MASTER

ORNL-2548
Chemistry – General
TID-4500 (15th ed.)

PHASE DIAGRAMS OF NUCLEAR REACTOR MATERIALS

R. E. Thoma, Editor

OAK RIDGE NATIONAL LABORATORY
operated by
UNION CARBIDE CORPORATION
for the
U.S. ATOMIC ENERGY COMMISSION

Printed in USA. Price $3.50. Available from the
Office of Technical Services
Department of Commerce
Washington 25, D.C.

DISCLAIMER

ORNL-2548
Chemistry – General
TID-4500 (15th ed.)

Contract No. W-7405-eng-26

REACTOR CHEMISTRY DIVISION

PHASE DIAGRAMS OF NUCLEAR REACTOR MATERIALS

R. E. Thoma, Editor

DATE ISSUED

OAK RIDGE NATIONAL LABORATORY
Oak Ridge, Tennessee
operated by
UNION CARBIDE CORPORATION
for the
U. S. ATOMIC ENERGY COMMISSION

CONTENTS

PHASE DIAGRAMS OF NUCLEAR REACTOR MATERIALS

INTRODUCTION

This compilation presents the phase diagrams for possible materials for nuclear reactors developed at the Oak Ridge National Laboratory over the period 1950–59. It represents the efforts of certain personnel in what are now the Chemical Technology, Metallurgy, Chemistry, and Reactor Chemistry Divisions of ORNL. This document also contains diagrams originated by other installations under contract to ORNL during that interval. In addition, a few diagrams from the unclassified literature have been included when they form part of completed systems sequences.

No general discussion of the principles of heterogeneous phase equilibrium has been included since excellent discussions are available in many well-known publications. Equilibria in several of the fused-salt systems presented below have been described in some detail in a recent publication by Ricci.[1] Nor has any attempt been made to assemble the phase equilibrium data on reactor materials available from many other sources. For such information the reader is referred to other recently published compilations of phase diagrams[2–6] and to the several new works dealing specifically with nuclear reactor materials.[7–9]

While some of the diagrams presented below are the result of fundamental researches, most were obtained in support of the ORNL programs in development of fluid-fueled reactors. Others have been developed as a consequence of ORNL interests in reprocessing of nuclear fuels, reactor metallurgy, production of uranium and thorium from raw materials, and studies of mechanisms of corrosion.

Much of the research effort was devoted to searches for systems of direct use as fluid fuels or blanket materials; unpromising systems were often given only casual attention. The diagrams in this collection, accordingly, vary widely in the degree of completeness of examination. A brief description of the status of the work is presented in each case; in a few cases, where no detailed description of the system has been published, the available data have been included with the diagram.

---

[1] J. E. Ricci, *Guide to the Phase Diagrams of the Fluoride Systems*, ORNL-2396 (Nov. 19, 1958).

[2] J. F. Hogerton and R. C. Grass (eds.), *The Reactor Handbook*, vol 2, AECD-3646 (May 1955).

[3] T. Lyman (ed.), *Metals Handbook*, American Society for Metals, Cleveland, Ohio, 1948.

[4] F. A. Rough and A. A. Bauer (eds.), *Constitution of Uranium and Thorium Alloys*, BMI-1300 (June 2, 1958).

[5] E. M. Levin, H. F. McMurdie, and F. P. Hall, *Phase Diagrams for Ceramists*, The American Ceramic Society, Columbus, Ohio, 1956.

[6] E. M. Levin, H. F. McMurdie, and F. P. Hall, *Supplement to Phase Diagrams for Ceramists*, The American Ceramic Society, Columbus, Ohio, 1959.

[7] B. Yates, *Materials for Use in Nuclear Reactors. Information Bibliography*, IGRL-IB/R-15 (2nd ed.), 1958.

[8] H. H. Hausner and S. B. Roboff, *Materials for Nuclear Power Reactors*, Reinhold Publishing Corp., New York, 1955.

[9] B. Kopelman (ed.), *Materials for Nuclear Reactors*, McGraw-Hill Book Co., New York, 1959.

1. METAL SYSTEMS

1.1. The System Silver–Zirconium

J. O. Betterton, Jr., and D. S. Easton, "The Silver–Zirconium System," *Trans. Met. Soc. AIME* **212**, 470–75 (1958).

A detailed investigation was made of the phase diagram of silver–zirconium, particularly in the region 0 to 36 at. % Ag. The system was found to be characterized by two intermediate phases, Zr_2Ag and ZrAg, and a eutectoid reaction in which the β-zirconium solid solution decomposes into α-zirconium and Zr_2Ag. It was found that impurities in the range 0.05% from the iodide-type zirconium were sufficient to introduce deviations from binary behavior; with partial removal of these impurities an increase in the α-phase solid solubility limit from 0.1 to 1.1 at. % Ag was observed.

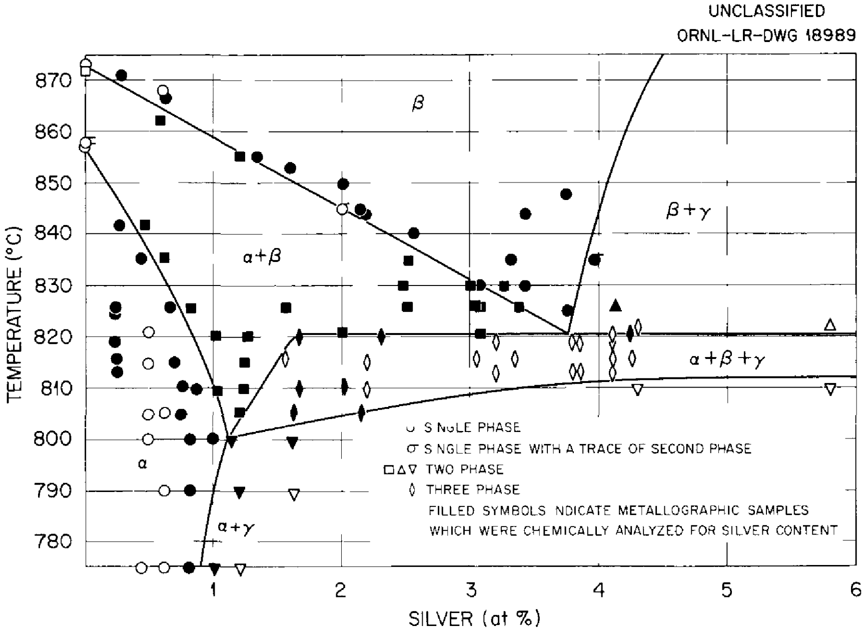

Fig. 1.1*a*. The System Silver–Zirconium in the Eutectoid Region (0–6 at. % Ag).

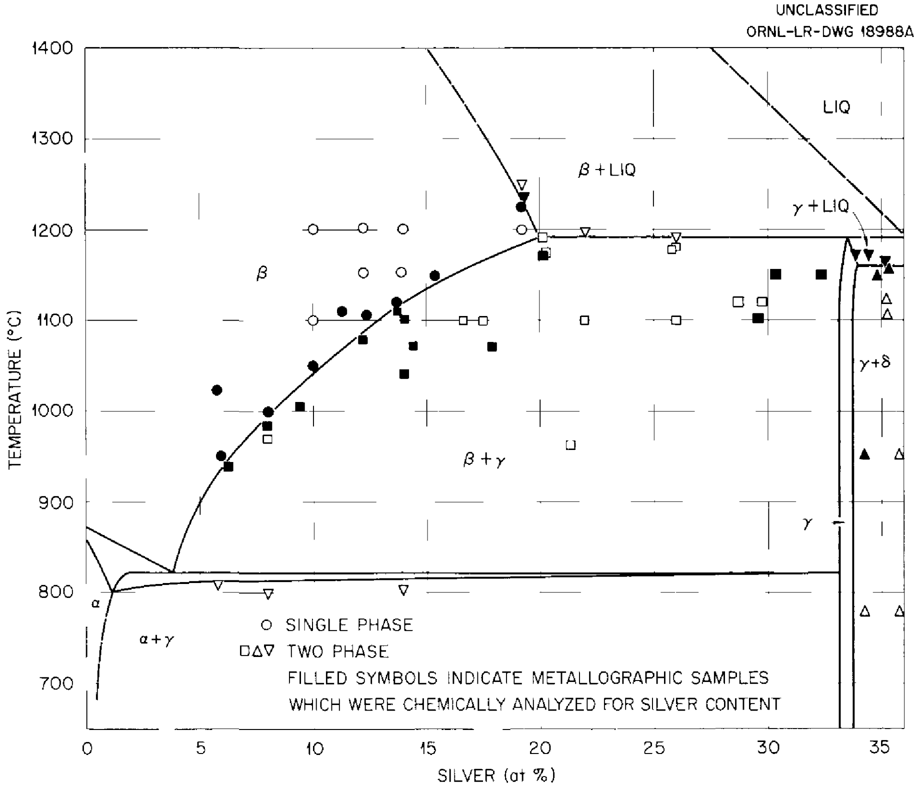

Fig. 1.1*b*. The System Silver–Zirconium in the Region 0–36 at. % Ag.

1.2. The System Indium–Zirconium

J. O. Betterton, Jr., and W. K. Noyce, "The Equilibrium Diagram of Indium–Zirconium in the Region 0–26 at. pct In," *Trans. Met. Soc. AIME* **212**, 340–42 (1958).

The zirconium-rich portion of the indium–zirconium phase diagram was determined as a study of the effect of alloying a trivalent B-subgroup element, indium, with zirconium in group IVA. The temperature of the allotropic transition was found to rise with indium, terminating in a peritectoid reaction, $\beta(9.3\%\ \mathrm{In}) + \gamma(22.4\%\ \mathrm{In}) \rightleftharpoons \alpha(10.1\%\ \mathrm{In})$ at 1003°C. In this respect the effect of indium is analogous to that of aluminum in zirconium and titanium alloys.

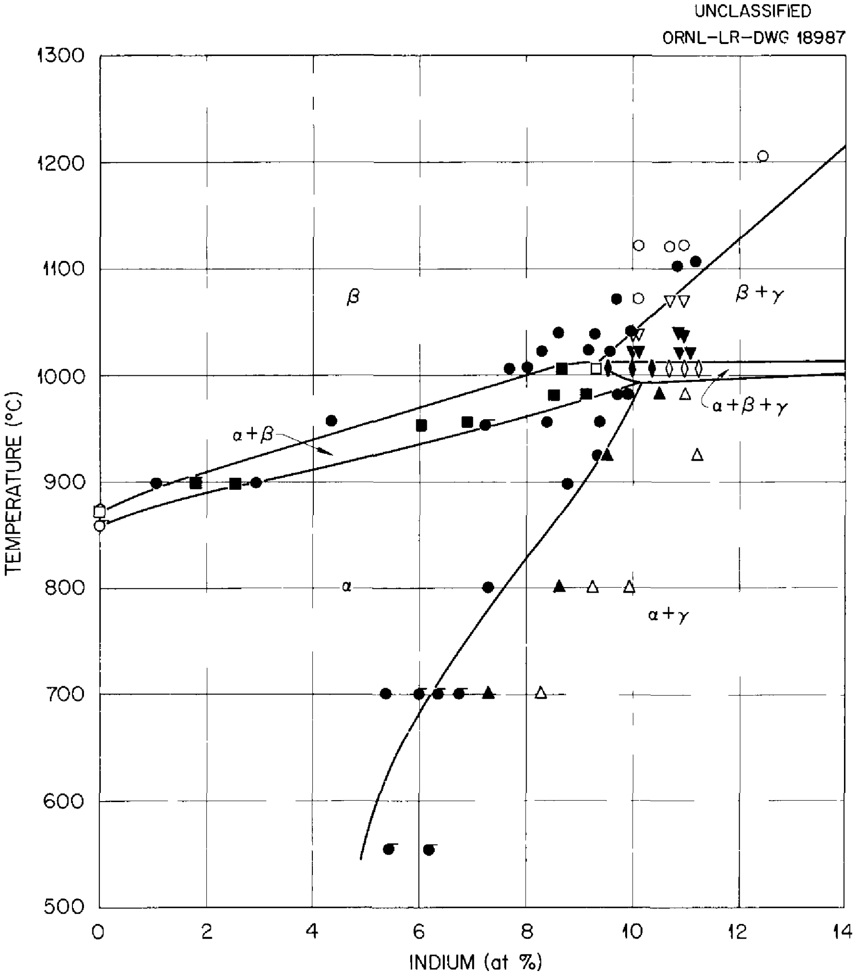

Fig. 1.2*a*. The System Indium–Zirconium in the Peritectoid Region (0–13 at. % In).

BLANK

BLANK

UNCLASSIFIED
ORNL-LR-DWG 18983

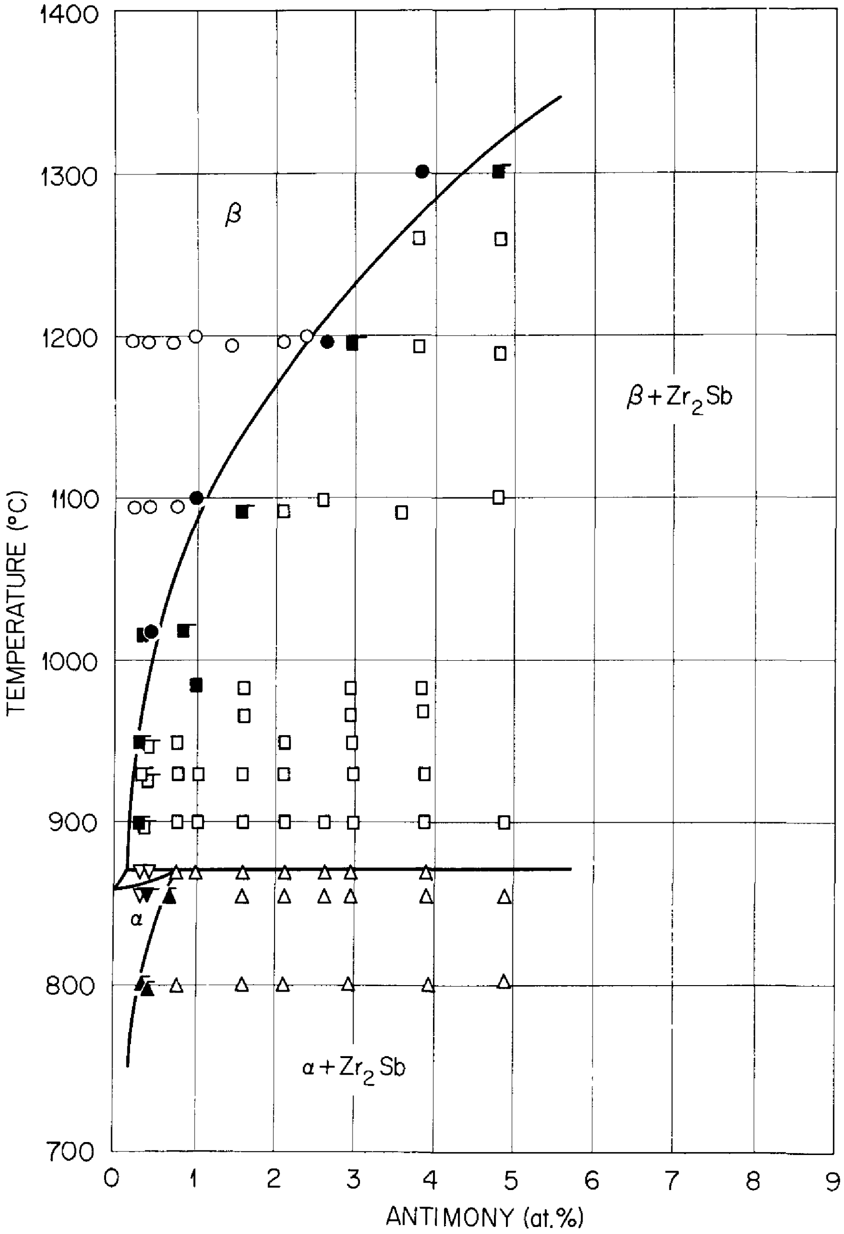

Fig. 1.3*b*. The System Antimony–Zirconium in the Peritectoid Region (0–6 at. % Sb).

1.4. The System Lead–Zirconium

G. D. Kneip, Jr., and J. O. Betterton, Jr., cited by E. T. Hayes and W. L. O'Brien, "Zirconium Equilibrium Diagrams," p 443–83 in *The Metallurgy of Zirconium*, ed. by B. Lustman and F. Kerze, Jr., McGraw-Hill Book Co., New York, 1955.

UNCLASSIFIED
ORNL–LR–DWG 1375

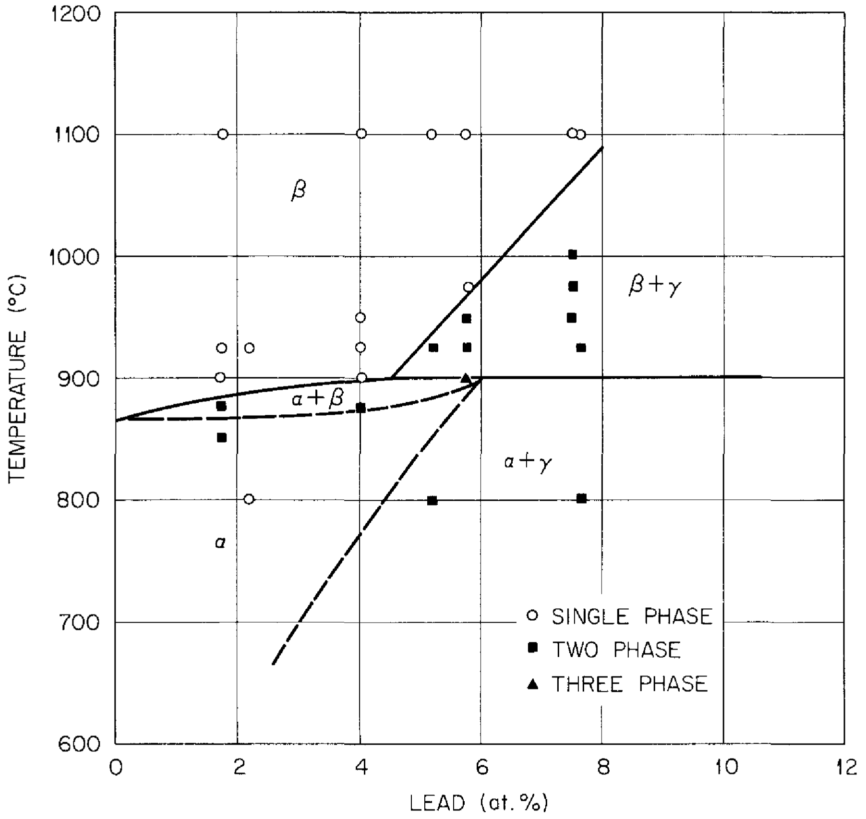

Fig. 1.4. The System Lead–Zirconium in the Peritectoid Region (0–12 at. % Pb).

2. METAL–FUSED-SALT SYSTEMS

2.1. The Sodium Metal–Sodium Halide Systems

M. A. Bredig and J. E. Sutherland, "High-Temperature Region of the Sodium–Sodium Halide Systems," *Chem. Ann. Prog. Rep. June 20, 1957*, ORNL-2386, p 119. Subsequent report on these systems to be published.

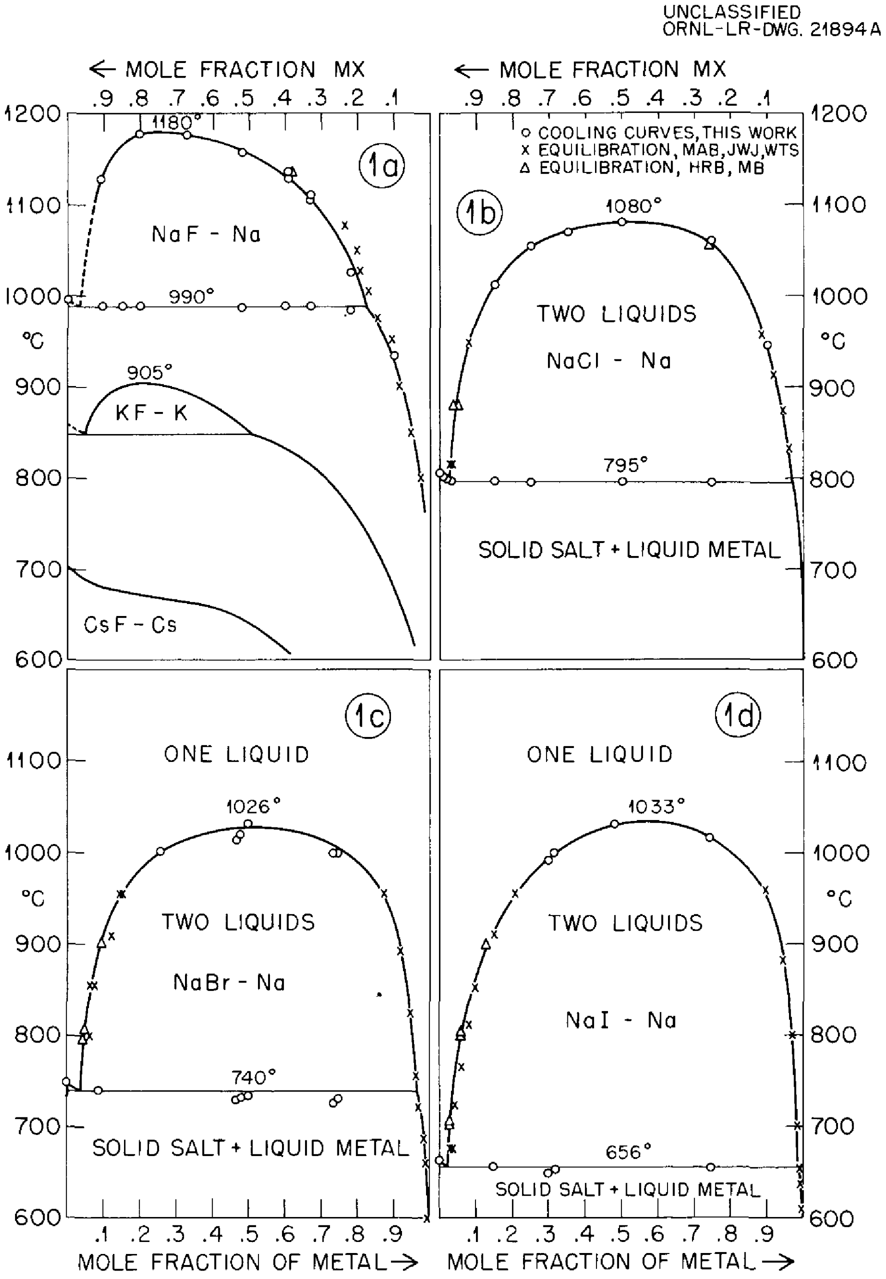

Fig. 2.1. The Sodium Metal–Sodium Halide Systems.

2.2. The Potassium Metal–Potassium Halide Systems

J. W. Johnson and M. A. Bredig, "Miscibility of Metals with Salts in the Molten State. III. The Potassium–Potassium Halide Systems," *J. Phys. Chem.* **62**, 604 (1958).

Complete miscibility of metal and salt exists in the KX–K systems, X = F, Cl, Br, and I, at and above 904, 790, 727, and 717°C, that is, as close as +47, +18, −7, and +22°, respectively, to the melting points of the salts. The asymmetry of the liquid-liquid coexistence areas, especially of the fluoride and chloride systems, as indicated by the consolute compositions (20, 39, 44, and 50 mole % metal, respectively), is largely explained by the difference in molar volumes of salt and metal. At the monotectic temperature, the solubility of the solid salts in the liquid metal, as well as of the metal in the liquid salt phase, is much larger than in the case of the sodium systems.

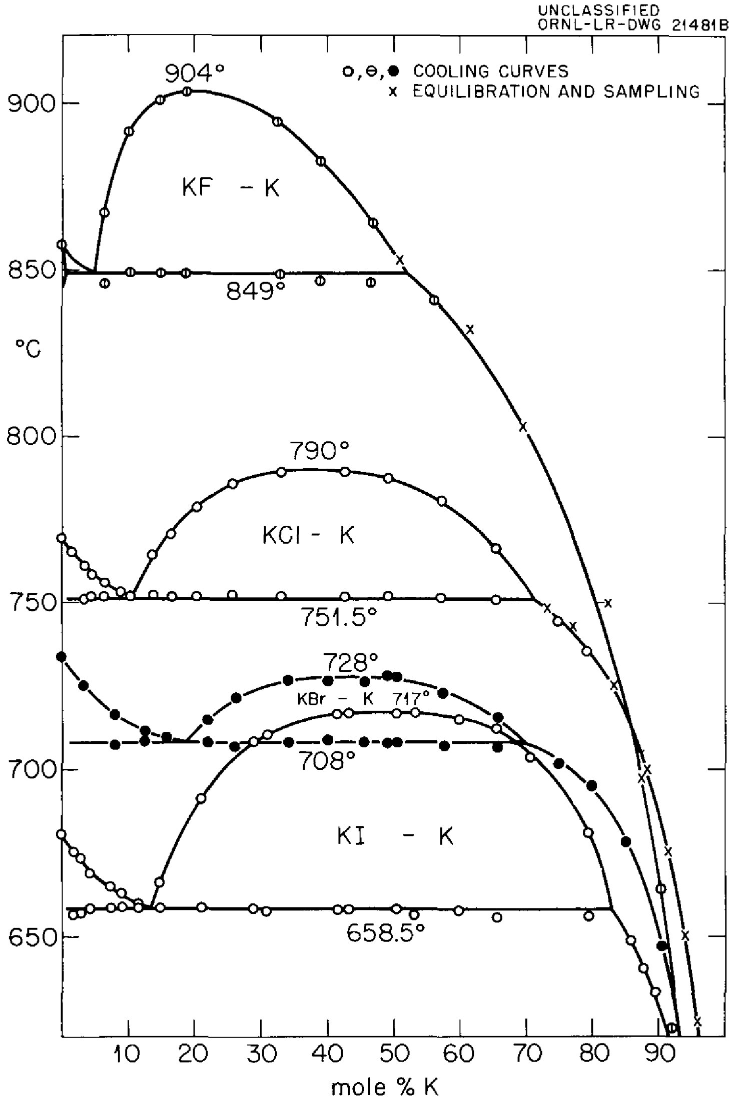

Fig. 2.2. The Potassium Metal–Potassium Halide Systems.

2.3. The Rubidium Metal–Rubidium Halide Systems

M. A. Bredig and J. W. Johnson, "Rubidium–Rubidium Halide Systems," *Chem. Ann. Prog. Rep. June 20, 1957*, ORNL-2386, p 122; M. A. Bredig, J. E. Sutherland, and A. S. Dworkin, "Molten Salt–Metal Solutions. Phase Equilibria," *Chem. Ann. Prog. Rep. June 20, 1958*, ORNL-2584, p 73. Subsequent report on these systems to be published.

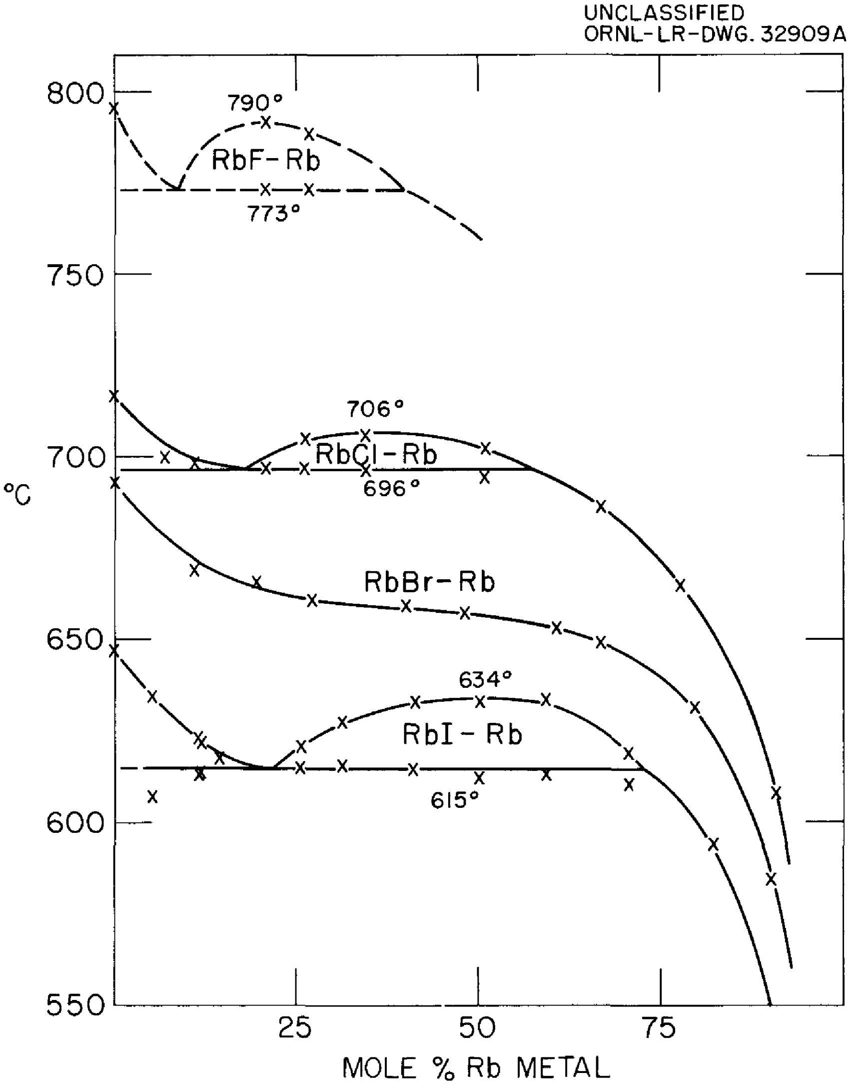

Fig. 2.3. The Rubidium Metal–Rubidium Halide Systems.

2.4. The Cesium Metal–Cesium Halide Systems

M. A. Bredig, H. R. Bronstein, and W. T. Smith, Jr., "Miscibility of Liquid Metals with Salts. II. The Potassium–Potassium Fluoride and Cesium–Cesium Halide Systems," *J. Am. Chem. Soc.* **77**, 1454 (1955).

Miscibility in all proportions of cesium metal with cesium halides at and above the melting points of the pure salts, and of potassium metal with potassium fluoride 50° above the melting point of the salt, occurs. The temperature-concentration range of coexistence of two liquid phases decreases in going from sodium to potassium systems and disappears altogether for the cesium systems. The solubility of the solid halides in the corresponding liquid alkali metals, at a given temperature, increases greatly with increase of atomic number of the metal.

UNCLASSIFIED
ORNL-LR-DWG. 37011

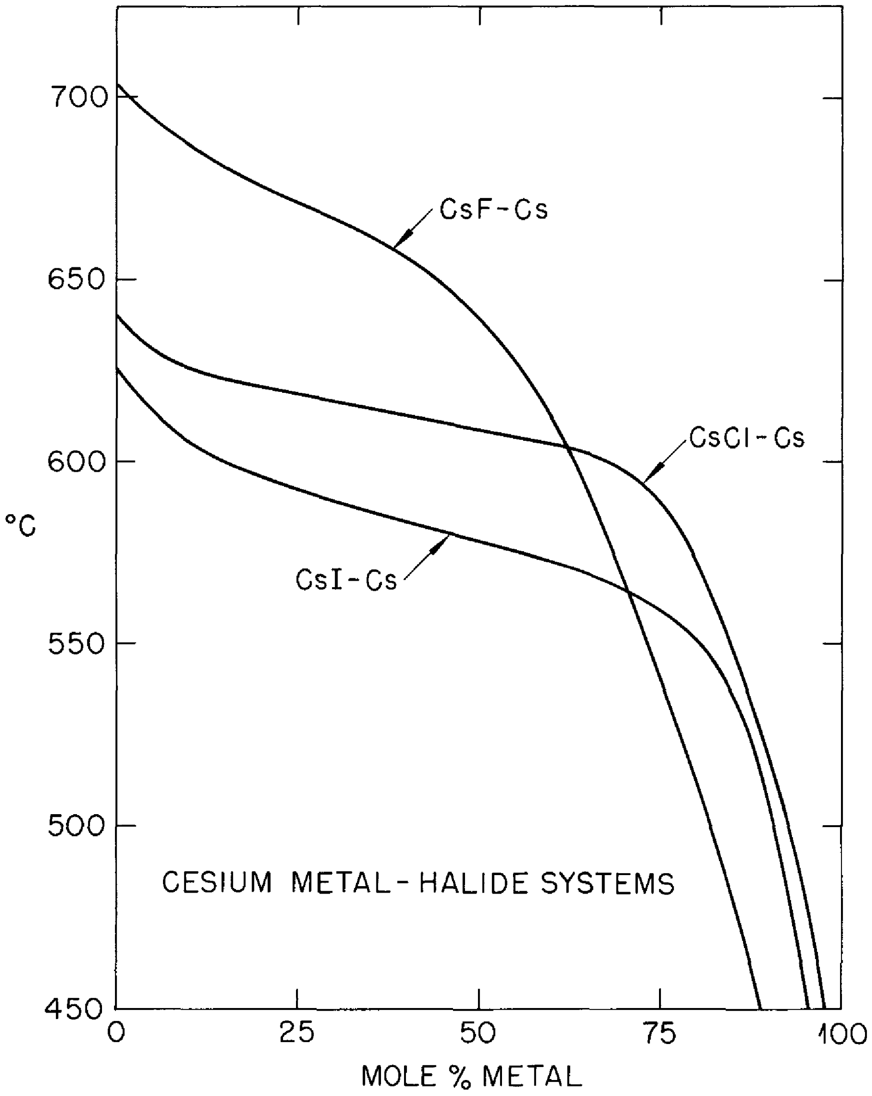

Fig. 2.4. The Cesium Metal–Cesium Halide Systems.

2.5. The Alkali Metal–Alkali Metal Fluoride Systems

M. A. Bredig, J. E. Sutherland, and A. S. Dworkin, "Molten Salt–Metal Solutions. Phase Equilibria," *Chem. Ann. Prog. Rep. June 20, 1958*, ORNL-2584, p 73.

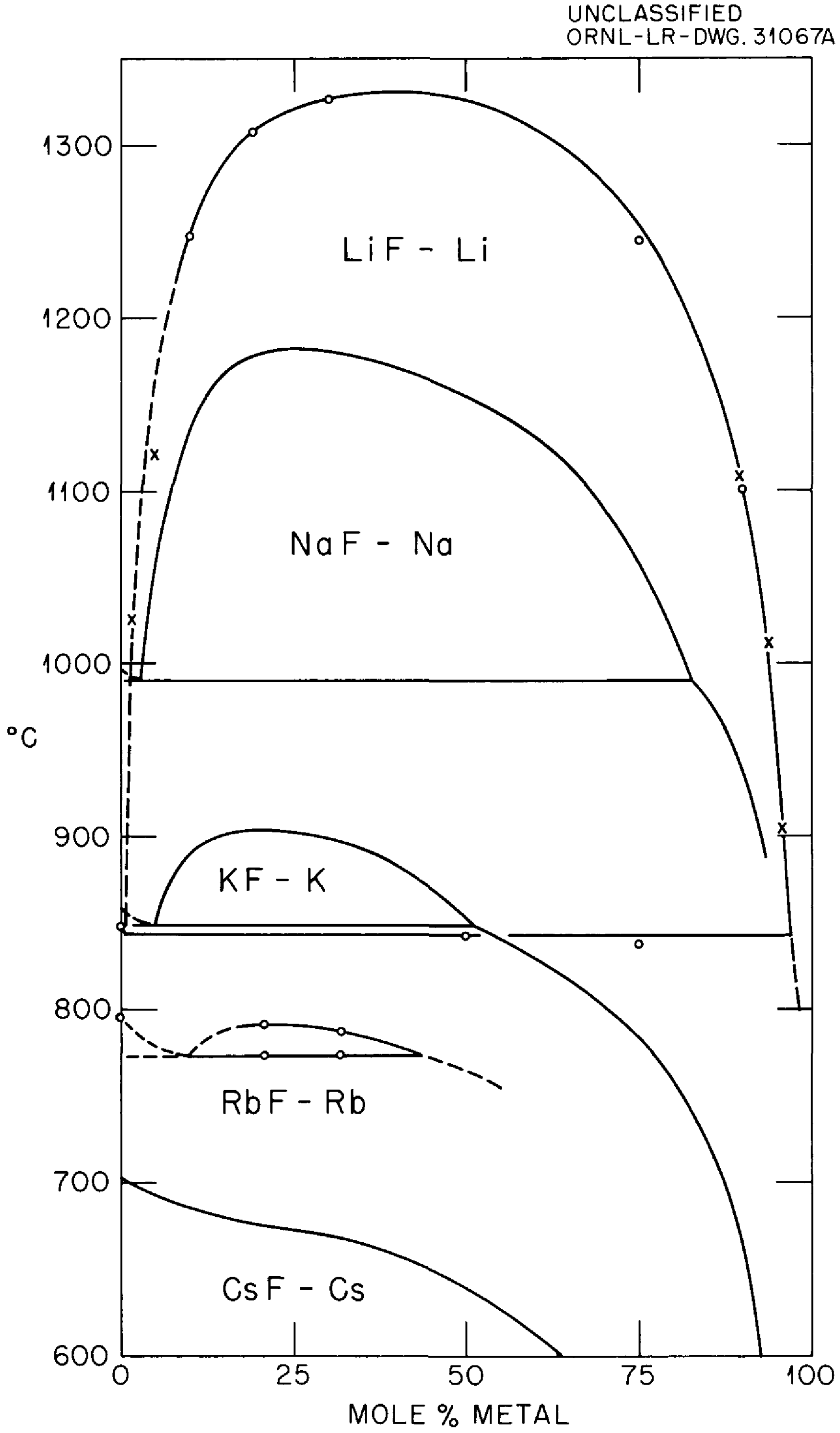

Fig. 2.5. The Alkali Metal–Alkali Metal Fluoride Systems.

3. FUSED-SALT SYSTEMS

3.1. The System LiF–NaF

A. G. Bergman and E. P. Dergunov, "Fusion Diagram of LiF–KF–NaF," *Compt. rend. acad. sci. U.R.S.S.* **31,** 753–54 (1941).

The system LiF–NaF contains a single eutectic at 60 LiF–40 NaF (mole %), m.p. 652°C.

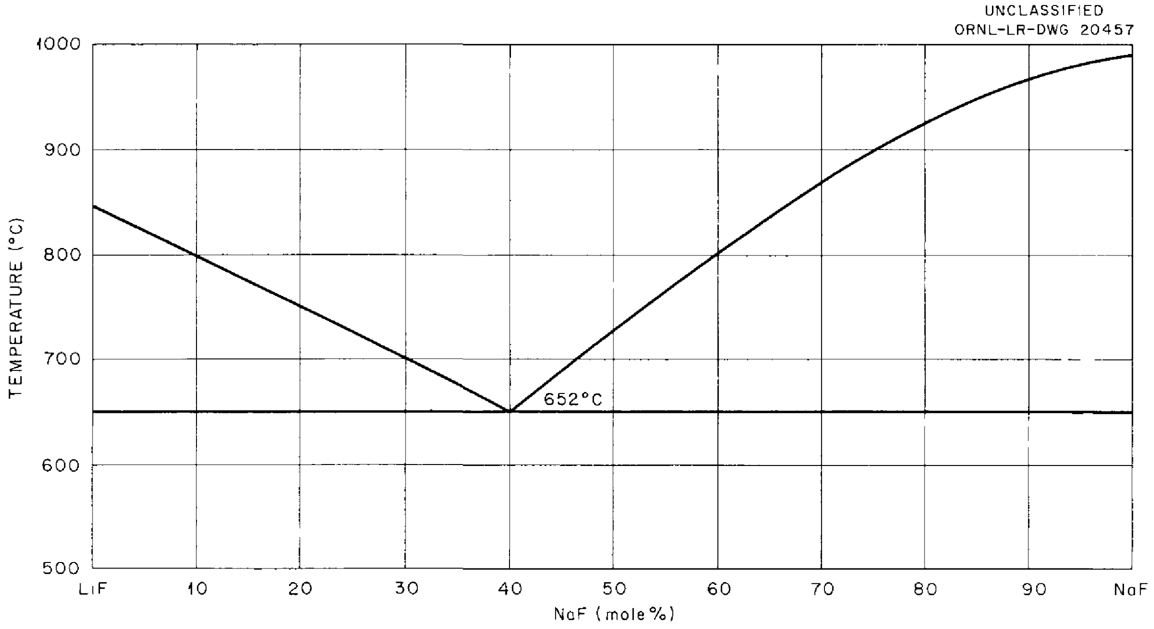

Fig. 3.1. The System LiF–NaF.

3.2. The System LiF–KF

A. G. Bergman and E. P. Dergunov, "Fusion Diagram of LiF–KF–NaF," *Compt. rend. acad. sci. U.R.S.S.* **31**, 753–54 (1941).

The system LiF–KF contains a single eutectic at 50 LiF–50 KF (mole %), m.p. 492°C.

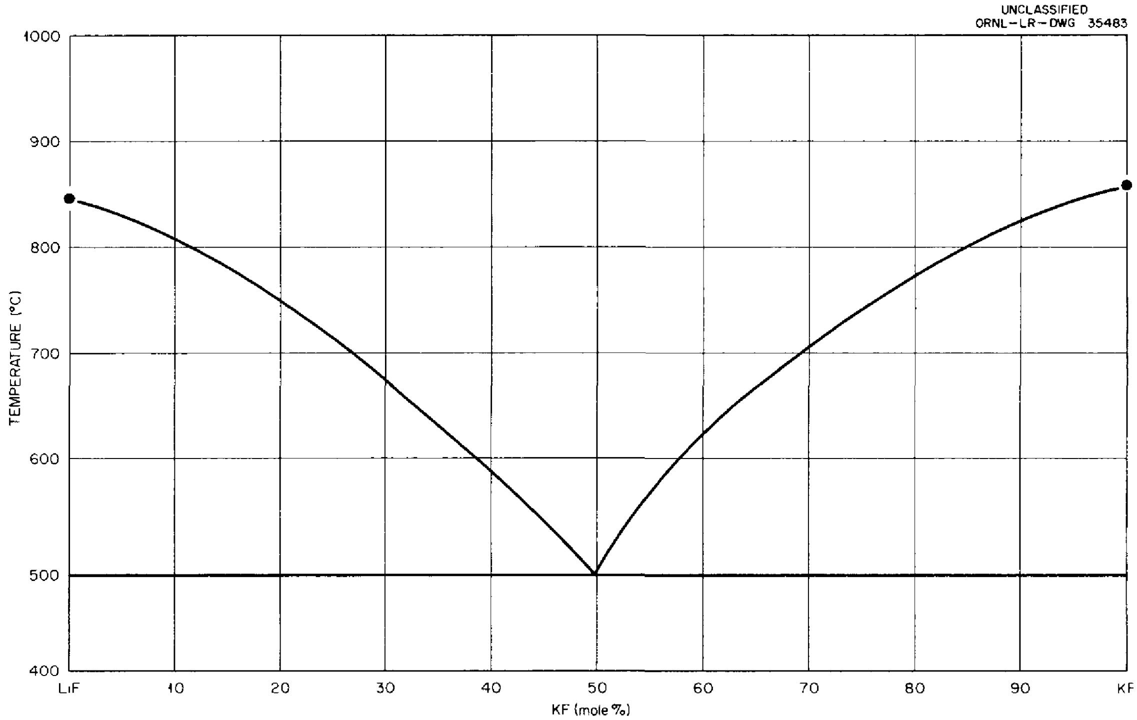

Fig. 3.2. The System LiF–KF.

3.3. The System LiF–RbF

C. J. Barton, T. N. McVay, L. M. Bratcher, and W. R. Grimes, unpublished work performed at the Oak Ridge National Laboratory, 1951–54.

Preliminary diagram.

Invariant Equilibria

Mole % LiF in Liquid	Invariant Temperature (°C)	Type of Equilibrium	Phase Reaction at Invariant Temperature
44	470	Eutectic	$L \rightleftharpoons \text{RbF} + \text{LiF}\cdot\text{RbF}$
47	475	Peritectic	$L + \text{LiF} \rightleftharpoons \text{LiF}\cdot\text{RbF}$

General characteristics of the system have been reported by E. P. Dergunov, "Fusion Diagrams of the Ternary Systems of the Fluorides of Lithium, Sodium, Potassium, and Rubidium," *Doklady Akad. Nauk S.S.S.R.* **58,** 1369–72 (1947).

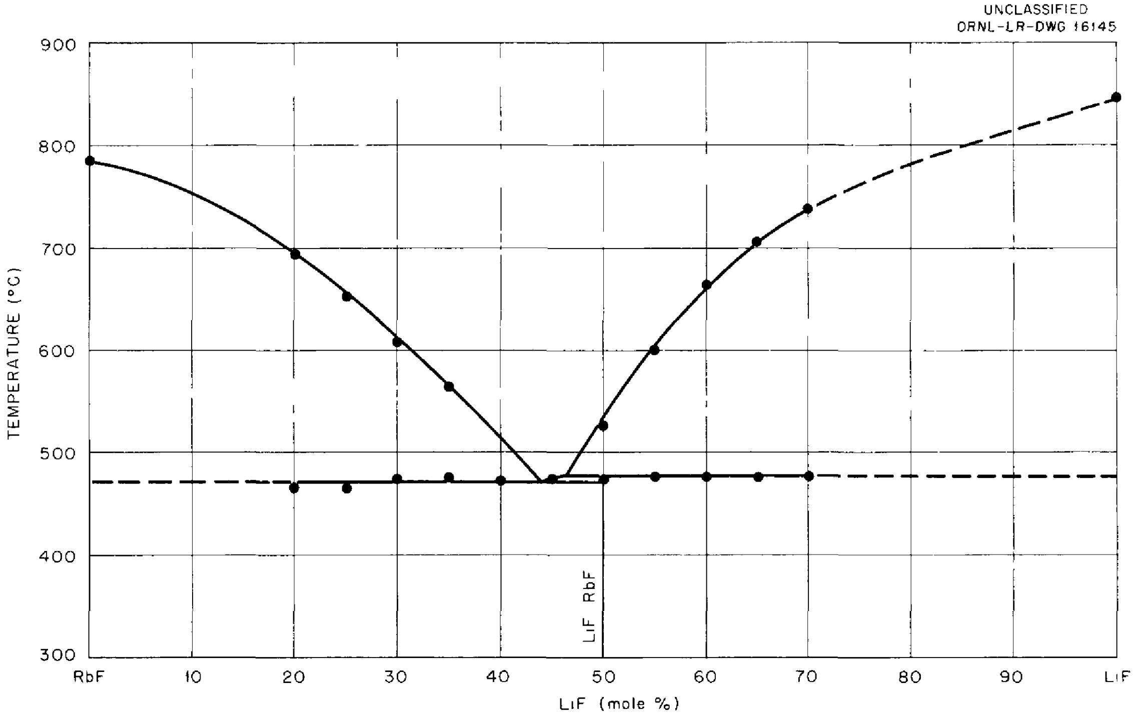

Fig. 3.3. The System LiF–RbF.

3.4. The System LiF–CsF

C. J. Barton, L. M. Bratcher, T. N. McVay, and W. R. Grimes, unpublished work performed at the Oak Ridge National Laboratory, 1952–54.

Preliminary diagram.

Invariant Equilibria

Mole % CsF in Liquid	Invariant Temperature (°C)	Type of Equilibrium	Phase Reaction at Invariant Temperature
55	495 ± 5	Peritectic	$\mathrm{LiF} + L \rightleftharpoons \mathrm{LiF{\cdot}CsF}$
63	475 ± 5	Eutectic	$L \rightleftharpoons \mathrm{LiF{\cdot}CsF} + \mathrm{CsF}$

UNCLASSIFIED
ORNL-LR-DWG 14632

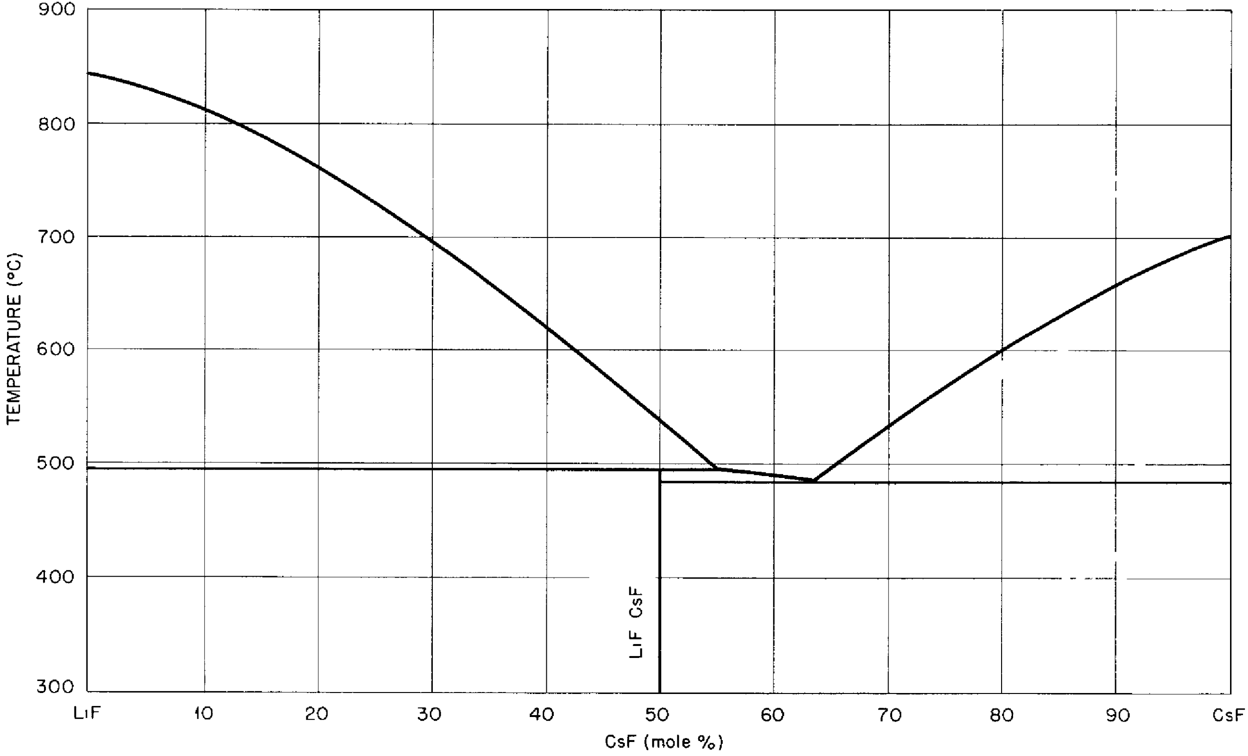

Fig. 3.4. The System LiF–CsF.

3.5. The System NaF–KF

A. G. Bergman and E. P. Dergunov, "Fusion Diagram of LiF–KF–NaF," *Compt. rend. acad. sci. U.R.S.S.* 31, 753–54 (1941).

The system NaF–KF contains a single eutectic at 40 NaF–60 KF (mole %), m.p. 710°C.

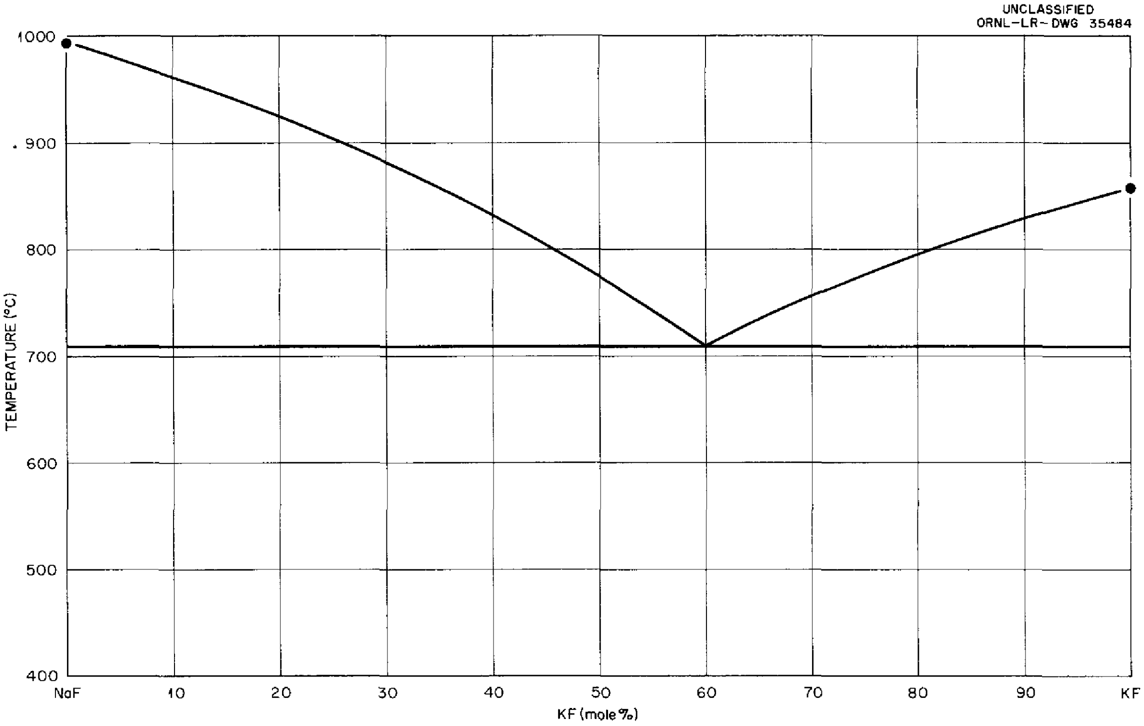

Fig. 3.5. The System NaF–KF.

3.6. The System NaF–RbF

C. J. Barton, J. P. Blakely, L. M. Bratcher, and W. R. Grimes, unpublished work performed at the Oak Ridge National Laboratory, 1951.

Preliminary diagram. The system NaF–RbF contains a single eutectic at 27 NaF–73 RbF (mole %), m.p. 675 ± 10°C.

General characteristics of the system have been reported by E. P. Dergunov, "Fusion Diagrams of the Ternary Systems of the Fluorides of Lithium, Sodium, Potassium, and Rubidium," *Doklady Akad. Nauk S.S.S.R.* **58,** 1369–72 (1947).

UNCLASSIFIED
ORNL-LR-DWG 35711

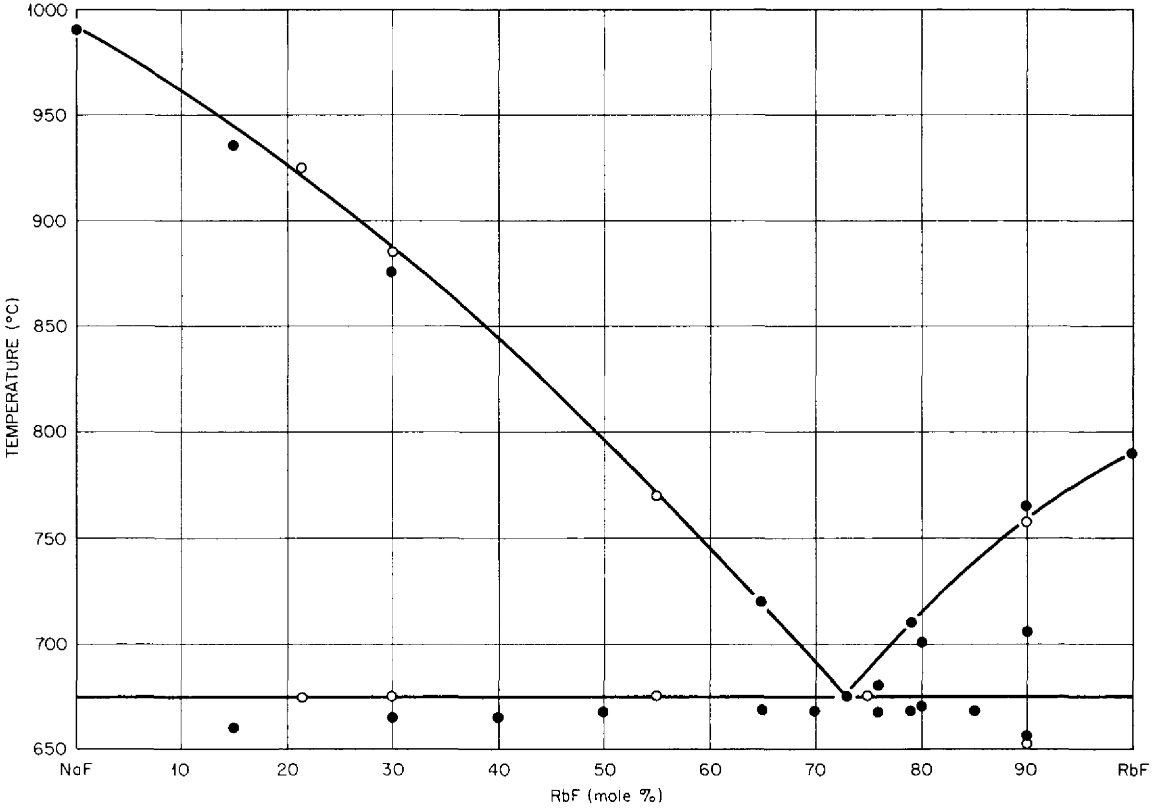

Fig. 3.6. The System NaF–RbF.

3.7. The System KF–RbF

C. J. Barton, J. P. Blakely, L. M. Bratcher, and W. R. Grimes, unpublished work performed at the Oak Ridge National Laboratory, 1951.

Preliminary diagram. The system KF–RbF contains a solid solution minimum at 28 KF–72 RbF (mole %), m.p. 770 ± 10°C.

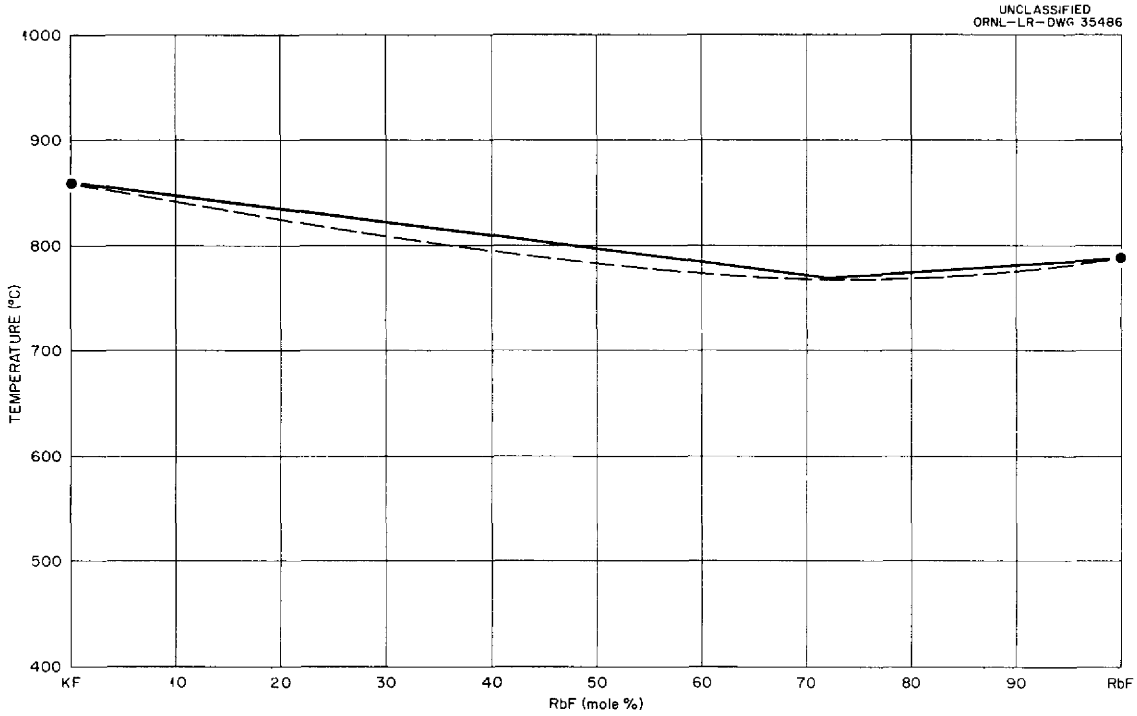

Fig. 3.7. The System KF–RbF.

3.8. The System LiF–NaF–KF

A. G. Bergman and E. P. Dergunov, "Fusion Diagram of LiF–KF–NaF," *Compt. rend. acad. sci. U.R.S.S.* **31**, 753–54 (1941).

The system LiF–NaF–KF contains a single eutectic at 46.5 LiF–11.5 NaF–42.0 KF (mole %), m.p. 454°C.

UNCLASSIFIED
ORNL-LR-DWG 1199A

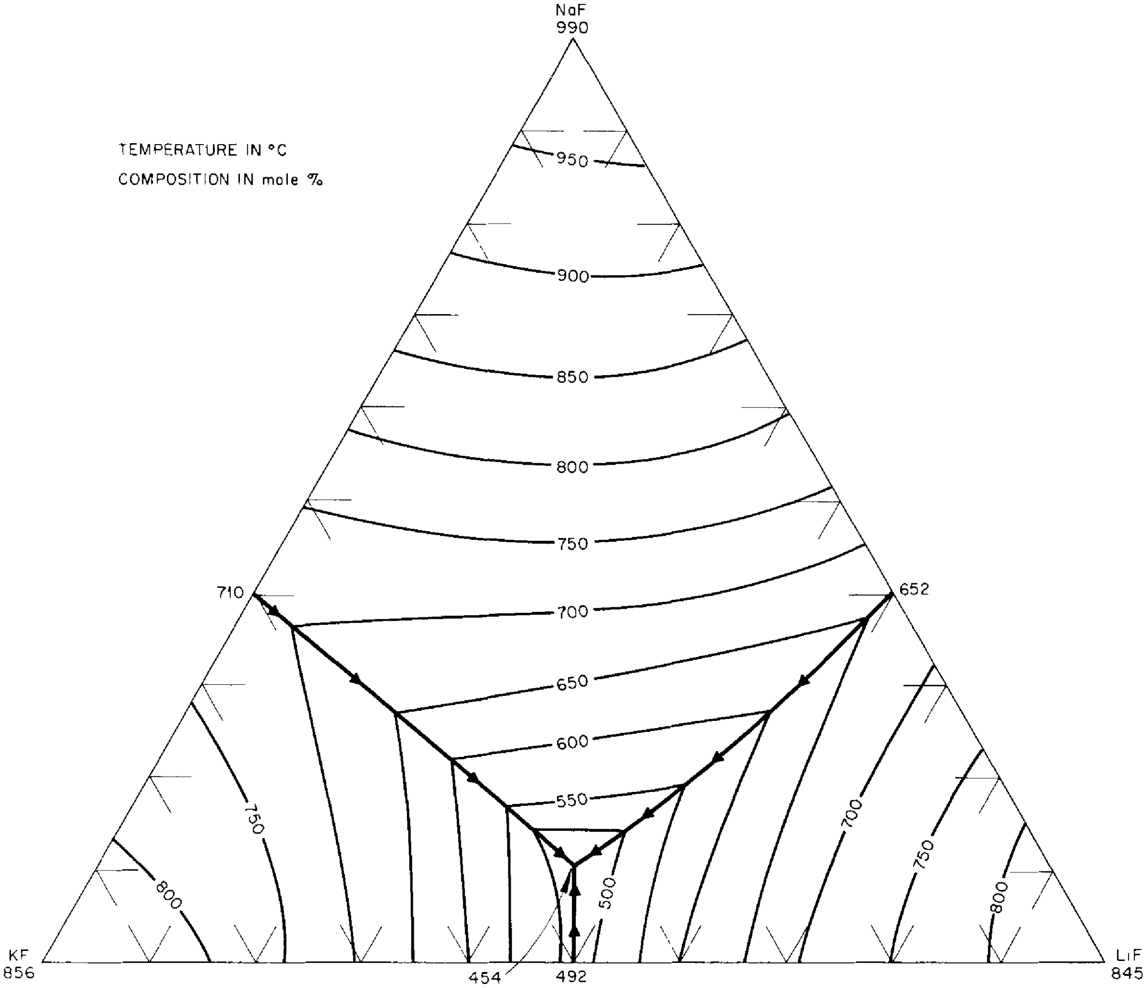

Fig. 3.8. The System LiF–NaF–KF.

3.9. The System LiF–NaF–RbF

C. J. Barton, L. M. Bratcher, J. P. Blakely, and W. R. Grimes, unpublished work performed at the Oak Ridge National Laboratory, 1951.

Preliminary diagram. The system LiF–NaF–RbF contains a single eutectic at 42 LiF–6 NaF–52 RbF (mole %), m.p. 430 ± 10°C. The composition and temperature of the ternary peritectic point have not yet been determined.

General characteristics of the system have been reported by E. P. Dergunov, "Fusion Diagrams of the Ternary systems of the Fluorides of Lithium, Sodium, Potassium, and Rubidium," *Doklady Akad. Nauk S.S.S.R.* **58,** 1369–72 (1947). Dergunov lists the composition and temperature of the ternary eutectic as 46.5 LiF–6.5 NaF–47 RbF (mole %), m.p. 426°C.

UNCLASSIFIED
ORNL-LR-DWG 1200A

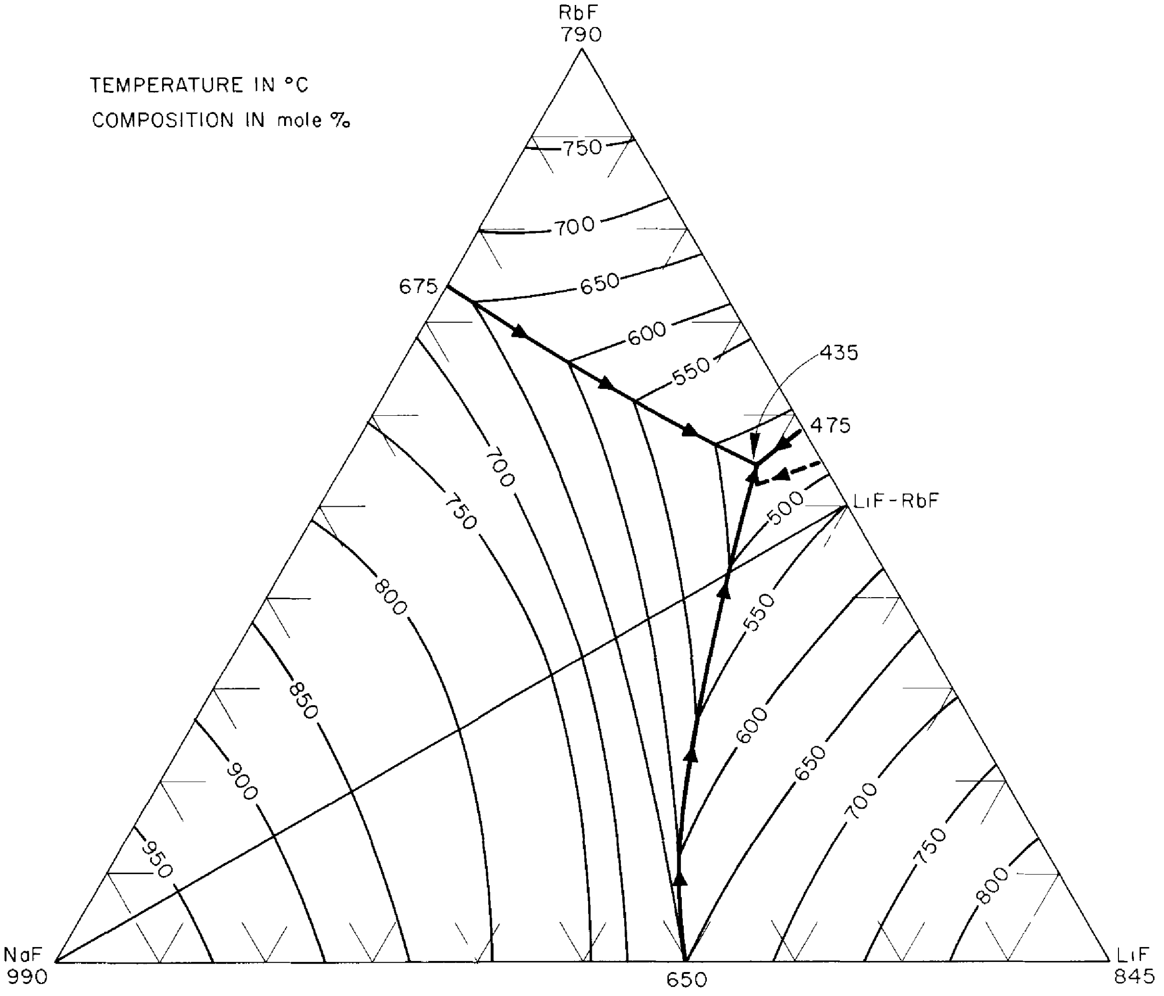

Fig. 3.9. The System LiF–NaF–RbF.

3.10. The System LiF–KF–RbF

C. J. Barton, J. P. Blakely, L. M. Bratcher, and W. R. Grimes, unpublished work performed at the Oak Ridge National Laboratory, 1951.

Preliminary diagram. The system LiF–KF–RbF contains a single eutectic at 40 LiF–32.5 KF–27.5 RbF (mole %), m.p. 440 ± 10°C.

General characteristics of the system have been reported by E. P. Dergunov, "Fusion Diagrams of the Ternary Systems of the Fluorides of Lithium, Sodium, Potassium, and Rubidium," *Doklady Akad. Nauk S.S.S.R.* **58,** 1369–72 (1947).

UNCLASSIFIED
ORNL-LR-DWG 35479

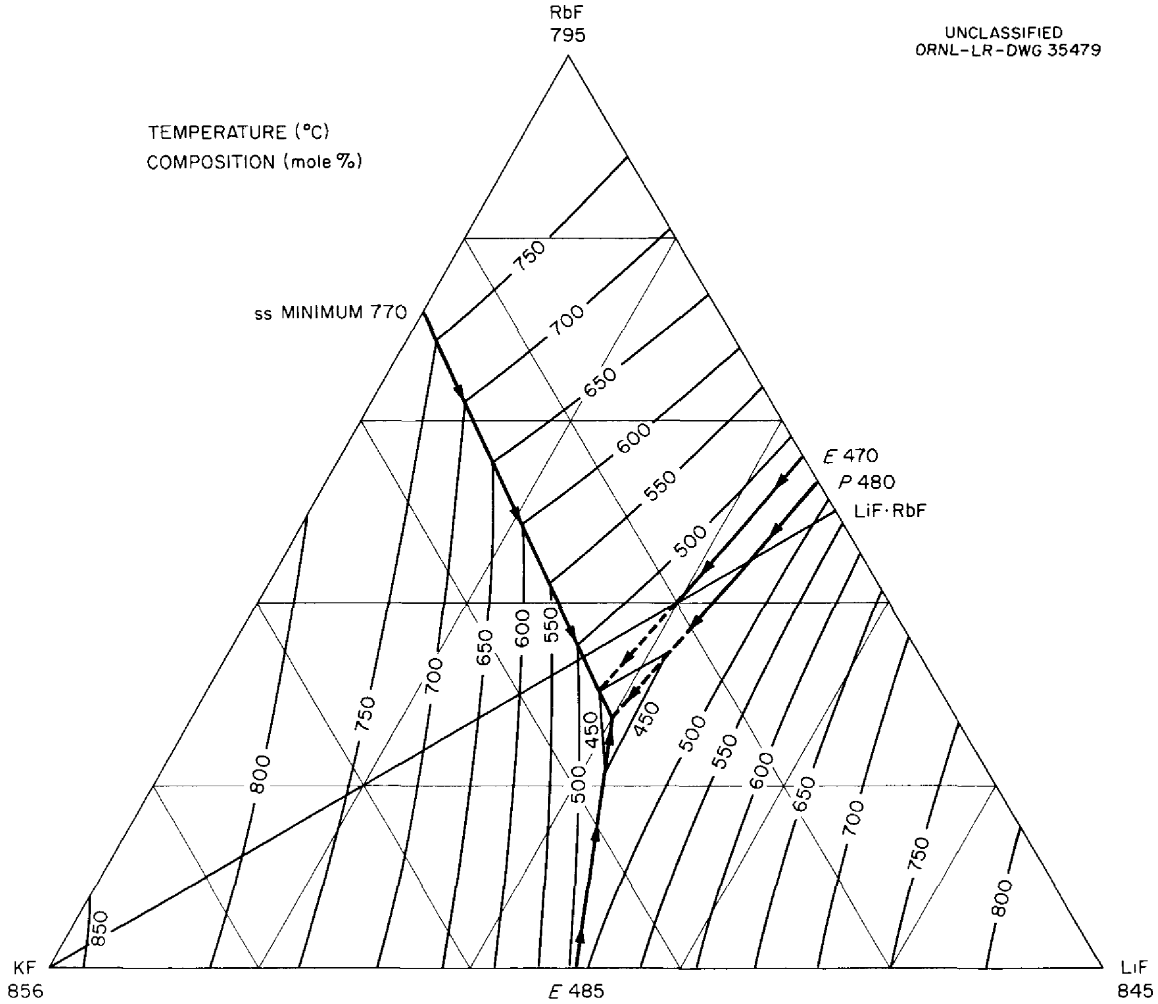

Fig. 3.10. The System LiF–KF–RbF.

3.11. The System NaF–KF–RbF

C. J. Barton, L. M. Bratcher, J. P. Blakely, and W. R. Grimes, unpublished work performed at the Oak Ridge National Laboratory, 1951.

Preliminary diagram. The system NaF–KF–RbF contains a single eutectic at 21 NaF–5 KF–74 RbF (mole %), m.p. 621 ± 10°C.

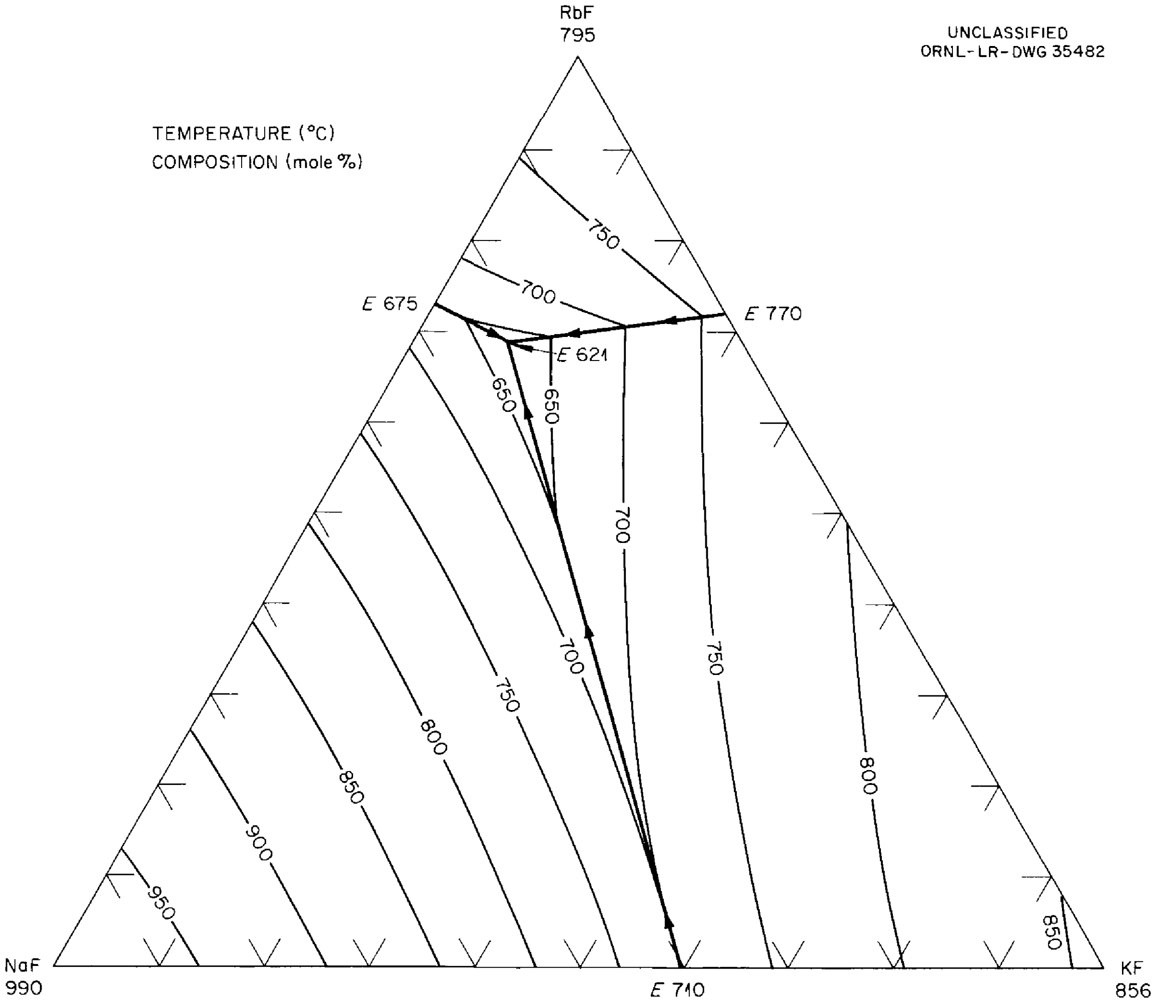

Fig. 3.11. The System NaF–KF–RbF.

3.12. The System $NaBF_4$–KBF_4

R. E. Moore, J. G. Surak, and W. R. Grimes, unpublished work performed at the Oak Ridge National Laboratory, 1957.

Preliminary diagram. The system $NaBF_4$–KBF_4 contains a single eutectic at 88 $NaBF_4$–12 KBF_4 (mole %), m.p. 355°C. The dotted line was obtained from thermal effects representing incompletely understood solid-phase transformations of KBF_4 and $NaBF_4$.

UNCLASSIFIED
ORNL-LR-DWG 35487

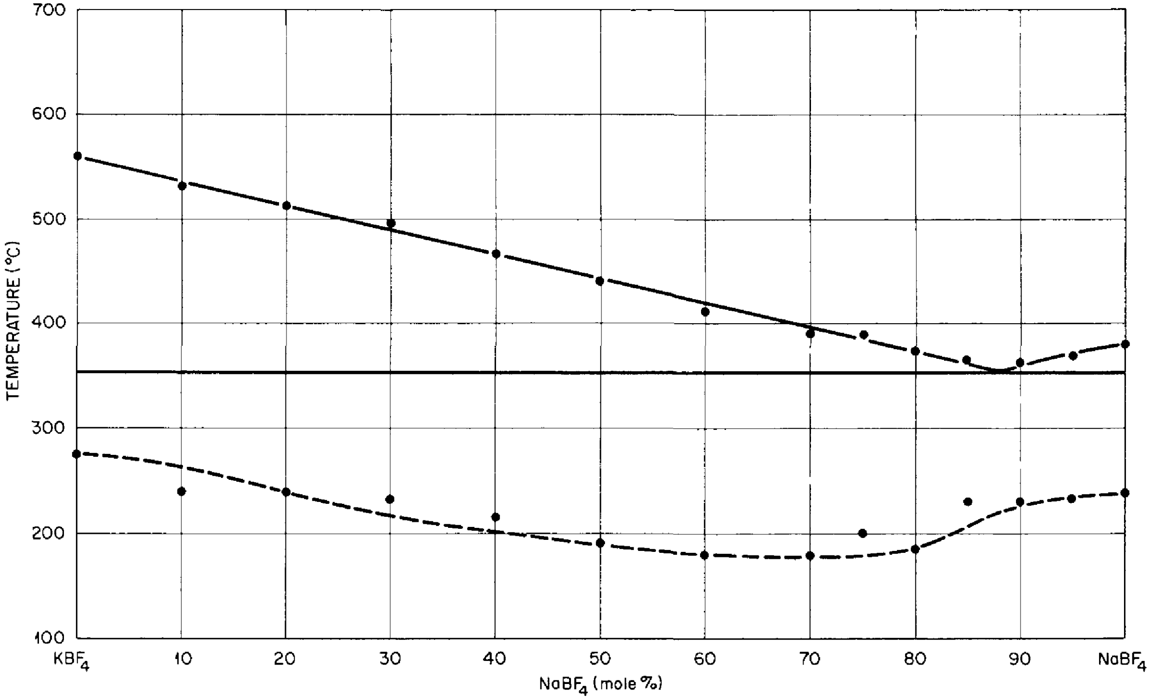

Fig. 3.12. The System $NaBF_4$–KBF_4.

3.13. The System NaF–FeF_2

R. E. Thoma, H. A. Friedman, B. S. Landau, and W. R. Grimes, unpublished work performed at the Oak Ridge National Laboratory, 1957.

Preliminary diagram.

Invariant Equilibria

Mole % FeF_2 in Liquid	Invariant Temperature (°C)	Type of Equilibrium	Phase Reaction at Invariant Temperature
30	680	Eutectic	$L \rightleftharpoons NaF + NaF \cdot FeF_2$
50	783	Congruent melting point	$L \rightleftharpoons NaF \cdot FeF_2$
63	745	Eutectic	$L \rightleftharpoons NaF \cdot FeF_2 + FeF_2$

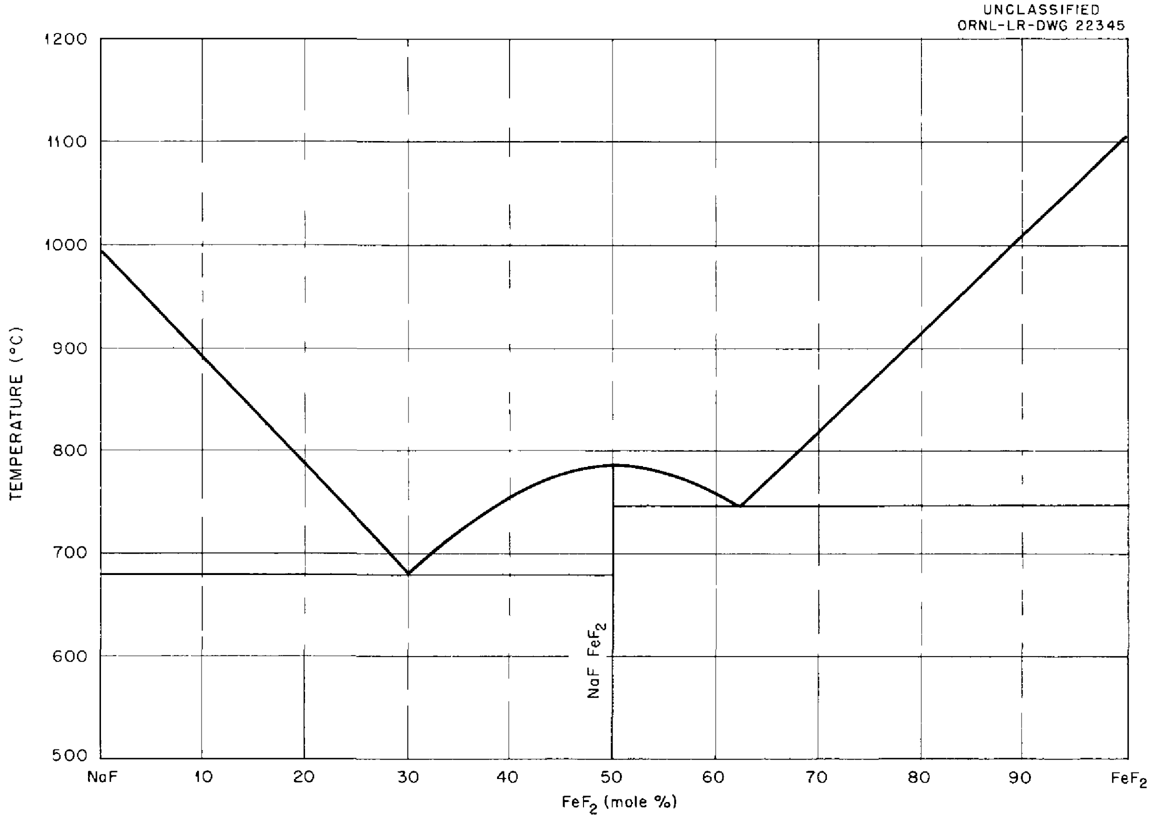

Fig. 3.13. The System NaF–FeF_2.

3.14. The System NaF–NiF_2

R. E. Thoma, H. A. Friedman, B. S. Landau, and W. R. Grimes, unpublished work performed at the Oak Ridge National Laboratory, 1957.

Preliminary diagram.

Invariant Equilibria

Mole % NiF_2 in Liquid	Invariant Temperature (°C)	Type of Equilibrium	Phase Reaction at Invariant Temperature
23	795	Eutectic	$L \rightleftharpoons NaF + NaF \cdot NiF_2$
50	1045	Congruent melting point	$L \rightleftharpoons NaF \cdot NiF_2$
57	1040	Eutectic	$L \rightleftharpoons NaF \cdot NiF_2 + NiF_2$

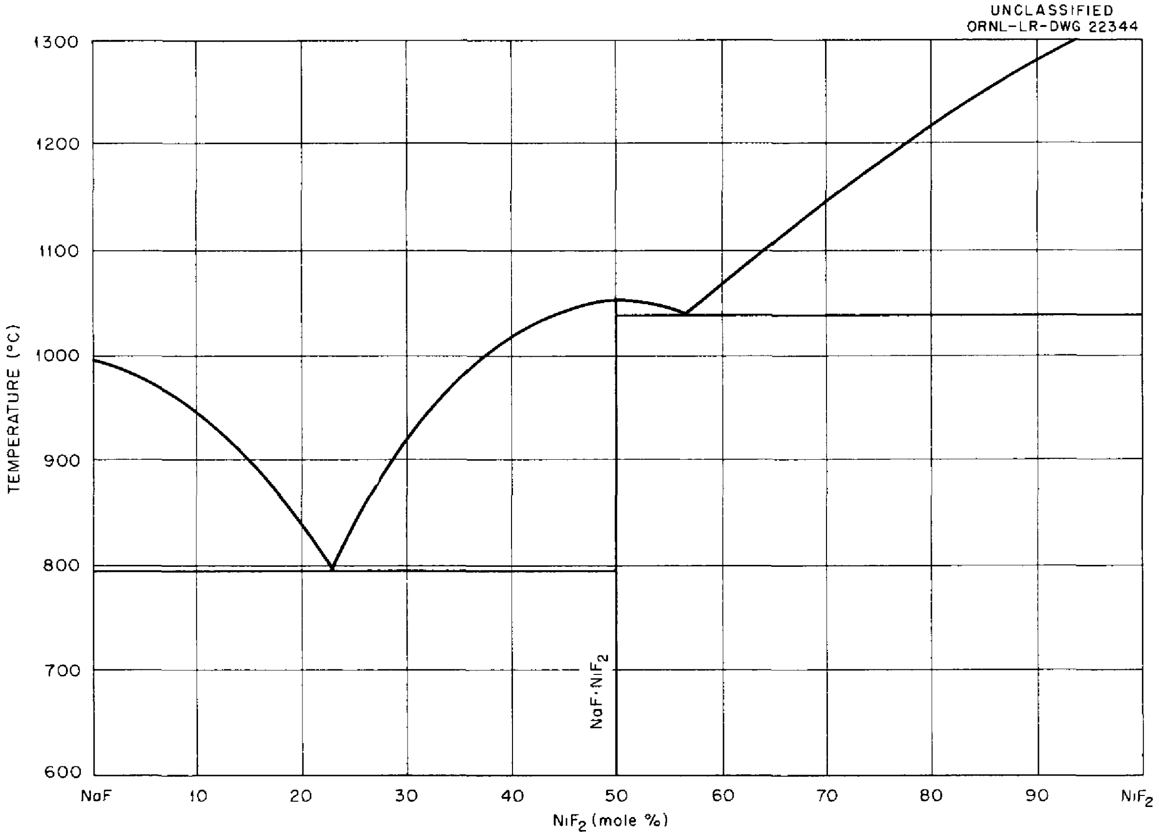

Fig. 3.14. The System NaF–NiF_2.

3.15. The System RbF–CaF$_2$

C. J. Barton, L. M. Bratcher, R. J. Sheil, and W. R. Grimes, unpublished work performed at the Oak Ridge National Laboratory, 1956.

Preliminary diagram.

Invariant Equilibria

Mole % CaF$_2$ in Liquid	Invariant Temperature (°C)	Type of Equilibrium	Phase Reaction at Invariant Temperature
9	760	Eutectic	$L \rightleftharpoons$ RbF + RbF·CaF$_2$
50	1110	Congruent melting point	$L \rightleftharpoons$ RbF·CaF$_2$
57	1090	Eutectic	$L \rightleftharpoons$ RbF·CaF$_2$ + CaF$_2$

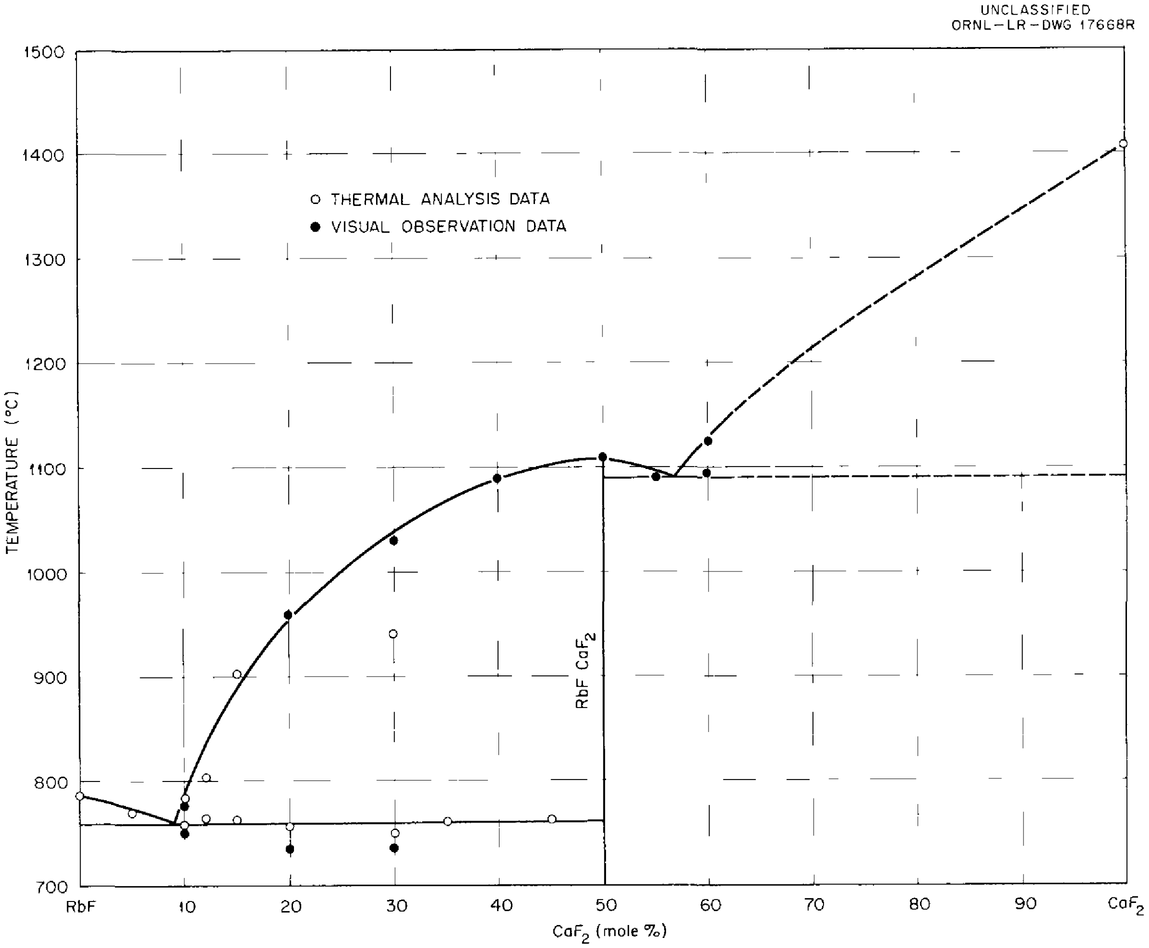

Fig. 3.15. The System RbF–CaF$_2$.

3.16. The System LiF–NaF–CaF_2

C. J. Barton, L. M. Bratcher, and W. R. Grimes, unpublished work performed at the Oak Ridge National Laboratory, 1955–56.

Preliminary diagram. The system LiF–NaF–CaF_2 contains a single eutectic at 53 LiF–36 NaF–11 CaF_2 (mole %), m.p. 616°C.

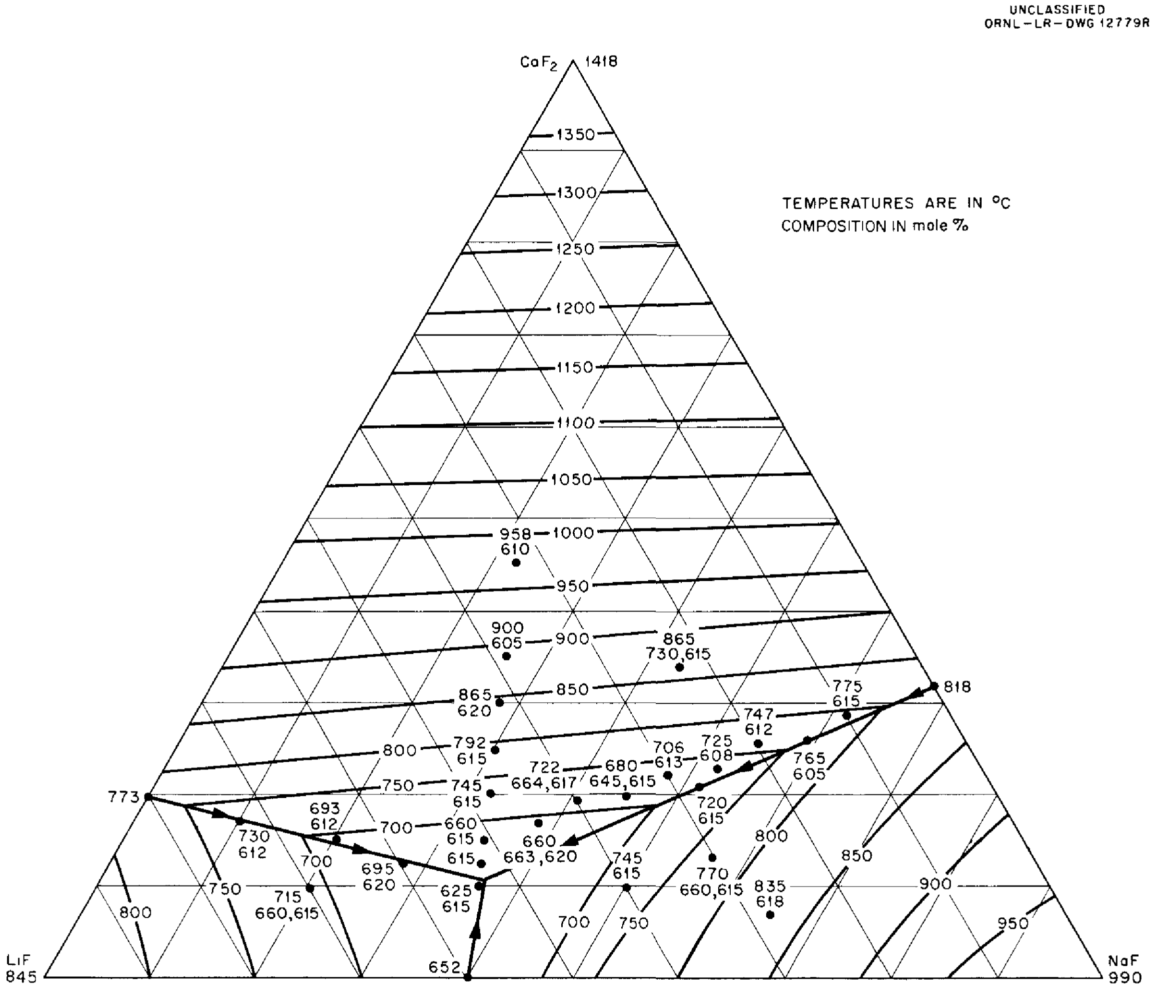

Fig. 3.16. The System LiF–NaF–CaF_2.

3.17. The System $NaF–MgF_2–CaF_2$

C. J. Barton, L. M. Bratcher, J. P. Blakely, and W. R. Grimes, unpublished work performed at the Oak Ridge National Laboratory, 1955–56.

Preliminary diagram.

Invariant Equilibria

Composition of Liquid (mole %)			Temperature (°C)	Type of Equilibrium	Solids Present at Invariant Temperature
NaF	CaF_2	MgF_2			
65	23	12	745	Eutectic	NaF, $NaF{\cdot}MgF_2$, and CaF_2
35	28	37	905	Eutectic	CaF_2, MgF_2, and $NaF{\cdot}MgF_2$

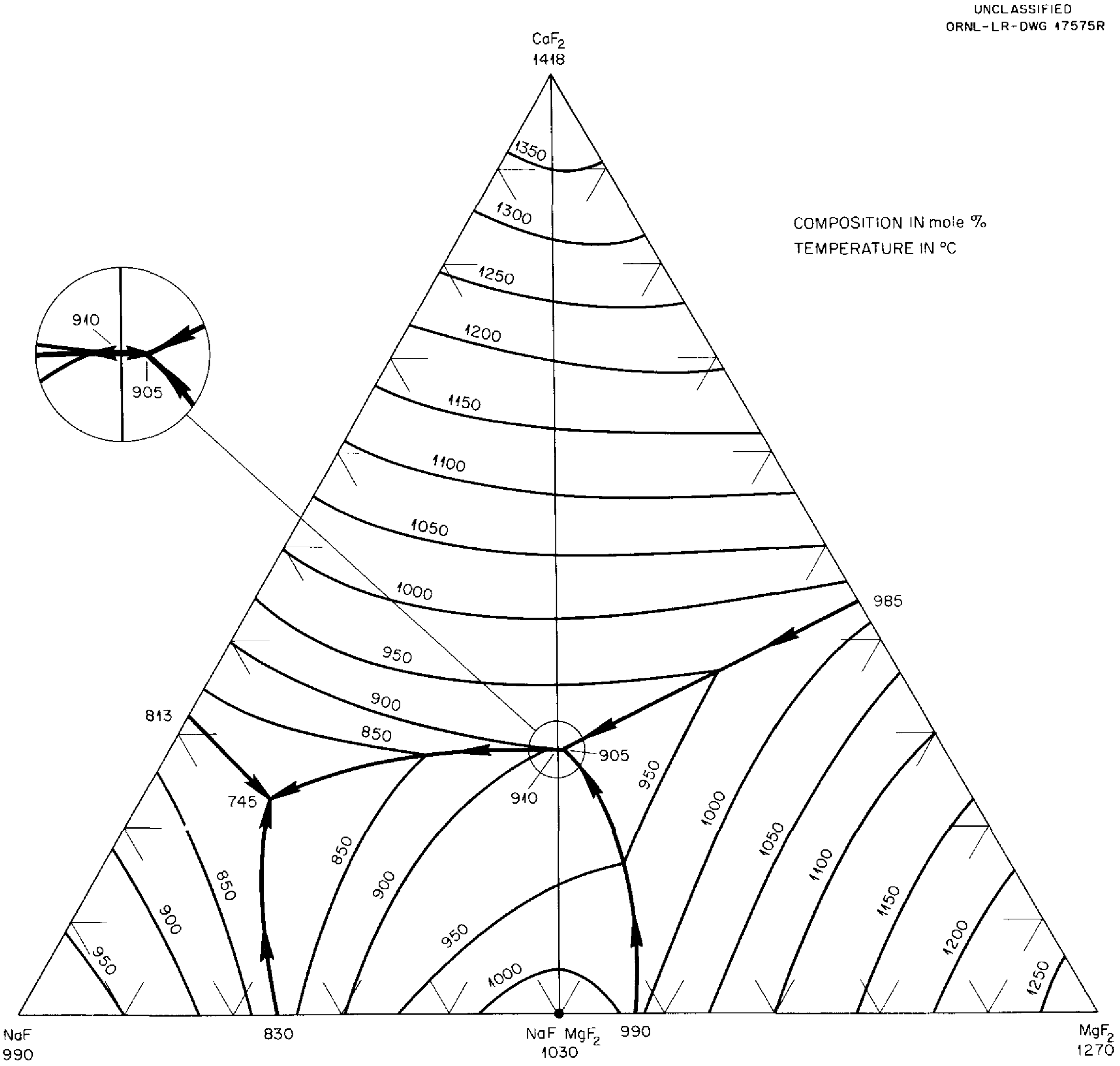

Fig. 3.17*a*. The System $NaF–MgF_2–CaF_2$.

The minimum temperature along the quasi-binary section NaF·MgF_2–CaF_2 occurs at the composition 36 NaF–36 MgF_2–28 CaF_2 (mole %), at 910°C.

The existence of the compound NaF·MgF_2 was previously reported by A. G. Bergman and E. P. Dergunov, *Compt. rend. acad. sci. U.R.S.S.* **31,** 755 (1941).

Ternary systems of alkali fluorides with MgF_2 have been reported by Bergman *et al.* as follows: the system LiF–NaF–MgF_2 by A. G. Bergman and E. P. Dergunov, *Compt. rend. acad. sci. U.R.S.S.* **31,** 755 (1941); the system LiF–KF–MgF_2 by A. G. Bergman and S. P. Parlenko, *Compt. rend. acad. sci. U.R.S.S.* **31,** 818–19 (1941); the system NaF–KF–MgF_2 by A. G. Bergman and E. P. Dergunov, *Compt. rend. acad. sci. U.R.S.S.* **48,** 330 (1945).

UNCLASSIFIED
ORNL–LR–DWG 12780

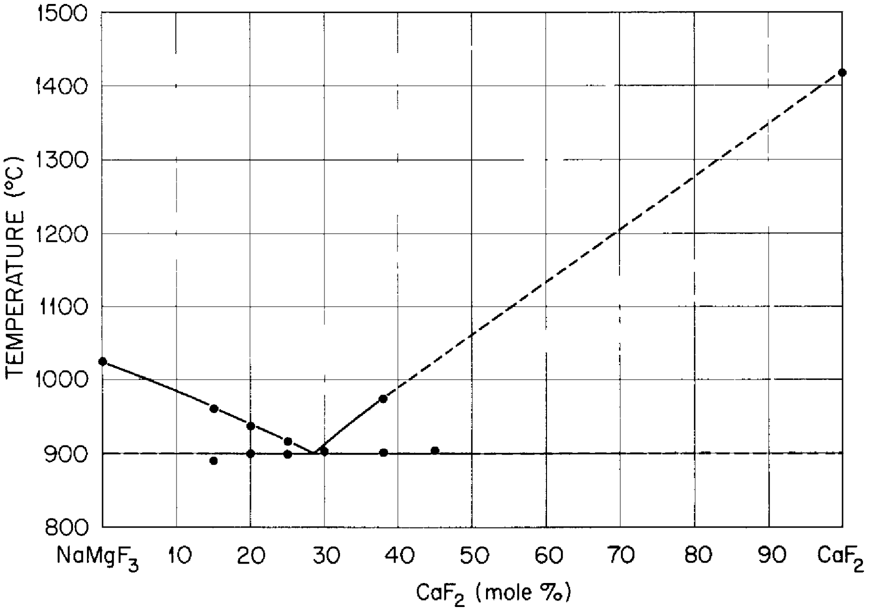

Fig. 3.17*b*. The Subsystem NaF·MgF_2–CaF_2.

3.18. The System $NaF-KF-AlF_3$

C. J. Barton, L. M. Bratcher, and W. R. Grimes, unpublished work performed at the Oak Ridge National Laboratory, 1951–52.

Preliminary diagram. No study has been made at the Oak Ridge National Laboratory of the phase relationships occurring within the system $NaF-KF-AlF_3$. Phase diagrams have been reported for the AlF_3 binary systems, $NaF-AlF_3$ [P. P. Fediotieff and W. P. Iljinsky, *Z. anorg. Chem.* **80,** 121 (1913); also N. A. Pushin and A. V. Baskow, *ibid.* **81,** 350 (1913)] and $KF-AlF_3$ [P. P. Fediotieff and K. Timofeef, *Z. anorg. u. allgem. Chem.* **206,** 265 (1932)].

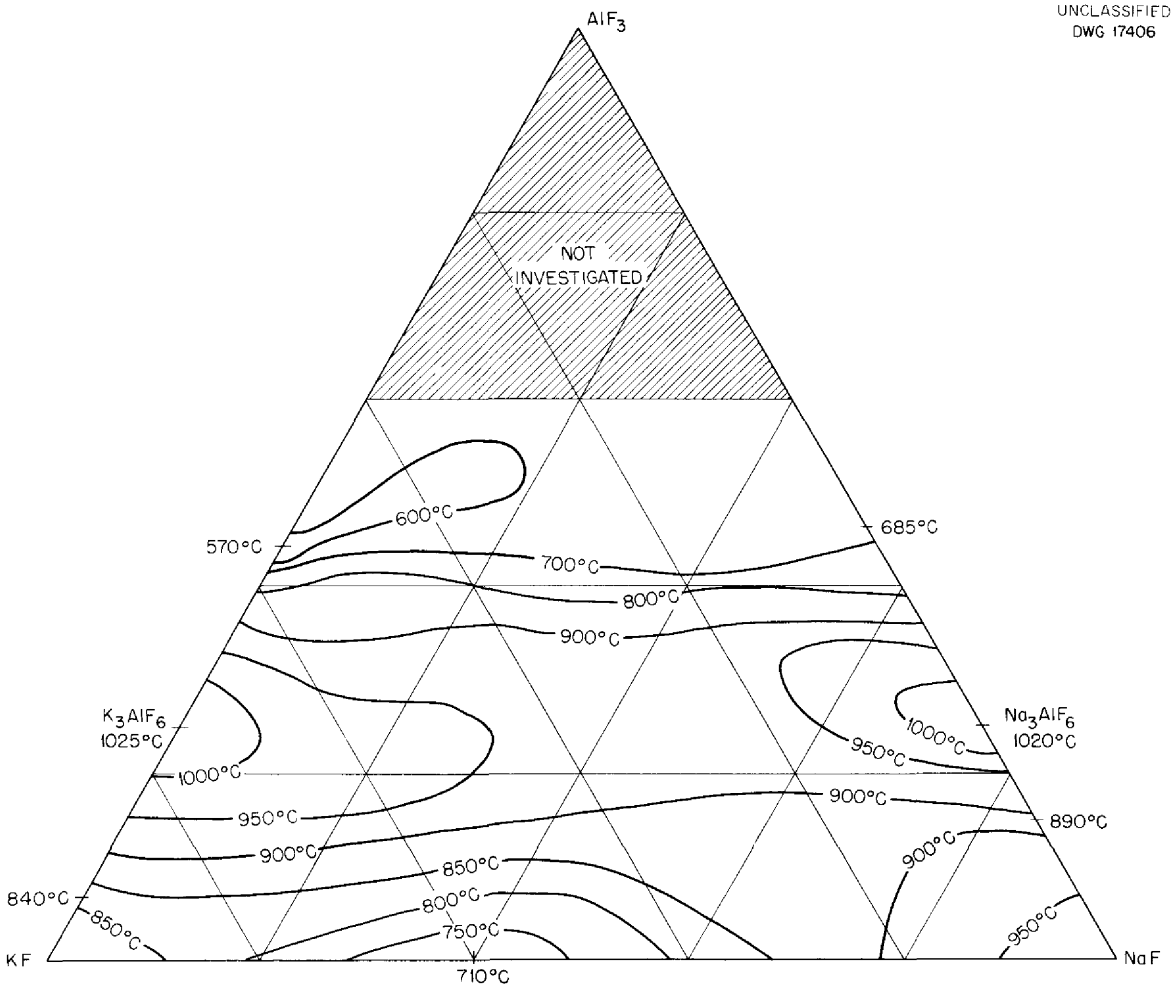

Fig. 3.18. The System $NaF-KF-AlF_3$.

3.19. The System LiF–BeF_2

This phase diagram is a composite from several published sources[1–3] and from unpublished data derived at the Oak Ridge National Laboratory (R. E. Moore, C. J. Barton, R. E. Thoma, and T. N. McVay) and at the Mound Laboratory (J. F. Eichelberger, C. R. Hudgens, L. V. Jones, and T. B. Rhinehammer). Thermal gradient quenching data (ORNL) and differential thermal analysis data (Mound Laboratory) have served to corroborate this composite diagram.

Invariant Equilibria

Mole % BeF_2 in Liquid	Invariant Temperature (°C)	Type of Equilibrium	Phase Reaction at Invariant Temperature
33.5*	454	Peritectic	$L + LiF \rightleftharpoons 2LiF{\cdot}BeF_2$
52	355	Eutectic	$L \rightleftharpoons 2LiF{\cdot}BeF_2 + BeF_2$
–	280	Upper temperature of stability for $LiF{\cdot}BeF_2$	$2LiF{\cdot}BeF_2 + BeF_2 \rightleftharpoons LiF{\cdot}BeF_2$

*Ref 3.

Roy, Roy, and Osborn have reported the presence of the compound $LiF{\cdot}2BeF_2$ in the system LiF–BeF_2 although neither the Mound Laboratory nor the ORNL data have indicated the existence of this compound.

---

[1] D. M. Roy, R. Roy, and E. F. Osborn, *J. Am. Ceram. Soc.* **37**, 300 (1954).

[2] A. V. Novoselova, Yu. P. Simanov, and E. I. Yarembash, *J. Phys. Chem. (U.S.S.R.)* **26**, 1244 (1952).

[3] John L. Speirs, *The Binary and Ternary Systems Formed by Calcium Fluoride, Lithium Fluoride, and Beryllium Fluoride: Phase Diagrams and Electrolytic Studies*, Ph.D. thesis, University of Michigan, May 29, 1952.

UNCLASSIFIED
ORNL-LR-DWG 16426R

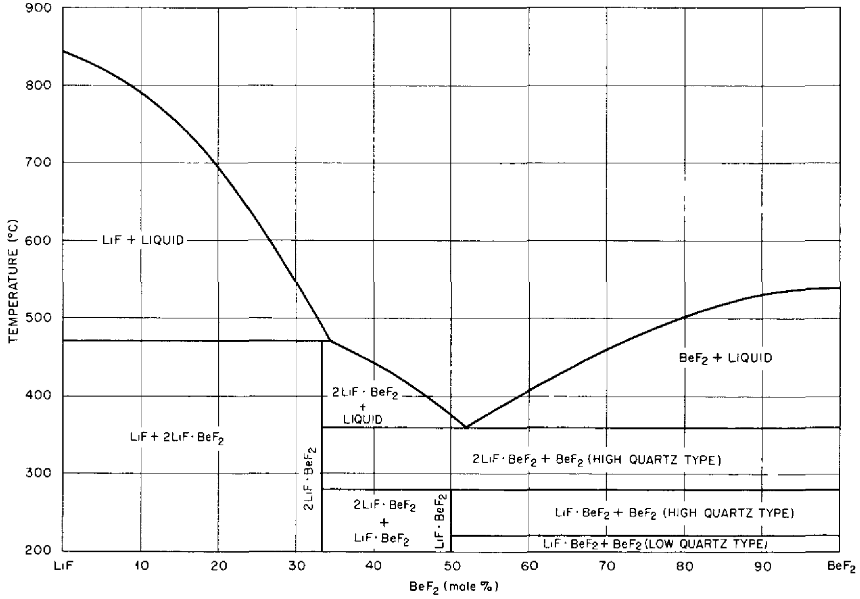

Fig. 3.19. The System LiF–BeF_2.

3.20. The System NaF–BeF_2

D. M. Roy, R. Roy, and E. F. Osborn, "Fluoride Model Systems: III. The System NaF–BeF_2 and the Polymorphism of Na_2BeF_4 and BeF_2," *J. Am. Ceram. Soc.* **36,** 185 (1953).

Invariant Equilibria*

Mole % BeF_2 in Liquid	Invariant Temperature (°C)	Type of Equilibrium	Phase Reaction at Invariant Temperature
31	570	Eutectic	$L \rightleftharpoons \text{NaF} + \alpha\text{-}2\text{NaF}\cdot\text{BeF}_2$
33.3	600	Congruent melting point	$L \rightleftharpoons \alpha\text{-}2\text{NaF}\cdot\text{BeF}_2$
–	320	Inversion	$\alpha\text{-}2\text{NaF}\cdot\text{BeF}_2 \rightleftharpoons \alpha'\text{-}2\text{NaF}\cdot\text{BeF}_2$
–	225	Inversion	$\alpha'\text{-}2\text{NaF}\cdot\text{BeF}_2 \rightleftharpoons \gamma\text{-}2\text{NaF}\cdot\text{BeF}_2$
43	340	Eutectic	$L \rightleftharpoons \alpha\text{-}2\text{NaF}\cdot\text{BeF}_2 + \beta\text{-NaF}\cdot\text{BeF}_2$
50	376 ± 5	Congruent melting point	$L \rightleftharpoons \beta'\text{-NaF}\cdot\text{BeF}_2$
55	365	Eutectic	$L \rightleftharpoons \beta'\text{-NaF}\cdot\text{BeF}_2 + \text{BeF}_2$

*Roy, Roy, and Osborn did not list invariant equilibria; those shown are estimates made from the reportec work and from experiments performed at the Oak Ridge National Laboratory.

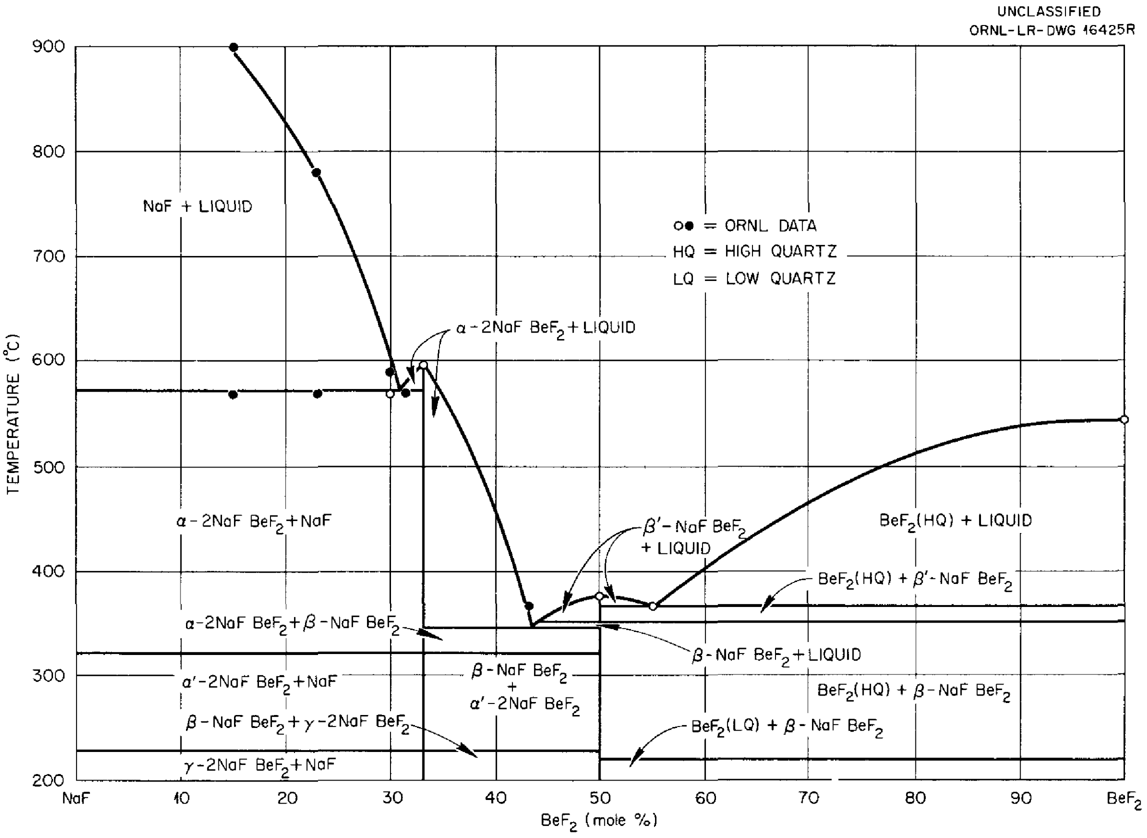

Fig. 3.20. The System NaF–BeF_2.

3.21. The System $KF-BeF_2$

R. E. Moore, C. J. Barton, L. M. Bratcher, T. N. McVay, G. D. White, R. J. Sheil, W. R. Grimes, R. E. Meadows, and L. A. Harris, unpublished work performed at the Oak Ridge National Laboratory, 1955–56.

Preliminary diagram.

Invariant Equilibria

Mole % BeF_2 In Liquid	Invariant Temperature (°C)	Type of Equilibrium	Phase Reaction at Invariant Temperature
19	720	Eutectic	$L \rightleftharpoons KF + 3KF \cdot BeF_2$
25	740	Congruent melting point	$L \rightleftharpoons 3KF \cdot BeF_2$
27	730	Eutectic	$L \rightleftharpoons 3KF \cdot BeF_2 + \alpha\text{-}2KF \cdot BeF_2$
33.3	787	Congruent melting point	$L \rightleftharpoons \alpha\text{-}2KF \cdot BeF_2$
–	685	Inversion	$\alpha\text{-}2KF \cdot BeF_2 \rightleftharpoons \beta\text{-}2KF \cdot BeF_2$
52	390	Peritectic	$\beta\text{-}2KF \cdot BeF_2 + L \rightleftharpoons KF \cdot BeF_2$
59	330	Eutectic	$L \rightleftharpoons KF \cdot BeF_2 + \beta\text{-}KF \cdot 2BeF_2$
66.7	358	Congruent melting point	$L \rightleftharpoons \alpha\text{-}KF \cdot 2BeF_2$
–	334	Inversion	$\alpha\text{-}KF \cdot 2BeF_2 \rightleftharpoons \beta\text{-}KF \cdot 2BeF_2$
72.5	323	Eutectic	$L \rightleftharpoons \beta\text{-}KF \cdot 2BeF_2 + BeF_2$

This system has been reported by M. P. Borzenkova, A. V. Novoselova, Yu. P. Simanov, V. I. Chernikh, and E. I. Yarembash, "Thermal and X-Ray Analysis of the $KF-BeF_2$ System," *Zhur. Neorg. Khim.* **1**, 2071–82 (1956).

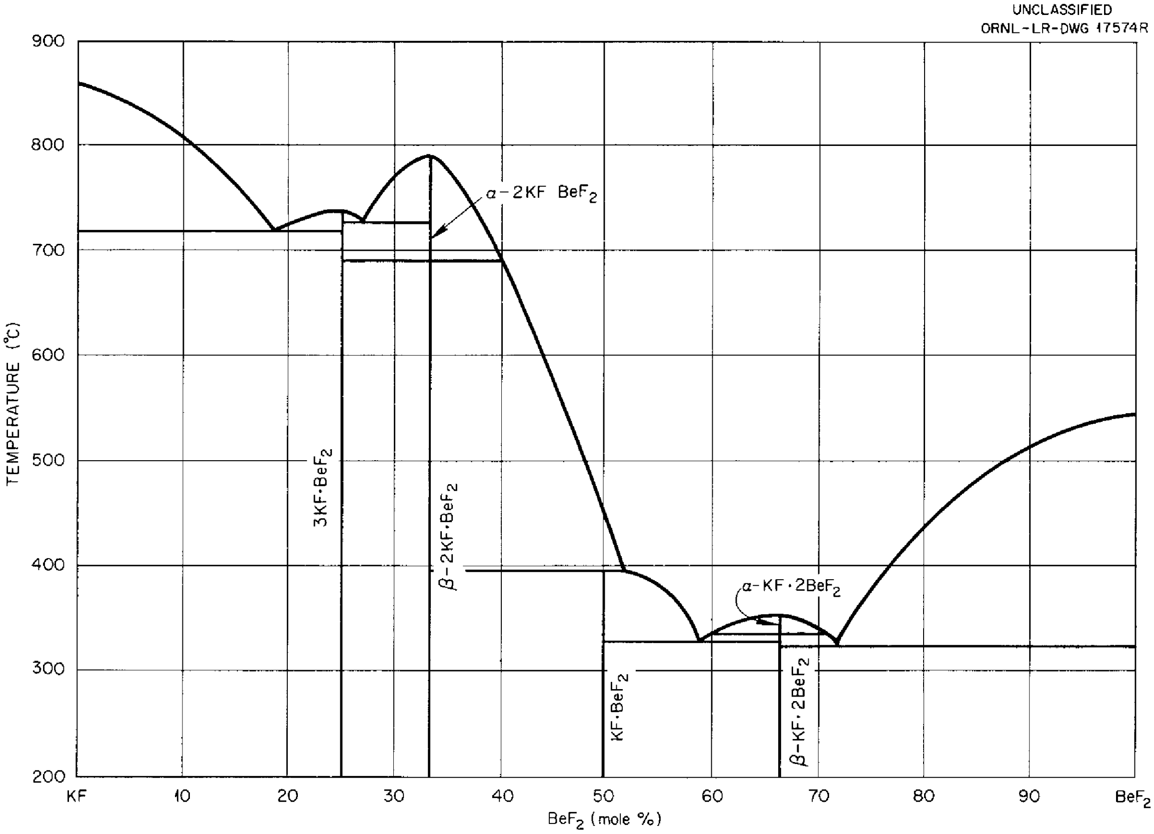

Fig. 3.21. The System KF–BeF_2.

3.22. The System $RbF-BeF_2$

R. E. Moore, C. J. Barton, L. M. Bratcher, T. N. McVay, G. D. White, R. J. Sheil, W. R. Grimes, and R. E. Meadows, unpublished work performed at the Oak Ridge National Laboratory, 1955–56.

Preliminary diagram.

Invariant Equilibria

Mole % BeF_2 in Liquid	Invariant Temperature (°C)	Type of Equilibrium	Phase Reaction at Invariant Temperature
16	675	Eutectic	$L \rightleftharpoons RbF + 3RbF \cdot BeF_2$
25	725	Congruent melting point	$L \rightleftharpoons 3RbF \cdot BeF_2$
27	720	Eutectic	$L \rightleftharpoons 3RbF \cdot BeF_2 + 2RbF \cdot BeF_2$
33.3	800	Congruent melting point	$L \rightleftharpoons 2RbF \cdot BeF_2$
50.5	442	Peritectic	$L + 2RbF \cdot BeF_2 \rightleftharpoons RbF \cdot BeF_2$
61	383	Eutectic	$L \rightleftharpoons RbF \cdot BeF_2 + RbF \cdot 2BeF_2$
66.7	464	Congruent melting point	$L \rightleftharpoons RbF \cdot 2BeF_2$
81	397	Eutectic	$L \rightleftharpoons RbF \cdot 2BeF_2 + BeF_2$

This system has also been reported by R. G. Grebenshchikov, "Investigation of the Phase Diagram of the $RbF-BeF_2$ System and of Its Relationship to the $BaO-SiO_2$ System," *Doklady Akad. Nauk S.S.S.R.* **114,** 316 (1957).

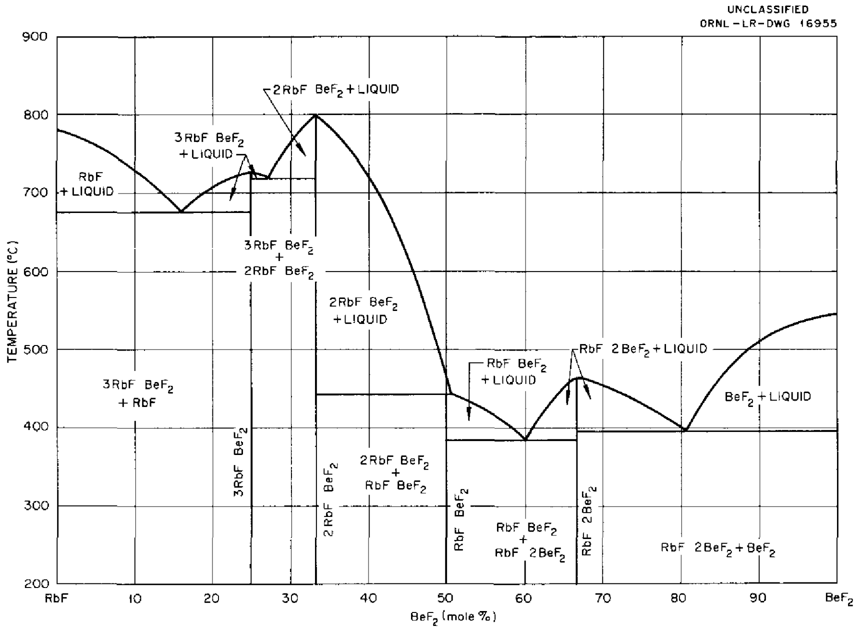

Fig. 3.22. The System RbF–BeF_2.

3.23. The System CsF–BeF$_2$

O. N. Breusov, A. V. Novoselova, and Yu. P. Simanov, "Thermal and X-Ray Phase Analysis of the System CsF–BeF$_2$ and Its Interrelationships with MeF and BeF$_2$ Systems," *Doklady Akad. Nauk S.S.S.R.* **118,** 935–37 (1958).

Invariant Equilibria

Mole % BeF$_2$ in Liquid	Invariant Temperature (°C)	Type of Equilibrium	Phase Reaction at Invariant Temperature
14	598	Eutectic	$L \rightleftharpoons \mathrm{CsF} + \beta\text{-}3\mathrm{CsF}\cdot\mathrm{BeF_2}$
23.5	659	Peritectic	$\alpha\text{-}2\mathrm{CsF}\cdot\mathrm{BeF_2} + L \rightleftharpoons \alpha\text{-}3\mathrm{CsF}\cdot\mathrm{BeF_2}$
–	617	Inversion	$\alpha\text{-}3\mathrm{CsF}\cdot\mathrm{BeF_2} \rightleftharpoons \beta\text{-}3\mathrm{CsF}\cdot\mathrm{BeF_2}$
33.3	793	Congruent melting point	$L \rightleftharpoons \alpha\text{-}2\mathrm{CsF}\cdot\mathrm{BeF_2}$
–	404	Inversion	$\alpha\text{-}2\mathrm{CsF}\cdot\mathrm{BeF_2} \rightleftharpoons \beta\text{-}2\mathrm{CsF}\cdot\mathrm{BeF_2}$
48	449	Eutectic	$L \rightleftharpoons \alpha\text{-}2\mathrm{CsF}\cdot\mathrm{BeF_2} + \alpha\text{-}\mathrm{CsF}\cdot\mathrm{BeF_2}$
50	475	Congruent melting point	$L \rightleftharpoons \alpha\text{-}\mathrm{CsF}\cdot\mathrm{BeF_2}$
–	360	Inversion	$\alpha\text{-}\mathrm{CsF}\cdot\mathrm{BeF_2} \rightleftharpoons \beta\text{-}\mathrm{CsF}\cdot\mathrm{BeF_2}$
–	140	Inversion	$\beta\text{-}\mathrm{CsF}\cdot\mathrm{BeF_2} \rightleftharpoons \gamma\text{-}\mathrm{CsF}\cdot\mathrm{BeF_2}$
58.4	393	Eutectic	$L \rightleftharpoons \alpha\text{-}\mathrm{CsF}\cdot\mathrm{BeF_2} + \beta\text{-}\mathrm{CsF}\cdot2\mathrm{BeF_2}$
66.7	480	Congruent melting point	$L \rightleftharpoons \alpha\text{-}\mathrm{CsF}\cdot2\mathrm{BeF_2}$
–	450	Inversion	$\alpha\text{-}\mathrm{CsF}\cdot2\mathrm{BeF_2} \rightleftharpoons \beta\text{-}\mathrm{CsF}\cdot2\mathrm{BeF_2}$
77.5	367	Eutectic	$L \rightleftharpoons \beta\text{-}\mathrm{CsF}\cdot2\mathrm{BeF_2} + \mathrm{BeF_2}$

UNCLASSIFIED
ORNL-LR-DWG 3548

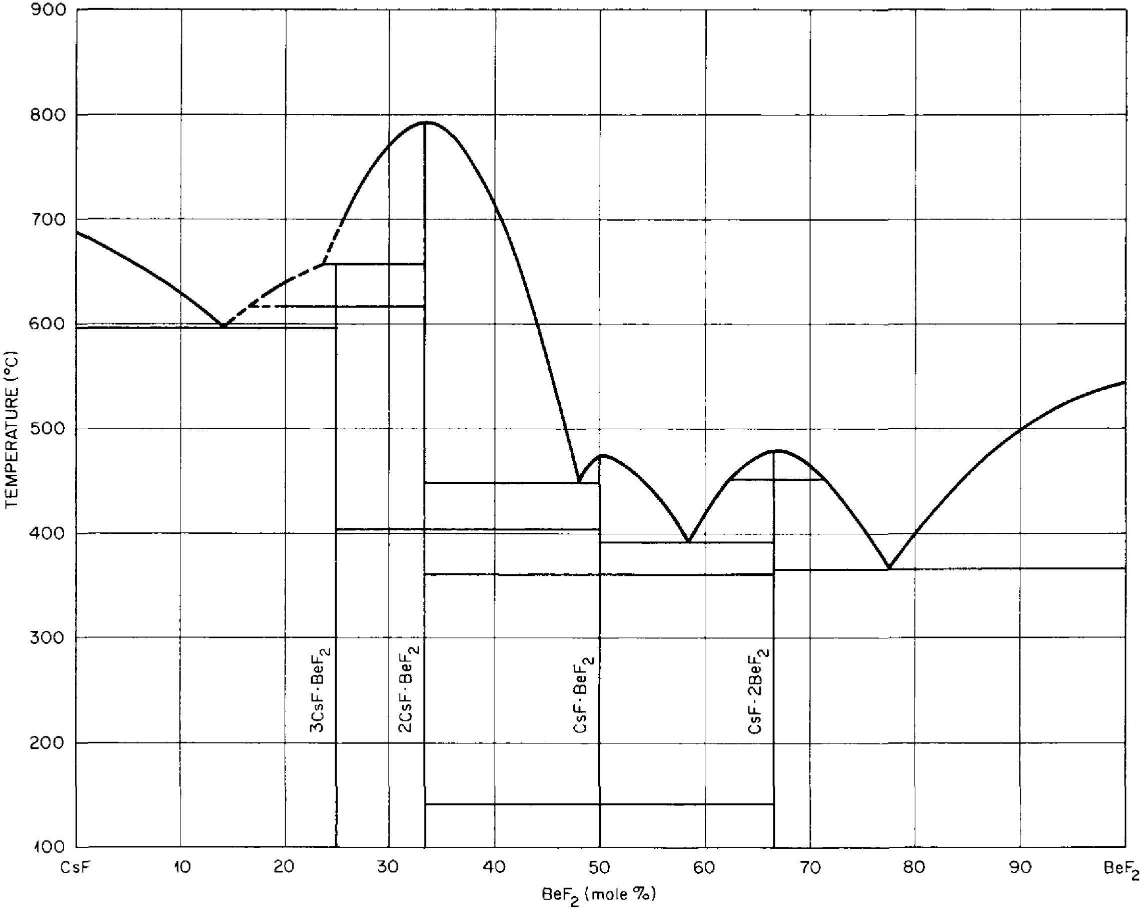

Fig. 3.23. The System CsF–BeF_2.

3.24. The System $LiF-NaF-BeF_2$

R. E. Moore, C. J. Barton, W. R. Grimes, R. E. Meadows, L. M. Bratcher, G. D. White, T. N. McVay, and L. A. Harris, unpublished work performed at the Oak Ridge National Laboratory, 1951–58.

Preliminary diagram.

Invariant Equilibria*

Composition of Liquid (mole %)			Invariant Temperature (°C)	Type of Equilibrium	Solids Present at Invariant Point
LiF	NaF	BeF_2			
15	58	27	480	Eutectic	NaF, LiF, and $2NaF \cdot BeF_2$
23	41	36	328	Eutectic	LiF, $2NaF \cdot BeF_2$, and $2NaF \cdot LiF \cdot 2BeF_2$
20	40	40	355	Congruent melting point	$2NaF \cdot LiF \cdot 2BeF_2$
5	53	42	318	Eutectic	$NaF \cdot BeF_2$, $2NaF \cdot BeF_2$, and $2NaF \cdot LiF \cdot 2BeF_2$
31.5	31	37.5	315	Eutectic	$2LiF \cdot BeF_2$, LiF, and $2NaF \cdot LiF \cdot 2BeF_2$

*Invariant equilibria shown in the phase diagram by the intersections of dotted-line boundary curves have not been determined with sufficient precision to be listed in the table.

Minimum Temperature on Alkemade Lines

Composition of Liquid (mole %)			Temperature (°C)	Alkemade Line
LiF	NaF	BeF_2		
16	56	28	485	$2NaF \cdot BeF_2-LiF$
26	37	37	340	$2NaF \cdot LiF \cdot 2BeF_2-LiF$
11	44	45	332	$NaF \cdot BeF_2-2NaF \cdot LiF \cdot 2BeF_2$
16	45	39	343	$2NaF \cdot BeF_2-2NaF \cdot LiF \cdot 2BeF_2$
30.5	31	38.5	316	$2LiF \cdot BeF_2-2NaF \cdot LiF \cdot 2BeF_2$

Phase relationships of two of the ternary compounds in this system have been reported by W. Jahn ["Silicate Models. V. $NaLi(BeF_4)$, a Model Substance for Monticellite, $CaMg(SiO_4)$;" *Z. anorg. u. allgem. Chem.* **276,** 113–27 (1954); "Silicate Models. VI. $Na_3Li(BeF_4)_2$, a New Compound in the Ternary System $NaF-LiF-BeF_2$, and Its Relation to Merwinite, $Ca_3Mg(SiO_4)_2$," *Z. anorg. u. allgem. Chem.* **277,** 274–86 (1954)].

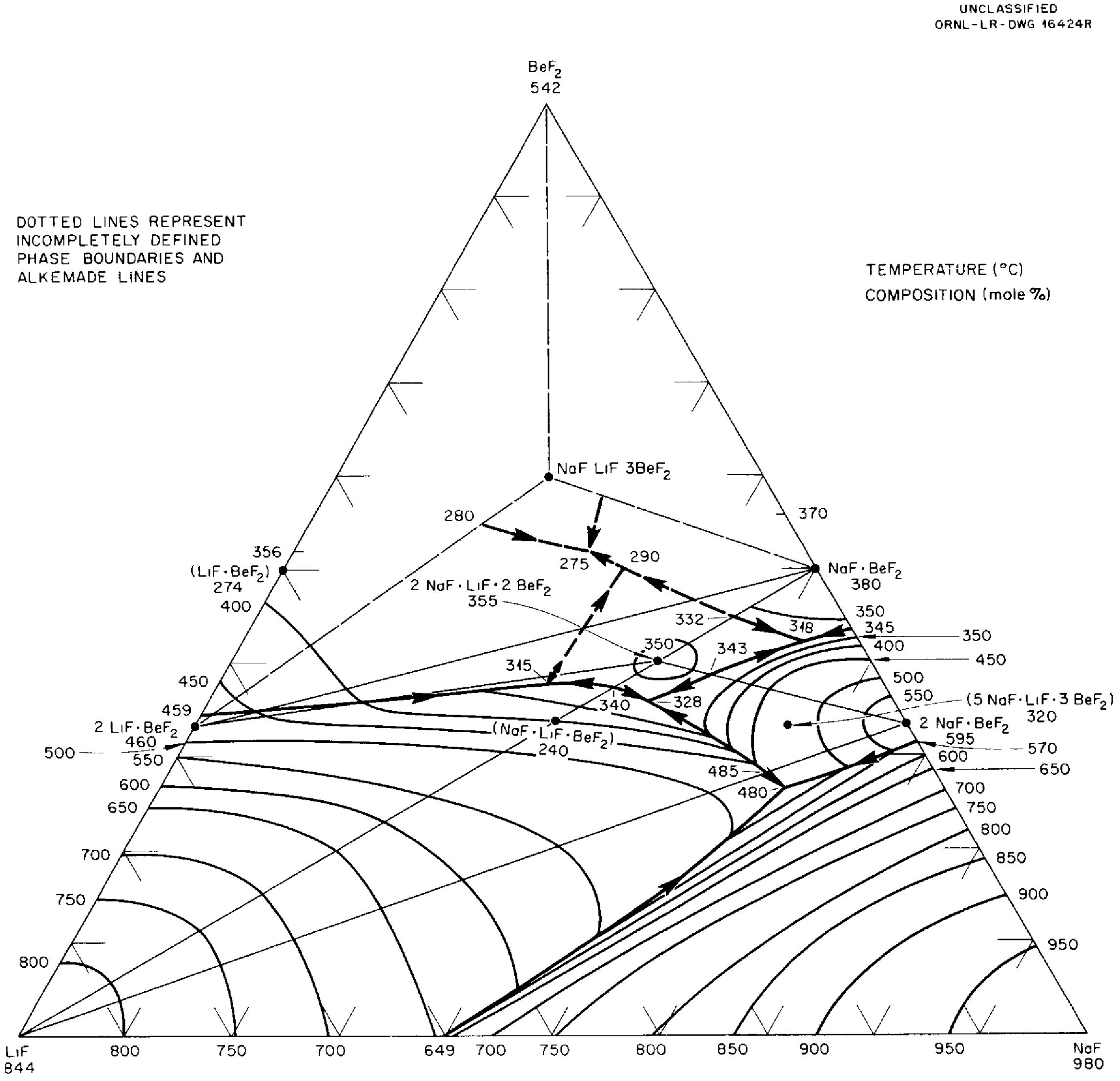

Fig. 3.24. The System LiF–NaF–BeF_2.

3.25. The System LiF–RbF–BeF_2

T. B. Rhinehammer, D. E. Etter, C. R. Hudgens, N. E. Rogers, and P. A. Tucker, unpublished work performed at the Mound Laboratory.

Preliminary diagram.

Invariant Equilibria and Singular Points

Composition of Liquid (mole %)			Temperature (°C)	Type of Equilibrium	Solid Phases Present
LiF	RbF	BeF_2			
40.0	20.0	40.0	485 ± 5	Congruent melting point	$2LiF \cdot RbF \cdot 2BeF_2$
33.3	33.3	33.3	544 ± 5	Incongruent melting point of $LiF \cdot RbF \cdot BeF_2$	
33.0	8.0	59.0	295 ± 5	Eutectic	$2LiF \cdot BeF_2$, $2LiF \cdot RbF \cdot 2BeF_2$, and BeF_2
26.0	12.0	62.0	305–320	Peritectic	$2LiF \cdot RbF \cdot 2BeF_2$, $RbF \cdot 2BeF_2$, and BeF_2
12.0	29.0	59.0	334 ± 5	Quasi-binary eutectic	$2LiF \cdot RbF \cdot 2BeF_2$ and $RbF \cdot 2BeF_2$
11.0	34.0	55.0	300 ± 5	Eutectic	$2LiF \cdot RbF \cdot 2BeF_2$, $RbF \cdot BeF_2$, and $RbF \cdot 2BeF_2$
11.5	35.5	53.0	335 ± 5	Peritectic	$2LiF \cdot RbF \cdot 2BeF_2$, $LiF \cdot RbF \cdot BeF_2$, and $RbF \cdot BeF_2$
9.0	40.0	51.0	380 ± 5	Peritectic	$LiF \cdot RbF \cdot BeF_2$, $2RbF \cdot BeF_2$, and $RbF \cdot BeF_2$
50.0	8.0	42.0	426 ± 5	Peritectic	LiF, $2LiF \cdot RbF \cdot 2BeF_2$, and $2LiF \cdot BeF_2$
41.5	19.5	39.0	473 ± 5	Quasi-binary eutectic	LiF and $2LiF \cdot RbF \cdot 2BeF_2$
35.0	25.5	39.5	470 ± 5	Peritectic	LiF, $2LiF \cdot RbF \cdot 2BeF_2$, and $LiF \cdot RbF \cdot BeF_2$
23.0	40.0	37.0	530 ± 5	Peritectic	LiF, $2RbF \cdot BeF_2$, and $LiF \cdot RbF \cdot BeF_2$
30.0	35.0	35.0	544 ± 5	Maximum on the boundary	LiF and $LiF \cdot RbF \cdot BeF_2$
41.0	39.5	19.5	640 ± 5	Quasi-binary eutectic	LiF and $2RbF \cdot BeF_2$
43.0	50.0	7.0	527 ± 5	Peritectic	LiF, $3RbF \cdot BeF_2$, and $2RbF \cdot BeF_2$
43.0	54.0	3.0	470 ± 5	Peritectic	LiF, $LiF \cdot RbF$, and $3RbF \cdot BeF_2$
43.0	55.0	2.0	462 ± 5	Eutectic	$LiF \cdot RbF$, RbF, and $3RbF \cdot BeF_2$

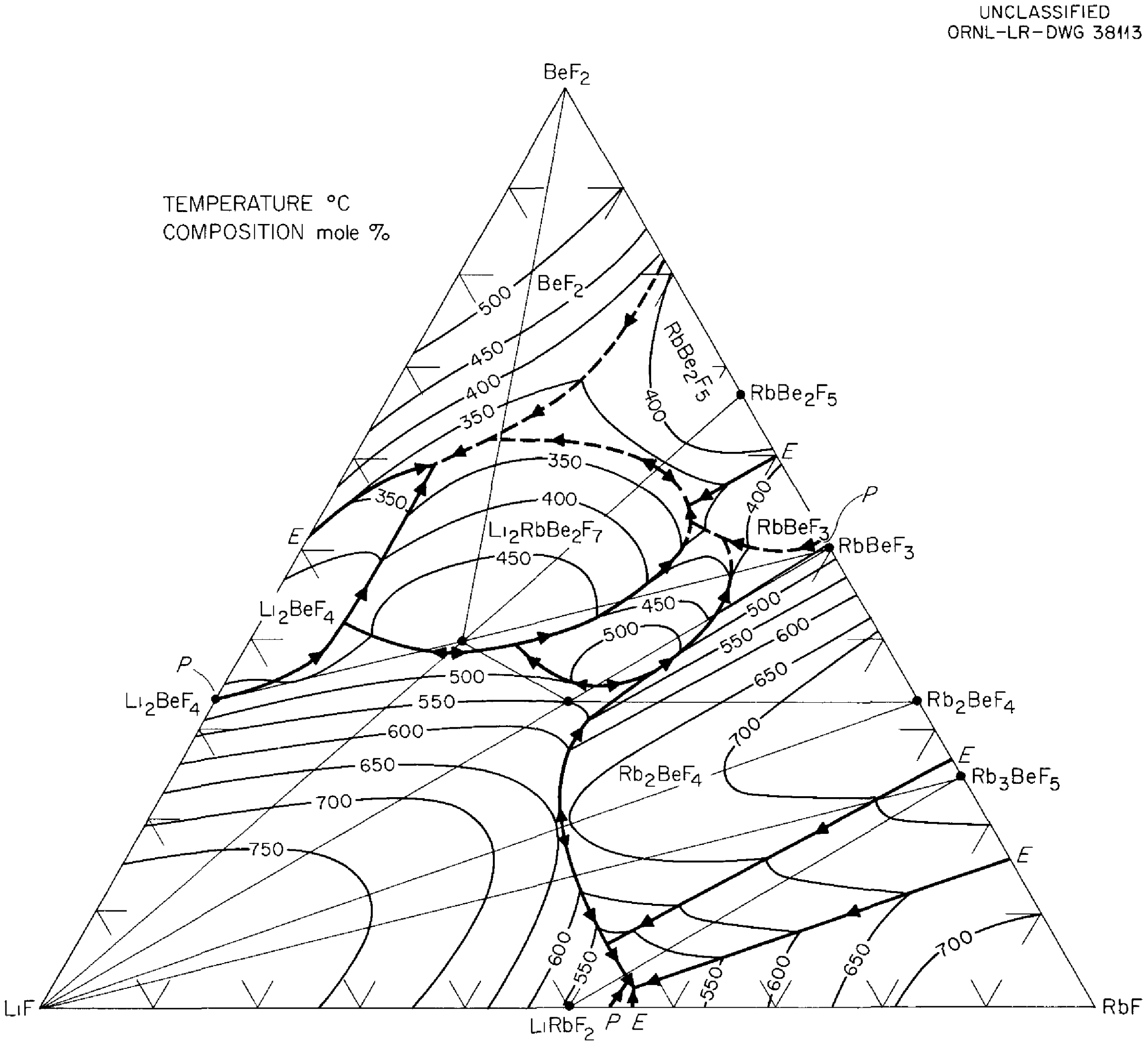

Fig. 3.25. The System LiF–RbF–BeF$_2$.

3.26. The System NaF–KF–BeF_2

R. E. Moore, C. J. Barton, L. M. Bratcher, T. N. McVay, and W. R. Grimes, unpublished work performed at the Oak Ridge National Laboratory, 1952–55.

Preliminary diagram. Phase relationships within the system NaF–KF–BeF_2 have not yet become so well defined at the Oak Ridge National Laboratory that the compositions and temperatures of the invariant points may be listed.

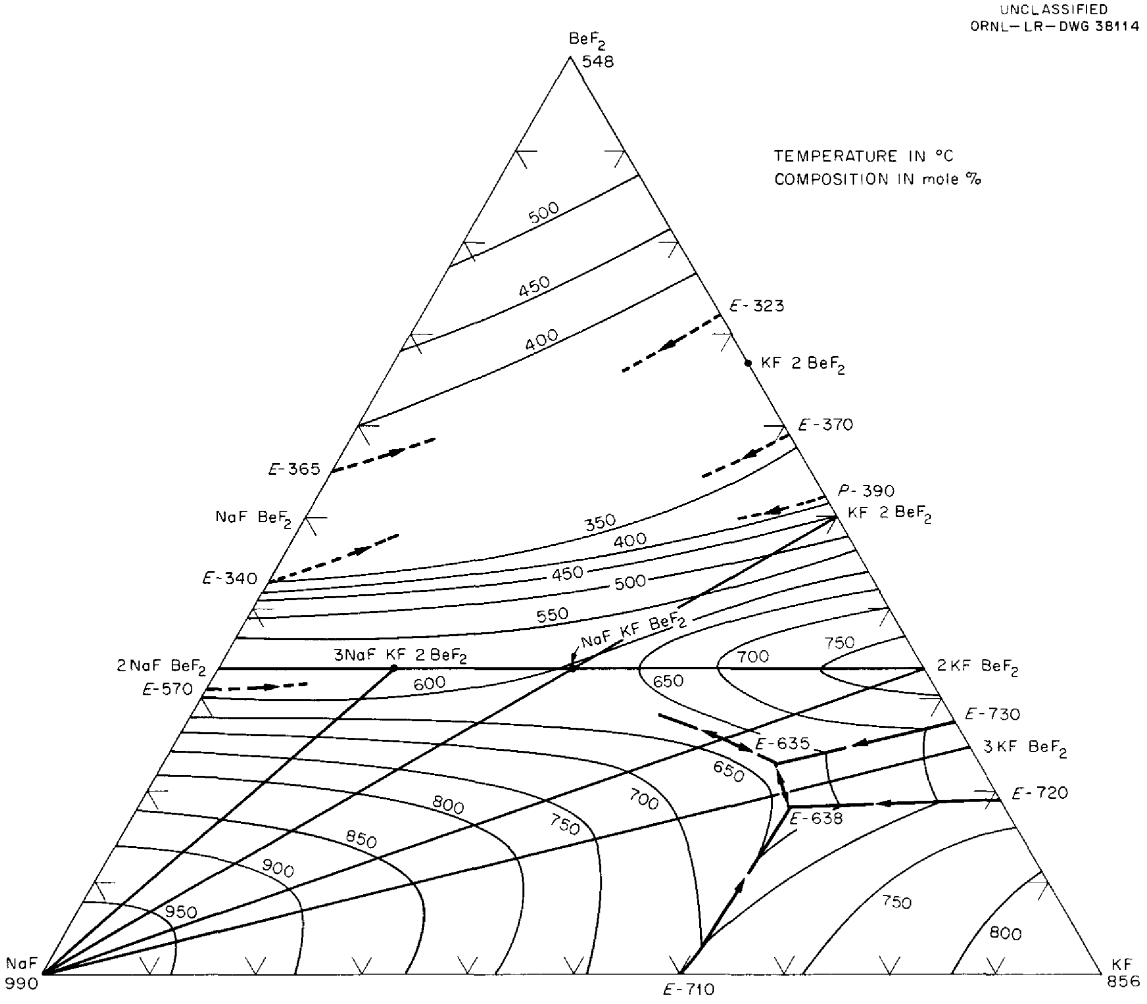

Fig. 3.26. The System NaF–KF–BeF_2.

3.27. The System NaF–RbF–BeF_2

R. E. Moore, C. J. Barton, L. M. Bratcher, and W. R. Grimes, unpublished work performed at the Oak Ridge National Laboratory, 1954–57.

Preliminary diagram.

Invariant Equilibria and Singular Points

Composition of Liquid (mole %)			Temperature (°C)	Type of Equilibrium	Solids Present at Invariant Temperature
NaF	RbF	BeF_2			
20.5	68.5	11.0	610	Eutectic	RbF, NaF, and $3RbF \cdot BeF_2$
50	37.5	12.5	640	Quasi-binary eutectic	$3RbF \cdot BeF_2$ and NaF
46	38	16	635	Eutectic	$3RbF \cdot BeF_2$, $2RbF \cdot BeF_2$, and NaF
45	37	18	650	Quasi-binary eutectic	$2RbF \cdot BeF_2$ and NaF
37	33	30	570	Peritectic	$2RbF \cdot BeF_2$, NaF, and $2NaF \cdot 4RbF \cdot 3BeF_2$
52	15	33	477	Eutectic	$2NaF \cdot 4RbF \cdot 3BeF_2$, NaF, and $2NaF \cdot BeF_2$
33	33.7	33.3	580	Peritectic	$2RbF \cdot BeF_2$ and $2NaF \cdot 4RbF \cdot 3BeF_2$
51.7	15	33.3	480	Quasi-binary eutectic	$2NaF \cdot 4RbF \cdot 3BeF_2$ and $2NaF \cdot BeF_2$

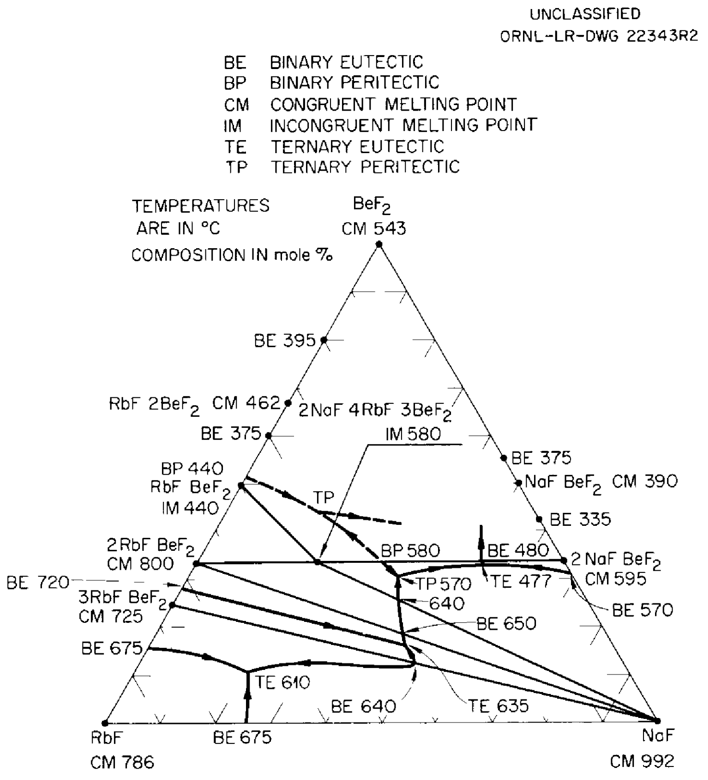

Fig. 3.27. The System NaF–RbF–BeF_2.

3.28. The System NaF–ZnF$_2$

C. J. Barton, L. M. Bratcher, and W. R. Grimes, unpublished work performed at the Oak Ridge National Laboratory, 1952.

Preliminary diagram.

Invariant Equilibria

Mole % ZnF$_2$ in Liquid	Invariant Temperature (°C)	Type of Equilibrium	Phase Reaction at Invariant Temperature
33	635	Eutectic	$L \rightleftharpoons$ NaF + NaF·ZnF$_2$
50	748 ± 10	Congruent melting point	$L \rightleftharpoons$ NaF·ZnF$_2$
69	685	Eutectic	$L \rightleftharpoons$ NaF·ZnF$_2$ + ZnF$_2$

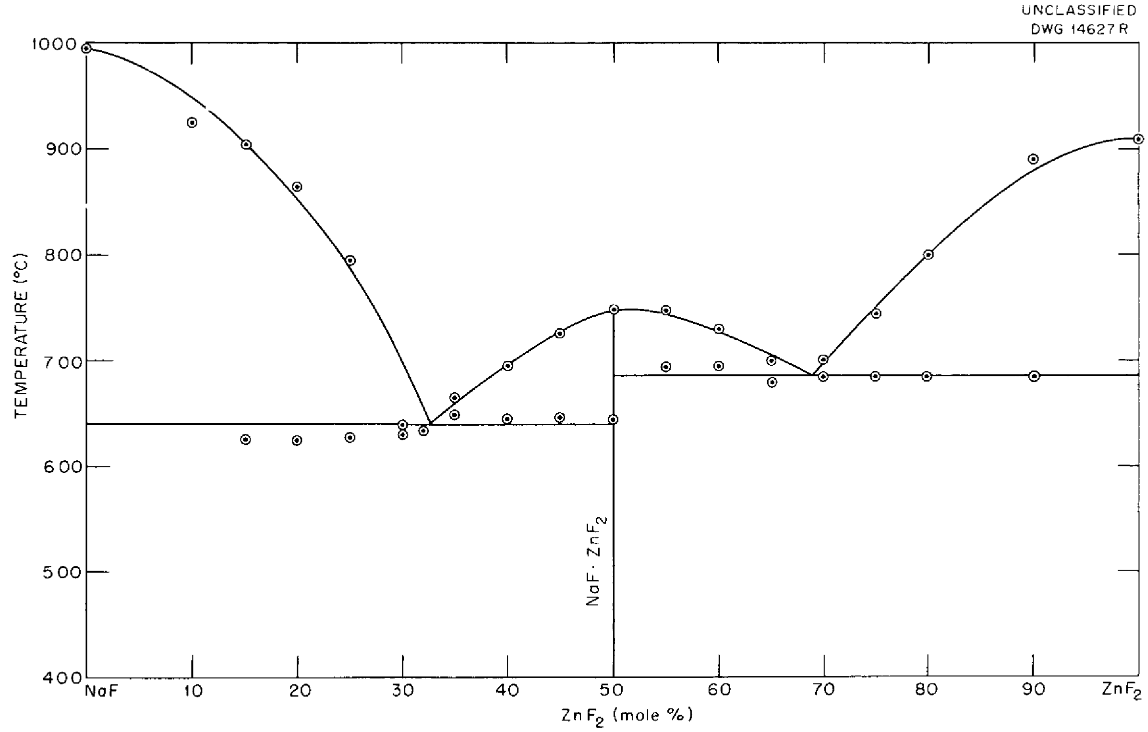

Fig. 3.28. The System NaF–ZnF$_2$.

3.29. The System $KF-ZnF_2$

C. J. Barton, L. M. Bratcher, and W. R. Grimes, unpublished work performed at the Oak Ridge National Laboratory, 1952.

Preliminary diagram.

Invariant Equilibria

Mole % ZnF_2 in Liquid	Invariant Temperature (°C)	Type of Equilibrium	Phase Reaction at Invariant Temperature
21	670	Eutectic	$L \rightleftharpoons KF + 2KF\cdot ZnF_2$
30	720 ± 10	Peritectic	$L + KF\cdot ZnF_2 \rightleftharpoons 2KF\cdot ZnF_2$
50	850 ± 10	Congruent melting point	$L \rightleftharpoons KF\cdot ZnF_2$
80	740 ± 5	Eutectic	$L \rightleftharpoons KF\cdot ZnF_2 + ZnF_2$

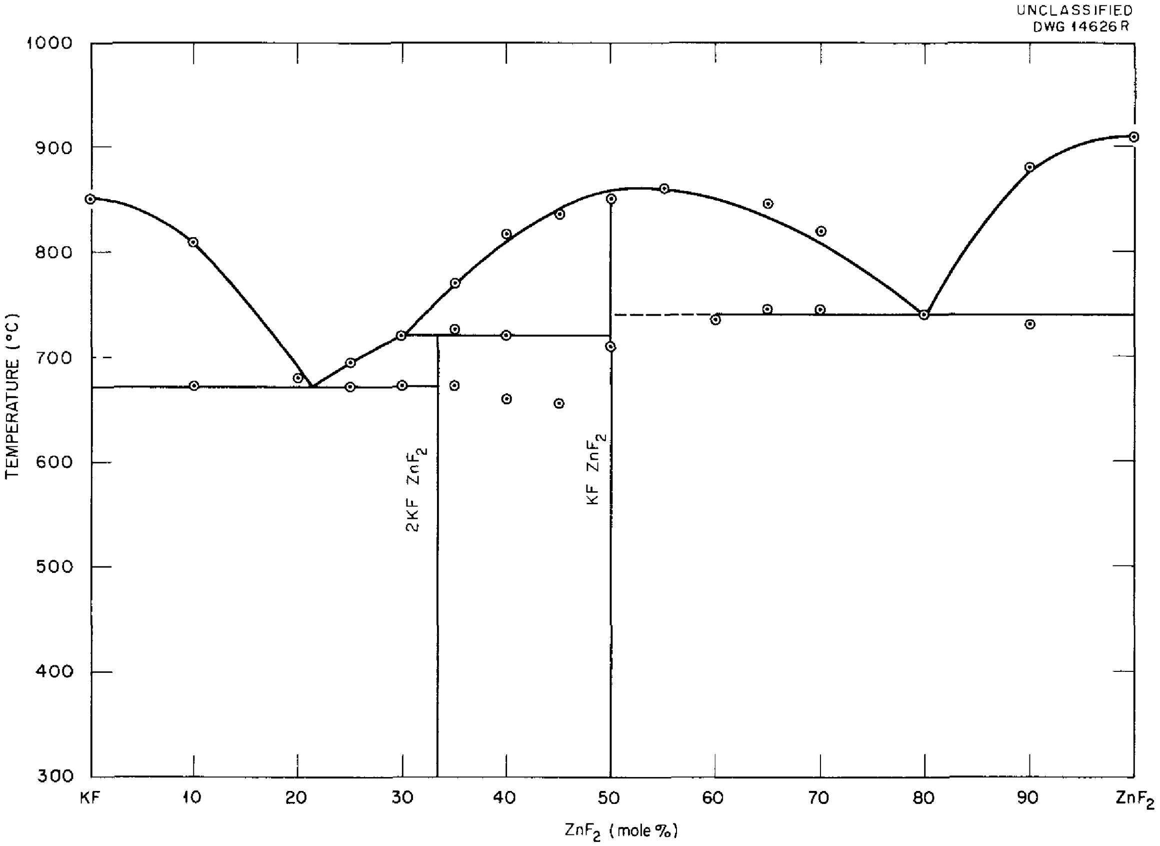

Fig. 3.29. The System $KF-ZnF_2$.

3.30. The System $RbF-ZnF_2$

C. J. Barton, L. M. Bratcher, and W. R. Grimes, unpublished work performed at the Oak Ridge National Laboratory, 1952.

Preliminary diagram.

Invariant Equilibria

Mole % ZnF_2 in Liquid	Invariant Temperature (°C)	Type of Equilibrium	Phase Reaction at Invariant Temperature
21	595 ± 10	Eutectic	$L \rightleftharpoons RbF + 2RbF\cdot ZnF_2$
32	620 ± 10	Peritectic	$L + RbF\cdot ZnF_2 \rightleftharpoons 2RbF\cdot ZnF_2$
50	730 ± 10	Congruent melting point	$L \rightleftharpoons RbF\cdot ZnF_2$
70	650	Eutectic	$L \rightleftharpoons RbF\cdot ZnF_2 + ZnF_2$

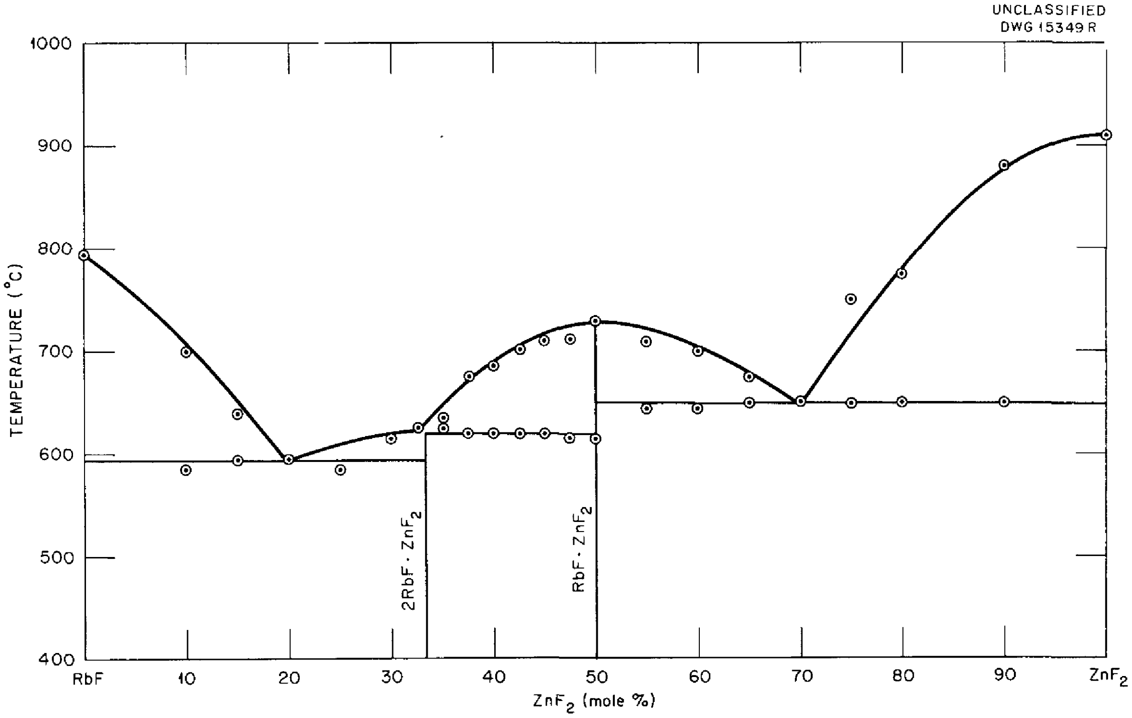

Fig. 3.30. The System $RbF-ZnF_2$.

3.31. The System LiF–YF_3

R. E. Thoma, C. F. Weaver, and H. A. Friedman, unpublished work performed at the Oak Ridge National Laboratory, 1958–59.

Preliminary diagram.

Invariant Equilibria

Mole % YF_3 in Liquid	Invariant Temperature (°C)	Type of Equilibrium	Phase Reaction at Invariant Temperature
19	695	Eutectic	$L \rightleftharpoons LiF + LiF \cdot YF_3$
49	815	Peritectic	$L + YF_3 \rightleftharpoons LiF \cdot YF_3$

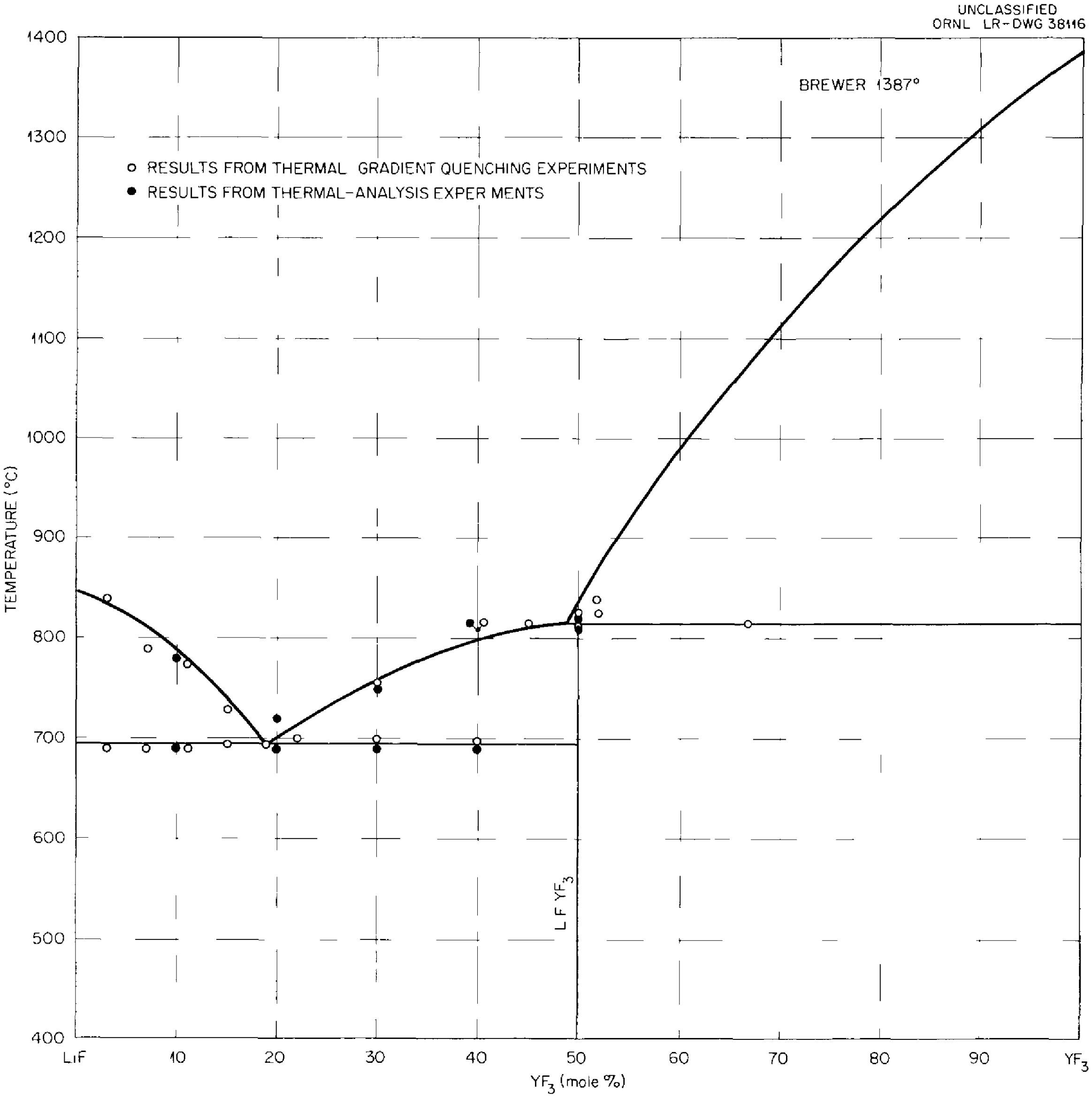

Fig. 3.31. The System LiF–YF_3.

3.32. The System $LiF-ZrF_4$

R. E. Moore, F. F. Blankenship, W. R. Grimes, H. A. Friedman, C. J. Barton, R. E. Thoma, and H. Insley, unpublished work performed at the Oak Ridge National Laboratory, 1951–56.

Preliminary diagram.

Invariant Equilibria

Mole % ZrF_4 in Liquid	Invariant Temperature (°C)	Type of Equilibrium	Phase Reaction at Invariant Temperature
21	598	Eutectic	$L \rightleftharpoons LiF + \alpha\text{-}3LiF\cdot ZrF_4$
25	662	Congruent melting point	$L \rightleftharpoons \alpha\text{-}3LiF\cdot ZrF_4$
–	475	Inversion	$\alpha\text{-}3LiF\cdot ZrF_4 \rightleftharpoons \beta\text{-}3LiF\cdot ZrF_4$
–	470	Decomposition	$\beta\text{-}3LiF\cdot ZrF_4 \rightleftharpoons LiF + 2LiF\cdot ZrF_4$
29.5	570	Eutectic	$L \rightleftharpoons \alpha\text{-}3LiF\cdot ZrF_4 + 2LiF\cdot ZrF_4$
33.3	596	Congruent melting point	$L \rightleftharpoons 2LiF\cdot ZrF_4$
49	507	Eutectic	$L \rightleftharpoons 2LiF\cdot ZrF_4 + 3LiF\cdot 4ZrF_4$
51.5	520	Peritectic	$L + ZrF_4 \rightleftharpoons 3LiF\cdot 4ZrF_4$
–	466	Decomposition	$3LiF\cdot 4ZrF_4 \rightleftharpoons 2LiF\cdot ZrF_4 + ZrF_4$

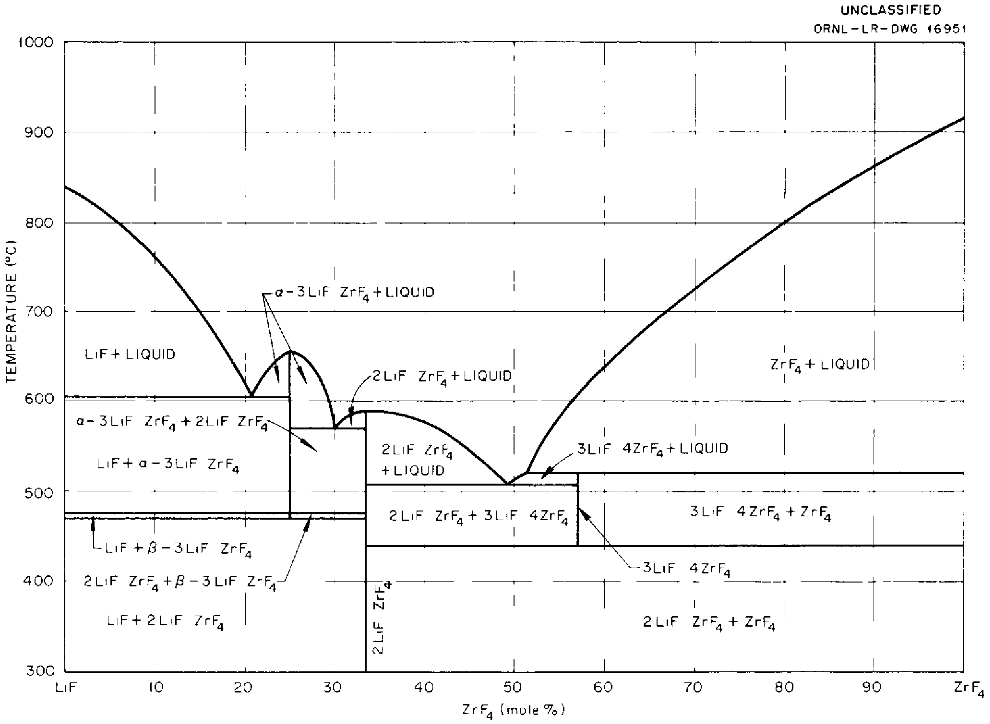

Fig. 3.32. The System LiF–ZrF_4.

3.33. The System NaF–ZrF$_4$

C. J. Barton, W. R. Grimes, H. Insley, R. E. Moore, and R. E. Thoma, "Phase Equilibria in the Systems NaF–ZrF$_4$, UF$_4$–ZrF$_4$, and NaF–ZrF$_4$–UF$_4$," *J. Phys. Chem.* **62**, 665–76 (1958).

Invariant Equilibria

Mole % ZrF$_4$ in Liquid	Invariant Temperature (°C)	Type of Equilibrium	Phase Reaction at Invariant Temperature
20	747	Eutectic	$L \rightleftharpoons NaF + 3NaF\cdot ZrF_4$
25	850	Congruent melting point	$L \rightleftharpoons 3NaF\cdot ZrF_4$*
–	523	Inversion	$\alpha\text{-}5NaF\cdot 2ZrF_4 \rightleftharpoons \beta\text{-}5NaF\cdot 2ZrF_4$
30.5	500	Eutectoid	$\alpha\text{-}5NaF\cdot 2ZrF_4\,ss \rightleftharpoons \beta\text{-}5NaF\cdot 2ZrF_4 + \gamma\text{-}2NaF\cdot ZrF_4$
34	640	Peritectic	$L + 3NaF\cdot ZrF_4$(*ss*, *ca.* 27.5 mole % ZrF$_4$) $\rightleftharpoons \alpha\text{-}5NaF\cdot 2ZrF_4$
39.5	544	Peritectic	$L + \alpha\text{-}5NaF\cdot 2ZrF_4$(*ss*, 30 mole % ZrF$_4$) $\rightleftharpoons \alpha\text{-}2NaF\cdot ZrF_4$
–	533	Inversion	$\alpha\text{-}2NaF\cdot ZrF_4 \rightleftharpoons \beta\text{-}2NaF\cdot ZrF_4$
–	505	Inversion	$\beta\text{-}2NaF\cdot ZrF_4 \rightleftharpoons \gamma\text{-}2NaF\cdot ZrF_4$
40.5	500	Eutectic	$L \rightleftharpoons \gamma\text{-}2NaF\cdot ZrF_4 + 7NaF\cdot 6ZrF_4\,ss$
46.2	525	Congruent melting point	$L \rightleftharpoons 7NaF\cdot 6ZrF_4$
49.5	512	Eutectic	$L \rightleftharpoons 7NaF\cdot 6ZrF_4 + 3NaF\cdot 4ZrF_4$
56.5	537	Peritectic	$L + ZrF_4 \rightleftharpoons 3NaF\cdot 4ZrF_4$

---

*A determination of the crystal structure of 3NaF·ZrF$_4$ has been reported by L. A. Harris, "The Crystal Structures of Na$_3$ZrF$_7$ and Na$_3$HfF$_7$," *Acta Cryst.* 12, 172 (1959).

UNCLASSIFIED
ORNL-LR-DWG-22105

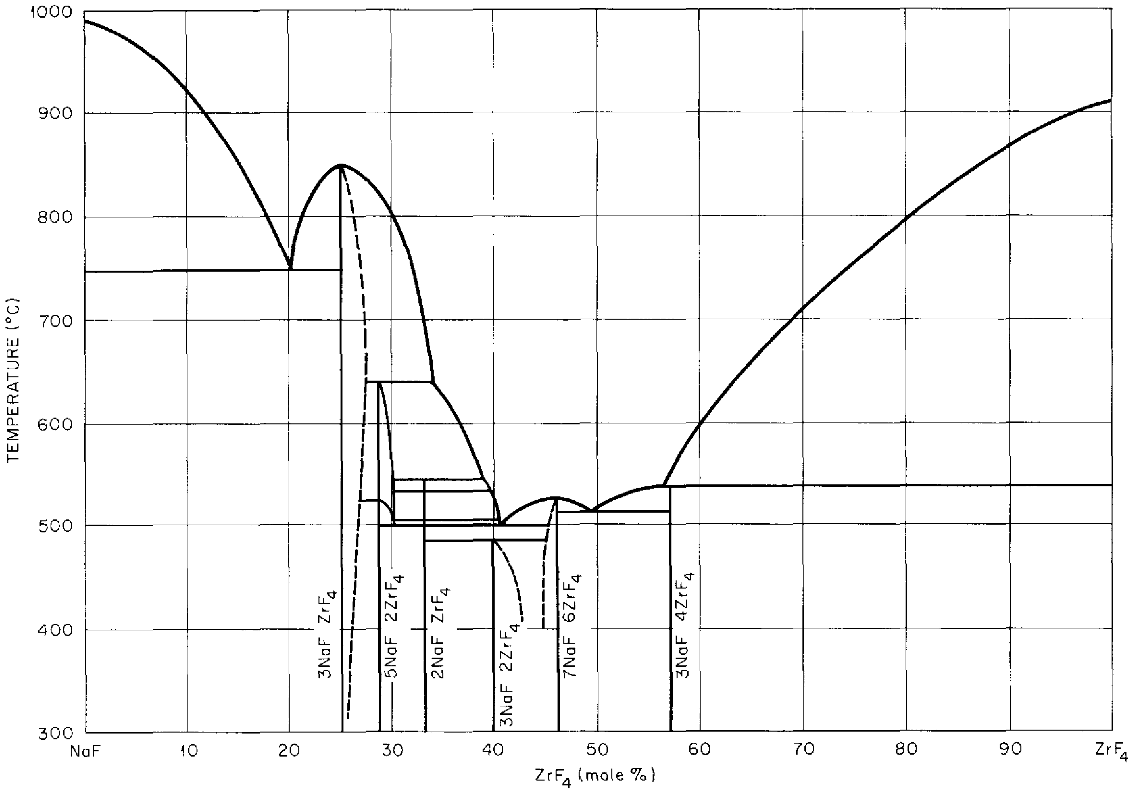

Fig. 3.33. The System NaF–ZrF_4.

3.34. The System KF–ZrF$_4$

C. J. Barton, H. Insley, R. P. Metcalf, R. E. Thoma, and W. R. Grimes, unpublished work performed at the Oak Ridge National Laboratory, 1951–55.

Preliminary diagram.

Invariant Equilibria

Mole % ZrF$_4$ in Liquid	Invariant Temperature (°C)	Type of Equilibrium	Phase Reaction at Invariant Temperature
14	765	Eutectic	$L \rightleftharpoons KF + 3KF \cdot ZrF_4$
25	910	Congruent melting point	$L \rightleftharpoons 3KF \cdot ZrF_4$
36	590	Peritectic	$3KF \cdot ZrF_4 + L \rightleftharpoons 2KF \cdot ZrF_4$
40.5	412	Peritectic	$2KF \cdot ZrF_4 + L \rightleftharpoons 3KF \cdot 2ZrF_4$
42	390	Eutectic	$L \rightleftharpoons 3KF \cdot 2ZrF_4 + KF \cdot ZrF_4$
50	475	Congruent melting point	$L \rightleftharpoons KF \cdot ZrF_4$
55	440	Eutectic	$L \rightleftharpoons KF \cdot ZrF_4 + ZrF_4$

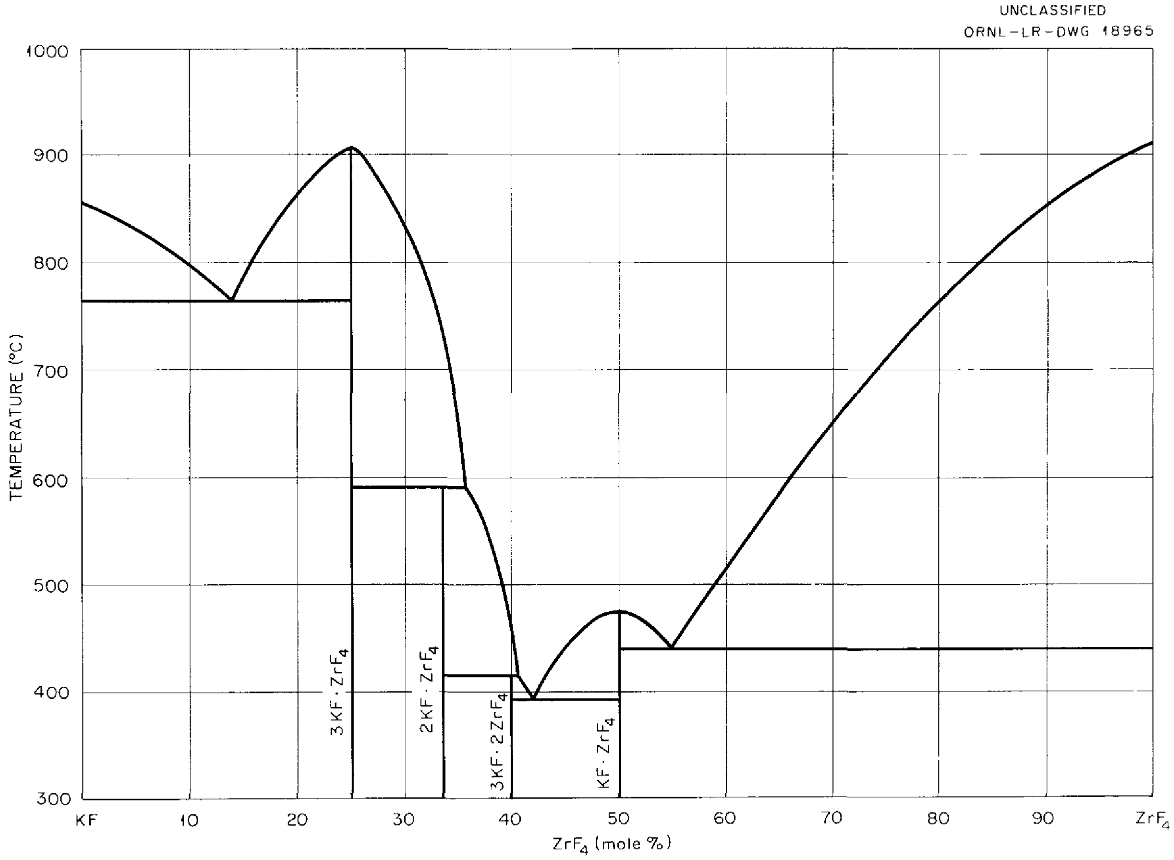

Fig. 3.34. The System KF–ZrF$_4$.

3.35. The System $RbF-ZrF_4$

R. E. Moore, R. E. Thoma, C. J. Barton, W. R. Grimes, H. Insley, B. S. Landau, and H. A. Friedman, unpublished work performed at the Oak Ridge National Laboratory, 1955–56.

Preliminary diagram.

Invariant Equilibria

Mole % ZrF_4 in Liquid	Invariant Temperature (°C)	Type of Equilibrium	Phase Reaction at Invariant Temperature
10	710	Eutectic	$L \rightleftharpoons RbF + 3RbF \cdot ZrF_4$
25	897	Congruent melting point	$L \rightleftharpoons 3RbF \cdot ZrF_4$
34	620	Peritectic	$L + 3RbF \cdot ZrF_4 ss \rightleftharpoons \alpha\text{-}2RbF \cdot ZrF_4$
–	460	Inversion	$\alpha\text{-}2RbF \cdot ZrF_4 \rightleftharpoons \beta\text{-}2RbF \cdot ZrF_4$
–	370	Lowered inversion and decomposition	$\alpha\text{-}2RbF \cdot ZrF_4 ss \rightleftharpoons \beta\text{-}2RbF \cdot ZrF_4 ss$
42	410	Eutectic	$L \rightleftharpoons \alpha\text{-}2RbF \cdot ZrF_4 ss + 5RbF \cdot 4ZrF_4$
44.4	445	Congruent melting point	$L \rightleftharpoons 5RbF \cdot 4ZrF_4$
48	390	Eutectic	$L \rightleftharpoons 5RbF \cdot 4ZrF_4 + \beta\text{-}RbF \cdot ZrF_4$
50	423	Congruent melting point	$L \rightleftharpoons \alpha\text{-}RbF \cdot ZrF_4$
–	391	Inversion	$\alpha\text{-}RbF \cdot ZrF_4 \rightleftharpoons \beta\text{-}RbF \cdot ZrF_4$
54	400	Eutectic	$L \rightleftharpoons \alpha\text{-}RbF \cdot ZrF_4 + RbF \cdot 2ZrF_4$
57	447	Peritectic	$L + ZrF_4 \rightleftharpoons RbF \cdot 2ZrF_4$

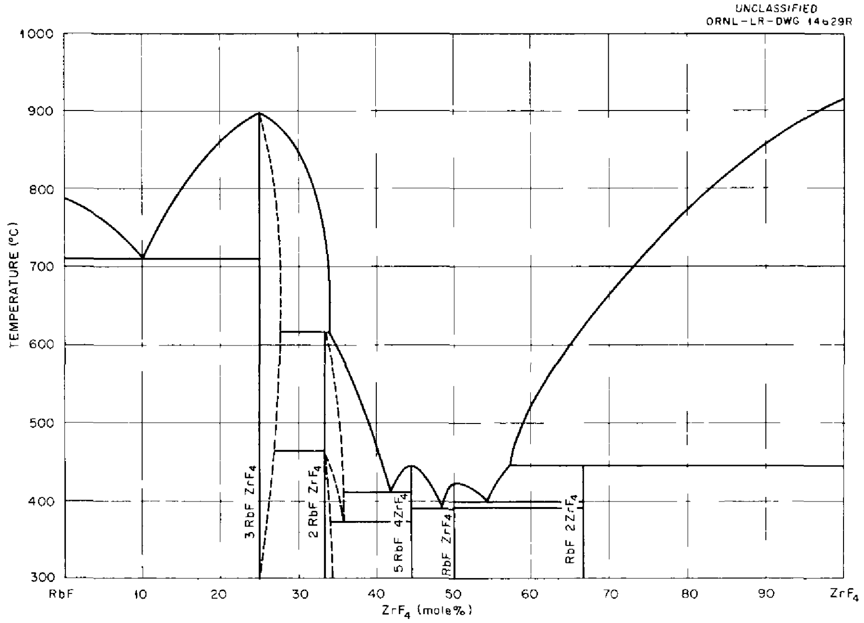

Fig. 3.35. The System $RbF-ZrF_4$.

3.36. The System $CsF-ZrF_4$

C. J. Barton, L. M. Bratcher, and W. R. Grimes, unpublished work performed at the Oak Ridge National Laboratory, 1952–53.

Preliminary diagram.

Invariant Equilibria

Mole % ZrF_4 in Liquid	Invariant Temperature (°C)	Type of Equilibrium	Phase Reaction at Invariant Temperature
9	640	Eutectic	$L \rightleftharpoons CsF + 3CsF \cdot ZrF_4$
25	775	Congruent melting point	$L \rightleftharpoons 3CsF \cdot ZrF_4$
35	520	Peritectic	$L + 3CsF \cdot ZrF_4 \rightleftharpoons 2CsF \cdot ZrF_4$
40	420	Eutectic	$L \rightleftharpoons 2CsF \cdot ZrF_4 + \alpha\text{-}CsF \cdot ZrF_4$
50	515	Congruent melting point	$L \rightleftharpoons \alpha\text{-}CsF \cdot ZrF_4$
–	320	Inversion	$\alpha\text{-}CsF \cdot ZrF_4 \rightleftharpoons \beta\text{-}CsF \cdot ZrF_4$
59	470	Eutectic	$L \rightleftharpoons \alpha\text{-}CsF \cdot ZrF_4 + ZrF_4$

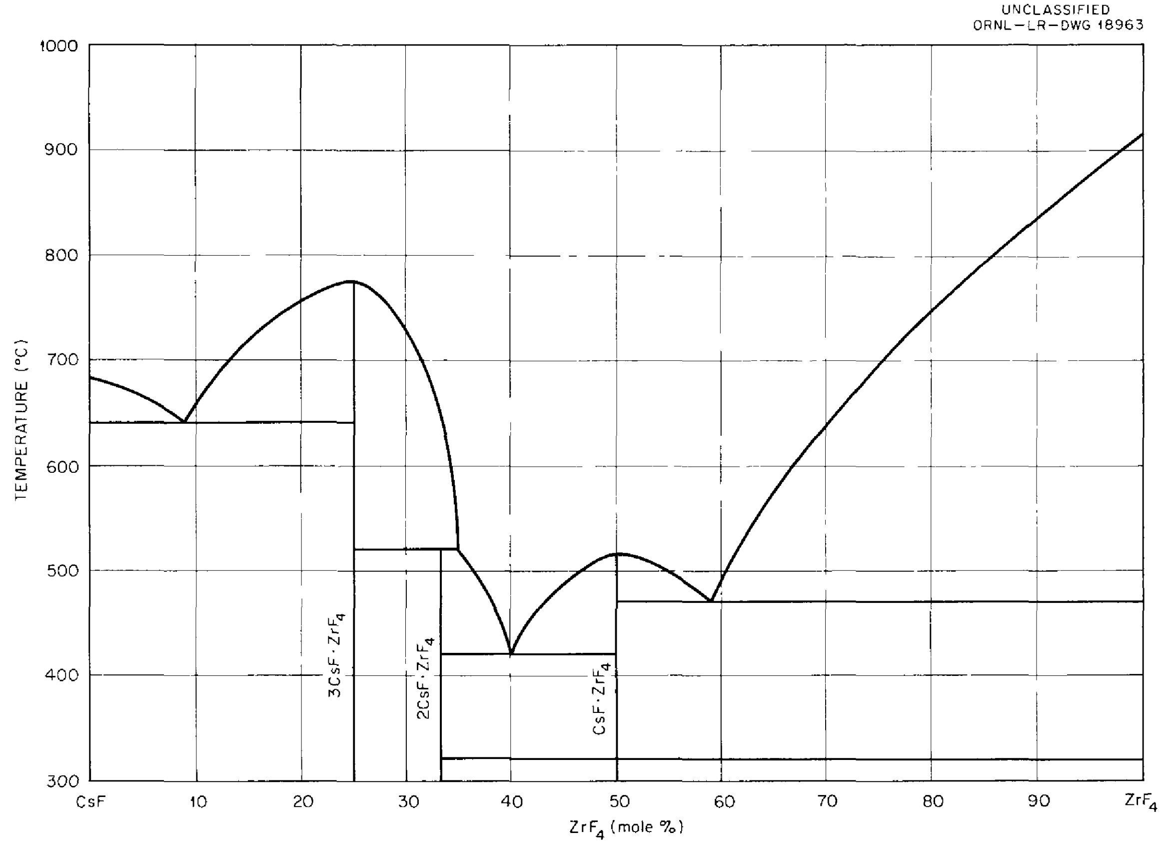

Fig. 3.36. The System CsF–ZrF_4.

3.37. The System LiF–NaF–ZrF_4

F. F. Blankenship, H. A. Friedman, H. Insley, R. E. Thoma, and W. R. Grimes, unpublished work performed at the Oak Ridge National Laboratory, 1953–59.

Preliminary diagram.

Invariant Equilibria

Composition of Liquid (mole %)			Temperature (°C)	Type of Invariant	Solids Present at Invariant Temperature
LiF	NaF	ZrF_4			
37	52	11	604	Eutectic	NaF, LiF, and $3NaF \cdot ZrF_4$
55	22	23	590	Eutectic	α-$3LiF \cdot ZrF_4$, $3NaF \cdot ZrF_4$*ss*, and LiF
32	36	32	450	Peritectic	β-$3LiF \cdot ZrF_4$, $3NaF \cdot ZrF_4$*ss*, and $2LiF \cdot ZrF_4$
31	35	34	448	Peritectic	$3NaF \cdot ZrF_4$, α-$5NaF \cdot 2ZrF_4$*ss*, and $2LiF \cdot ZrF_4$
31	34.5	34.5	445	Peritectic	$2NaF \cdot ZrF_4$, α-$5NaF \cdot 2ZrF_4$*ss*, and $2LiF \cdot ZrF_4$
26	37	37	425	Eutectic	$2NaF \cdot ZrF_4$, $7NaF \cdot 6ZrF_4$, and $2LiF \cdot ZrF_4$
29	25.5	45.5	449	Eutectic	$7NaF \cdot 6ZrF_4$, $3NaF \cdot 4ZrF_4$*ss*, and $2LiF \cdot ZrF_4$
29	24.5	46.5	453	Peritectic	$3NaF \cdot 4ZrF_4$*ss*, $3LiF \cdot 4ZrF_4$*ss*, and $2LiF \cdot ZrF_4$
28	24	48	475	Peritectic	$3NaF \cdot 4ZrF_4$*ss*, $3LiF \cdot 4ZrF_4$*ss*, and ZrF_4

UNCLASSIFIED
ORNL-LR-DWG 38115

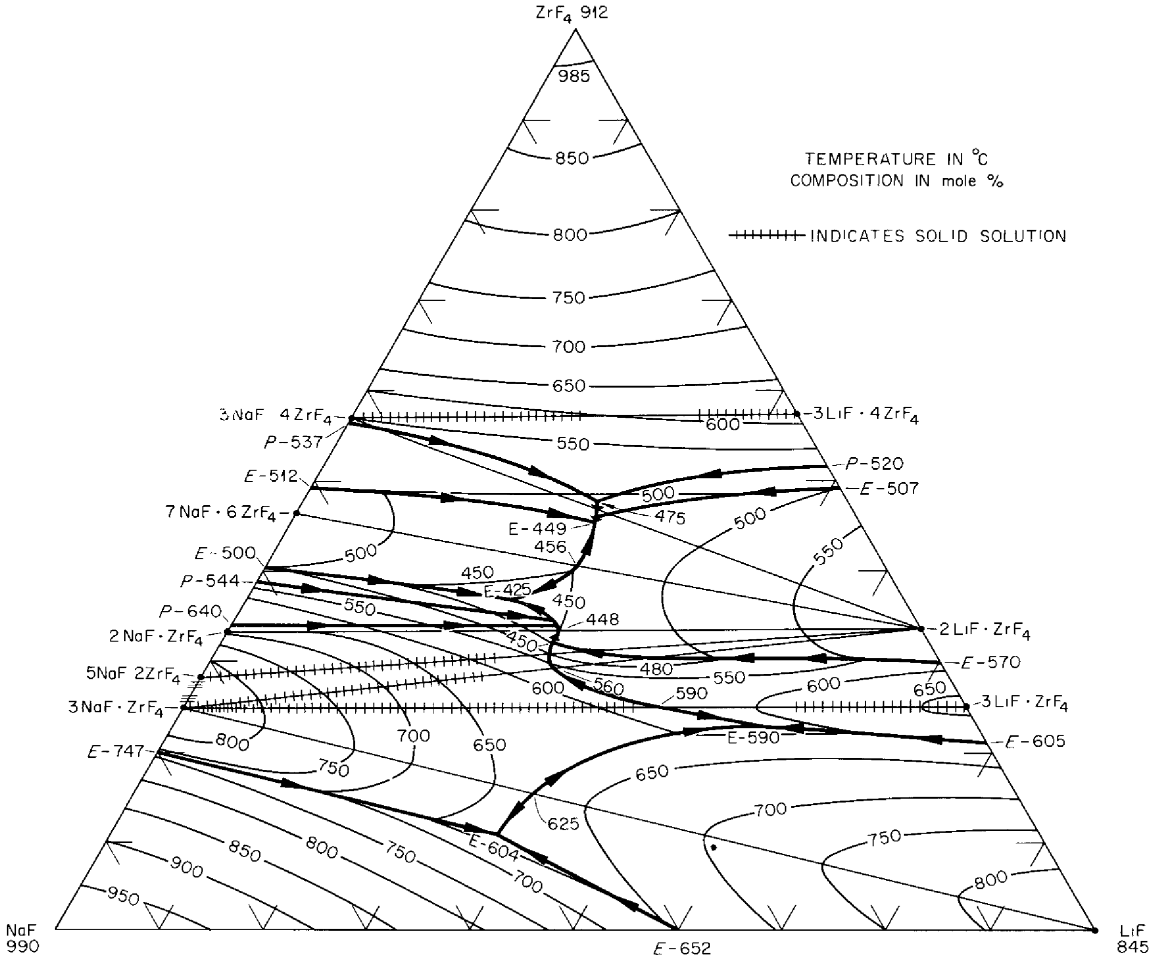

Fig. 3.37. The System LiF–NaF–ZrF_4.

3.38. The System NaF–KF–ZrF_4

R. E. Thoma, C. J. Barton, H. Insley, H. A. Friedman, and W. R. Grimes, unpublished work performed at the Oak Ridge National Laboratory, 1951–55.

Preliminary diagram.

Invariant Equilibria*

Composition of Liquid (mole %)**			Invariant Temperature (°C)	Type of Equilibrium	Solids Present at Invariant Point
NaF	KF	ZrF_4			
34	58	8	695	Eutectic	NaF, KF, and $3KF \cdot ZrF_4$
45	38	17	720	Eutectic	NaF, $3KF \cdot ZrF_4$, and $3NaF \cdot 3KF \cdot 2ZrF_4$
61	19	20	710	Eutectic	NaF, $3NaF \cdot ZrF_4$, and $3NaF \cdot 3KF \cdot 2ZrF_4$
52	17	31		Peritectic	$3NaF \cdot ZrF_4$, $3NaF \cdot 3KF \cdot 2ZrF_4$, and $NaF \cdot KF \cdot ZrF_4$
48	18	34		Peritectic	$3NaF \cdot ZrF_4$, $NaF \cdot KF \cdot ZrF_4$, and $5NaF \cdot 2ZrF_4$
33	32	35		Peritectic	$3NaF \cdot 3KF \cdot 2ZrF_4$, $3KF \cdot ZrF_4$, and $NaF \cdot KF \cdot ZrF_4$
12	51	37		Peritectic	$3KF \cdot ZrF_4$, $2KF \cdot ZrF_4$, and $NaF \cdot KF \cdot ZrF_4$
40	21	39		Peritectic	$5NaF \cdot 2ZrF_4$, $2NaF \cdot ZrF_4$, and $NaF \cdot KF \cdot ZrF_4$
39	21	40		Peritectic	$2NaF \cdot ZrF_4$, $7NaF \cdot 6ZrF_4$, and $NaF \cdot KF \cdot ZrF_4$
11	49	40		Peritectic	$2KF \cdot ZrF_4$, $3KF \cdot 2ZrF_4$, and $NaF \cdot KF \cdot ZrF_4$
10	48	42	385	Eutectic	$3KF \cdot 2ZrF_4$, $KF \cdot ZrF_4$, and $NaF \cdot KF \cdot ZrF_4$
15	40	45		Eutectic	$KF \cdot ZrF_4$, $NaF \cdot KF \cdot ZrF_4$, and $2NaF \cdot 3KF \cdot 5ZrF_4$
22	33	45		Peritectic	$NaF \cdot KF \cdot ZrF_4$, $7NaF \cdot 6ZrF_4$, and $2NaF \cdot 3KF \cdot 5ZrF_4$
25	25	50		Eutectic	$7NaF \cdot 6ZrF_4$, $3NaF \cdot 4ZrF_4$, and $2NaF \cdot 3KF \cdot 5ZrF_4$
21	29	51		Eutectic	$3NaF \cdot 4ZrF_4$, ZrF_4, and $2NaF \cdot 3KF \cdot 5ZrF_4$
20	30	50	432	Congruent melting point	$2NaF \cdot 3KF \cdot 5ZrF_4$

*Three solid phases have been observed routinely in the composition region 30–50 mole % ZrF_4 which have not been identified as to composition. Whether these exhibit primary phases at the liquidus surface has not yet been determined.

**Compositions of invariant points shown by the intersection of dotted boundary curves are approximate.

UNCLASSIFIED
ORNL-LR-DWG 35480

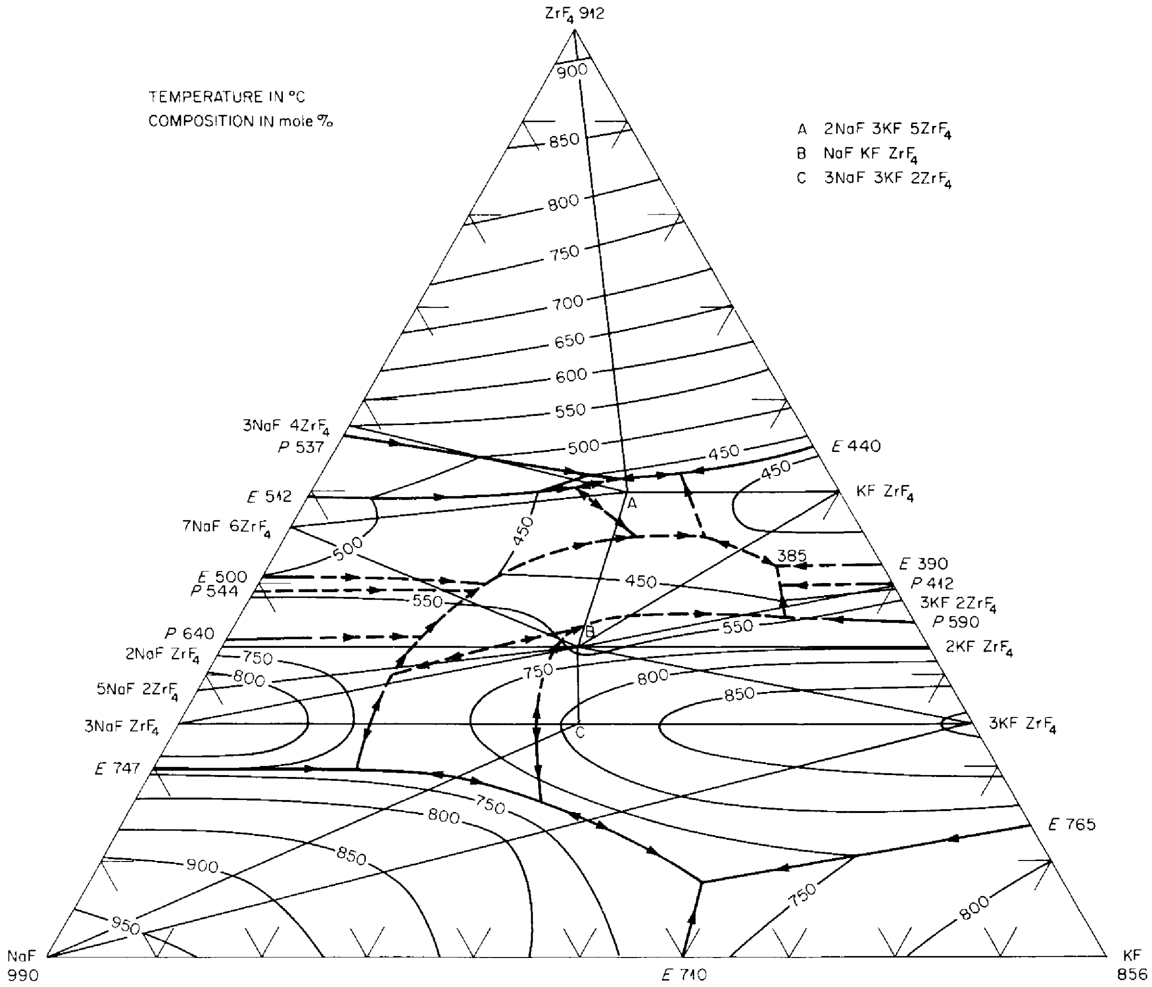

Fig. 3.38. The System NaF–KF–ZrF$_4$. The isotherms for the temperatures 600, 650, and 700°C between the 30 and 40 mole % ZrF$_4$ compositions have been omitted in order not to obscure the phase relationships in this polythermal projection.

3.39. The System NaF–RbF–ZrF_4

R. E. Thoma, H. Insley, H. A. Friedman, and W. R. Grimes, unpublished work performed at the Oak Ridge National Laboratory, 1951–56.

Preliminary diagram.

Invariant Equilibria

Composition of Liquid (mole %)			Invariant Temperature (°C)	Type of Equilibrium	Solids Present at Invariant Point
NaF	RbF	ZrF_4			
23	72	5	643	Eutectic	NaF, RbF, and $3RbF \cdot ZrF_4$
50	27	23	720	Eutectic	NaF, $3RbF \cdot ZrF_4$, and $3NaF \cdot ZrF_4$
37	32	31	605	Eutectic	$3NaF \cdot ZrF_4$, $3RbF \cdot ZrF_4$, and $NaF \cdot RbF \cdot ZrF_4$
39	26	35	545	Peritectic	$3NaF \cdot ZrF_4$, $5NaF \cdot 2ZrF_4$, and $NaF \cdot RbF \cdot ZrF_4$
36.3	24.2	39.5	427	Peritectic	$5NaF \cdot 2ZrF_4$, $2NaF \cdot ZrF_4$, and $NaF \cdot RbF \cdot ZrF_4$
34.5	24	41.5	424	Peritectic	$2NaF \cdot ZrF_4$, $NaF \cdot RbF \cdot ZrF_4$, and $3NaF \cdot 3RbF \cdot 4ZrF_4$
34	23.5	42.5	422	Peritectic	$2NaF \cdot ZrF_4$, $7NaF \cdot 6ZrF_4$, and $3NaF \cdot 3RbF \cdot 4ZrF_4$
33	23.5	43.5	420	Eutectic	$7NaF \cdot 6ZrF_4$, $3NaF \cdot 3RbF \cdot 4ZrF_4$, and $NaF \cdot RbF \cdot 2ZrF_4$
28.5	21.5	50	443	Eutectic	$3NaF \cdot 4ZrF_4$, $7NaF \cdot 6ZrF_4$, and $NaF \cdot RbF \cdot 2ZrF_4$
28	21.5	50.5	446	Peritectic	$3NaF \cdot 4ZrF_4$, ZrF_4, and $NaF \cdot RbF \cdot 2ZrF_4$
23.5	39.5	37	470	Peritectic	$NaF \cdot RbF \cdot ZrF_4$, $2RbF \cdot ZrF_4$, and $3RbF \cdot ZrF_4$
21	40	39	438	Peritectic	$NaF \cdot RbF \cdot ZrF_4$, $2RbF \cdot ZrF_4$, and $3NaF \cdot 3RbF \cdot 4ZrF_4$
8	50	42	400	Eutectic	$3NaF \cdot 3RbF \cdot 4ZrF_4$, $2RbF \cdot ZrF_4$, and $5RbF \cdot 4ZrF_4$
8.5	47	44.5	395	Eutectic	$3NaF \cdot 3RbF \cdot 4ZrF_4$, $5RbF \cdot ZrF_4$, and $NaF \cdot RbF \cdot 2ZrF_4$
6.2	45.8	48	380	Eutectic	$NaF \cdot RbF \cdot 2ZrF_4$, $5RbF \cdot 4ZrF_4$, and $RbF \cdot ZrF_4$
5	42	53	398	Eutectic	$NaF \cdot RbF \cdot 2ZrF_4$, $RbF \cdot ZrF_4$, and $RbF \cdot 2ZrF_4$
6.5	39	54.5	423	Peritectic	ZrF_4, $NaF \cdot RbF \cdot 2ZrF_4$, and $RbF \cdot 2ZrF_4$
33.3	33.3	33.3	642	Congruent melting point	$NaF \cdot RbF \cdot ZrF_4$
25	25	50	462	Congruent melting point	$NaF \cdot RbF \cdot 2ZrF_4$

Minimum Temperatures on Alkemade Lines

Composition of Liquid (mole %)			Temperature (°C)	Alkemade Line
NaF	RbF	ZrF_4		
24.75	24.75	51.5	455	$NaF{\cdot}RbF{\cdot}2ZrF_4$–$ZrF_4$
6	44	50	402	$NaF{\cdot}RbF{\cdot}2ZrF_4$–$RbF{\cdot}ZrF_4$
7.5	46.5	46	405	$NaF{\cdot}RbF{\cdot}2ZrF_4$–$5RbF{\cdot}4ZrF_4$
8.5	48.5	43	405	$3NaF{\cdot}RbF{\cdot}4ZrF_4$–$5RbF{\cdot}4ZrF_4$
28	28	44	435	$3NaF{\cdot}RbF{\cdot}4ZrF_4$–$NaF{\cdot}RbF{\cdot}2ZrF_4$
22	40	38	442	$3NaF{\cdot}3RbF{\cdot}4ZrF_4$–$2RbF{\cdot}ZrF_4$
29	41.5	49.5	450	$NaF{\cdot}RbF{\cdot}2ZrF_4$–$7NaF{\cdot}6ZrF_4$
37	24.5	38.5	610	$NaF{\cdot}RbF{\cdot}ZrF_4$–$3NaF{\cdot}ZrF_4$
47	28	25	732	$3NaF{\cdot}ZrF_4$–$3RbF{\cdot}ZrF_4$
36	48	16	777	NaF–$3RbF{\cdot}ZrF_4$
30	36.7	33.3	598	$NaF{\cdot}RbF{\cdot}ZrF_4$–$3RbF{\cdot}ZrF_4$

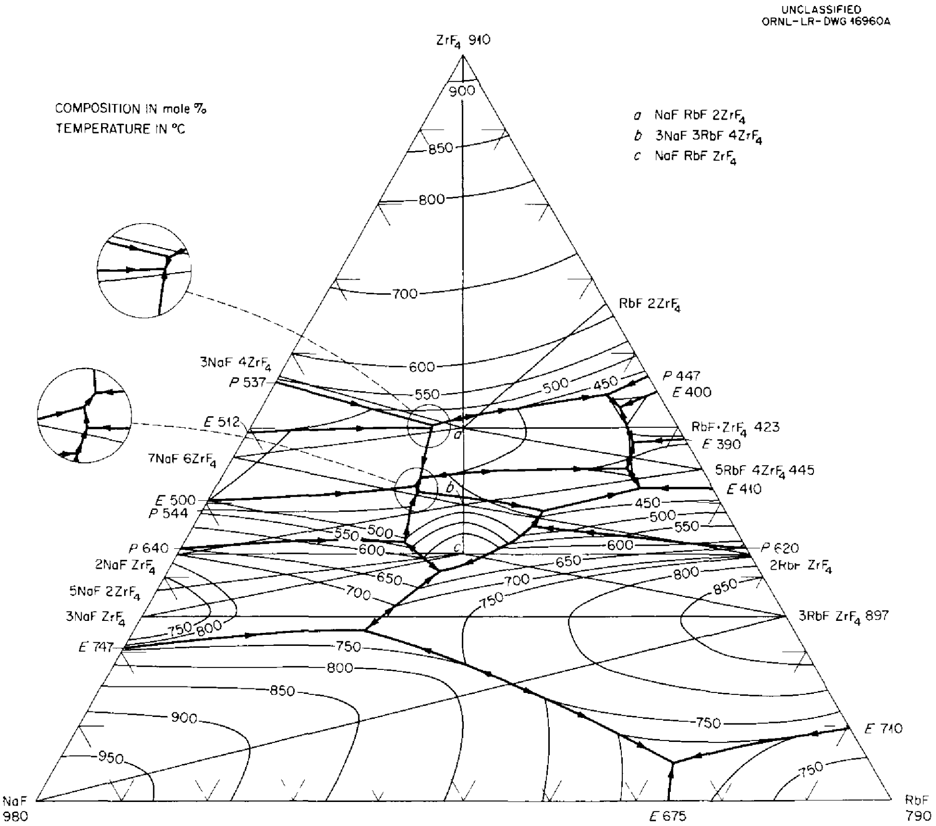

Fig. 3.39. The System NaF–RbF–ZrF_4.

3.40. The System $NaF-CrF_2-ZrF_4$: The Section $NaF \cdot CrF_2 - ZrF_4$

R. E. Thoma, H. A. Friedman, B. S. Landau, and W. R. Grimes, unpublished work performed at the Oak Ridge National Laboratory, 1956–57.

Preliminary diagram. No invariant equilibria occur for compositions lying on the section $NaF \cdot CrF_2-ZrF_4$.

UNCLASSIFIED
ORNL-LR-DWG 19367R

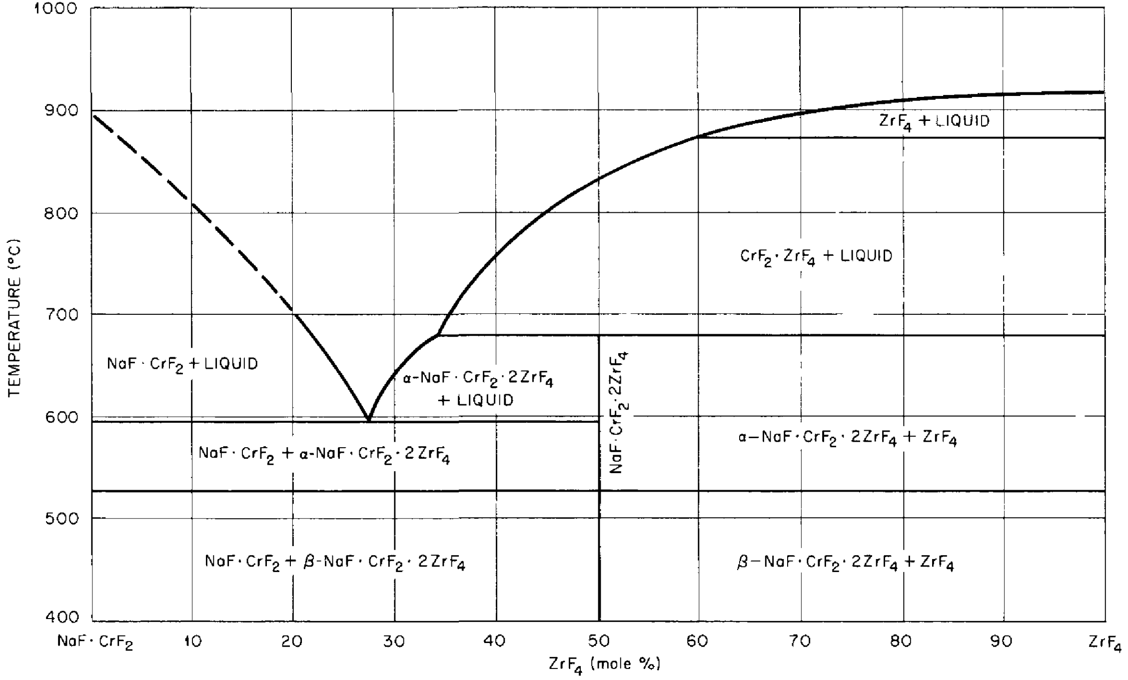

Fig. 3.40. The Section $NaF \cdot CrF_2-ZrF_4$.

3.41. The System NaF–CeF_3–ZrF_4

W. T. Ward, R. A. Strehlow, W. R. Grimes, and G. M. Watson, "Solubility Relationships of Rare Earth Fluorides and Yttrium Fluoride in Various Molten NaF–ZrF_4 and NaF–ZrF_4–UF_4 Solvents," *J. Chem. Eng. Data* (in press).

UNCLASSIFIED
ORNL-LR-DWG 29164R

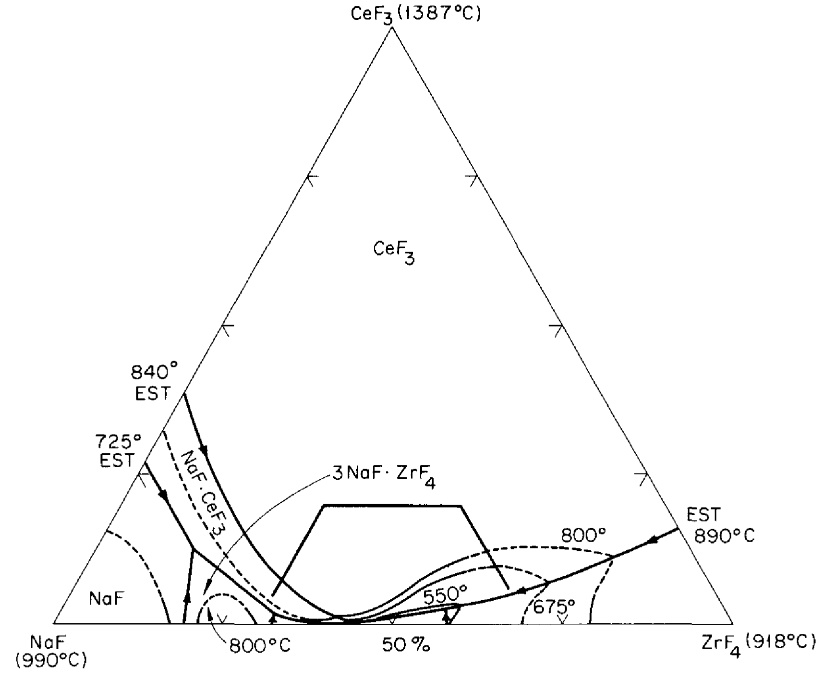

Fig. 3.41*a*. The System NaF–CeF_3–ZrF_4.

UNCLASSIFIED
ORNL-LR-DWG 29165R

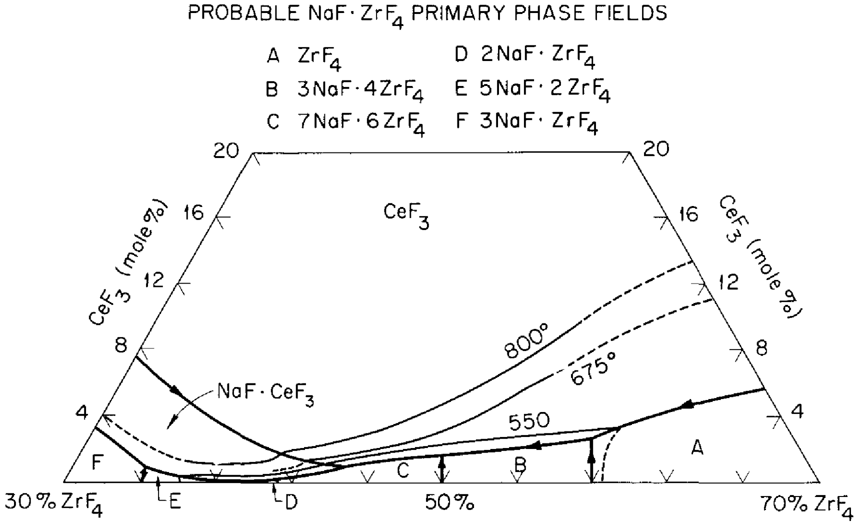

Fig. 3.41*b*. The System NaF–CeF_3–ZrF_4 in the Region 30–70 Mole % NaF, 0–20 Mole % CeF_3, 30–70 Mole % ZrF_4.

3.42. The System LiF–CeF_3

C. J. Barton, L. M. Bratcher, R. J. Sheil, and W. R. Grimes, unpublished work performed at the Oak Ridge National Laboratory, 1956–57.

Preliminary diagram. The system LiF–CeF_3 contains a single eutectic at 81 LiF–19 CeF_3 (mole %), m.p. 755 ± 5°C.

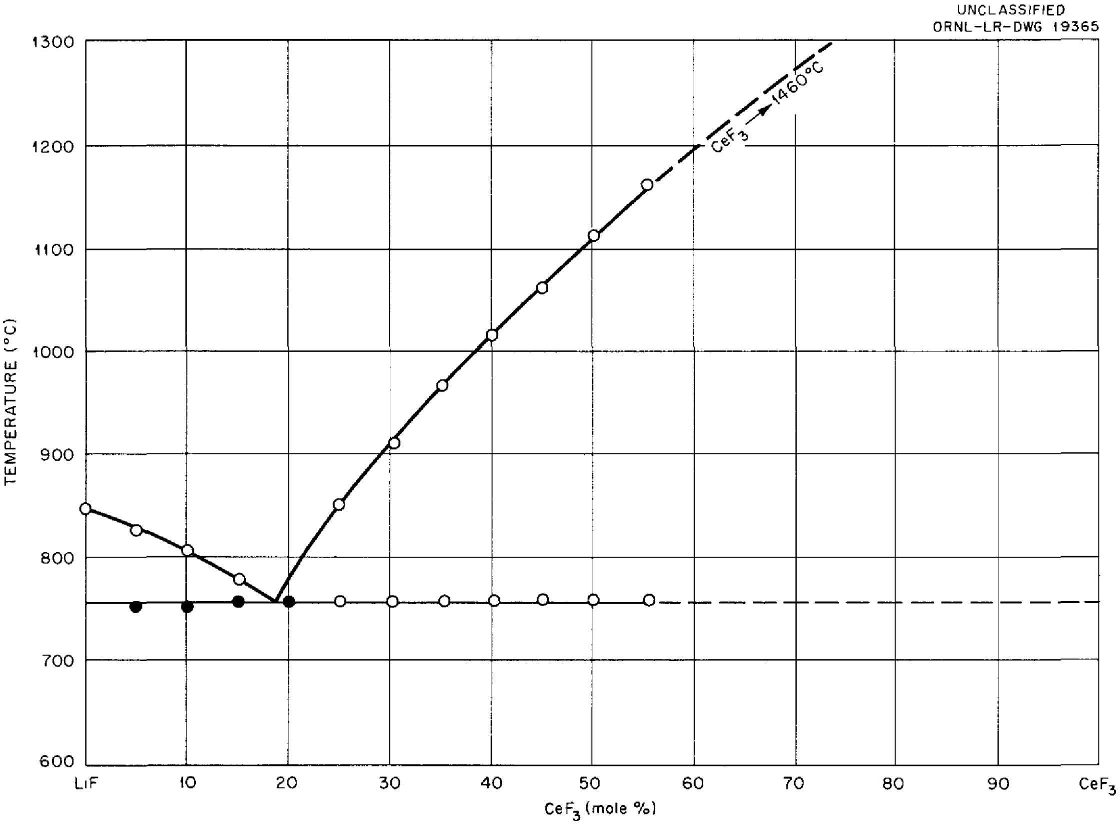

Fig. 3.42. The System LiF–CeF$_3$.

3.43. The System NaF–HfF_4

R. E. Thoma, C. F. Weaver, T. N. McVay, H. A. Friedman, and W. R. Grimes, unpublished work performed at the Oak Ridge National Laboratory, 1956–58.

Preliminary diagram.

Invariant Equilibria

Mole % HfF_4 in Liquid	Invariant Temperature (°C)	Type of Equilibrium	Phase Reaction at Invariant Temperature
18.5	695	Eutectic	$L \rightleftharpoons NaF + 3NaF{\cdot}HfF_4$
25	863	Congruent melting point	$L \rightleftharpoons 3NaF{\cdot}HfF_4$*
34	606	Peritectic	$L + 3NaF{\cdot}HfF_4 \rightleftharpoons \alpha\text{-}5NaF{\cdot}2HfF_4$
–	535	Inversion	$\alpha\text{-}5NaF{\cdot}2HfF_4 \rightleftharpoons \beta\text{-}5NaF{\cdot}2HfF_4$
35	586	Peritectic	$L + \alpha\text{-}5NaF{\cdot}2HfF_4 \rightleftharpoons \beta\text{-}2NaF{\cdot}HfF_4$
–	Below 350	Inversion	$\beta\text{-}2NaF{\cdot}HfF_4 \rightleftharpoons \gamma\text{-}2NaF{\cdot}HfF_4$
–	Below 350	Inversion	$\gamma\text{-}2NaF{\cdot}HfF_4 \rightleftharpoons \delta\text{-}2NaF{\cdot}HfF_4$
43	510	Eutectic	$L \rightleftharpoons \beta\text{-}2NaF{\cdot}HfF_4 + 7NaF{\cdot}6HfF_4$
45	531	Peritectic	$L + NaF{\cdot}HfF_4 \rightleftharpoons 7NaF{\cdot}6HfF_4$
50	557	Congruent melting point	$L \rightleftharpoons NaF{\cdot}HfF_4$
53	535	Eutectic	$L \rightleftharpoons NaF{\cdot}HfF_4 + HfF_4$

*A determination of the crystal structure of $3NaF{\cdot}HfF_4$ has been reported by L. A. Harris, "The Crystal Structures of Na_3ZrF_7 and Na_3HfF_7," *Acta Cryst.* 12, 172 (1959).

UNCLASSIFIED
ORNL-LR-DWG 35488

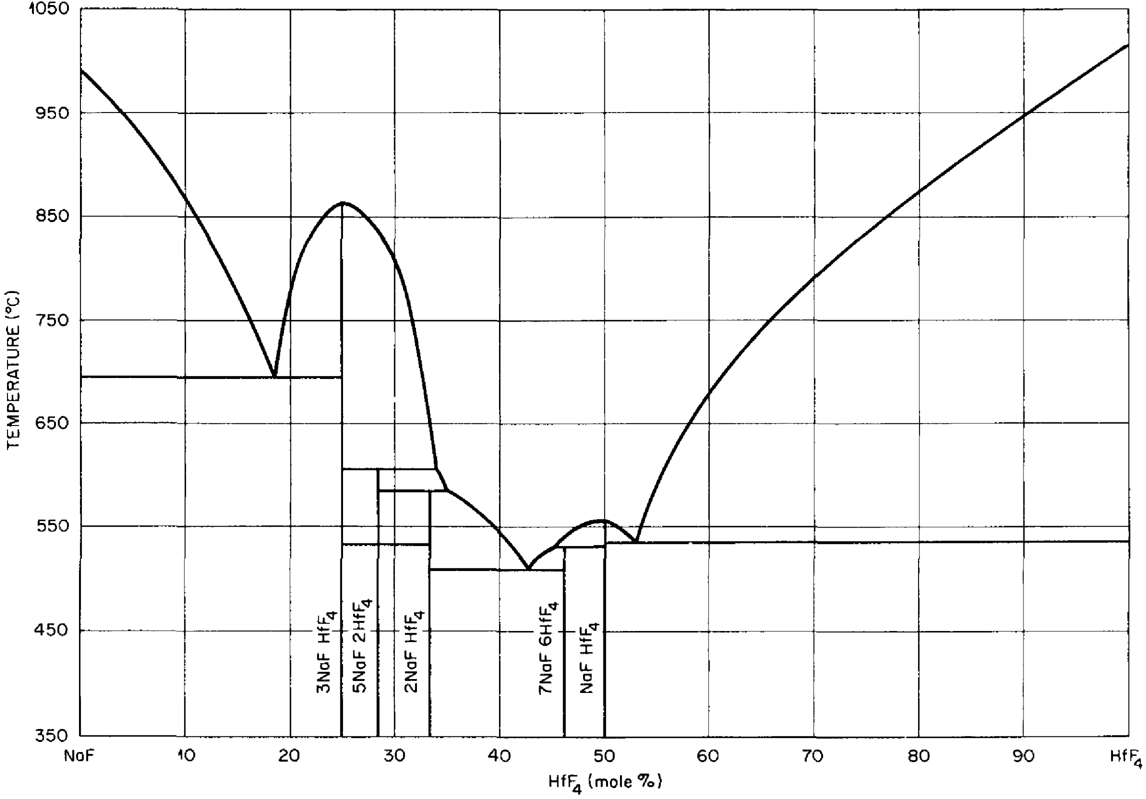

Fig. 3.43. The System NaF–HfF_4.

3.44. The System LiF–ThF_4

R. E. Thoma, H. Insley, B. S. Landau, H. A. Friedman, and W. R. Grimes, "Phase Equilibria in the Fused Salt Systems LiF–ThF_4 and NaF–ThF_4," *J. Phys. Chem.* **63,** 1266–74 (1959).

Invariant Equilibria

Mole % ThF_4 in Liquid	Invariant Temperature (°C)	Type of Equilibrium	Phase Reaction at Invariant Temperature
23	568	Eutectic	$L \rightleftharpoons LiF + 3LiF \cdot ThF_4$
25	573	Congruent melting point	$L \rightleftharpoons 3LiF \cdot ThF_4$
29	565	Eutectic	$L \rightleftharpoons 3LiF \cdot ThF_4 + 7LiF \cdot 6ThF_4$
30.5	597	Peritectic	$LiF \cdot 2ThF_4 + L \rightleftharpoons 7LiF \cdot 6ThF_4$
42	762	Peritectic	$LiF \cdot 4ThF_4 + L \rightleftharpoons LiF \cdot 2ThF_4$
62	897	Peritectic	$ThF_4 + L \rightleftharpoons LiF \cdot 4ThF_4$

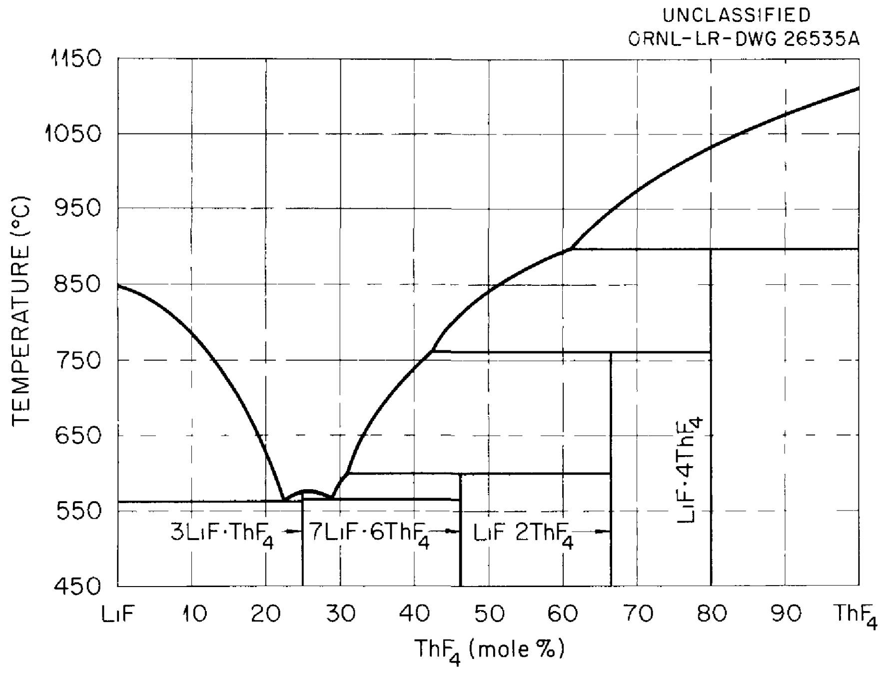

Fig. 3.44. The System LiF–ThF_4.

3.45. The System NaF–ThF$_4$

R. E. Thoma, H. Insley, B. S. Landau, H. A. Friedman, and W. R. Grimes, "Phase Equilibria in the Fused Salt Systems LiF–ThF$_4$ and NaF–ThF$_4$," *J. Phys. Chem.* **63,** 1266–74 (1959).

Invariant Equilibria

Mole % ThF$_4$ in Liquid	Invariant Temperature (°C)	Type of Equilibrium	Phase Reaction at Invariant Temperature
21.5	645	Peritectic	$NaF + L \rightleftharpoons \alpha\text{-}4NaF\cdot ThF_4$
22.5	618	Eutectic	$L \rightleftharpoons \alpha\text{-}4NaF\cdot ThF_4 + 2NaF\cdot ThF_4$
–	604	Inversion	$\alpha\text{-}4NaF\cdot ThF_4 \rightleftharpoons \beta\text{-}4NaF\cdot ThF_4$
–	558	Decomposition	$\beta\text{-}4NaF\cdot ThF_4 \rightleftharpoons NaF + 2NaF\cdot ThF_4$
33.3	705	Congruent melting point	$L \rightleftharpoons 2NaF\cdot ThF_4$
37	690	Eutectic	$L \rightleftharpoons 2NaF\cdot ThF_4 + 3NaF\cdot 2ThF_4$
40	712	Congruent melting point	$L \rightleftharpoons 3NaF\cdot 2ThF_4$
41	705	Eutectic	$L \rightleftharpoons 3NaF\cdot 2ThF_4 + \alpha\text{-}NaF\cdot ThF_4$
–	683	Decomposition	$3NaF\cdot 2ThF_4 \rightleftharpoons 2NaF\cdot ThF_4 + \alpha\text{-}NaF\cdot ThF_4$
45.5	730	Peritectic	$NaF\cdot 2ThF_4 + L \rightleftharpoons \alpha\text{-}NaF\cdot ThF_4$
58	831	Peritectic	$ThF_4 + L \rightleftharpoons NaF\cdot 2ThF_4$

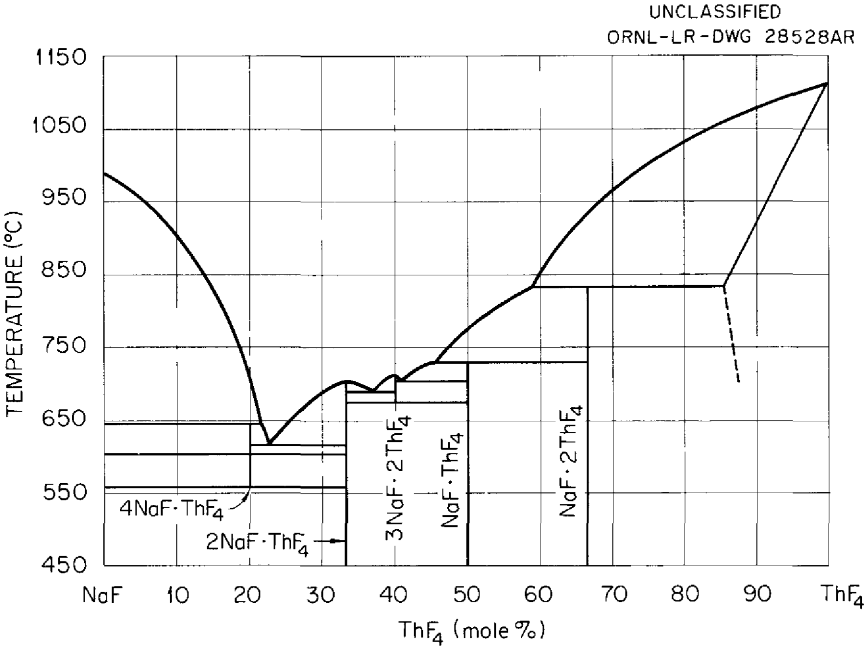

Fig. 3.45. The System NaF–ThF$_4$.

3.46. The System KF–ThF_4

W. J. Asker, E. R. Segnit, and A. W. Wylie, "The Potassium Thorium Fluorides," *J. Chem. Soc.* **1952,** 4470–79.

This system has also been reported by A. G. Bergman and E. P. Dergunov, *Doklady Akad. Nauk S.S.S.R.* **53,** 753 (1941) and by V. S. Emelyanov and A. J. Evstyukhin, "An Investigation of Fused-Salt Systems Based on Thorium Fluoride – II. NaF–KF–ThF_4, NaF–ThF_4, and KF–ThF_4," *J. Nuclear Energy* **5,** 108–14 (1957).

Invariant Equilibria

Mole % ThF_4 in Liquid	Invariant Temperature (°C)	Type of Equilibrium	Phase Reaction at Invariant Temperature
14	694	Eutectic	$L \rightleftharpoons KF + \beta\text{-}5KF\cdot ThF_4$
–	635	Inversion	$\alpha\text{-}5KF\cdot ThF_4 \rightleftharpoons \beta\text{-}5KF\cdot ThF_4$
–	712	Peritectic	$L + 3KF\cdot ThF_4 \rightleftharpoons \alpha\text{-}5KF\cdot ThF_4$
25	865	Congruent melting point	$L \rightleftharpoons 3KF\cdot ThF_4$
–	570	Decomposition	$3KF\cdot ThF_4 \rightleftharpoons \beta\text{-}5KF\cdot ThF_4 + \beta\text{-}2KF\cdot ThF_4$
31	691	Eutectic	$L \rightleftharpoons 3KF\cdot ThF_4 + \alpha\text{-}2KF\cdot ThF_4$
–	747	Peritectic	$L + KF\cdot ThF_4 \rightleftharpoons \alpha\text{-}2KF\cdot ThF_4$
–	645	Inversion	$\alpha\text{-}2KF\cdot ThF_4 \rightleftharpoons \beta\text{-}2KF\cdot ThF_4$
50*	905	Congruent melting point	$L \rightleftharpoons KF\cdot ThF_4$
56	875	Eutectic	$L \rightleftharpoons KF\cdot ThF_4 + KF\cdot 2ThF_4$
66	930	Peritectic	$L + KF\cdot 3ThF_4 \rightleftharpoons KF\cdot 2ThF_4$
75	990	Congruent melting point	$L \rightleftharpoons KF\cdot 3ThF_4$
78	980	Eutectic	$L \rightleftharpoons KF\cdot 3ThF_4 + ThF_4ss$

*It has been shown that the compound labeled by Asker *et al.* has the actual formula $7KF\cdot 6ThF_4$, cf. R. E. Thoma, *Crystal Structures of Some Compounds of* UF_4 *and* ThF_4 *with Alkali Fluorides*, ORNL CF-58-12-40 (December 11, 1958).

UNCLASSIFIED
ORNL—LR—DWG 18966

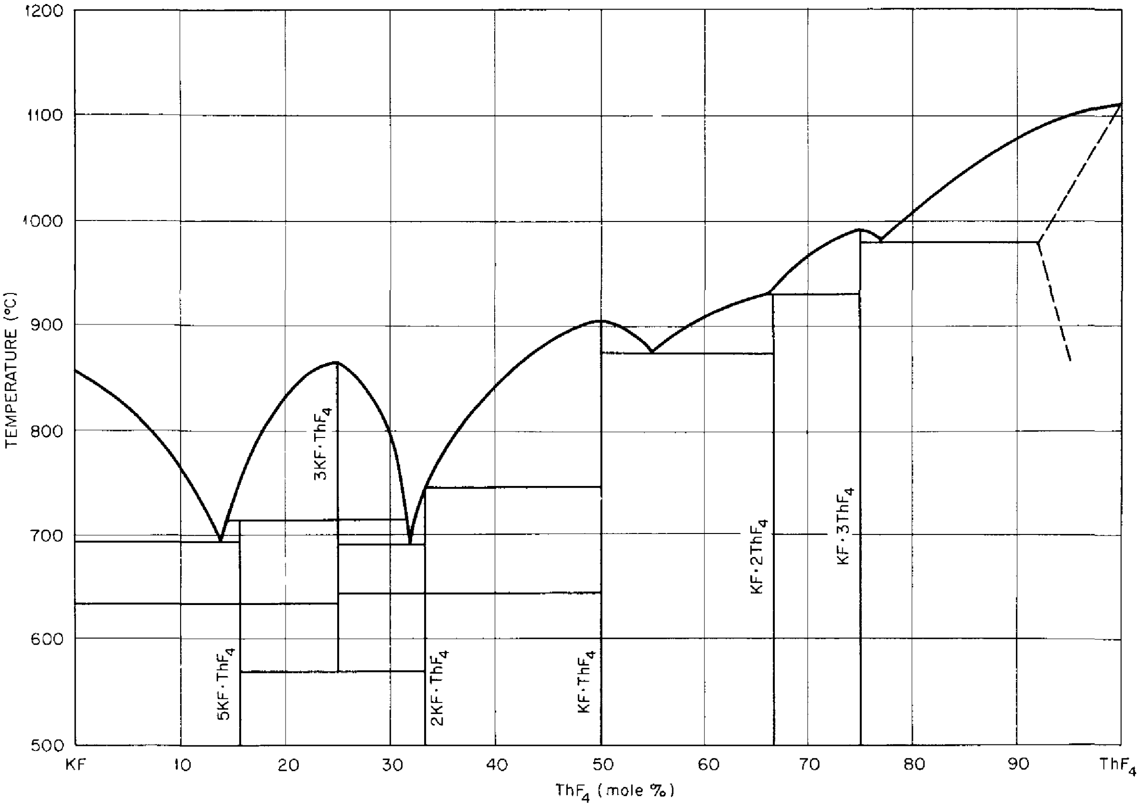

Fig. 3.46. The System KF–ThF_4.

3.47. The System RbF–ThF$_4$

E. P. Dergunov and A. G. Bergman, "Complex Formation Between Alkali Metal Fluorides and Fluorides of Metals of the Fourth Group," *Doklady Akad. Nauk S.S.S.R.* **60,** 391–94 (1948).

Invariant Equilibria

Mole % ThF$_4$ in Liquid	Invariant Temperature (°C)	Type of Equilibrium	Phase Reaction at Invariant Temperature
15	664	Eutectic	$L \rightleftharpoons$ RbF + 3RbF·ThF$_4$
25	974	Congruent melting point	$L \rightleftharpoons$ 3RbF·ThF$_4$
37	762	Eutectic	$L \rightleftharpoons$ 3RbF·ThF$_4$ + RbF·ThF$_4$
50	852	Congruent melting point	$L \rightleftharpoons$ RbF·ThF$_4$
54	848	Eutectic	$L \rightleftharpoons$ RbF·ThF$_4$ + RbF·3ThF$_4$
75	1004	Congruent melting point	$L \rightleftharpoons$ RbF·3ThF$_4$
80	1000	Eutectic	$L \rightleftharpoons$ RbF·3ThF$_4$ + ThF$_4$

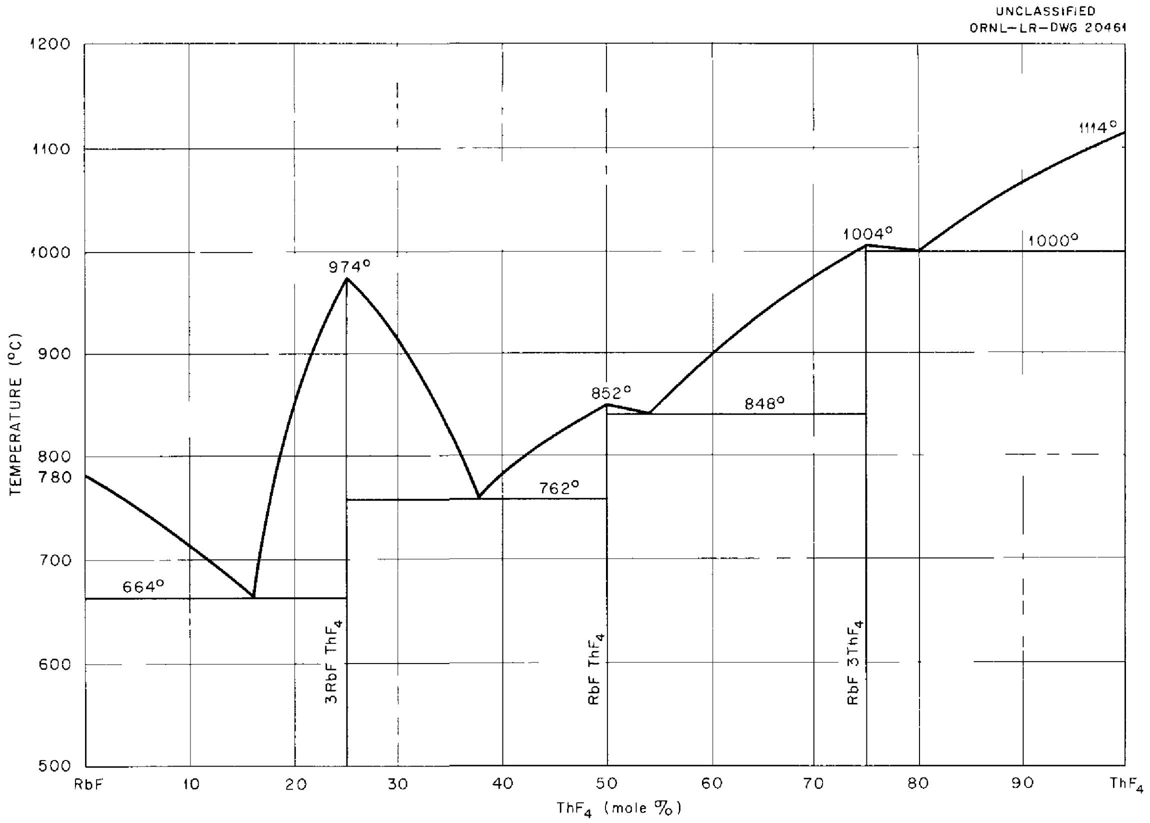

Fig. 3.47. The System RbF–ThF$_4$.

3.48. The System BeF_2–ThF_4

R. E. Thoma, H. Insley, H. A. Friedman, and C. F. Weaver, "Phase Equilibria in the Systems BeF_2–ThF_4 and LiF–BeF_2–ThF_4," paper to be presented at the 136th National Meeting of the American Chemical Society, Atlantic City, N. J., Sept. 13–18, 1959.

The system BeF_2–ThF_4 contains a single eutectic at 98.5 BeF_2–1.5 ThF_4 (mole %), m.p. 526 ± 3°C.

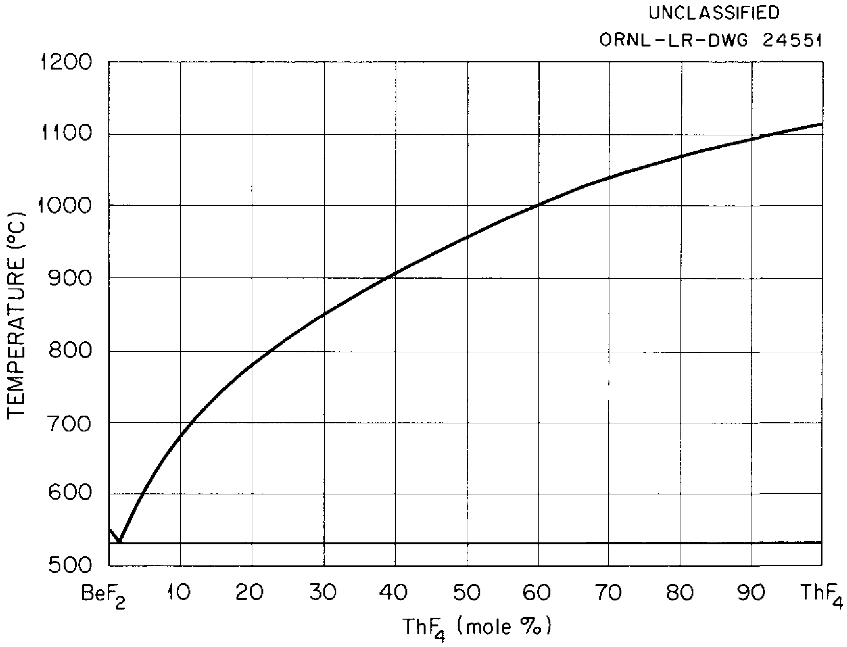

Fig. 3.48. The System BeF_2–ThF_4.

3.49. The System BeF_2–UF_4

T. B. Rhinehammer, P. A. Tucker, and E. F. Joy, *Phase Equilibria in the System* BeF_2–UF_4, MLM-1082 (to be published).

Preliminary diagram. The system BeF_2–UF_4 contains a single eutectic at 99.5 BeF_2–0.5 UF_4 (mole %), m.p. 535 ± 2°C.

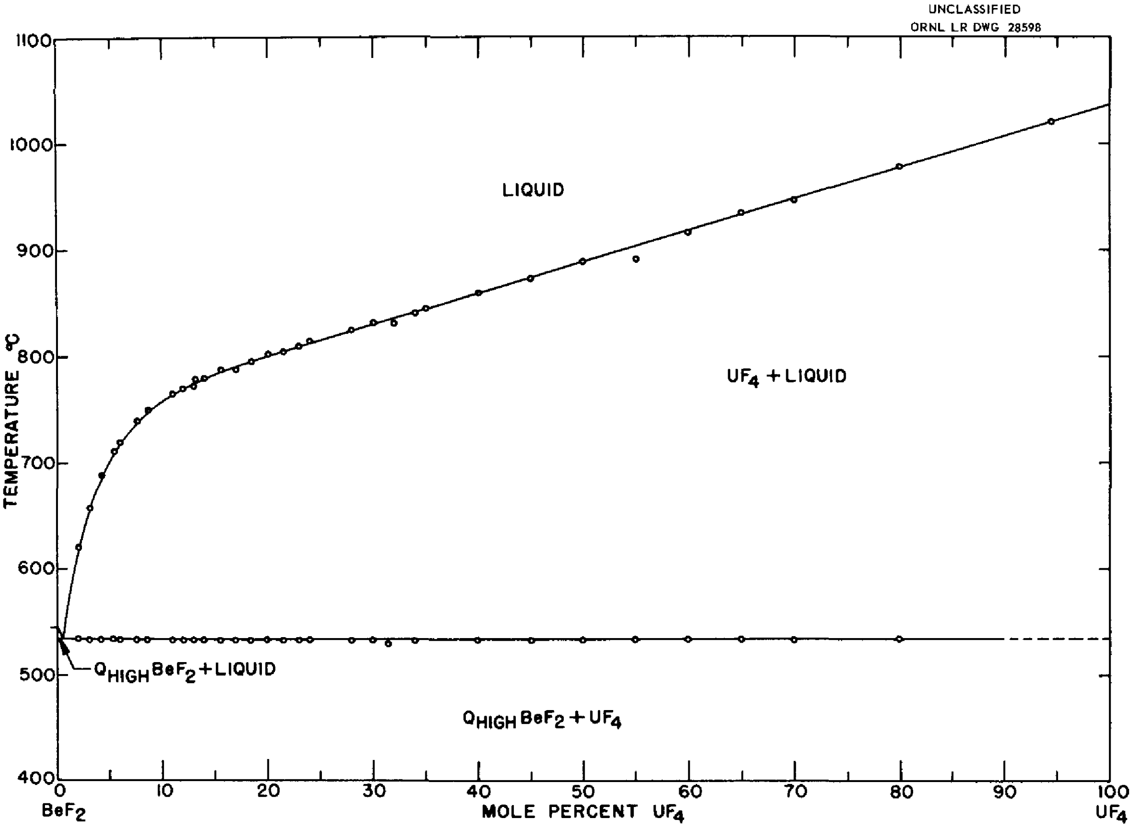

Fig. 3.49. The System BeF_2–UF_4.

3.50. The System MgF_2–ThF_4

J. O. Blomeke, *An Investigation of the ThF_4–Fused Salt Solutions for Homogeneous Reactors*, ORNL-1030 (June 19, 1951) (declassified with deletions).

Invariant Equilibria

Mole % ThF_4 in Liquid	Invariant Temperature (°C)	Type of Equilibrium	Phase Reaction at Invariant Temperature
25	915	Eutectic	$L \rightleftharpoons ThF_4 + MgF_2 \cdot 2ThF_4$
33.3	937	Congruent melting point	$L \rightleftharpoons MgF_2 \cdot 2ThF_4$
40	925	Eutectic	$L \rightleftharpoons MgF_2 \cdot 2ThF_4 + MgF_2$

UNCLASSIFIED
ORNL-LR-DWG 20465

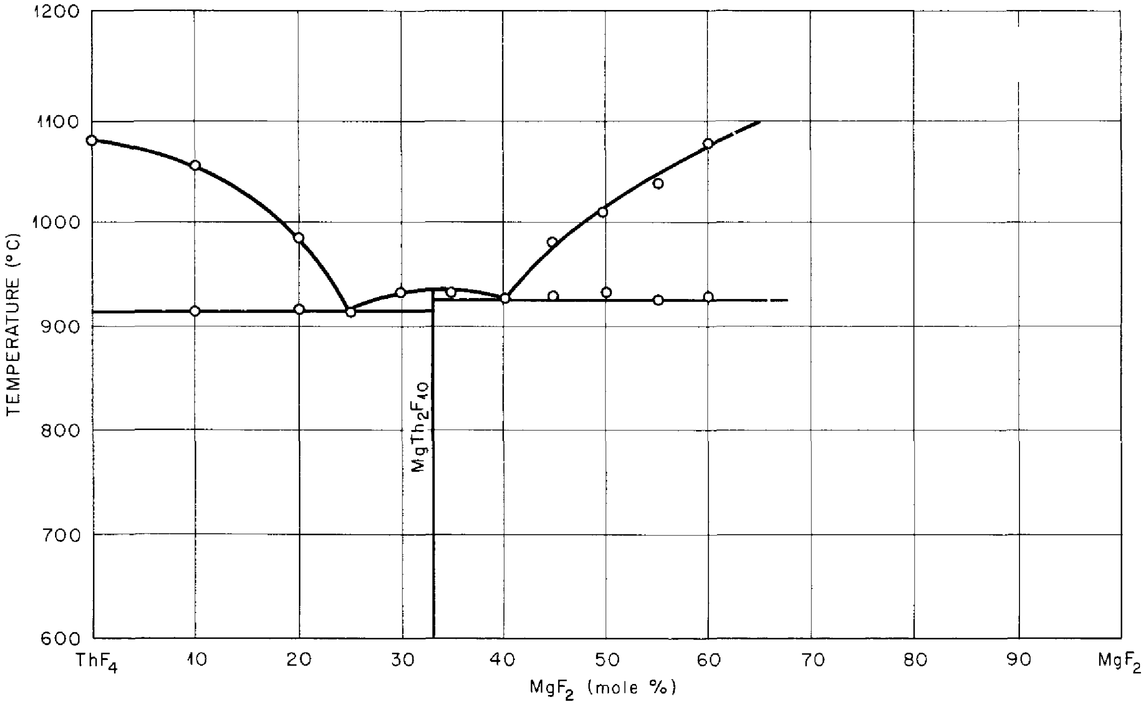

Fig. 3.50. The System MgF_2–ThF_4.

3.51. The System LiF–BeF_2–ThF_4

R. E. Thoma, H. Insley, H. A. Friedman, and C. F. Weaver, "Phase Equilibria in the Systems BeF_2–ThF_4 and LiF–BeF_2–ThF_4," paper to be presented at the 136th National Meeting of the American Chemical Society, Atlantic City, N. J., Sept. 13–18, 1959.

Invariant Equilibria

Composition of Liquid (mole %)			Invariant Temperature (°C)	Type of Invariant	Solids Present at Invariant Point
LiF	BeF_2	ThF_4			
15	83	2	497 ± 4	Peritectic	ThF_4, LiF·4ThF_4, and BeF_2
33.5	64	2.5	455 ± 4	Peritectic	LiF·4ThF_4, LiF·2ThF_4, and BeF_2
47	51.5	1.5	356 ± 6	Eutectic	2LiF·BeF_2, LiF·2ThF_4, and BeF_2
60.5	36.5	3	433 ± 5	Peritectic	LiF·2ThF_4, 3LiF·ThF_4*ss*, and 2LiF·BeF_2
65.5	30.5	4	444 ± 4	Peritectic	LiF, 2LiF·BeF_2, and 3LiF·ThF_4*ss*
63	30.5	6.5	448 ± 5	Peritectic	3LiF·ThF_4*ss*, 7LiF·6ThF_4, and LiF·2ThF_4

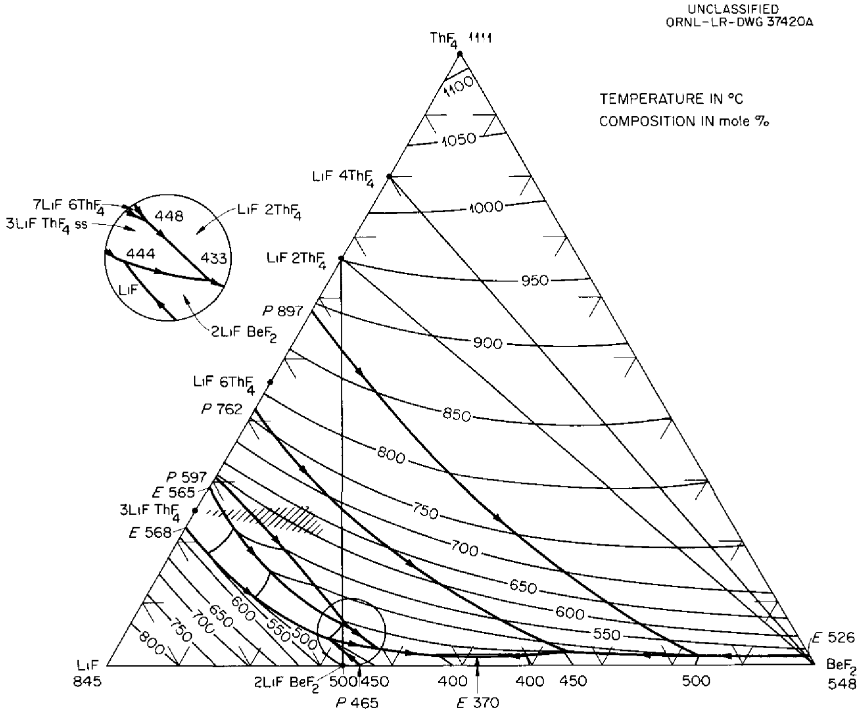

Fig. 3.51*a*. The System LiF–BeF_2–ThF_4.

Limits of Single-Phase $3LiF \cdot ThF_4$ Solid Solution

Composition (mole %)		
LiF	BeF_2	ThF_4
75	0	25
58	16	26
59	20	21

A three-dimensional model of the system $LiF-BeF_2-ThF_4$ is shown in Fig. 3.51*b*.

UNCLASSIFIED
PHOTO 32551

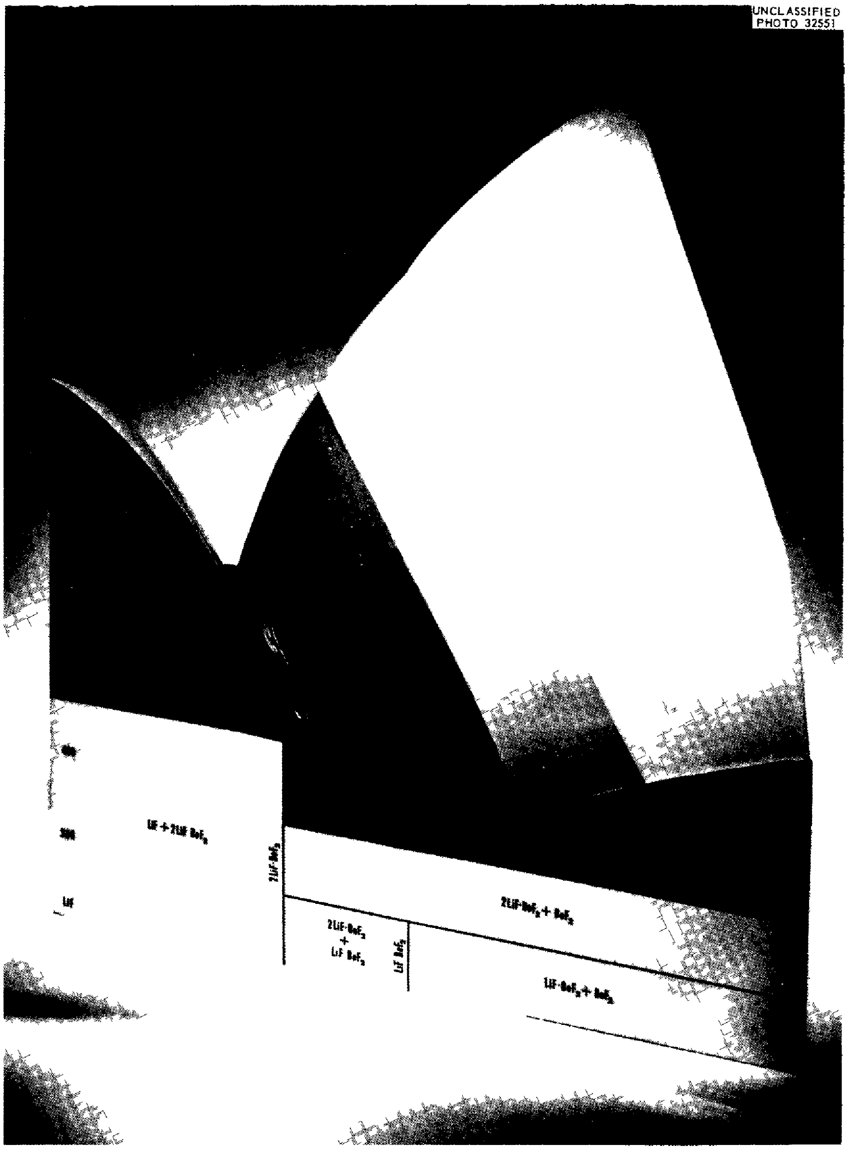

Fig. 3.51*b*. Model of the System $LiF-BeF_2-ThF_4$.

3.52. The System $NaF-ZrF_4-ThF_4$

R. E. Thoma, H. Insley, B. S. Landau, H. A. Friedman, and W. R. Grimes, unpublished work performed at the Oak Ridge National Laboratory, 1956–57.

Preliminary diagram.

Invariant Equilibria

Composition of Liquid (mole %)			Invariant Temperature (°C)	Type of Equilibrium	Solids Present at Invariant Point
NaF	ZrF_4	ThF_4			
77	3	20	645	Peritectic	NaF, α-$4NaF \cdot ThF_4$, and $3NaF \cdot ZrF_4$
75.5	2.5	22	618	Eutectic	α-$4NaF \cdot ThF_4$, $2NaF \cdot ThF_4$, and $3NaF \cdot ZrF_4$
63	6	31*	683	Decomposition point of $3NaF \cdot 2ThF_4$ in ternary system	$3NaF \cdot 2ThF_4$, $2NaF \cdot ThF_4$, and $NaF \cdot ThF_4$
65.5	21.5	13	622	Peritectic	$2NaF \cdot ThF_4$, $3NaF \cdot ZrF_4$, and $NaF \cdot ThF_4$
65.5	24.5	10	615	Peritectic	$3NaF \cdot ZrF_4$, $NaF \cdot ThF_4$, and α-$5NaF \cdot 2ZrF_4$
64.5	25.5	10	593	Peritectic	α-$5NaF \cdot 2ZrF_4$, $NaF \cdot ThF_4$, and $NaF \cdot 2ThF_4$
58	38	4	538	Peritectic	α-$5NaF \cdot 2ZrF_4$, α-$2NaF \cdot ZrF_4$, and $NaF \cdot 2ThF_4$
58	40	2	495	Eutectic	β-$2NaF \cdot ZrF_4$, $NaF \cdot 2ThF_4$, and $7NaF \cdot 6ZrF_4$–$3NaF \cdot 2ZrF_4$ *ss*
53	42	4	510	Peritectic	$NaF \cdot 2ThF_4$, $Th(Zr)F_4$ *ss* , and $7NaF \cdot 6ZrF_4$–$3NaF \cdot 2ThF_4$ *ss*
49.5	48	2.5	505	Eutectic	$7NaF \cdot 6ZrF_4$, $3NaF \cdot 4ZrF_4$, and $Zr(Th)F_4$ *ss*

*Approximate composition.

Note: The boundary curve maximum on the Alkemade line $7NaF \cdot 6ZrF_4$–ThF_4 is unlikely to fall exactly on this line, because pure ThF_4 does not occur along this line. Since ThF_4 forms solid solutions with both ZrF_4 and $NaF \cdot 2ThF_4$, it is not readily determined on which side of the Alkemade line this maximum occurs.

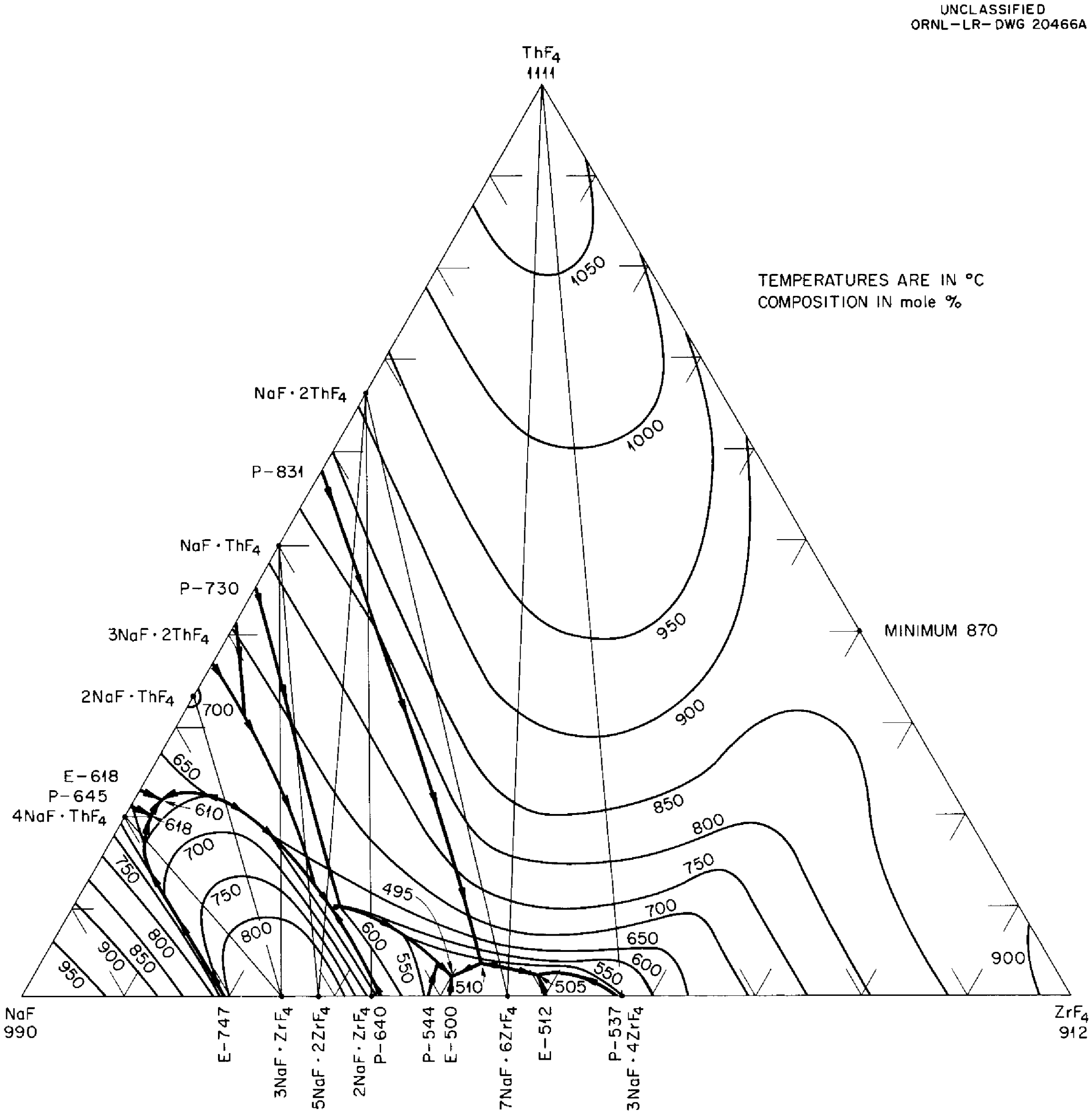

Fig. 3.52. The System NaF–ZrF$_4$–ThF$_4$.

3.53. The System LiF–UF_3

C. J. Barton, V. S. Coleman, L. M. Bratcher, and W. R. Grimes, unpublished work performed at the Oak Ridge National Laboratory, 1953–54.

Preliminary diagram. The system LiF–UF_3 contains a single eutectic at 73 LiF–27 UF_3 (mole %), m.p. 770°C.

UNCLASSIFIED
ORNL-LR-DWG 2923

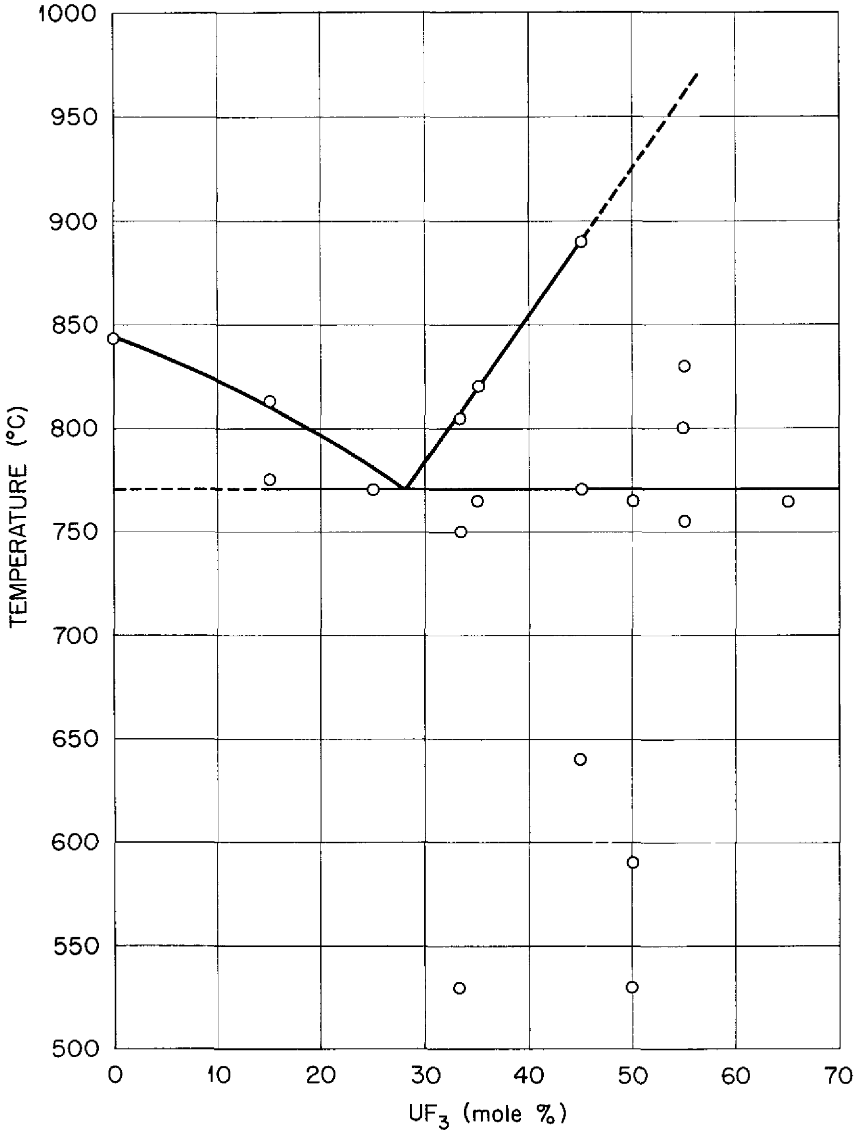

Fig. 3.53. The System LiF–UF_3.

3.54. The System LiF–UF_4

C. J. Barton, H. A. Friedman, W. R. Grimes, H. Insley, R. E. Moore, and R. E. Thoma, "Phase Equilibria in the Alkali Fluoride–Uranium Tetrafluoride Fused Salt Systems: I. The Systems LiF–UF_4 and NaF–UF_4," *J. Am. Ceram. Soc.* 41, 63–69 (1958).

Invariant Equilibria

Mole % UF_4 in Liquid	Invariant Temperature (°C)	Type of Equilibrium	Phase Reaction at Invariant Temperature
–	470	Decomposition	$4LiF{\cdot}UF_4 \rightleftharpoons LiF + 7LiF{\cdot}6UF_4$
26	500	Peritectic	$LiF + L \rightleftharpoons 4LiF{\cdot}UF_4$
27	490	Eutectic	$L \rightleftharpoons 4LiF{\cdot}UF_4 + 7LiF{\cdot}6UF_4$
40	610	Peritectic	$L + LiF{\cdot}4UF_4 \rightleftharpoons 7LiF{\cdot}6UF_4$
57	775	Peritectic	$L + UF_4 \rightleftharpoons LiF{\cdot}4UF_4$

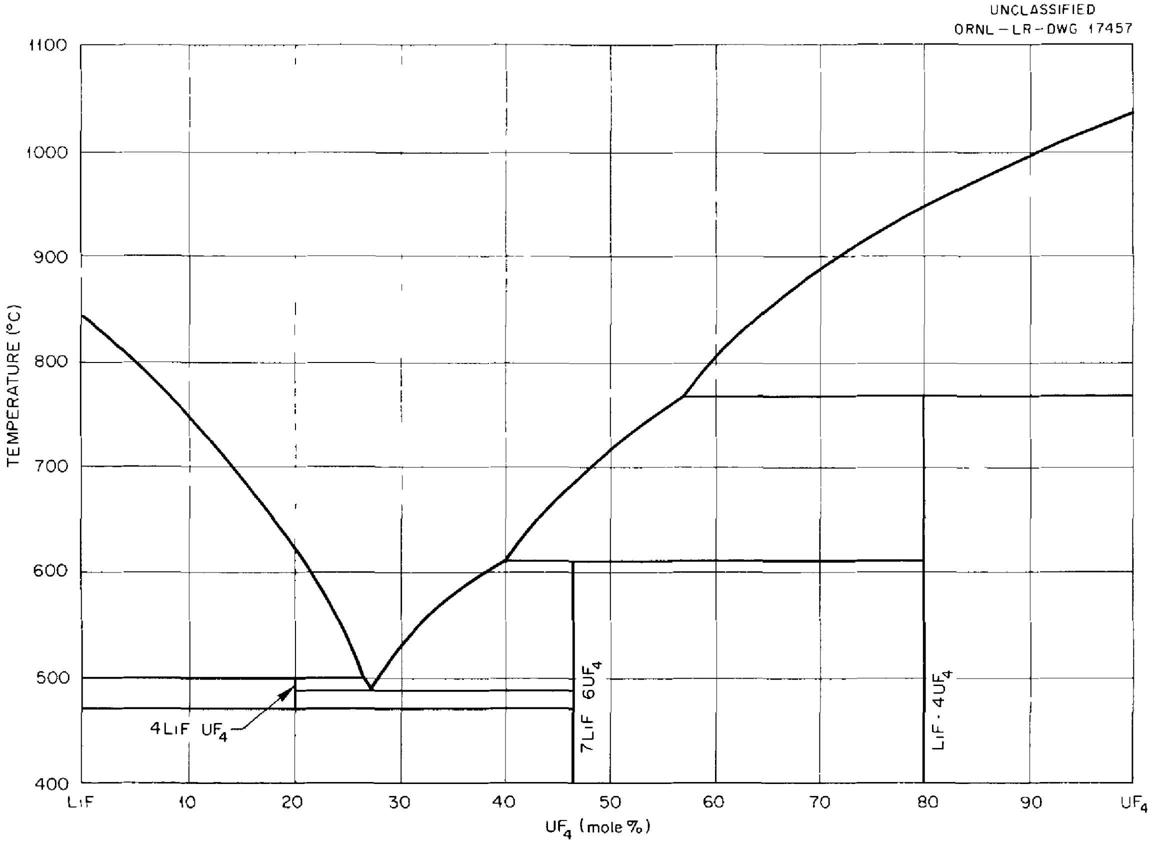

Fig. 3.54. The System LiF–UF_4.

3.55. The System NaF–UF_3

C. J. Barton, V. S. Coleman, T. N. McVay, and W. R. Grimes, unpublished work performed at the Oak Ridge National Laboratory, 1953–54.

Preliminary diagram.

Invariant Equilibria

Mole % UF_3 in Liquid	Invariant Temperature (°C)	Type of Equilibrium	Phase Reaction at Invariant Temperature
27	715	Eutectic	$L \rightleftharpoons \text{NaF} + \alpha\text{-NaF}\cdot\text{UF}_3$
35	775	Peritectic	$L + \text{UF}_3 \rightleftharpoons \alpha\text{-NaF}\cdot\text{UF}_3$
–	595	Inversion	$\alpha\text{-NaF}\cdot\text{UF}_3 \rightleftharpoons \beta\text{-NaF}\cdot\text{UF}_3$

UNCLASSIFIED
ORNL-LR-DWG 2924R

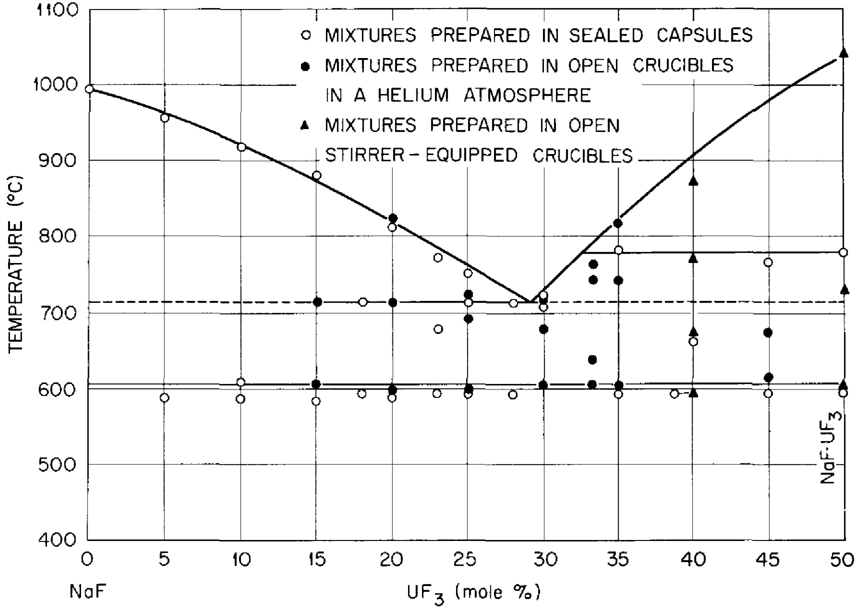

Fig. 3.55. The System $NaF-UF_3$.

3.56. The System $NaF–UF_4$

C. J. Barton, H. A. Friedman, W. R. Grimes, H. Insley, R. E. Moore, and R. E. Thoma, "Phase Equilibria in the Alkali Fluoride–Uranium Tetrafluoride Fused Salt Systems: I. The Systems $LiF–UF_4$ and $NaF–UF_4$," *J. Am. Ceram. Soc.* 41, 63–69 (1958).

Invariant Equilibria

Mole % UF_4 in Liquid	Invariant Temperature (°C)	Type of Equilibrium	Phase Reaction at Invariant Temperature
21.5	618	Eutectic	$L \rightleftharpoons \alpha\text{-}3NaF \cdot UF_4 + NaF$
25	629	Congruent melting point	$L \rightleftharpoons \alpha\text{-}3NaF \cdot UF_4$
–	528	Inversion	$\alpha\text{-}3NaF \cdot UF_4 \rightleftharpoons \beta\text{-}3NaF \cdot UF_4$
–	497	Decomposition	$\beta\text{-}3NaF \cdot UF_4 \rightleftharpoons NaF + 2NaF \cdot UF_4$
28	623	Eutectic	$L \rightleftharpoons \alpha\text{-}3NaF \cdot UF_4 + 2NaF \cdot UF_4$
32.5	648	Peritectic	$L + 5NaF \cdot 3UF_4 \rightleftharpoons 2NaF \cdot UF_4$
37	673	Peritectic	$L + 7NaF \cdot 6UF_4 \rightleftharpoons 5NaF \cdot 3UF_4$
–	630	Decomposition	$5NaF \cdot 3UF_4 \rightleftharpoons 2NaF \cdot UF_4 + 7NaF \cdot 6UF_4$
46.2	718	Congruent melting point	$L \rightleftharpoons 7NaF \cdot 6UF_4$
56	680	Eutectic	$L \rightleftharpoons 7NaF \cdot 6UF_4 + UF_4$
–	660	Upper stability limit of $NaF \cdot 2UF_4$	$7NaF \cdot 6UF_4 + UF_4 \rightleftharpoons NaF \cdot 2UF_4$

UNCLASSIFIED
ORNL-LR-DWG 19364

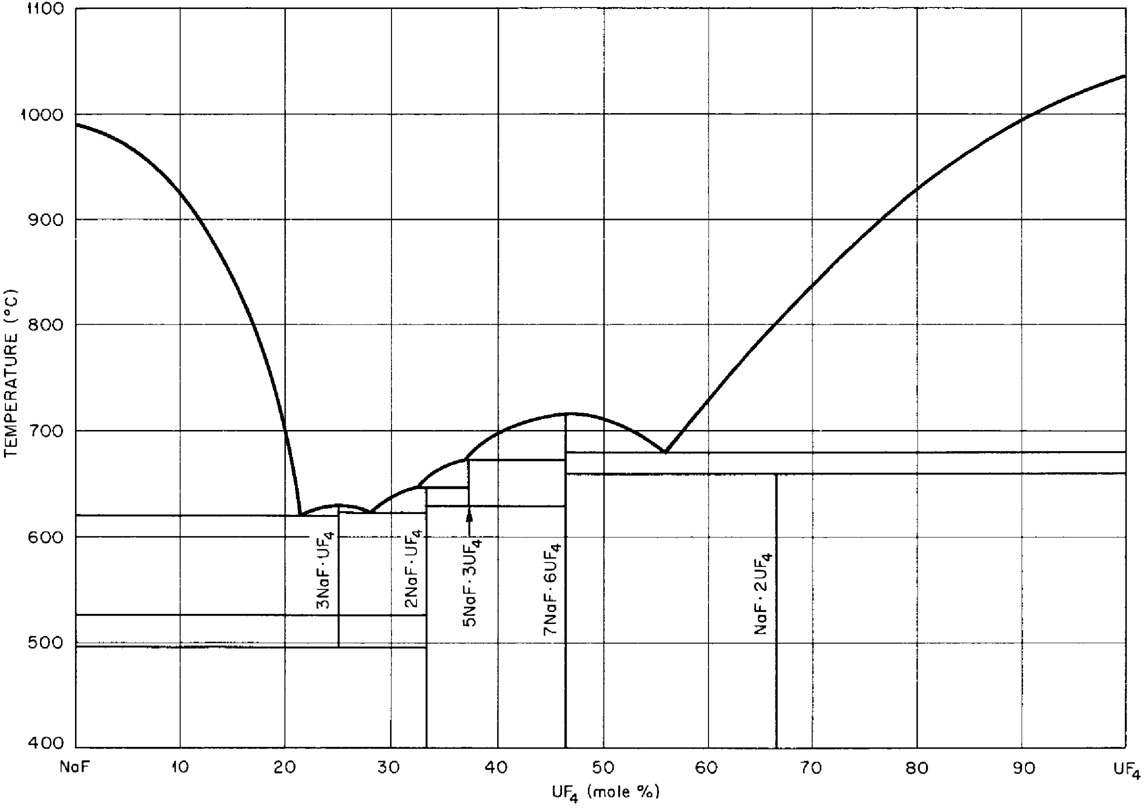

Fig. 3.56. The System NaF–UF_4.

3.57. The System $KF-UF_4$

R. E. Thoma, H. Insley, B. S. Landau, H. A. Friedman, and W. R. Grimes, "Phase Equilibria in the Alkali Fluoride–Uranium Tetrafluoride Fused Salt Systems: II. The Systems $KF-UF_4$ and $RbF-UF_4$," *J. Am. Ceram. Soc.* **41,** 538–44 (1958).

Invariant Equilibria

Mole % UF_4 in Liquid	Invariant Temperature (°C)	Type of Equilibrium	Phase Reaction at Invariant Temperature
15	735	Eutectic	$L \rightleftharpoons KF + 3KF \cdot UF_4$
25	957	Congruent melting point	$L \rightleftharpoons 3KF \cdot UF_4$
–	608	Decomposition	$2KF \cdot UF_4 \rightleftharpoons 3KF \cdot UF_4 + 7KF \cdot 6UF_4$
35	755	Peritectic	$3KF \cdot UF_4 + L \rightleftharpoons 2KF \cdot UF_4$
38.5	740	Eutectic	$L \rightleftharpoons 2KF \cdot UF_4 + 7KF \cdot 6UF_4$
46.2	789	Congruent melting point	$L \rightleftharpoons 7KF \cdot 6UF_4$
54.5	735	Eutectic	$L \rightleftharpoons 7KF \cdot 6UF_4 + KF \cdot 2UF_4$
65	765	Peritectic	$UF_4 + L \rightleftharpoons KF \cdot 2UF_4$

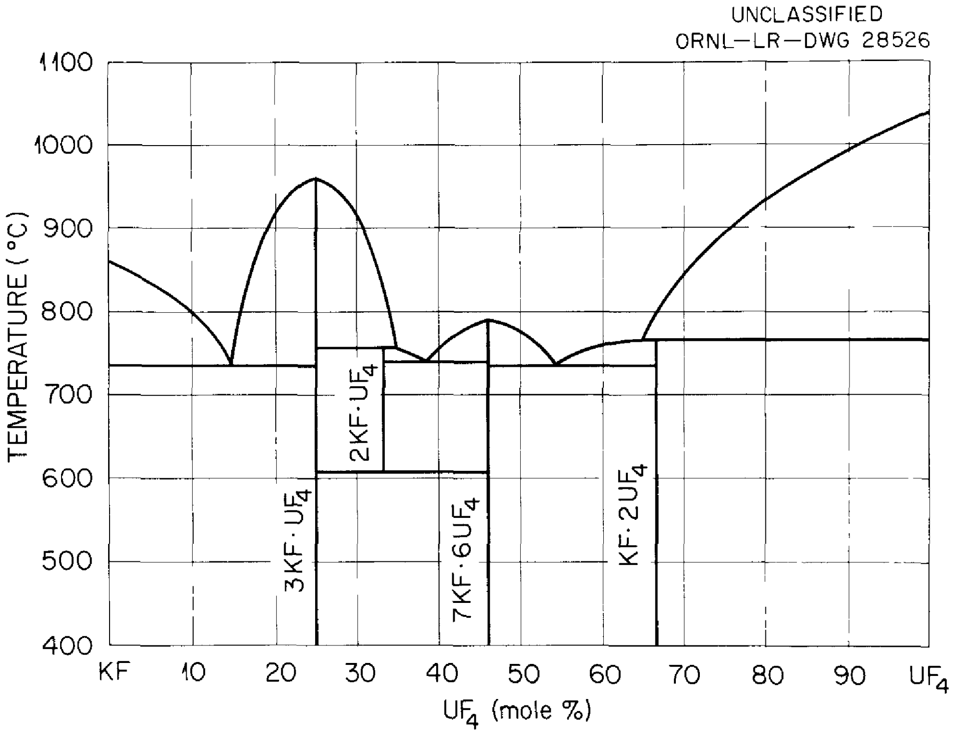

Fig. 3.57. The System $KF-UF_4$.

3.58. The System RbF–UF_4

R. E. Thoma, H. Insley, B. S. Landau, H. A. Friedman, and W. R. Grimes, "Phase Equilibria in the Alkali Fluoride–Uranium Tetrafluoride Fused Salt Systems: II. The Systems KF–UF_4 and RbF–UF_4," *J. Am. Ceram. Soc.* **41,** 538–44 (1958).

Invariant Equilibria

Mole % UF_4 in Liquid	Invariant Temperature (°C)	Type of Equilibrium	Phase Reaction at Invariant Temperature
10	710	Eutectic	$L \rightleftharpoons RbF + 3RbF\cdot UF_4$
25	995	Congruent melting point	$L \rightleftharpoons 3RbF\cdot UF_4$
38	818	Peritectic	$L + 3RbF\cdot UF_4 \rightleftharpoons 2RbF\cdot UF_4$
43.5	675	Eutectic	$L \rightleftharpoons 2RbF\cdot UF_4 + 7RbF\cdot 6UF_4$
44	693	Peritectic	$RbF\cdot UF_4 + L \rightleftharpoons 7RbF\cdot 6UF_4$
50	735	Congruent melting point	$L \rightleftharpoons RbF\cdot UF_4$
55	714	Eutectic	$L \rightleftharpoons RbF\cdot UF_4 + 2RbF\cdot 3UF_4$
56.5	722	Peritectic	$RbF\cdot 3UF_4 + L \rightleftharpoons 2RbF\cdot 3UF_4$
57	730	Peritectic	$RbF\cdot 6UF_4 + L \rightleftharpoons RbF\cdot 3UF_4$
70.5	832	Peritectic	$UF_4 + L \rightleftharpoons RbF\cdot 6UF_4$

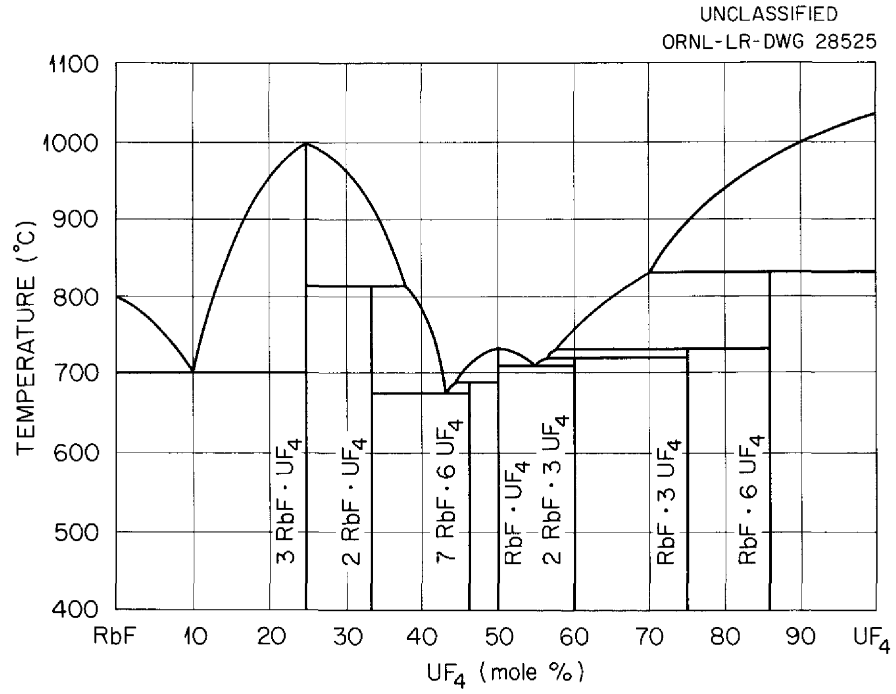

Fig. 3.58. The System RbF–UF_4.

3.59. The System $CsF-UF_4$

C. J. Barton, L. M. Bratcher, J. P. Blakely, G. J. Nessle, and W. R. Grimes, unpublished work performed at the Oak Ridge National Laboratory, 1951–53.

Preliminary diagram.

Invariant Equilibria

Mole % UF_4 in Liquid	Invariant Temperature (°C)	Type of Equilibrium	Phase Reaction at Invariant Temperature
7.5	650	Eutectic	$L \rightleftharpoons CsF + 3CsF \cdot UF_4$
25	970	Congruent melting point	$L \rightleftharpoons 3CsF \cdot UF_4$
34	800	Peritectic	$L + 3CsF \cdot UF_4 \rightleftharpoons 2CsF \cdot UF_4$
41	695	Eutectic	$L \rightleftharpoons 2CsF \cdot UF_4 + \alpha\text{-}CsF \cdot UF_4$
50	735	Congruent melting point	$L \rightleftharpoons \alpha\text{-}CsF \cdot UF_4$
–	550	Inversion	$\alpha\text{-}CsF \cdot UF_4 \rightleftharpoons \beta\text{-}CsF \cdot UF_4$
53	725	Eutectic	$L \rightleftharpoons \alpha\text{-}CsF \cdot UF_4 + UF_4$

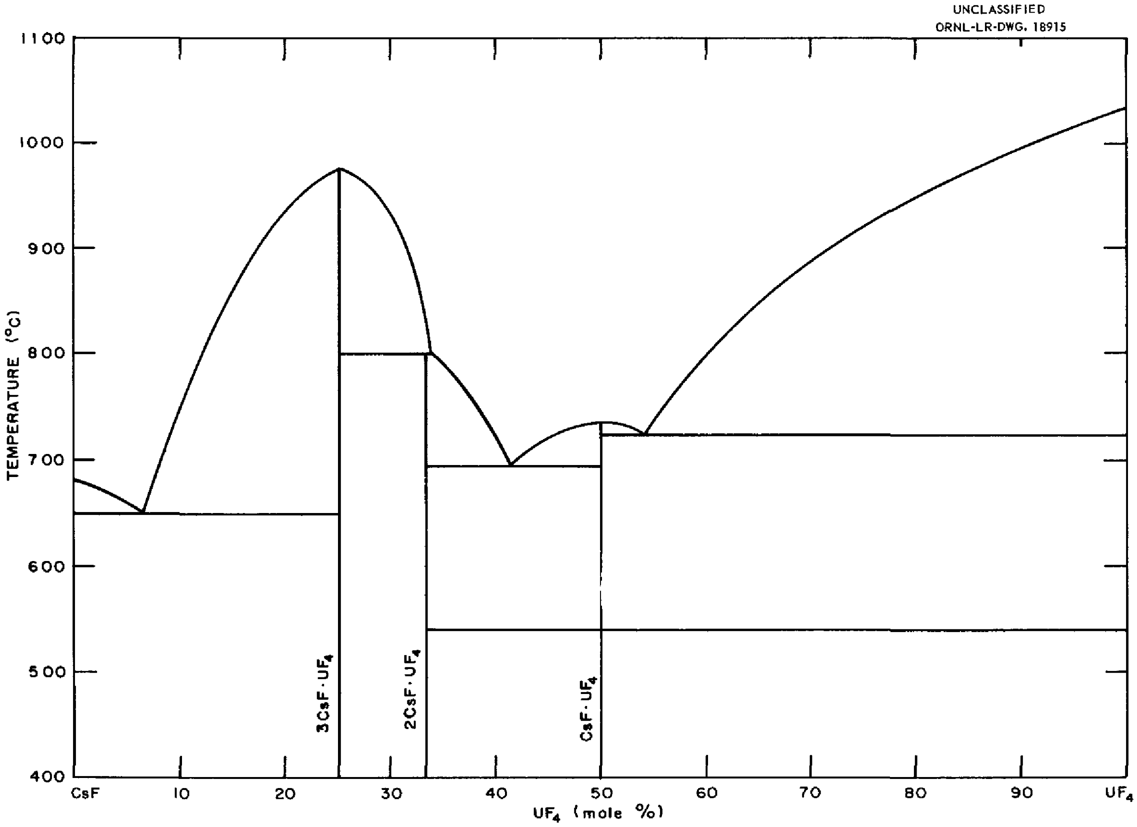

Fig. 3.59. The System $CsF-UF_4$.

3.60. The System ZrF_4–UF_4

C. J. Barton, W. R. Grimes, H. Insley, R. E. Moore, and R. E. Thoma, "Phase Equilibria in the Systems NaF–ZrF_4, UF_4–ZrF_4, and NaF–ZrF_4–UF_4," *J. Phys. Chem.* **62,** 665–76 (1958).

The system ZrF_4–UF_4 forms a continuous series of solid solutions having a minimum melting temperature of 765°C at 77 ZrF_4–23 UF_4 (mole %).

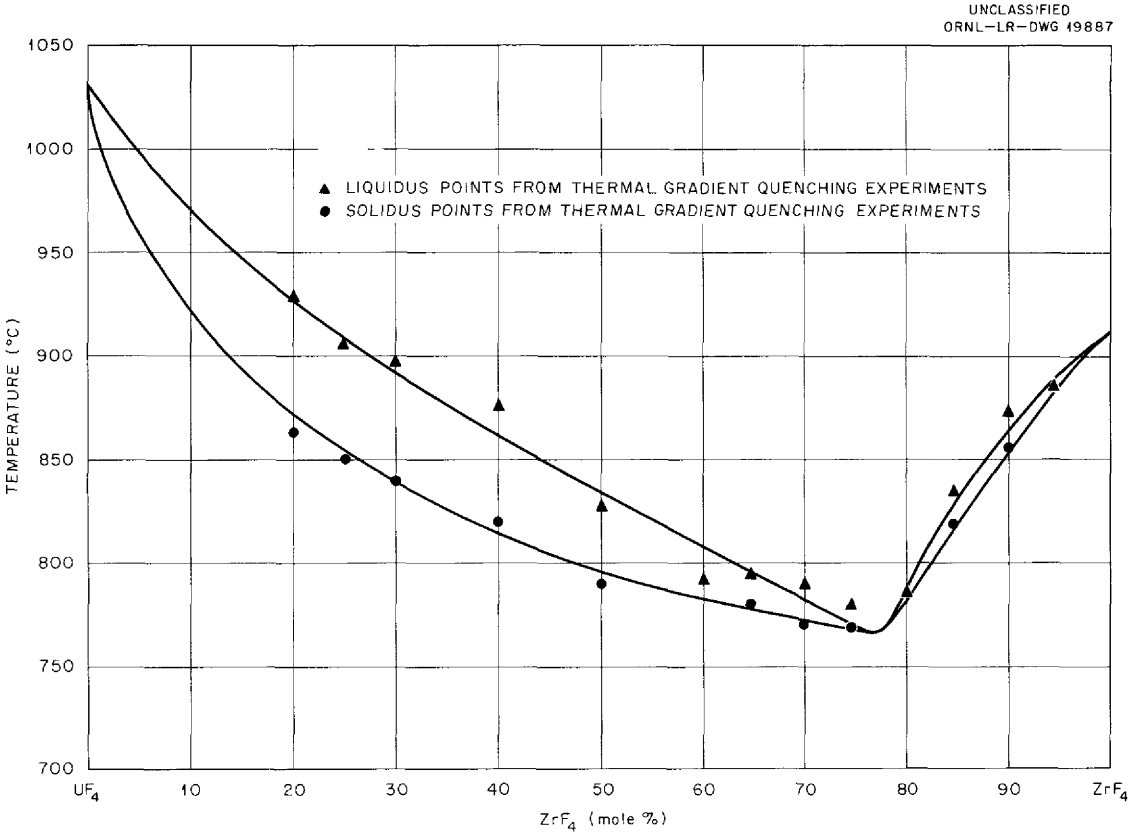

Fig. 3.60. The System ZrF_4–UF_4.

3.61. The System SnF_2–UF_4

B. J. Thamer and G. E. Meadows, *The Systems UF_4–SnF_2 and PuF_3–SnF_2*, LA-2286 (July 1959).

Invariant Equilibria

Mole % UF_4 in Liquid	Invariant Temperature (°C)	Type of Equilibrium	Phase Reaction at Invariant Temperature
0.5	212	Eutectic	$L \rightleftharpoons SnF_2 + 2SnF_2{\cdot}UF_4$
4.5	340	Peritectic	$L + SnF_2{\cdot}UF_4 \rightleftharpoons 2SnF_2{\cdot}UF_4$
7.8	371	Peritectic	$L + UF_4 \rightleftharpoons SnF_2{\cdot}UF_4$

UNCLASSIFIED
ORNL-LR-DWG 36864

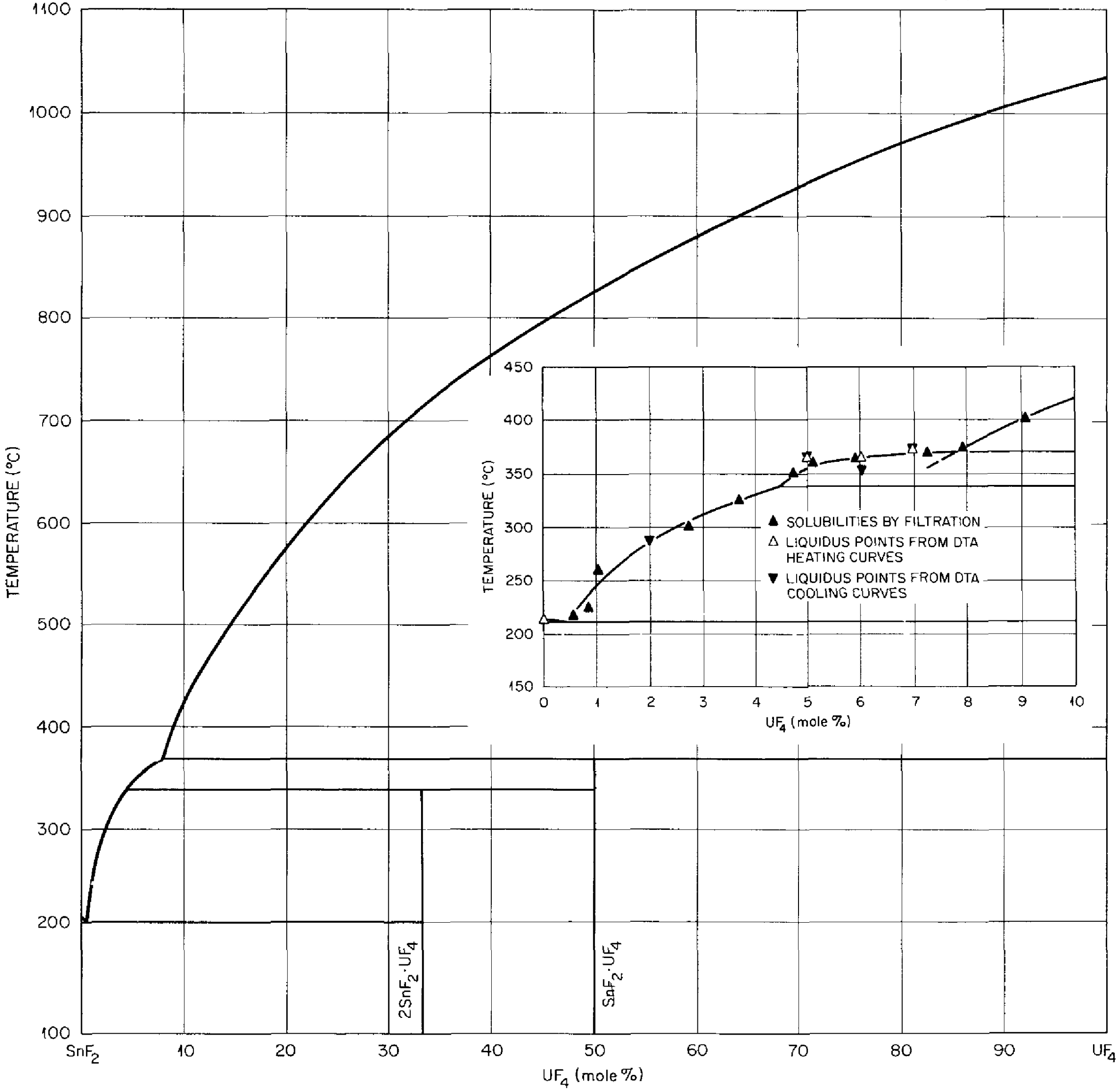

Fig. 3.61. The System SnF_2–UF_4.

3.62. The System PbF_2–UF_4

C. J. Barton, L. M. Bratcher, J. P. Blakely, G. J. Nessle, and W. R. Grimes, unpublished work performed at the Oak Ridge National Laboratory, 1950–51.

Preliminary diagram.

Invariant Equilibria

Mole % UF_4 in Liquid	Invariant Temperature (°C)	Type of Equilibrium	Phase Reaction at Invariant Temperature
14.3	920	Congruent melting point	$L \rightleftharpoons 6PbF_2 \cdot UF_4$
35	835	Eutectic	$L \rightleftharpoons 6PbF_2 \cdot UF_4 + 3PbF_2 \cdot 2UF_4$
40	840	Congruent melting point	$L \rightleftharpoons 3PbF_2 \cdot 2UF_4$
62	762 ± 10	Eutectic	$L \rightleftharpoons 3PbF_2 \cdot 2UF_4 + UF_4$

The eutectic at quite high PbF_2 concentrations is not shown on this diagram. The authors examined thermal data but found no evidence of a eutectic thermal effect.

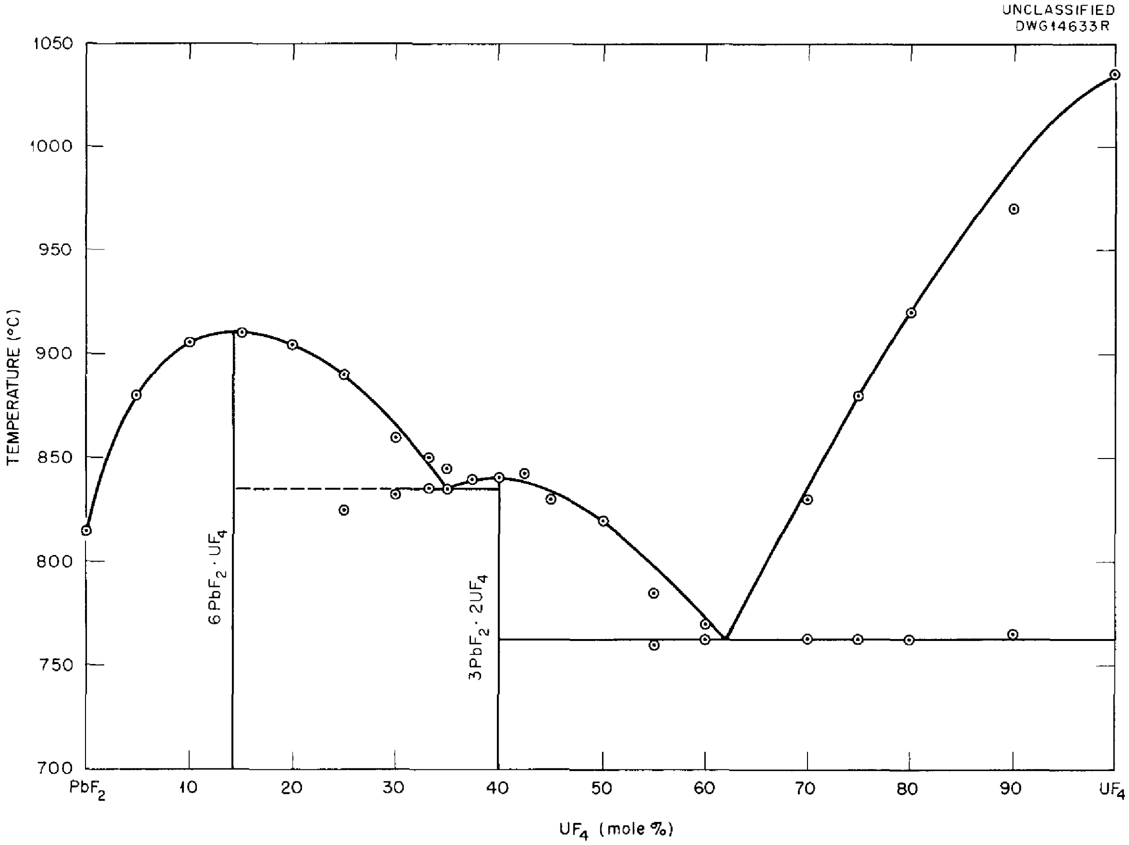

Fig. 3.62. The System PbF_2–UF_4.

3.63. The System ThF_4–UF_4

C. F. Weaver, R. E. Thoma, H. A. Friedman, and H. Insley, "Phase Equilibria in the Systems UF_4–ThF_4 and LiF–ThF_4–UF_4," paper presented at the 61st National Meeting of the American Ceramic Society, Chicago, Ill., May 17–21, 1959.

The system ThF_4–UF_4 forms a continuous series of solid solutions without a minimum.

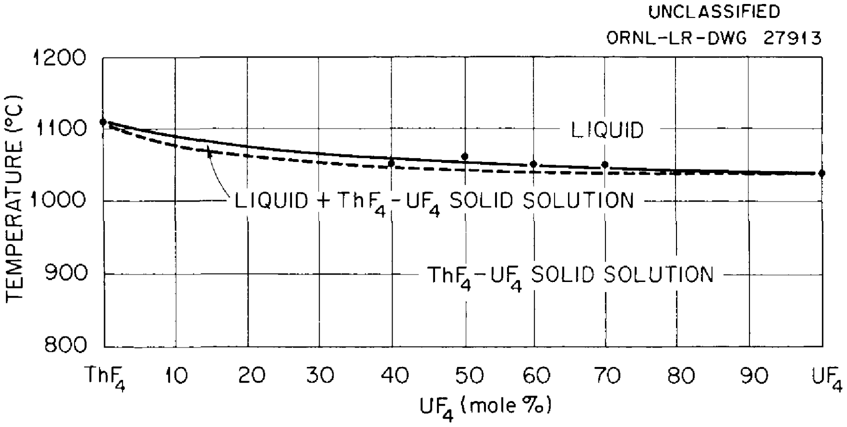

Fig. 3.63. The System ThF_4–UF_4.

3.64. The System $LiF-NaF-UF_4$

R. E. Thoma, H. Insley, B. S. Landau, H. A. Friedman, and W. R. Grimes, "Phase Equilibria in the Alkali Fluoride–Uranium Tetrafluoride Fused Salt Systems: III. The System $NaF-LiF-UF_4$," *J. Am. Ceram. Soc.* **42,** 21–26 (1959).

Invariant Equilibria

Composition of Liquid (mole %)			Invariant Temperature (°C)	Type of Equilibrium	Solid Phases Present at Invariant Point
NaF	LiF	UF_4			
60	21	19	480	Eutectic	$2NaF \cdot UF_4$, NaF, and LiF
65	13	22	497	Peritectic	β-$3NaF \cdot UF_4$, $2NaF \cdot UF_4$, and NaF
7	65.5	27.5	470	Peritectic	$7LiF \cdot 6UF_4$*ss*,* $4LiF \cdot UF_4$, and LiF
35	37	28	480	Eutectic	$2NaF \cdot UF_4$, $7NaF \cdot 6UF_4$*ss*, and LiF
57	13	30	630	Peritectic	$2NaF \cdot UF_4$, $5NaF \cdot 3UF_4$, and $7NaF \cdot 6UF_4$*ss*
24.3	43.5	32.2	445	Eutectic	$7NaF \cdot 6UF_4$*ss*, LiF, and $7LiF \cdot 6UF_4$*ss*
24.5	29	46.5	602	Eutectic	$NaF \cdot 2UF_4$, $7LiF \cdot 6UF_4$*ss*, and $7NaF \cdot 6UF_4$*ss*
24.3	28.7	47	605	Peritectic	$NaF \cdot 2UF_4$, $LiF \cdot 4UF_4$, and $7LiF \cdot 6UF_4$*ss*
23.5	28	48.5	640	Peritectic	UF_4, $NaF \cdot 2UF_4$, and $LiF \cdot 4UF_4$
37.5	10.5	52	660	Peritectic	UF_4, $NaF \cdot 2UF_4$, and $7NaF \cdot 6UF_4$*ss*

*The compounds $7LiF \cdot 6UF_4$ and $7NaF \cdot 6UF_4$ as they occur in the ternary system are members of the solid solution $7LiF \cdot 6UF_4-7NaF \cdot 6UF_4$.

UNCLASSIFIED
ORNL-LR-DWG 28214R

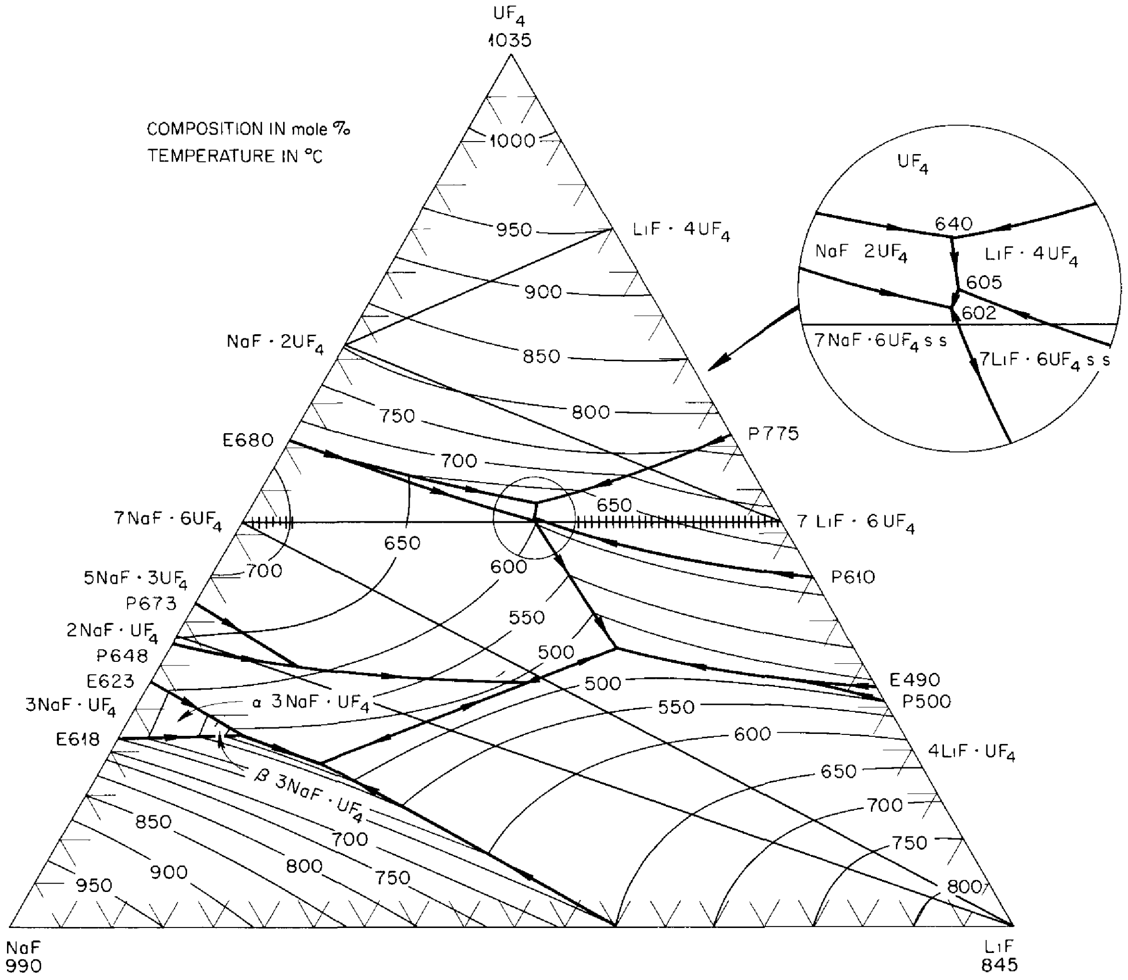

Fig. 3.64*a*. The System $LiF-NaF-UF_4$.

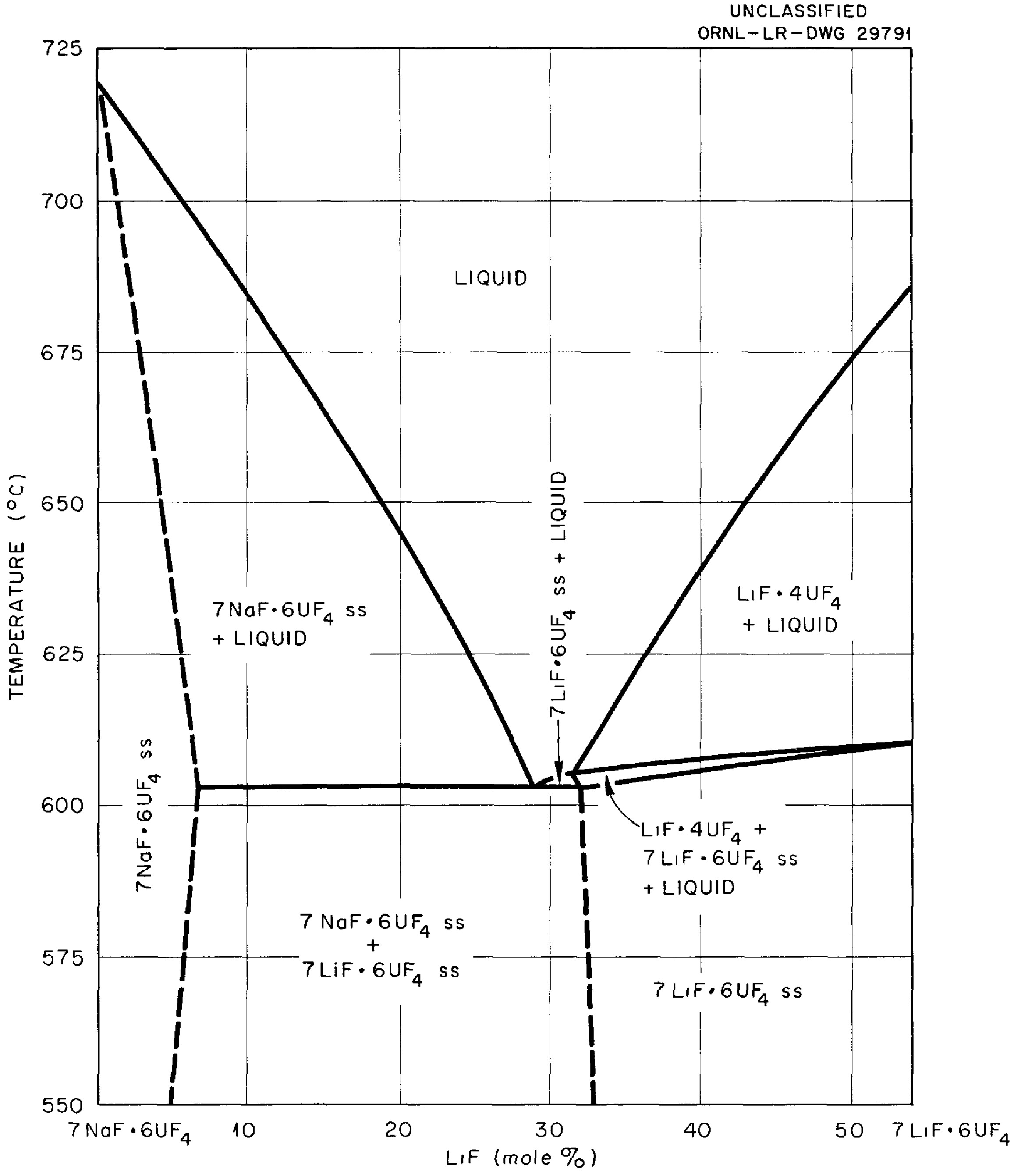

Fig. 3.64b. The Join $7NaF{\cdot}6UF_4$–$7LiF{\cdot}6UF_4$.

3.65. The System LiF–KF–UF$_4$

C. J. Barton, J. P. Blakely, L. M. Bratcher, and W. R. Grimes, unpublished work performed at the Oak Ridge National Laboratory, 1950–51.

Preliminary diagram. The system LiF–KF–UF$_4$ has not yet been defined at the Oak Ridge National Laboratory with sufficient precision to permit the temperatures and compositions of the invariant equilibria to be listed.

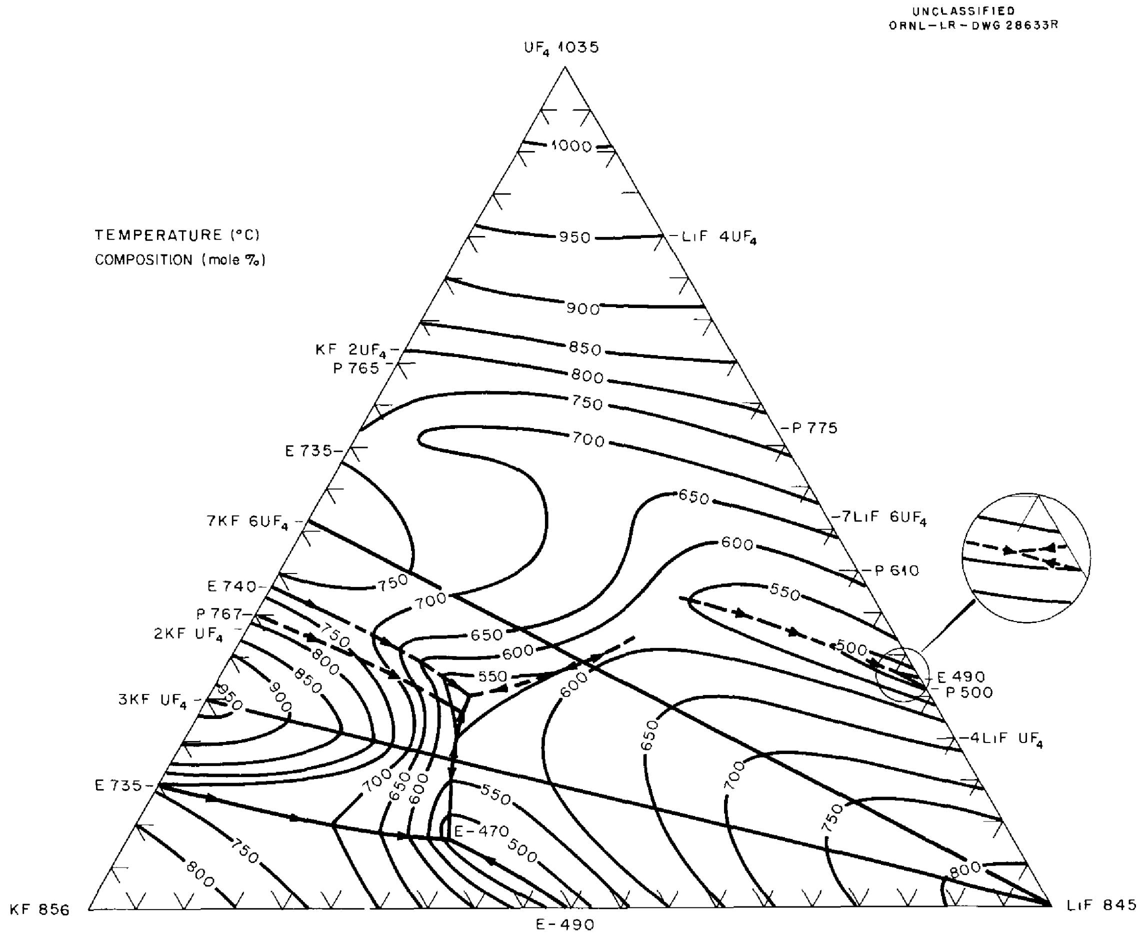

Fig. 3.65. The System LiF–KF–UF$_4$.

3.66. The System LiF–RbF–UF_4

C. J. Barton, J. P. Blakely, L. M. Bratcher, and W. R. Grimes, unpublished work performed at the Oak Ridge National Laboratory, 1950–51.

Preliminary diagram. Phase relationships within the system LiF–RbF–UF_4 have not yet become so well defined at the Oak Ridge National Laboratory that the compositions and temperatures of the invariant points may be listed.

UNCLASSIFIED
ORNL-LR-DWG 28634R

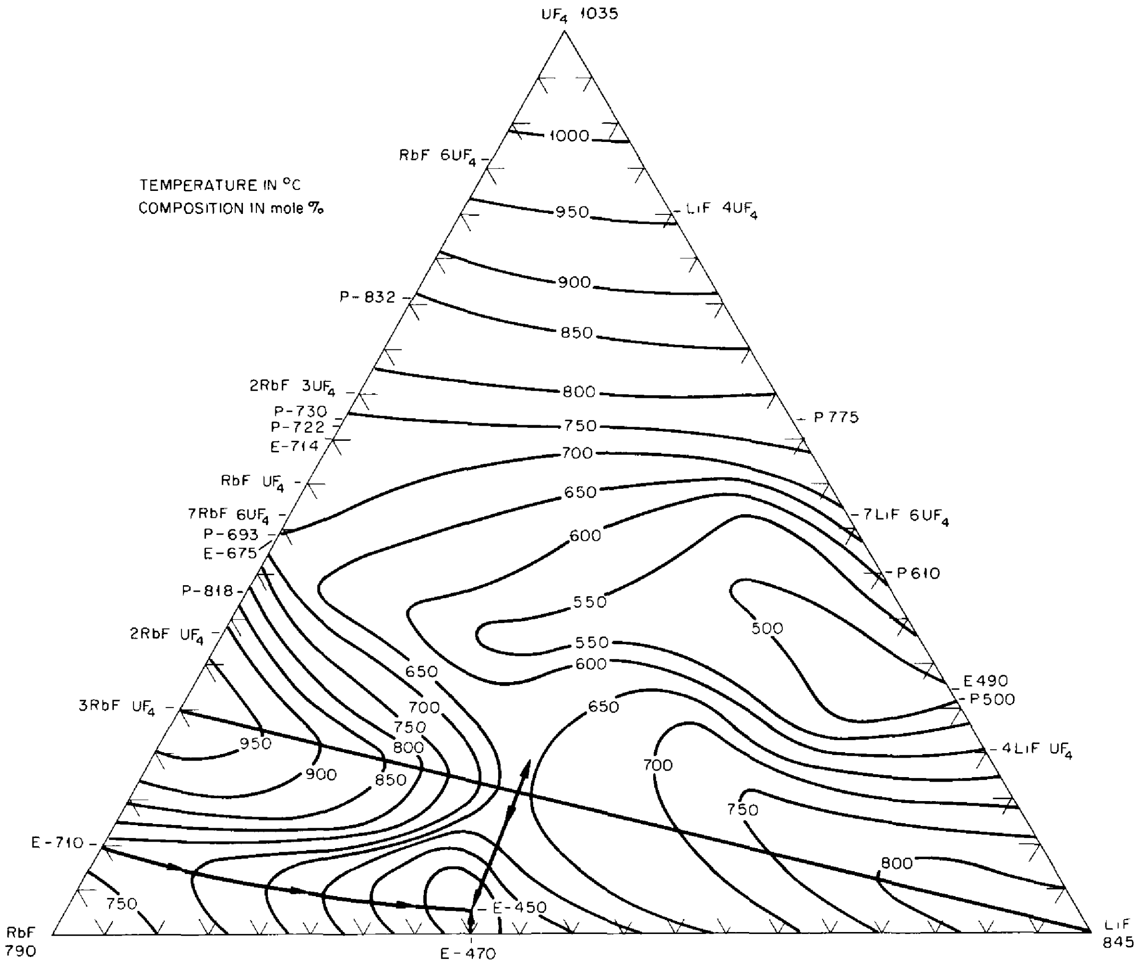

Fig. 3.66. The System LiF–RbF–UF_4.

3.67. The System NaF–KF–UF_4

R. E. Thoma, C. J. Barton, J. P. Blakely, R. E. Moore, G. J. Nessle, H. Insley, and H. A. Friedman, unpublished work performed at the Oak Ridge National Laboratory, 1950–58.

Preliminary diagram. Phase relationships within the system NaF–KF–UF_4 have not yet become so well defined at the Oak Ridge National Laboratory that the compositions and temperatures of the invariant points may be listed.

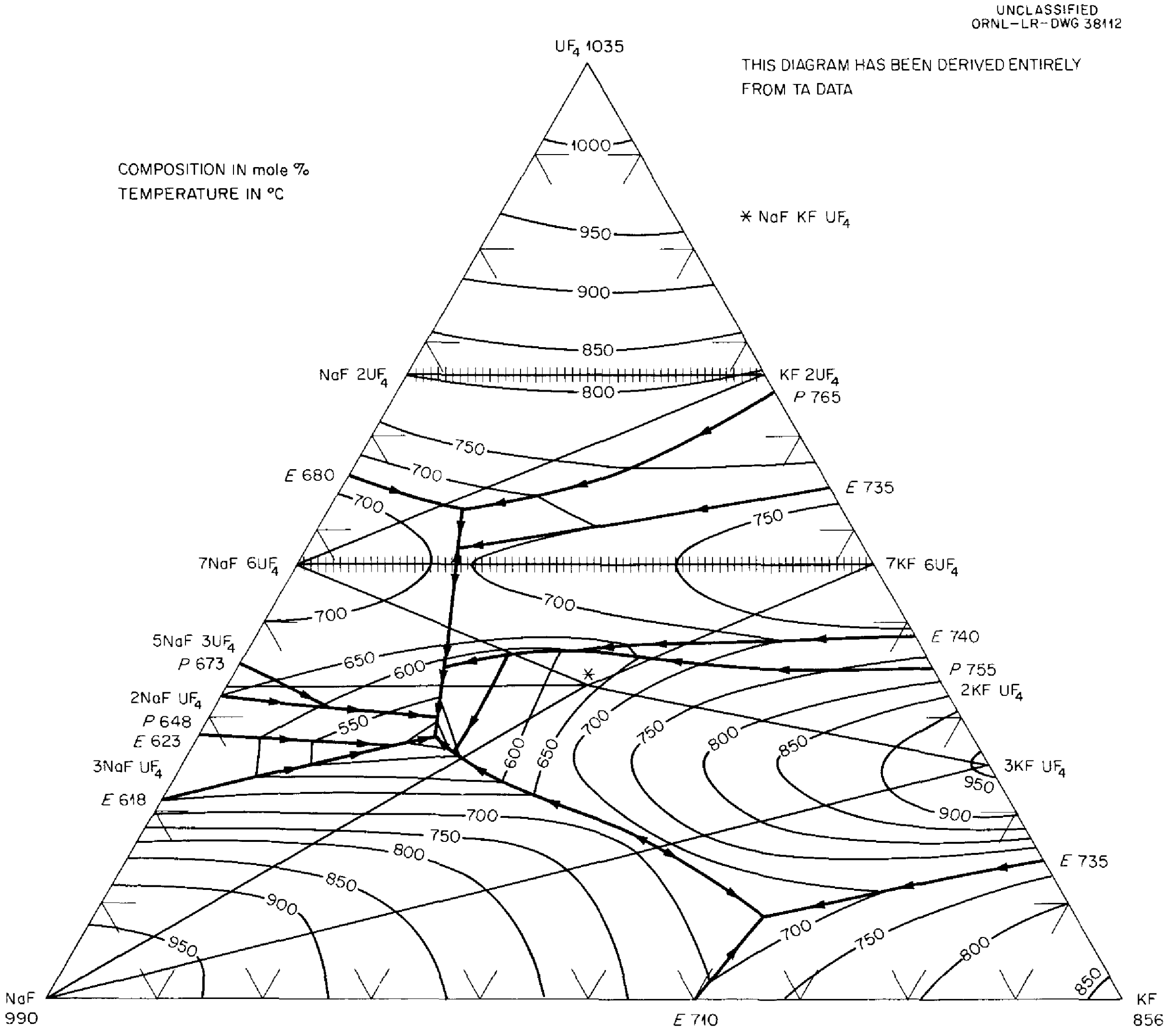

THIS DIAGRAM HAS BEEN DERIVED ENTIRELY FROM TA DATA

COMPOSITION IN mole %
TEMPERATURE IN °C

Fig. 3.67. The System NaF–KF–UF_4.

3.68. The System NaF–RbF–UF_4

R. E. Thoma, H. Insley, H. A. Friedman, and W. R. Grimes, unpublished work performed at the Oak Ridge National Laboratory, 1955–56.

Preliminary diagram.

Invariant Equilibria

Composition of Liquid (mole %)			Invariant Temperature (°C)	Type of Equilibrium	Solid Phases Present at Invariant Point
NaF	RbF	UF_4			
18	73	9	670	Eutectic	RbF, NaF, and $3RbF{\cdot}UF_4$
46	33	21	470	Eutectic	NaF, $NaF{\cdot}RbF{\cdot}UF_4$, and $3RbF{\cdot}UF_4$
44	33	23	500	Peritectic	$NaF{\cdot}RbF{\cdot}UF_4$, $2RbF{\cdot}UF_4$, and $3RbF{\cdot}UF_4$
45	30	25	485	Peritectic	NaF, $2NaF{\cdot}UF_4$, and $NaF{\cdot}RbF{\cdot}UF_4$
52	23	25	500	Decomposition	$3NaF{\cdot}UF_4$, NaF, and $2NaF{\cdot}UF_4$
41	26	33	555	Peritectic	$2RbF{\cdot}UF_4$, $2NaF{\cdot}UF_4$, and $NaF{\cdot}RbF{\cdot}UF_4$
57	8	35	630	Decomposition	$2NaF{\cdot}UF_4$, $5NaF{\cdot}3UF_4$, and $7NaF{\cdot}6UF_4$
33	30	37	535	Eutectic	$2RbF{\cdot}UF_4$, $2NaF{\cdot}UF_4$, and $7RbF{\cdot}6UF_4$
32	29	39	540	Peritectic	$7RbF{\cdot}6UF_4$, $2NaF{\cdot}UF_4$, and $7NaF{\cdot}6UF_4$
26	27	47	620	Eutectic	$7RbF{\cdot}6UF_4$, $7NaF{\cdot}6UF_4$, and $RbF{\cdot}UF_4$
25	25	50	630	Eutectic	$7NaF{\cdot}6UF_4$, $RbF{\cdot}UF_4$, and $2RbF{\cdot}3UF_4$
27	22	51	633	Peritectic	$7NaF{\cdot}6UF_4$, $2RbF{\cdot}3UF_4$, and $RbF{\cdot}3UF_4$
33	14	53	655	Peritectic	$7NaF{\cdot}6UF_4$, $RbF{\cdot}3UF_4$, and $RbF{\cdot}6UF_4$
42	3	55	678	Peritectic	$7NaF{\cdot}6UF_4$, $RbF{\cdot}6UF_4$, and UF_4

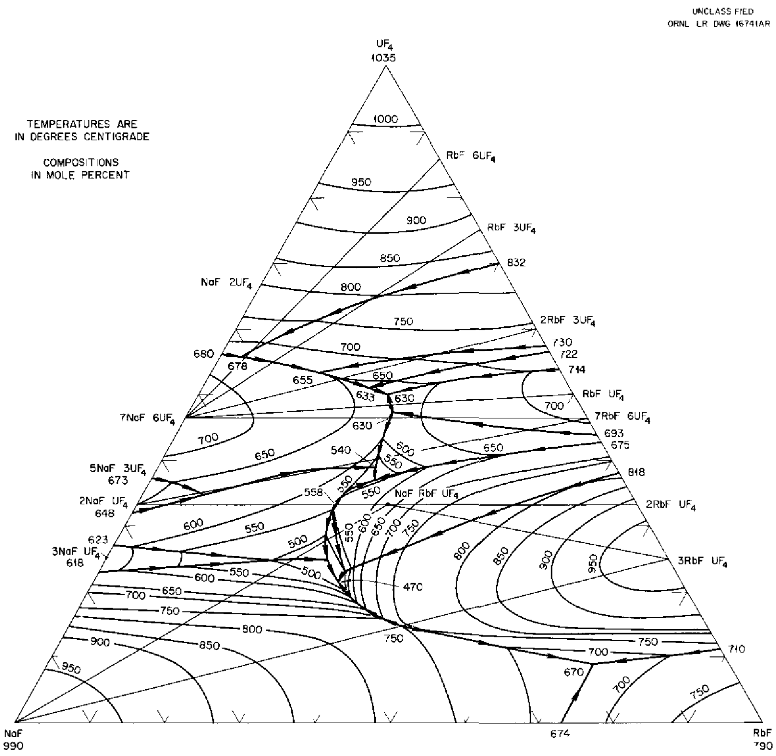

Fig. 3.68*a*. The System NaF–RbF–UF_4.

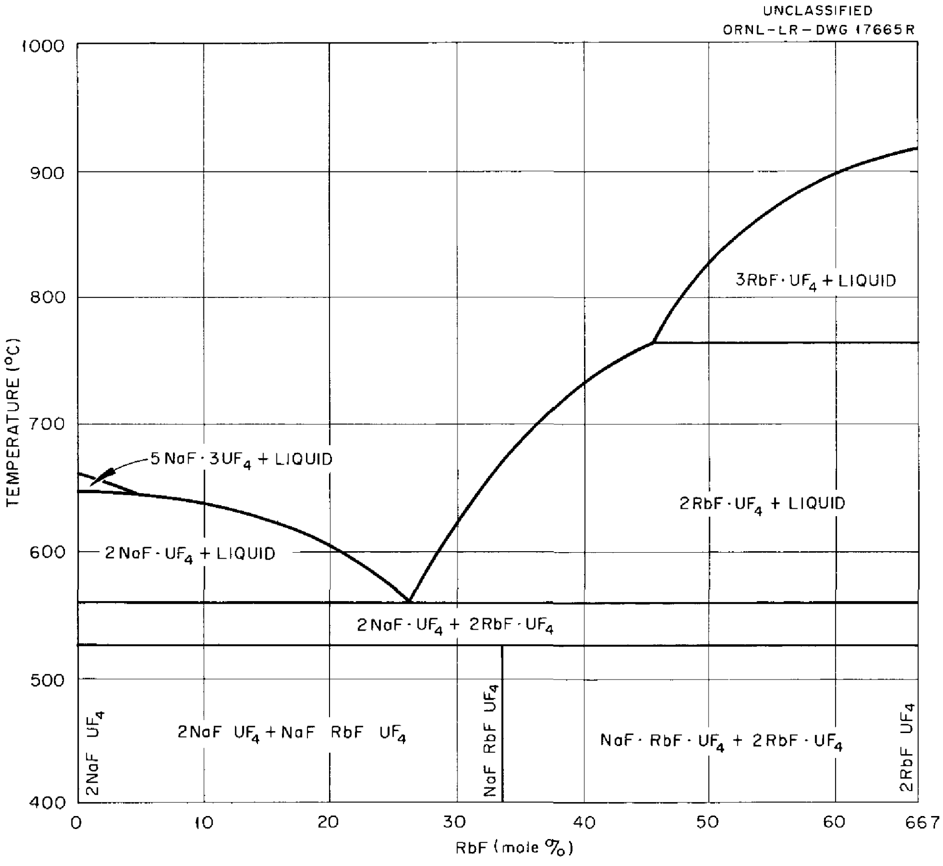

Fig. 3.68*b*. The Section $2NaF\cdot UF_4$–$2RbF\cdot UF_4$.

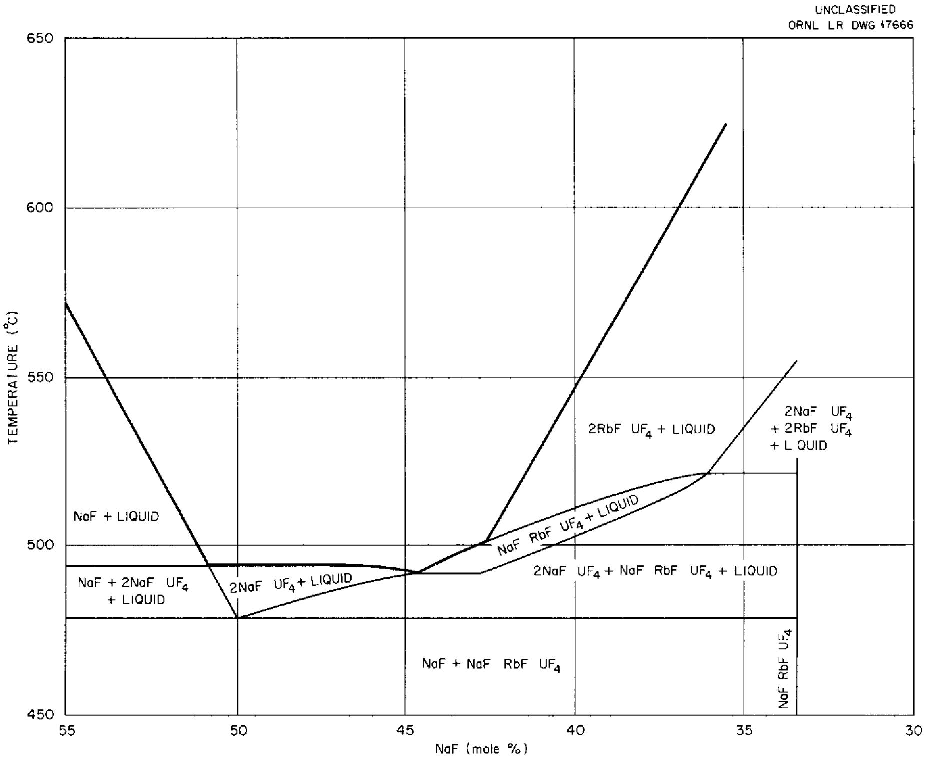

Fig. 3.68*c*. The Section NaF–NaF·RbF·UF_4.

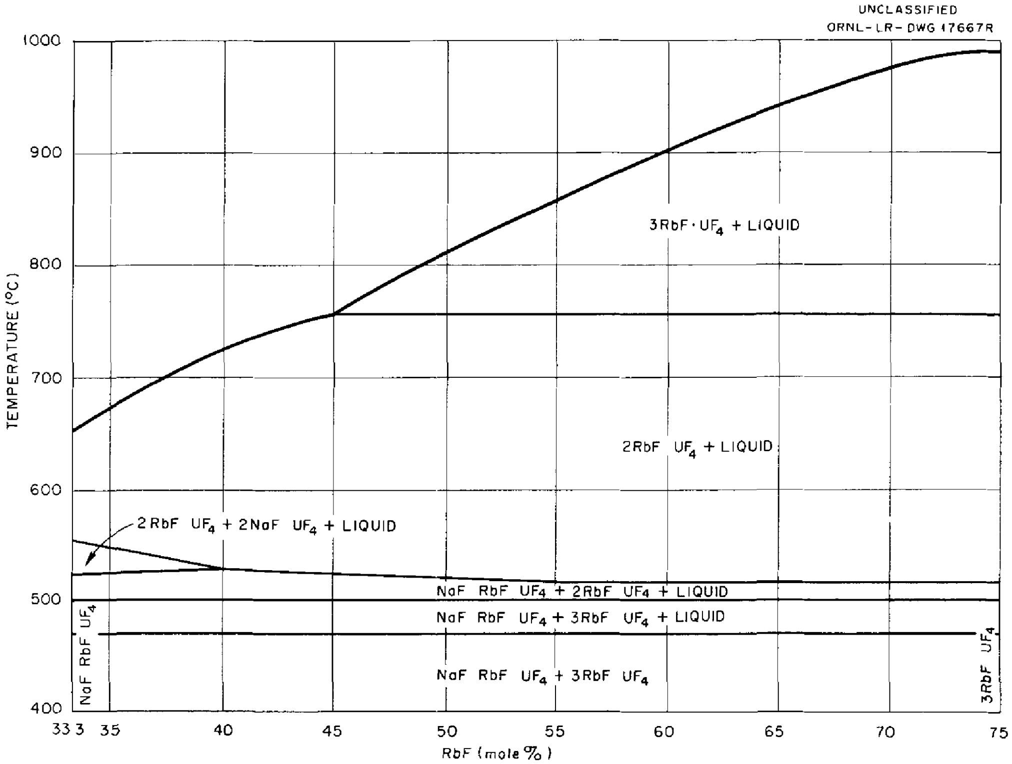

Fig. 3.68*d*. The Section $3RbF \cdot UF_4$–$NaF \cdot RbF \cdot UF_4$.

3.69. The System LiF–BeF$_2$–UF$_4$

L. V. Jones, D. E. Etter, C. R. Hudgens, A. A. Huffman, T. B. Rhinehammer, N. E. Rogers, P. A. Tucker, and L. J. Wittenberg, *Phase Equilibria in the LiF–BeF$_2$–UF$_4$ Ternary Fused Salt System*, MLM-1080 (Aug. 24, 1959).

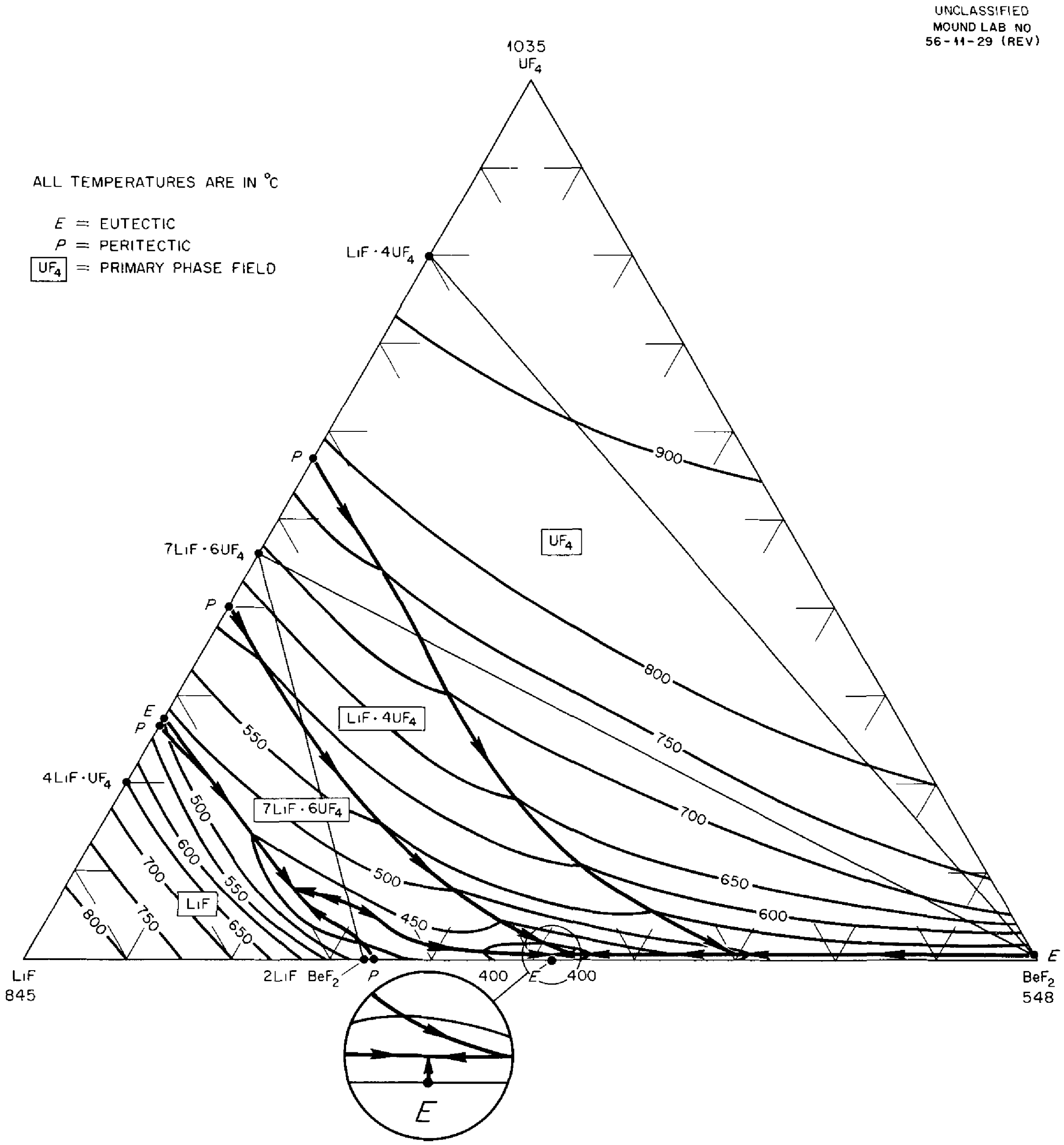

Fig. 3.69*a*. The System LiF–BeF$_2$–UF$_4$.

Preliminary diagram.

Invariant Equilibria

Composition of Liquid (mole %)			Temperature (°C)	Type of Equilibrium	Solid Phases Present at Invariant Temperature
LiF	BeF_2	UF_4			
72	6	22	480	Peritectic (decomposition of $4LiF \cdot UF_4$ in the ternary system)	$4LiF \cdot UF_4$, LiF, and $7LiF \cdot 6UF_4$
69	23	8	426	Eutectic	LiF, $2LiF \cdot BeF_2$, and $7LiF \cdot 6UF_4$
48	51.5	0.5	350	Eutectic	$7LiF \cdot 6UF_4$, $2LiF \cdot BeF_2$, and BeF_2
45.5	54	0.5	381	Peritectic	$LiF \cdot 4UF_4$, $7LiF \cdot 6UF_4$, and BeF_2
29.5	70	0.5	483	Peritectic	UF_4, $LiF \cdot 4UF_4$, and BeF_2

The minimum temperature in the quasi-binary system $2LiF \cdot BeF_2$–$7LiF \cdot 6UF_4$ occurs at 65 LiF–29 BeF_2–6 UF_4 (mole %) at 438°C.

A three-dimensional model of the system LiF–BeF_2-UF_4 is shown in Fig. 3.69*b*.

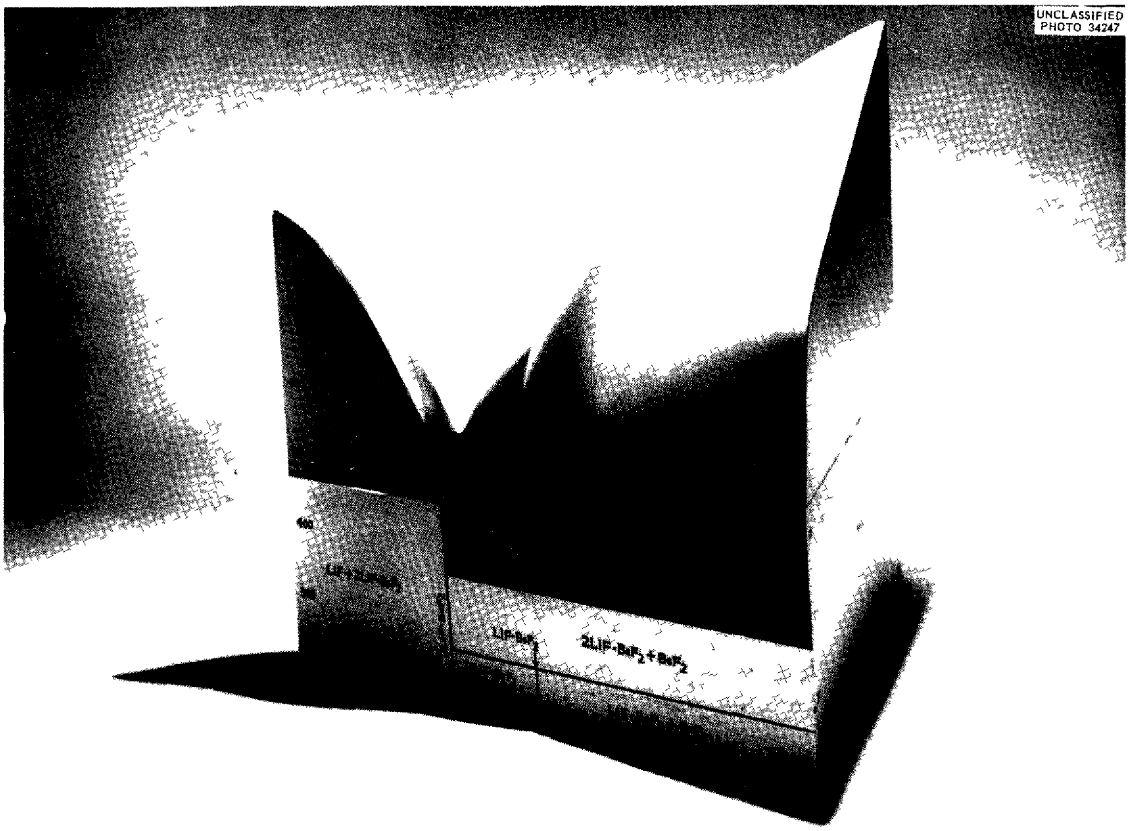

Fig. 3.69*b*. Model of the System LiF–BeF_2–UF_4.

3.70. The System $NaF–BeF_2–UF_4$

J. F. Eichelberger, C. R. Hudgens, L. V. Jones, G. Pish, T. B. Rhinehammer, P. A. Tucker, and L. J. Wittenberg, unpublished work performed at the Mound Laboratory, 1956–57.

Preliminary diagram.

Invariant Equilibria

Composition of Liquid (mole %)			Temperature (°C)	Type of Equilibrium	Solid Phases Present at Invariant Temperature
NaF	BeF_2	UF_4			
74	12	14	500	Peritectic (decomposition of $3NaF\cdot UF_4$ in ternary system)	$3NaF\cdot UF_4$, NaF, and $2NaF\cdot UF_4$
72.5	17	19.5	486	Eutectic	NaF, $2NaF\cdot UF_4$, and $2NaF\cdot BeF_2$
64.5	9	26.5	630	Peritectic (decomposition of $5NaF\cdot 3UF_4$ in the ternary system)	$5NaF\cdot 3UF_4$, $2NaF\cdot UF_4$, and $7NaF\cdot 6UF_4$
57	42	1	378	Peritectic	$2NaF\cdot BeF_2$, $2NaF\cdot UF_4$, and $7NaF\cdot 6UF_4$
56	43.5	0.5	339	Eutectic	$2NaF\cdot BeF_2$, $NaF\cdot BeF_2$, and $7NaF\cdot 6UF_4$
43.5	55.5	1	357	Eutectic	$7NaF\cdot 6UF_4$, BeF_2, and $NaF\cdot BeF_2$
41	58	1	375	Peritectic	$7NaF\cdot 6UF_4$, $NaF\cdot 2UF_4$, and BeF_2
26	63	1	409	Peritectic	$NaF\cdot 2UF_4$, $NaF\cdot 4UF_4$, and BeF_2
44	18	38	665	Peritectic	$7NaF\cdot 6UF_4$, UF_4, and $NaF\cdot 2UF_4$
40	47	13	548	Peritectic	UF_4, $NaF\cdot 2UF_4$, and $NaF\cdot 4UF_4$
27	72	1	498	Peritectic	UF_4, BeF_2, and $NaF\cdot 4UF_4$

The minimum temperature in the quasi-binary system $2NaF\cdot BeF_2–2NaF\cdot UF_4$ occurs at 66.7 LiF–25 BeF_2–8.3 UF_4 (mole %) at 528°C. The minimum temperature in the quasi-binary system $NaF\cdot BeF_2–7NaF\cdot 6UF_4$ occurs at 50.5 NaF–48.5 BeF_2–1.0 UF_4 (mole %) at 367°C.

A three-dimensional model of the system $NaF–BeF_2–UF_4$ has been constructed by the authors and is shown in Fig. 3.70*b*.

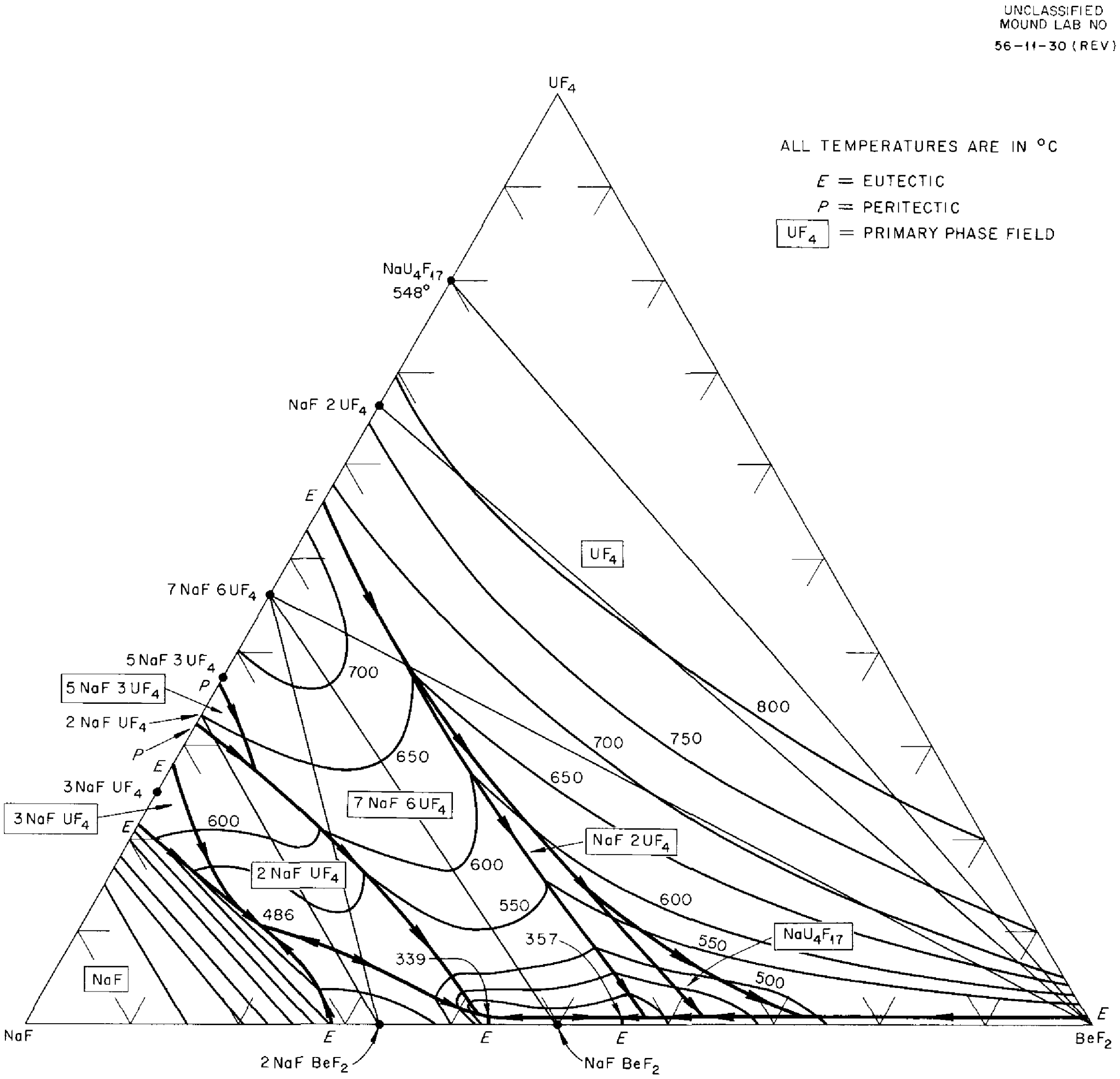

Fig. 3.70*a*. The System NaF–BeF_2–UF_4.

UNCLASSIFIED
PHOTO 47483

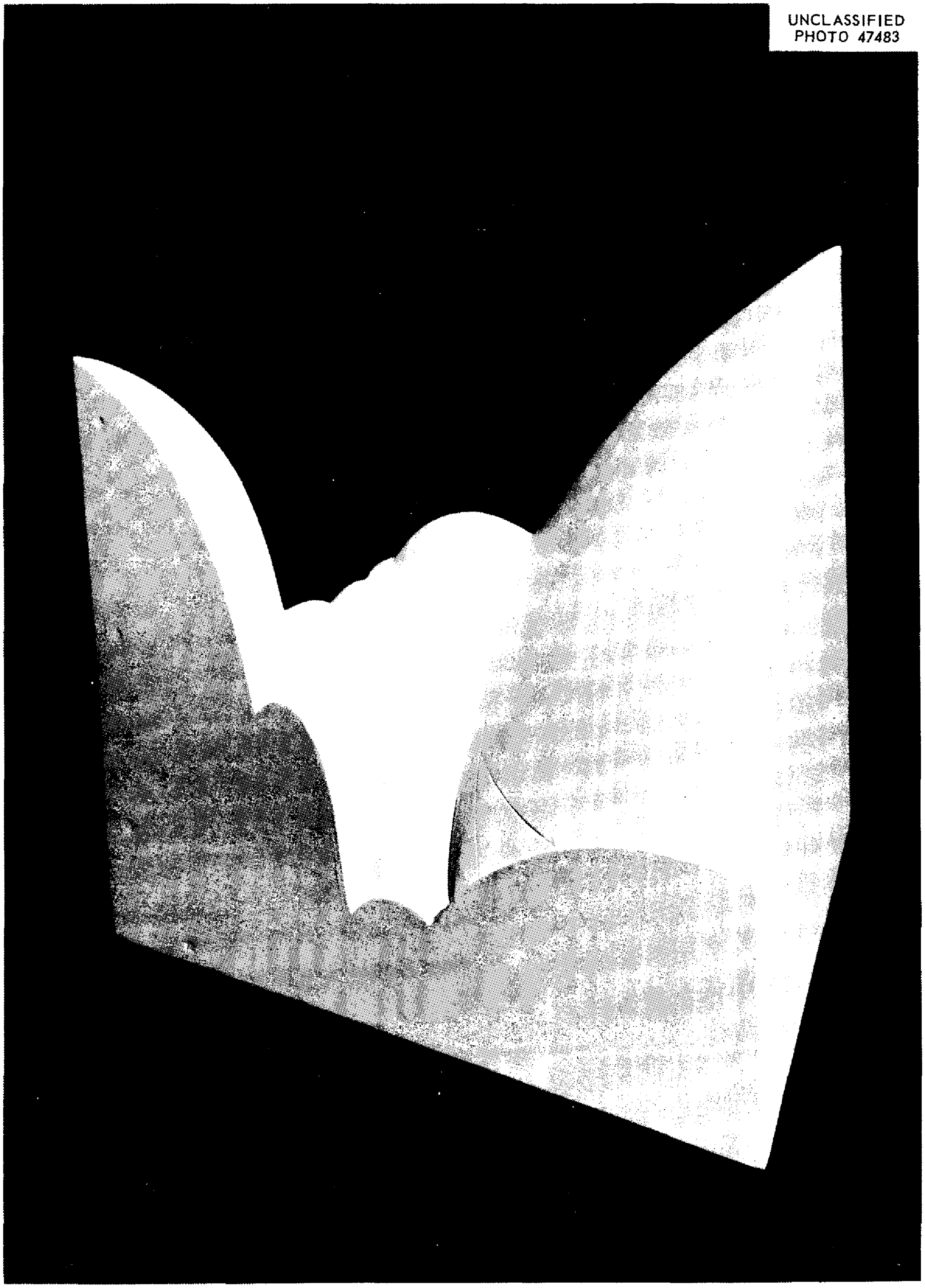

Fig. 3.70*b*. Model of the System NaF–BeF_2–UF_4.

3.71. The System NaF–PbF_2–UF_4

C. J. Barton, J. P. Blakely, G. J. Nessle, L. M. Bratcher, and W. R. Grimes, unpublished work performed at the Oak Ridge National Laboratory, 1950–51.

Preliminary diagram. No study has been made at the Oak Ridge National Laboratory of the phase relationships within the system NaF–PbF_2–UF_4.

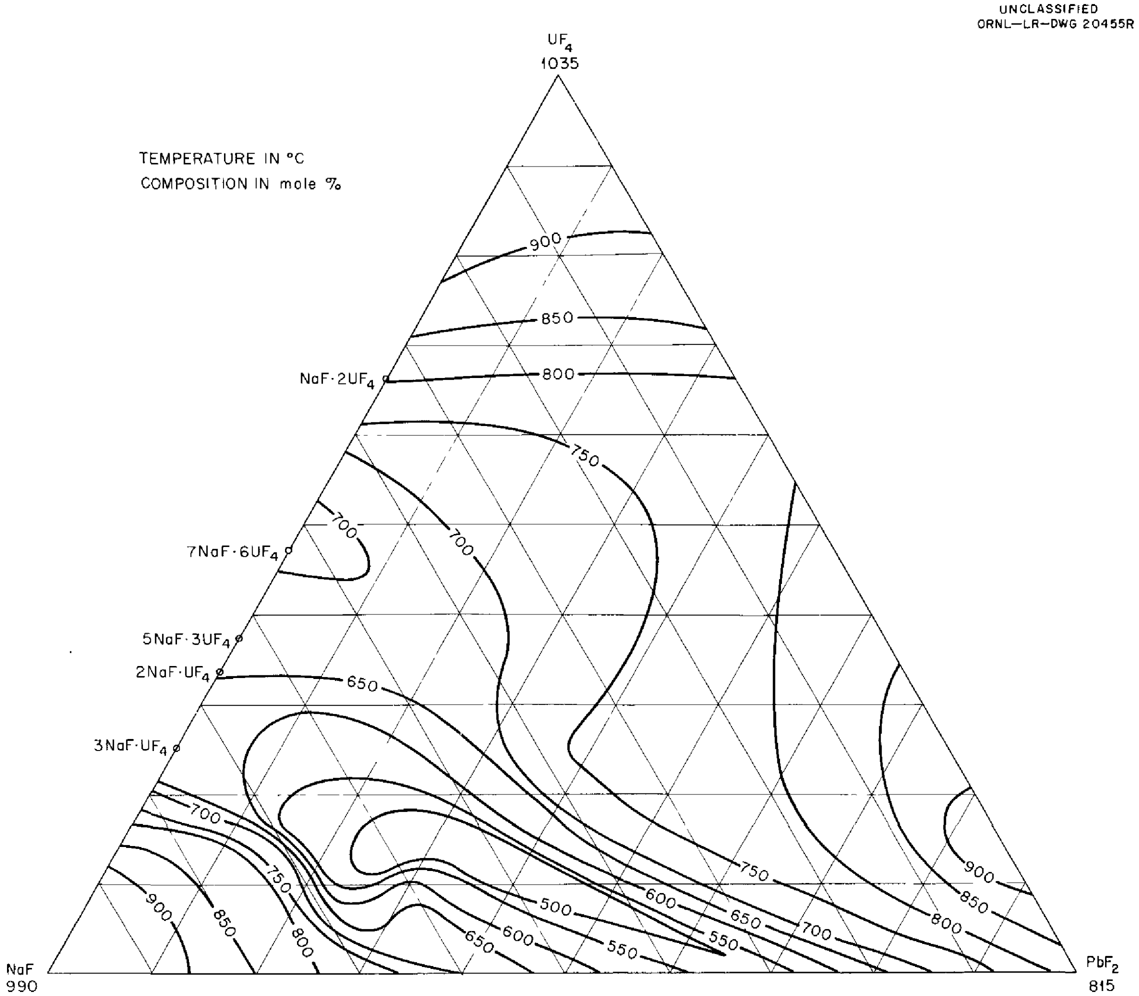

Fig. 3.71. The System NaF–PbF_2–UF_4.

3.72. The system $KF-PbF_2-UF_4$

C. J. Barton, J. P. Blakely, G. J. Nessle, L. M. Bratcher, and W. R. Grimes, unpublished work performed at the Oak Ridge National Laboratory, 1950–51.

Preliminary diagram. No study has been made at the Oak Ridge National Laboratory of the phase relationships within the system $KF-PbF_2-UF_4$.

UNCLASSIFIED
DWG 11514A

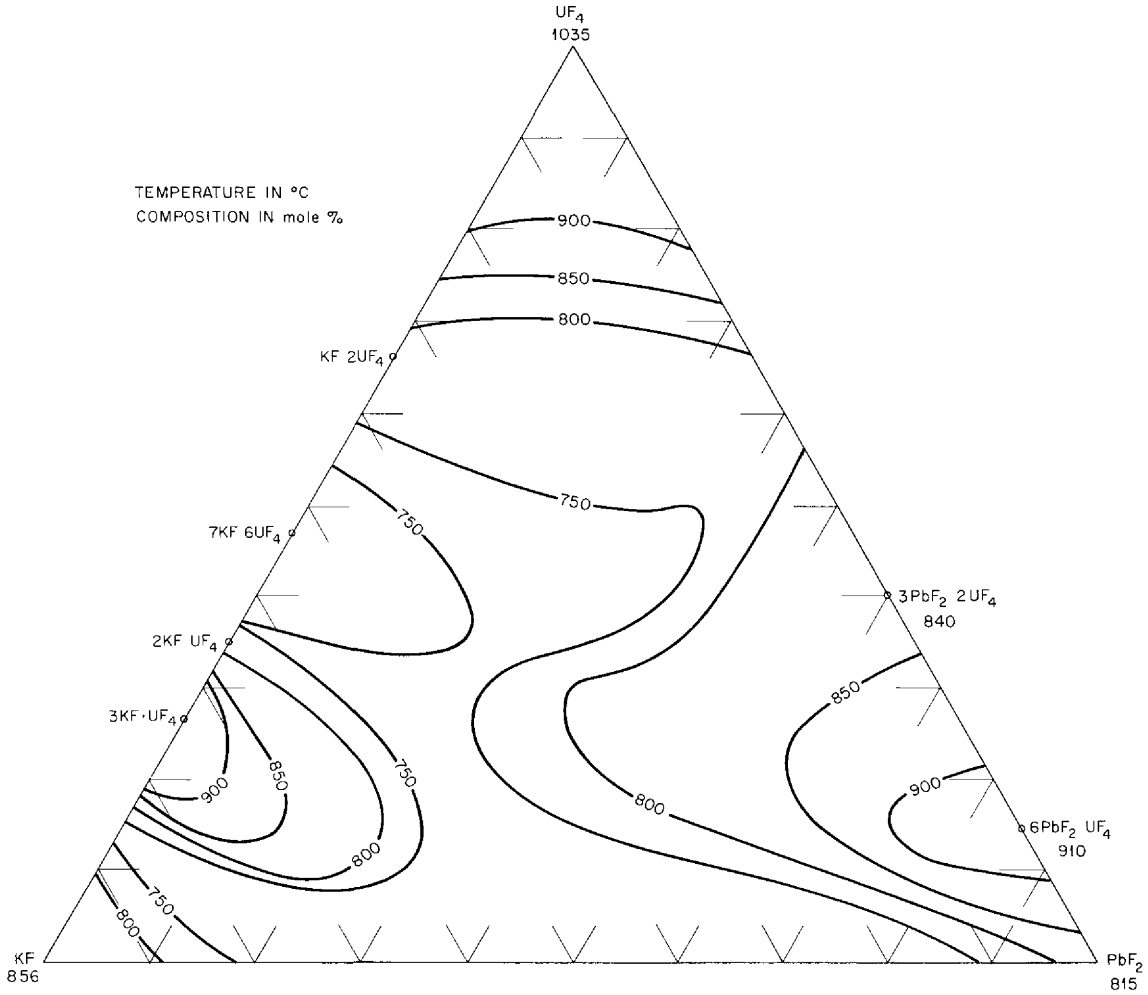

Fig. 3.72. The System KF–PbF$_2$–UF$_4$.

3.73. The System NaF–ZrF_4–UF_4

C. J. Barton, W. R. Grimes, H. Insley, R. E. Moore, and R. E. Thoma, "Phase Equilibria in the Systems NaF–ZrF_4, UF_4–ZrF_4, and NaF–ZrF_4–UF_4," *J. Phys. Chem.* **62, 665–76 (1958).**

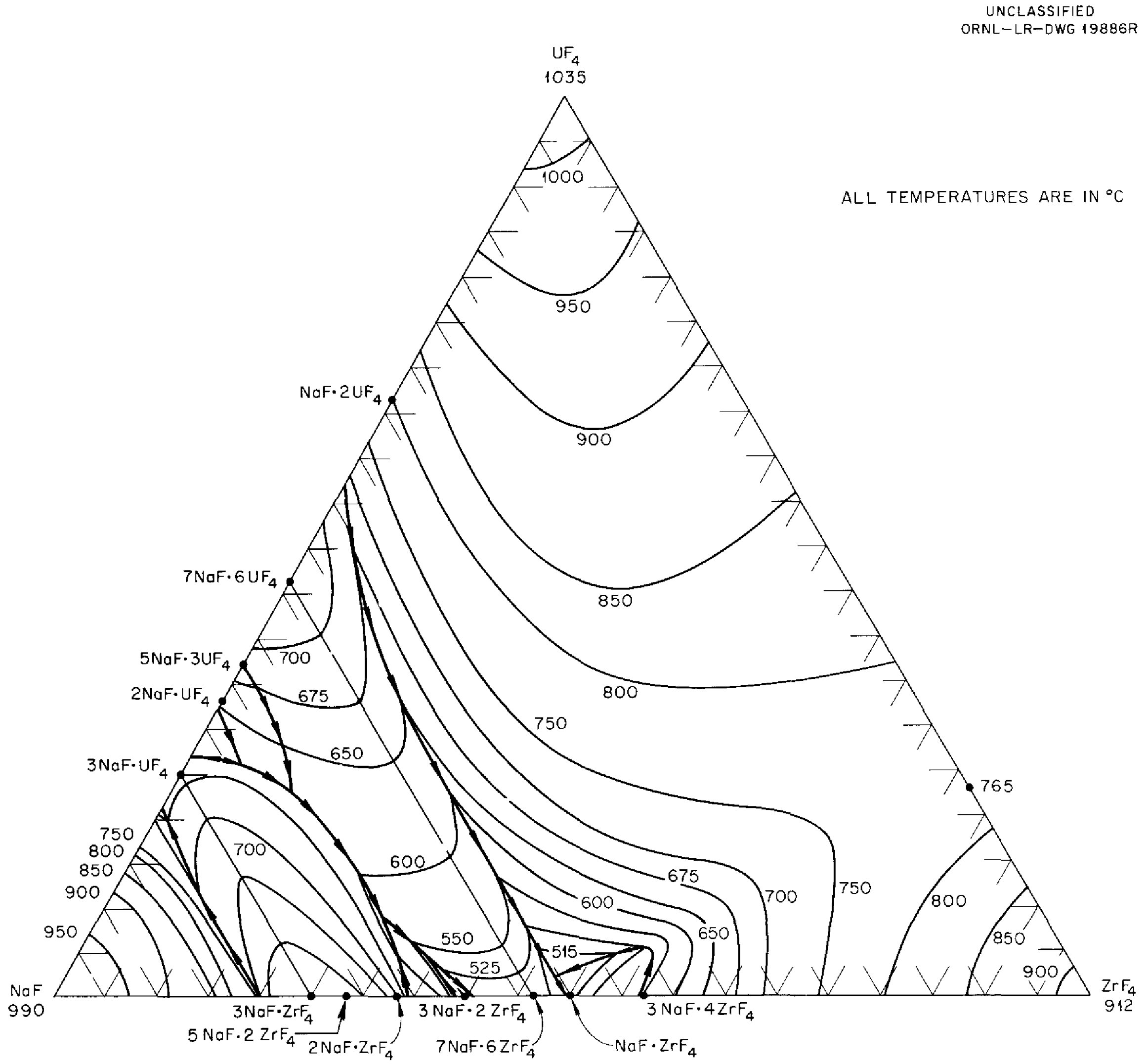

Fig. 3.73*a*. The System NaF–ZrF_4–UF_4.

Invariant Equilibria and Singular Points

Composition of Liquid (mole %)			Temperature (°C)	Type of Equilibrium	Solids Present at Invariant Point
NaF	ZrF_4	UF_4			
69.5	4.0	26.5	646	Maximum temperature of boundary curve	$3NaF\cdot(U,Zr)F_4$ and $2NaF\cdot UF_4$
68.5	5.5	26.0	640	Peritectic	$3NaF\cdot(U,Zr)F_4$, $2NaF\cdot UF_4$, and $5NaF\cdot 3UF_4$*ss*
65.5	12.0	22.5	613	Peritectic or decomposition	$3NaF\cdot(U,Zr)F_4$, $5NaF\cdot 3UF_4$*ss*, and $7NaF\cdot 6(U,Zr)F_4$
64.0	27.0	9.0	592	Peritectic	$3NaF\cdot(U,Zr)F_4$, $5NaF\cdot 2ZrF_4$*ss*, and $7NaF\cdot 6(U,Zr)F_4$
61.5	34.5	4.0	540	Peritectic	$5NaF\cdot 2ZrF_4$*ss*, $2NaF\cdot ZrF_4$, and $7NaF\cdot 6(U,Zr)F_4$
50.5	47	2.5	513	Peritectic	$7NaF\cdot 6(U,Zr)F_4$, $(U,Zr)F_4$, and $3NaF\cdot 4ZrF_4$

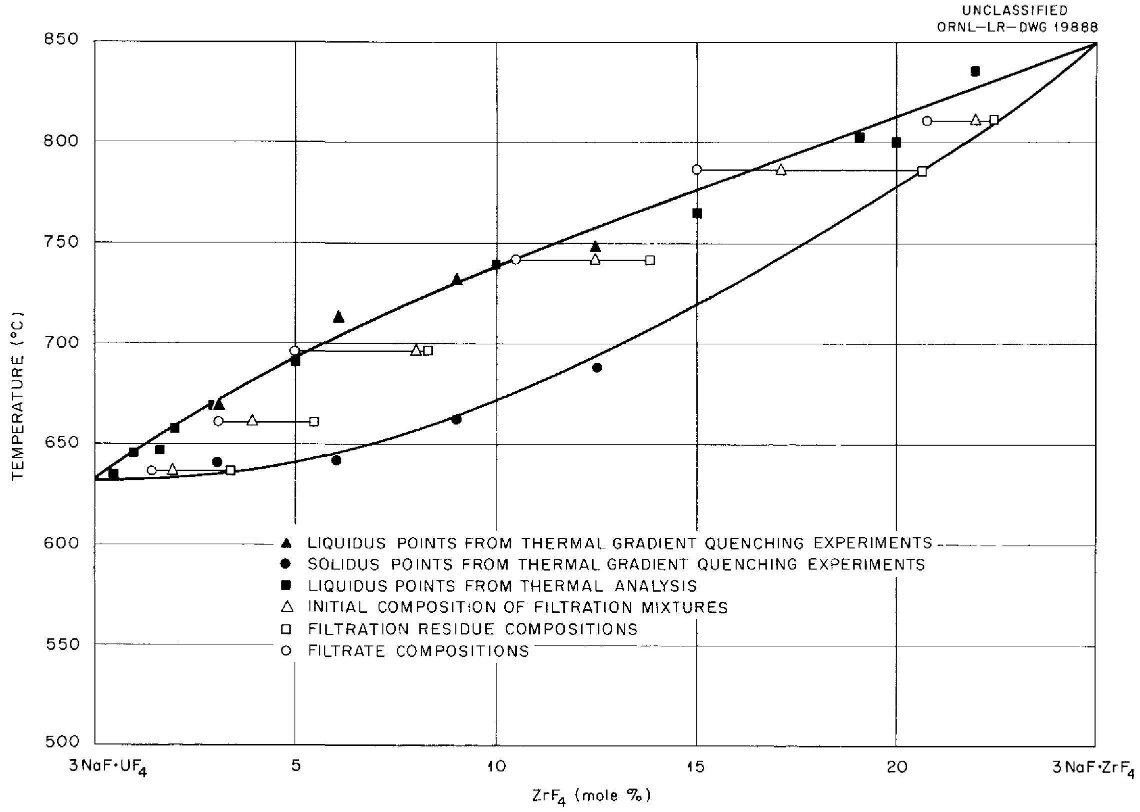

Fig. 3.73*b*. The Subsystem $3NaF\cdot UF_4$–$3NaF\cdot ZrF_4$.

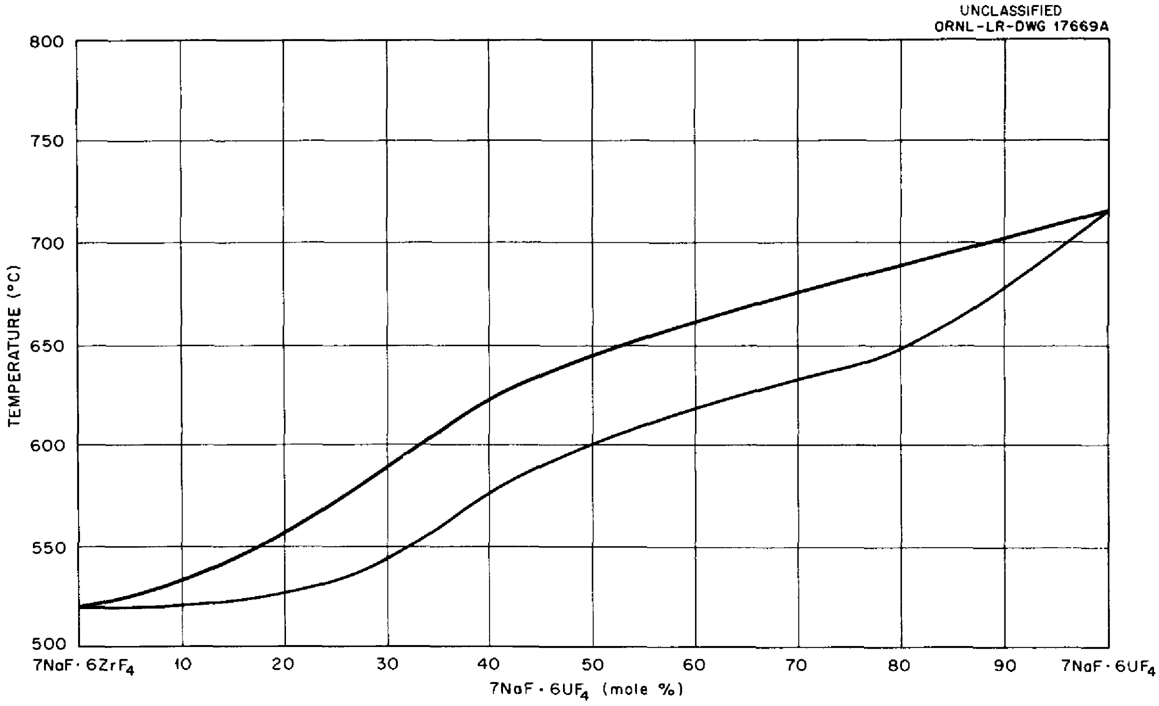

Fig. 3.73c. The Subsystem $7NaF \cdot 6ZrF_4$–$7NaF \cdot 6UF_4$.

3.74. The System LiF–ThF$_4$–UF$_4$

C. F. Weaver, R. E. Thoma, H. Insley, and H. A. Friedman, "Phase Equilibria in the Systems UF$_4$–ThF$_4$ and LiF–ThF$_4$–UF$_4$," paper presented at the 61st National Meeting of the American Ceramic Society, Chicago, Ill., May 17–21, 1959.

Invariant Equilibria

Composition of Liquid (mole %)			Invariant Temperature (°C)	Type of Equilibrium	Solids Present at Invariant Point
LiF	ThF$_4$	UF$_4$			
72.5	7.0	20.5	500	Peritectic	LiF, 3LiF·(Th,U)F$_4$, and 7LiF·6(U,Th)F$_4$
72.0	1.5	26.5	488	Eutectic	LiF, 4LiF·UF$_4$, and 7LiF·6(U,Th)F$_4$
53	18	19	609	Peritectic	7LiF·6(U,Th)F$_4$, LiF·2(Th,U)F$_4$, and LiF·4(U,Th)F$_4$

A three-dimensional model of the system LiF–ThF$_4$–UF$_4$ is shown in Fig. 3.74*e*.

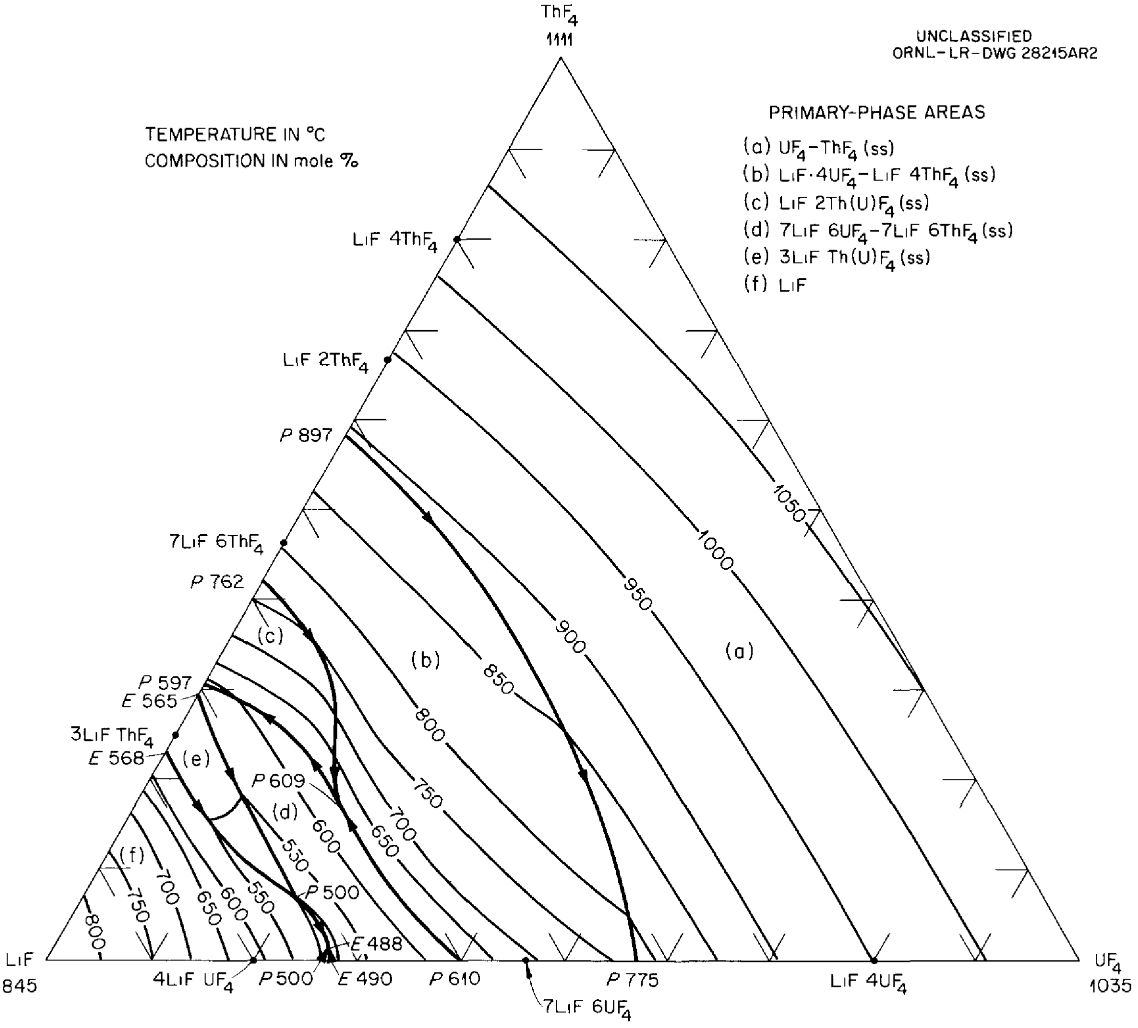

Fig. 3.74*a*. The System LiF–ThF$_4$–UF$_4$.

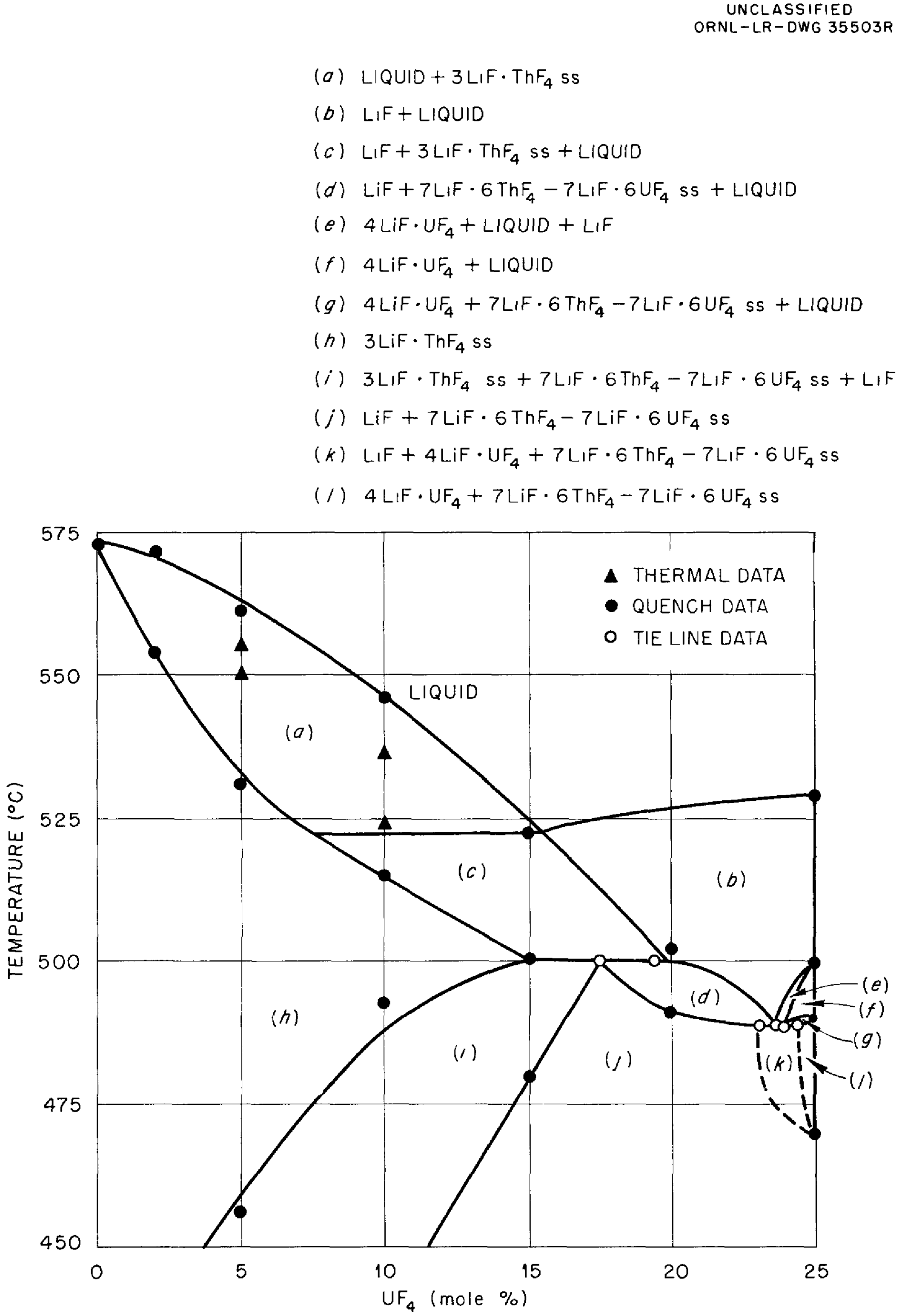

Fig. 3.74*b*. The System $LiF-ThF_4-UF_4$: The Section at 75 Mole % LiF.

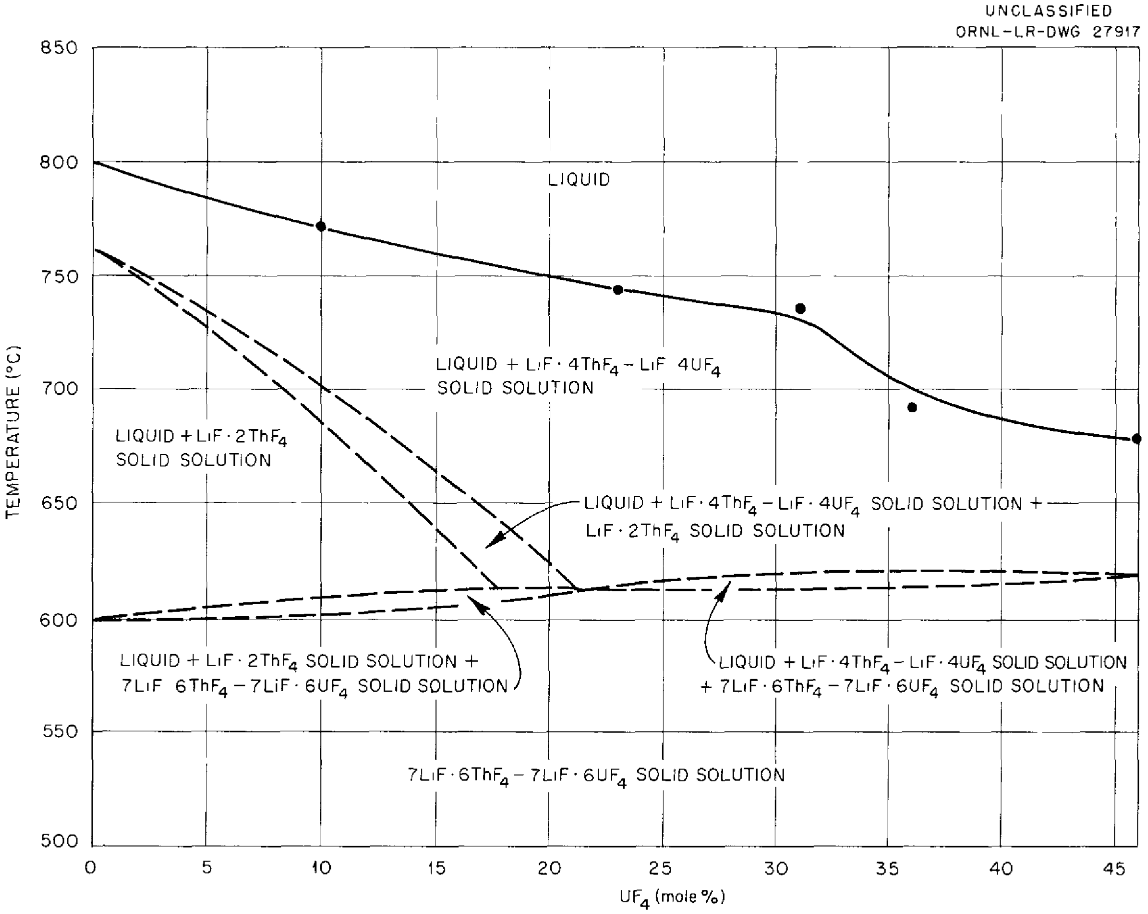

Fig. 3.74c. The System LiF–ThF$_4$–UF$_4$: The Section at 53.8 Mole % LiF.

UNCLASSIFIED
ORNL-LR-DWG 35506R

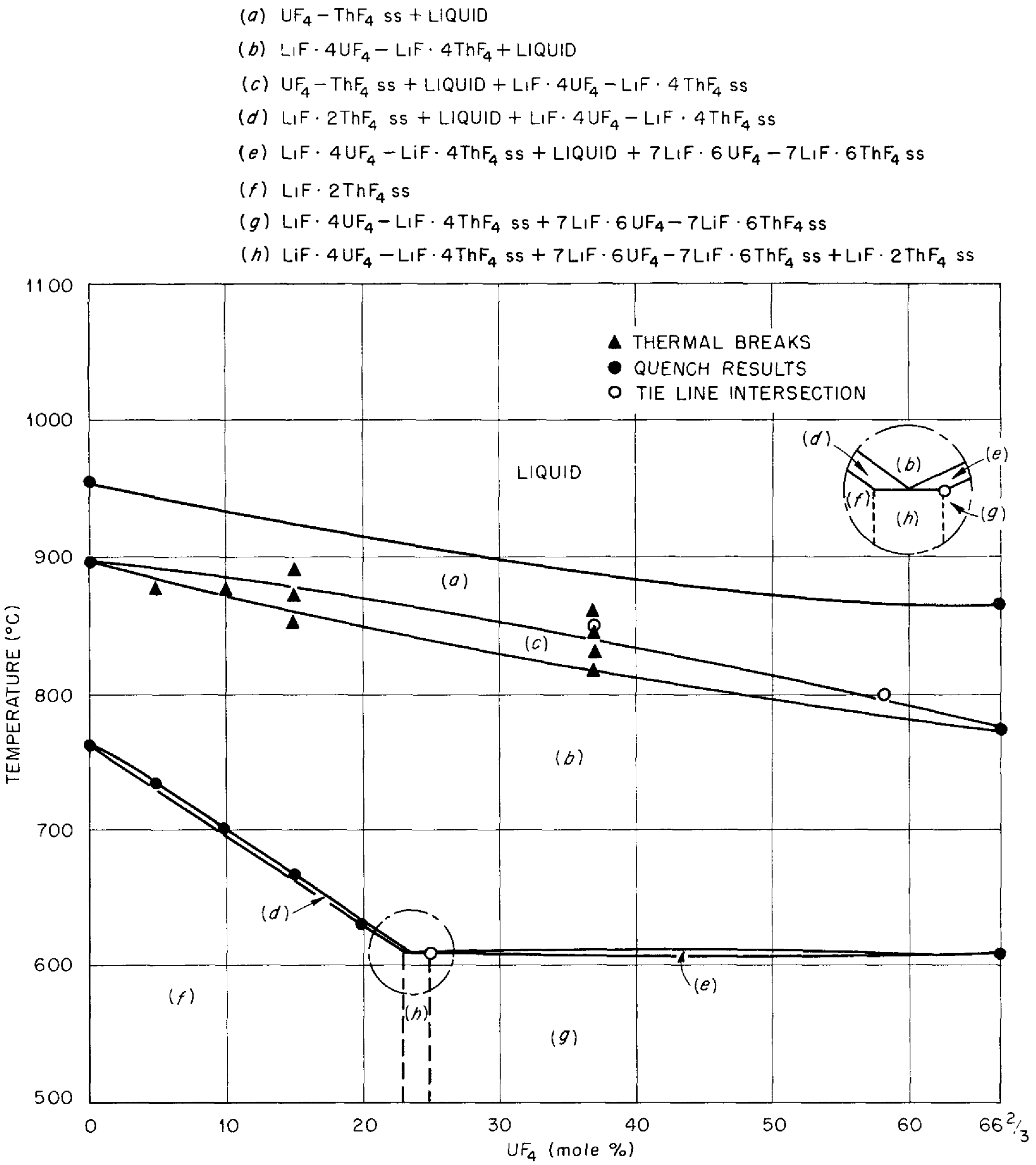

Fig. 3.74*d*. The System LiF–ThF$_4$–UF$_4$: The Section at 33.3 Mole % LiF.

UNCLASSIFIED
PHOTO 34246

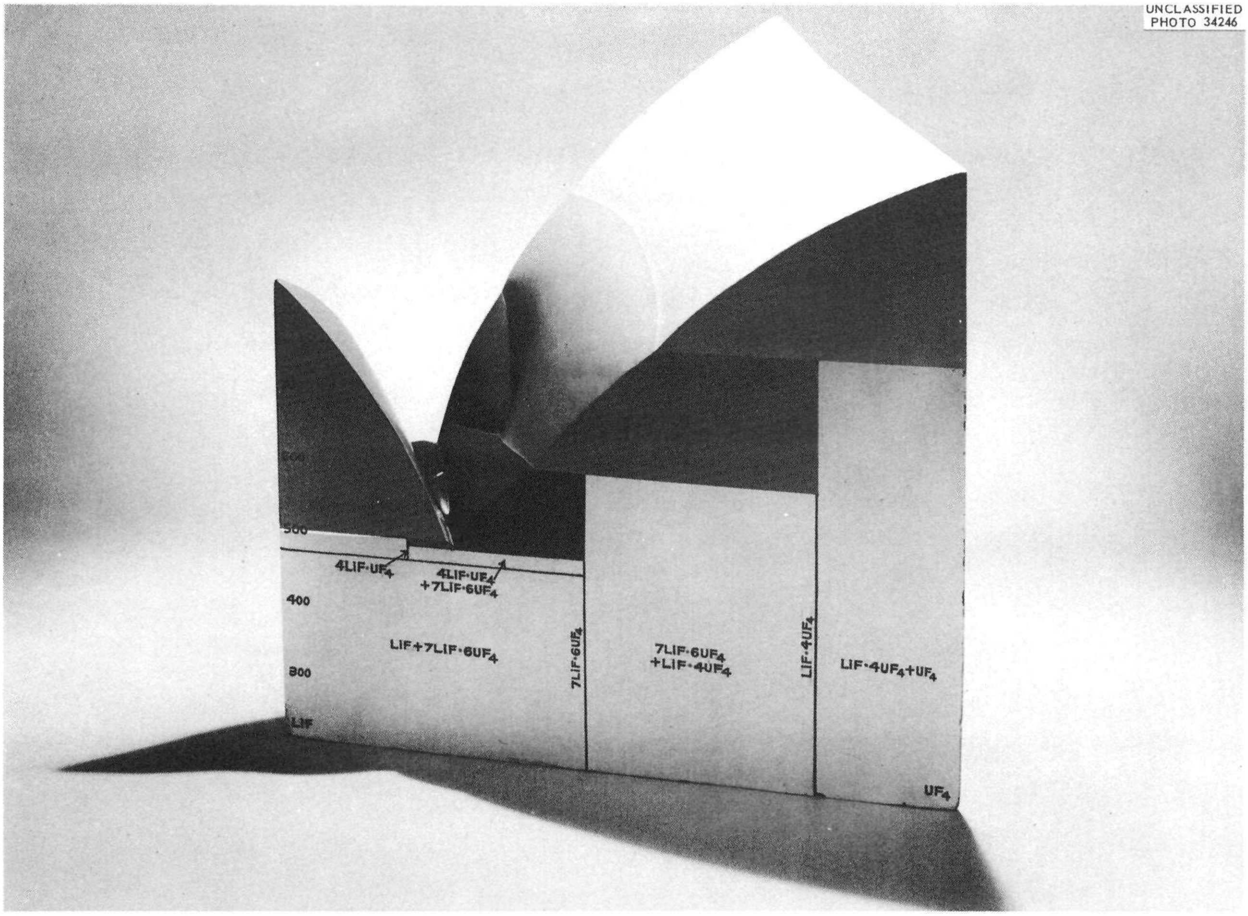

Fig. 3.74*e*. Model of the System LiF–ThF_4–UF_4.

3.75. The System NaF–ThF_4–UF_4: The Section $2NaF \cdot ThF_4$–$2NaF \cdot UF_4$

R. E. Thoma, H. Insley, H. A. Friedman, and C. F. Weaver, unpublished work performed at the Oak Ridge National Laboratory, 1958–59.

Preliminary diagram.

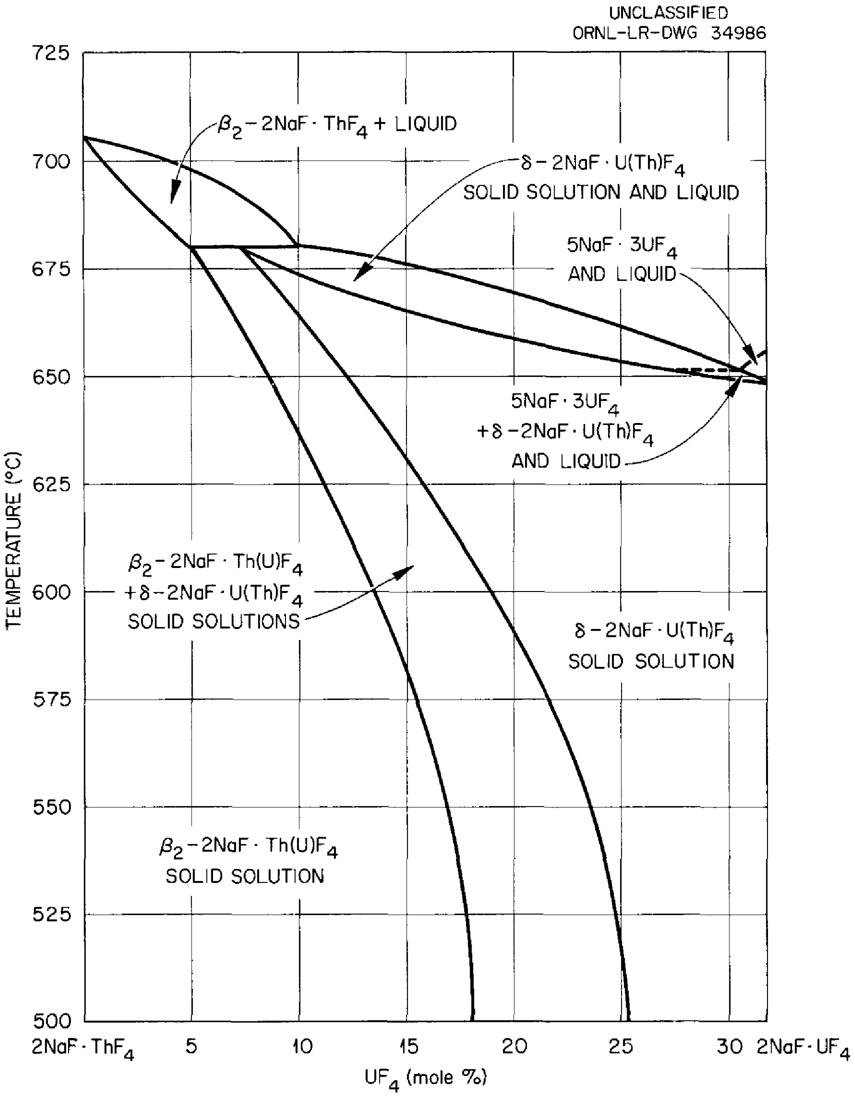

Fig. 3.75. The Section $2NaF \cdot ThF_4$–$2NaF \cdot UF_4$.

3.76. The System LiF–PuF$_3$

C. J. Barton and R. A. Strehlow, "Phase Relationships in the System Lithium Fluoride–Plutonium Fluoride," paper presented at the 135th National Meeting of the American Chemical Society, Boston, Mass., Apr. 5–10, 1959.

The system LiF–PuF$_3$ contains a single eutectic at 80.5 LiF–19.5 PuF$_3$ (mole %), m.p. 743°C.

UNCLASSIFIED
ORNL-LR-DWG 34817

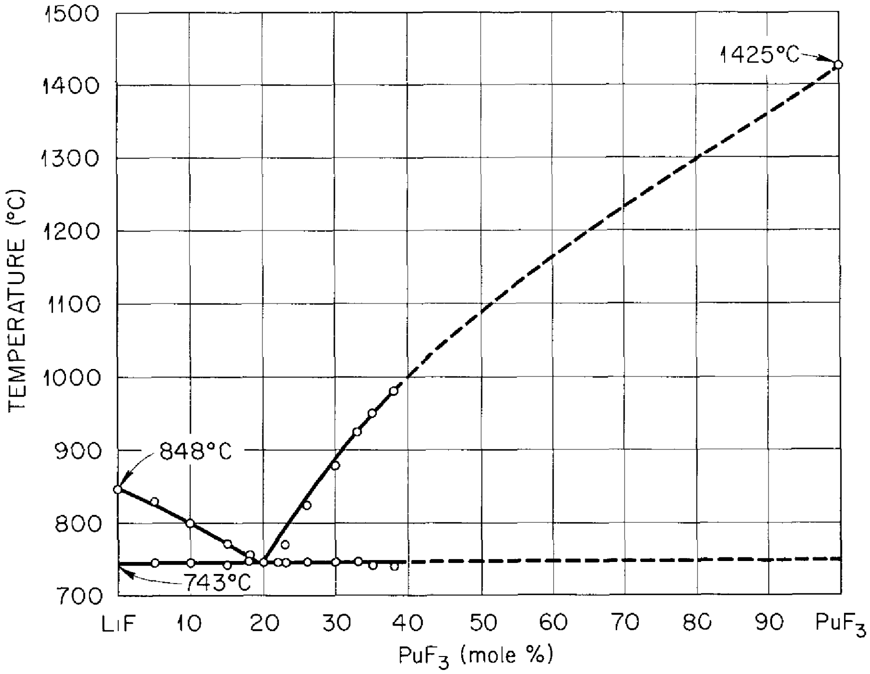

Fig. 3.76. The System LiF–PuF$_3$.

3.77. The System LiCl–FeCl$_2$

C. Beusman, *Activities in the KCl–FeCl$_2$ and LiCl–FeCl$_2$ Systems*, ORNL-2323 (May 15, 1957).

The system LiCl–FeCl$_2$ forms a continuous series of solid solutions with a minimum at 60 LiCl–40 FeCl$_2$ (mole %), m.p. 540°C.

UNCLASSIFIED
ORNL-LR-DWG. 20942

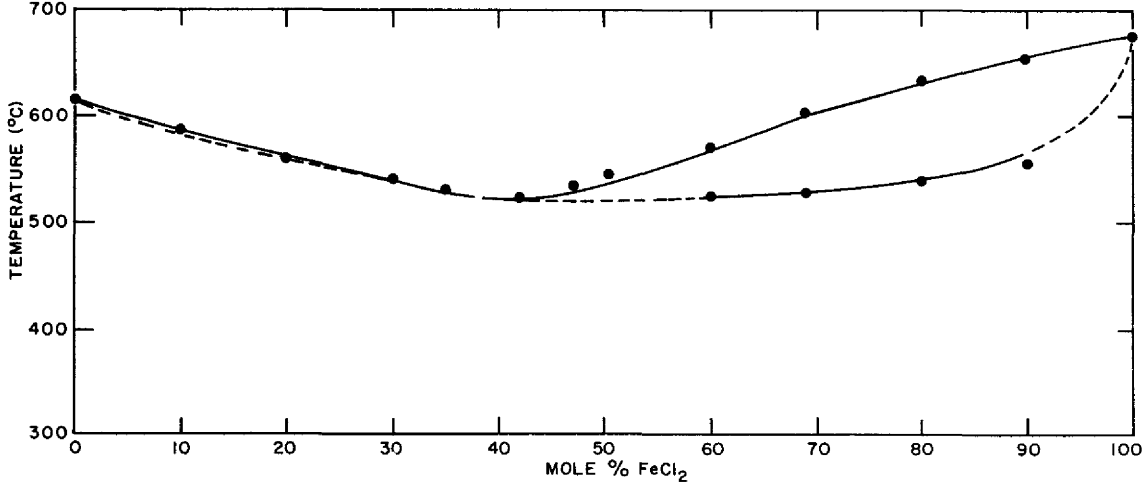

Fig. 3.77. The System LiCl–FeCl$_2$.

3.78. The System $KCl-FeCl_2$

C. Beusman, *Activities in the $KCl-FeCl_2$ and $LiCl-FeCl_2$ Systems*, ORNL-2323 (May 15, 1957). A nearly identical diagram to this one has been reported by H. L. Pinch and J. M. Hirshon, "Thermal Analysis of the Ferrous Chloride–Potassium Chloride System," *J. Am. Chem. Soc.* **79**, 6149–50 (1957).

Invariant Equilibria

Mole % $FeCl_2$ in Liquid	Invariant Temperature (°C)	Type of Equilibrium	Phase Reaction at Invariant Temperature
35	385	Peritectic	$L + KCl \rightleftharpoons \alpha\text{-}2KCl\cdot FeCl_2$
–	255	Inversion	$\alpha\text{-}2KCl\cdot FeCl_2 \rightleftharpoons \beta\text{-}2KCl\cdot FeCl_2$
39	355	Eutectic	$L \rightleftharpoons \alpha\text{-}2KCl\cdot FeCl_2 + \alpha\text{-}KCl\cdot FeCl_2$
50	400	Congruent melting point	$L \rightleftharpoons \alpha\text{-}KCl\cdot FeCl_2$
–	300	Inversion	$\alpha\text{-}KCl\cdot FeCl_2 \rightleftharpoons \beta\text{-}KCl\cdot FeCl_2$
53	390	Eutectic	$L \rightleftharpoons \alpha\text{-}KCl\cdot FeCl_2 + FeCl_2$

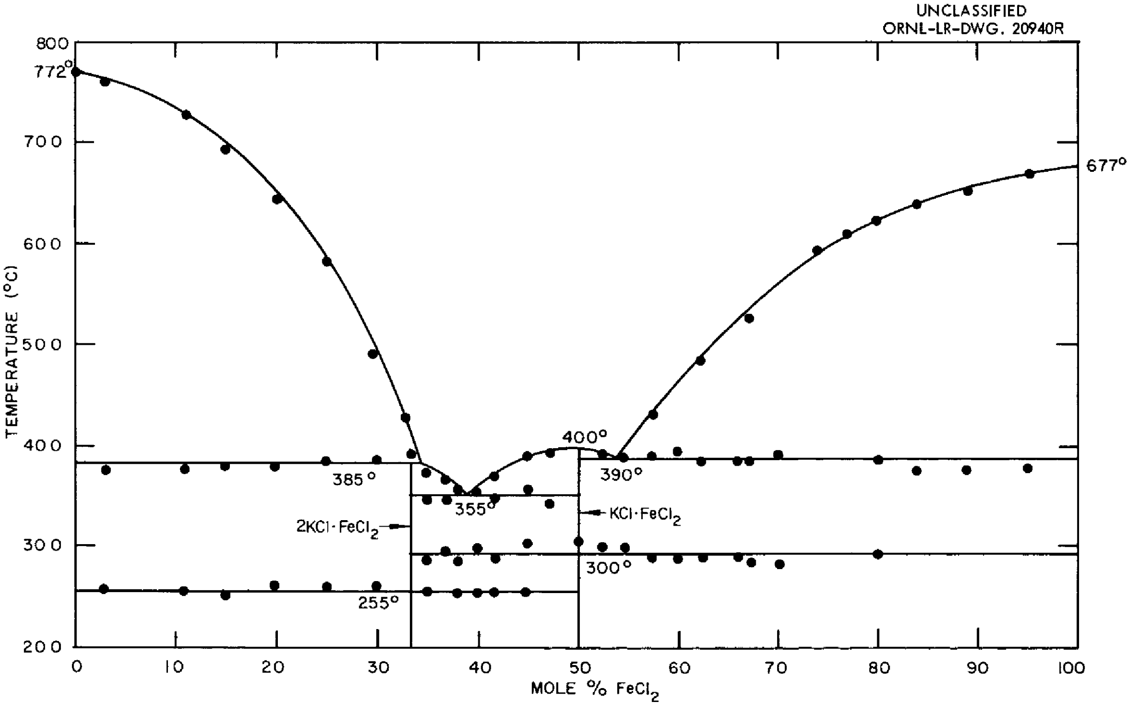

Fig. 3.78. The System $KCl-FeCl_2$.

3.79. The System $\mathrm{NaCl{-}ZrCl_4}$

C. J. Barton, R. J. Sheil, and W. R. Grimes, unpublished work performed at the Oak Ridge National Laboratory, 1956.

Preliminary diagram.

Invariant Equilibria

Mole % $\mathrm{ZrCl_4}$ in Liquid	Invariant Temperature (°C)	Type of Equilibrium	Phase Reaction at Invariant Temperature
28.0	535 ± 5	Peritectic	$L + \mathrm{NaCl} \rightleftharpoons \mathrm{3NaCl{\cdot}ZrCl_4}$
–	445 ± 5	Decomposition	$\mathrm{3NaCl{\cdot}ZrCl_4} \rightleftharpoons \mathrm{NaCl} + \alpha\text{-}\mathrm{2NaCl{\cdot}ZrCl_4}$
28.5	525 ± 5	Eutectic	$L \rightleftharpoons \mathrm{3NaCl{\cdot}ZrCl_4} + \alpha\text{-}\mathrm{2NaCl{\cdot}ZrCl_4}$
33.3	626 + 5	Congruent melting point	$L \rightleftharpoons \alpha\text{-}\mathrm{2NaCl{\cdot}ZrCl_4}$
–	370 ± 5	Inversion	$\alpha\text{-}\mathrm{2NaCl{\cdot}ZrCl_4} \rightleftharpoons \beta\text{-}\mathrm{2NaCl{\cdot}ZrCl_4}$
58	352 ± 5	Peritectic	$L + \beta\text{-}\mathrm{2NaCl{\cdot}ZrCl_4} \rightleftharpoons \alpha\text{-}\mathrm{3NaCl{\cdot}4ZrCl_4}$
–	312 ± 5	Inversion	$\alpha\text{-}\mathrm{3NaCl{\cdot}4ZrCl_4} \rightleftharpoons \beta\text{-}\mathrm{3NaCl{\cdot}4ZrCl_4}$
63	312 ± 5	Eutectic	$L \rightleftharpoons \beta\text{-}\mathrm{3NaCl{\cdot}4ZrCl_4} + \mathrm{ZrCl_4}$

Previous reports on the system $\mathrm{NaCl{-}ZrCl_4}$ have been made by N. A. Berlozerskts and O. A. Kucherenko, *Zhur. Priklad. Khim.* **13**, 1552 (1940), I. S. Morozov and B. G. Korshunov, *Zhur. Neorg. Khim.* **1**, 145(1956), and H. H. Kellogg, L. J. Howell, and R. C. Sommer, *Physical Chemical Properties of the Systems* $\mathrm{NaCl{-}ZrCl_4}$, $\mathrm{KCl{-}ZrCl_4}$, *and* $\mathrm{NaCl{-}KCl{-}ZrCl_4}$, *Summary Report*, NYO-3108 (April 7, 1955).

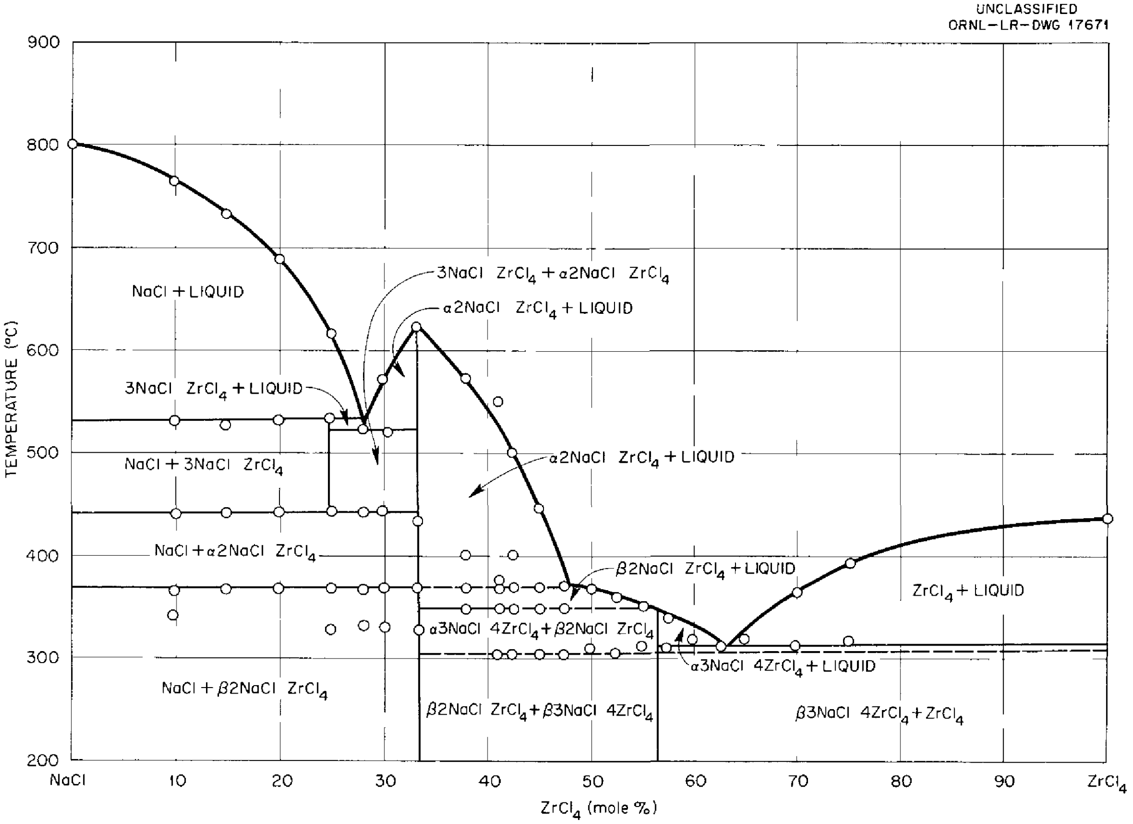

Fig. 3.79. The System NaCl–$ZrCl_4$.

3.80. The System $KCl-ZrCl_4$

C. J. Barton, R. J. Sheil, and W. R. Grimes, unpublished work performed at the Oak Ridge National Laboratory, 1955.

Preliminary diagram.

Invariant Equilibria

Mole % $ZrCl_4$ in Liquid	Invariant Temperature (°C)	Type of Equilibrium	Phase Reaction at Invariant Temperature
23	600 ± 5	Eutectic	$L \rightleftharpoons KCl + 2KCl\cdot ZrCl_4$
33.3	790 ± 5	Congruent melting point	$L \rightleftharpoons 2KCl\cdot ZrCl_4$
48	565 ± 5	Peritectic	$L + 2KCl\cdot ZrCl_4 \rightleftharpoons \alpha\text{-}7KCl\cdot 6ZrCl_4$
–	222 ± 4	Inversion	$\alpha\text{-}7KCl\cdot 6ZrCl_4 \rightleftharpoons \beta\text{-}7KCl\cdot 6ZrCl_4$
65	225 ± 4	Eutectic	$L \rightleftharpoons \alpha\text{-}7KCl\cdot 6ZrCl_4 + ZrCl_4$

Some phase work on this system has been reported by H. H. Kellogg, L. J. Howell, and R. C. Sommer, *Physical Chemical Properties of the Systems NaCl–ZrCl₄, KCl–ZrCl₄, and NaCl–KCl–ZrCl₄, Summary Report,* NYO-3108 (April 7, 1955).

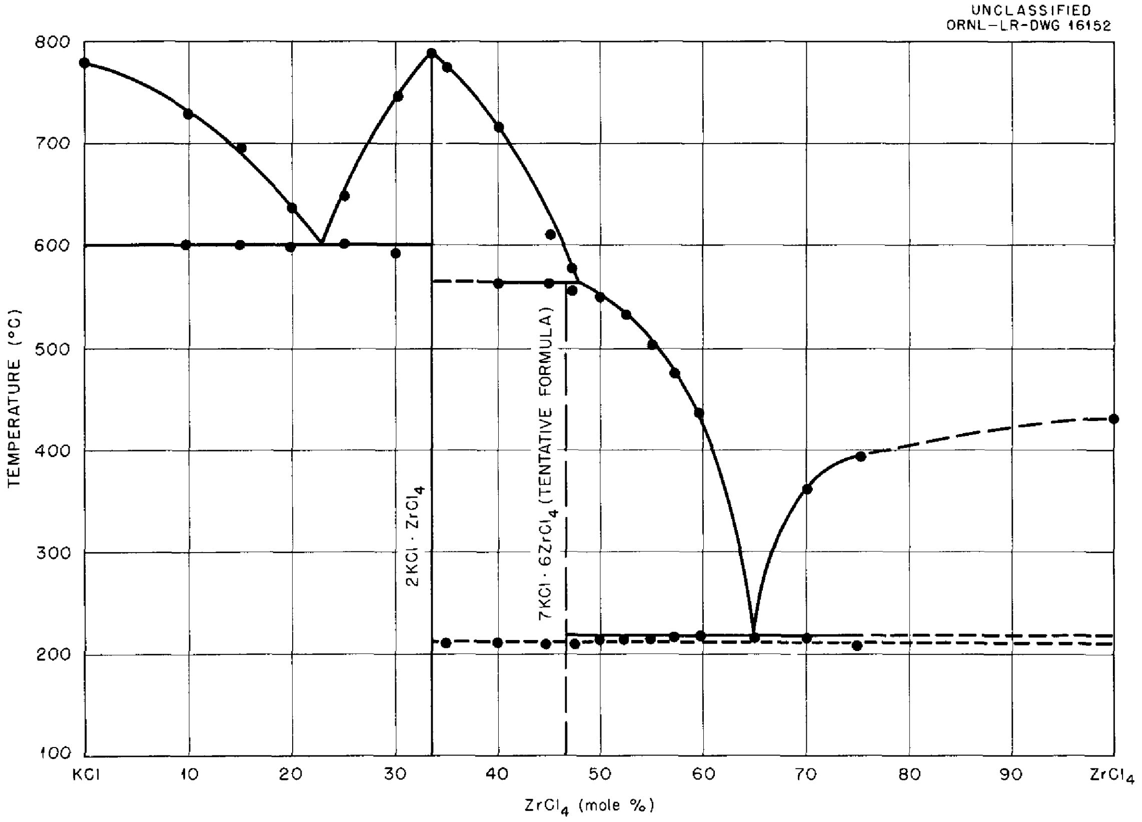

Fig. 3.80. The System $KCl-ZrCl_4$.

3.81. The System LiCl–UCl_3

C. J. Barton, A. B. Wilkerson, and W. R. Grimes, unpublished work performed at the Oak Ridge National Laboratory, 1953.

Preliminary diagram. The system LiCl–UCl_3 contains a single eutectic at 75 LiCl–25 UCl_3 (mole %), m.p. 495 ± 5°C.

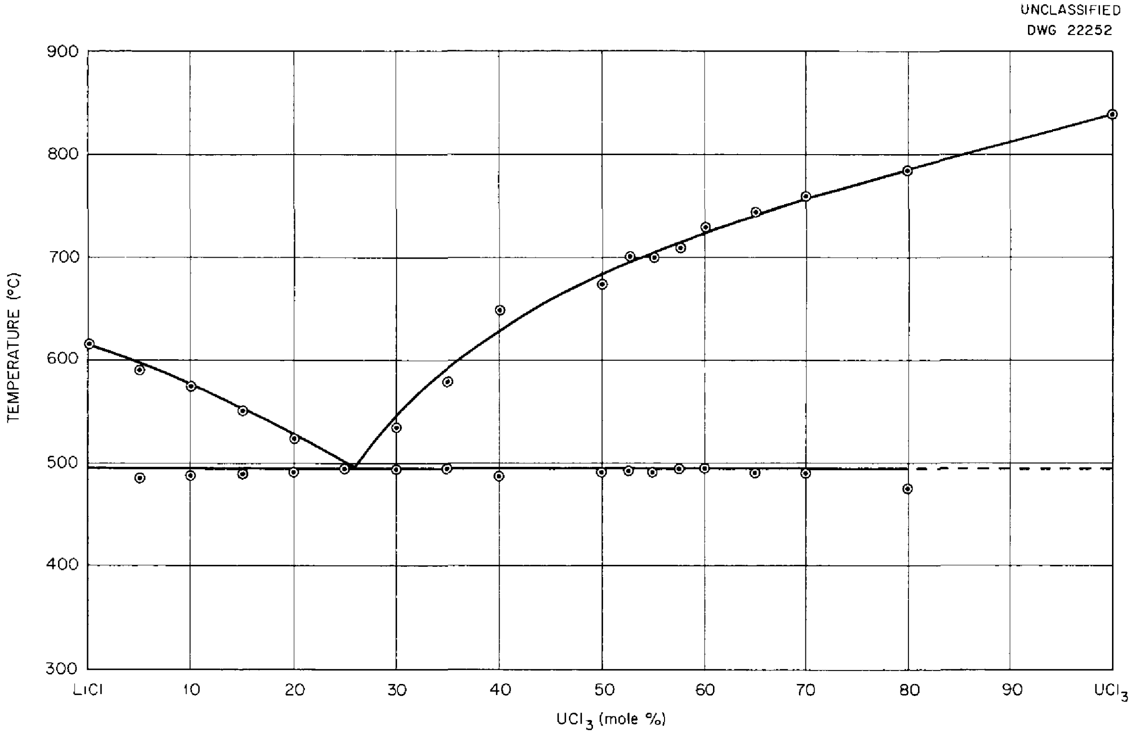

Fig. 3.81. The System LiCl–UCl_3.

3.82. The System $LiCl-UCl_4$

C. J. Barton, R. J. Sheil, and W. R. Grimes, unpublished work performed at the Oak Ridge National Laboratory, 1953.

Preliminary diagram.

Invariant Equilibria

Mole % UCl_4 in Liquid	Invariant Temperature (°C)	Type of Equilibrium	Phase Reaction at Invariant Temperature
29	415	Eutectic	$L \rightleftharpoons 2LiCl \cdot UCl_4 + LiCl$
33.3	430 ± 10	Congruent melting point	$L \rightleftharpoons 2LiCl \cdot UCl_4$
48	405	Eutectic	$L \rightleftharpoons 2LiCl \cdot UCl_4 + UCl_4$

Some data on this system were reported by C. A. Kraus in *Phase Diagrams of Some Complex Salts of Uranium with Halides of the Alkali and Alkaline Earth Metals,* M-251 (July 1, 1943).

UNCLASSIFIED
DWG 19904R

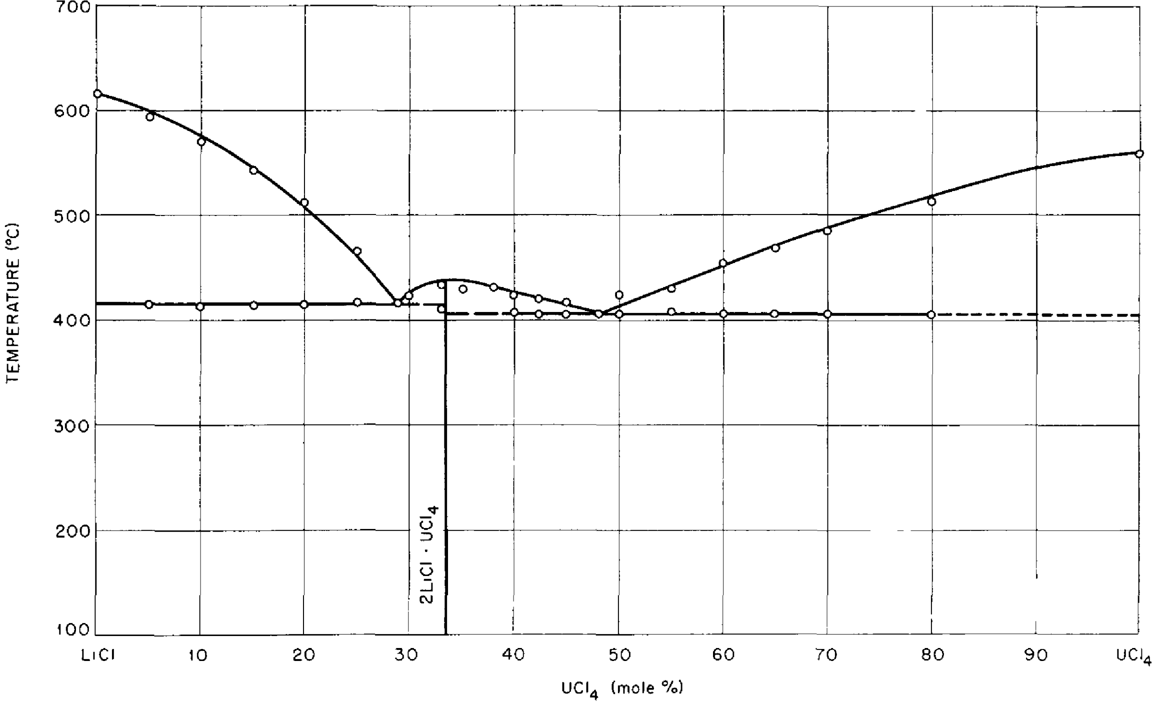

Fig. 3.82. The System $LiCl-UCl_4$.

3.83. The System $NaCl-UCl_3$

C. A. Kraus, unpublished work.

Preliminary diagram constructed with the author's permission from data reported in *Phase Diagrams of Some Complex Salts of Uranium with Halides of the Alkali and Alkaline Earth Metals*, M-251 (July 1, 1943).

The system $NaCl-UCl_3$ contains a single eutectic at 67 NaCl–33 UCl_3 (mole %), m.p. 525°C.

UNCLASSIFIED
ORNL-LR-DWG 20464

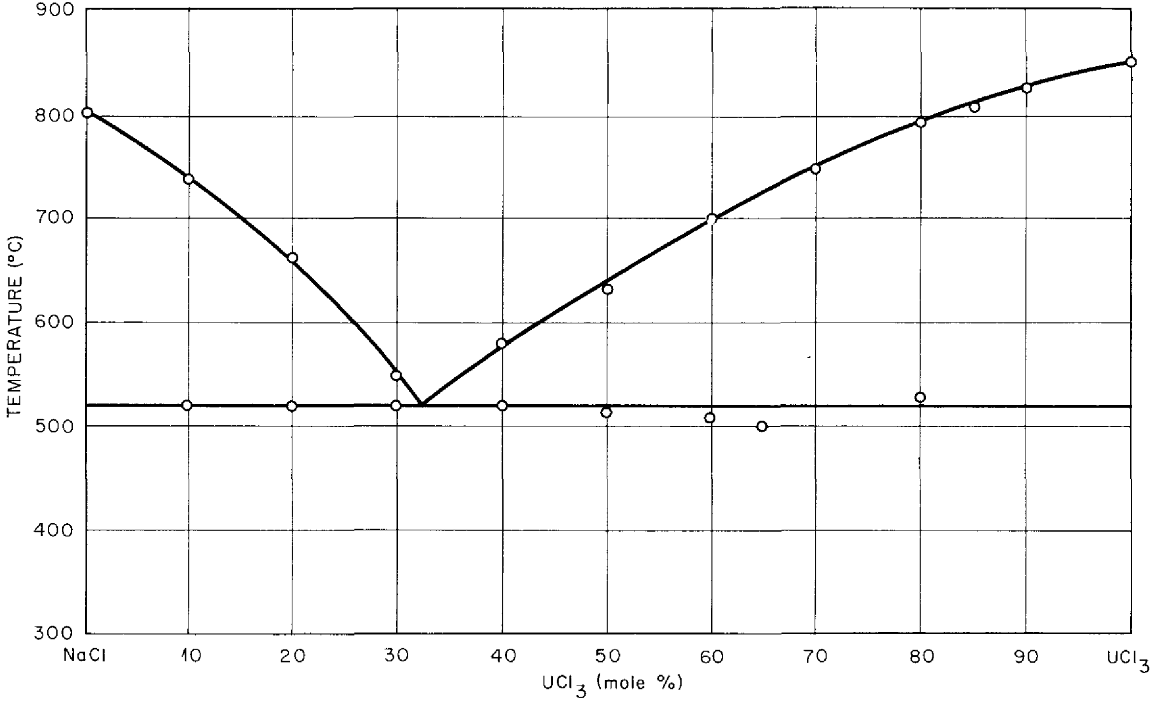

Fig. 3.83. The System $NaCl-UCl_3$.

3.84. The System $NaCl-UCl_4$

C. J. Barton, R. J. Sheil, A. B. Wilkerson, and W. R. Grimes, unpublished work performed at the Oak Ridge National Laboratory, 1953.

Preliminary diagram.

Invariant Equilibria

Mole % UCl_4 in Liquid	Invariant Temperature (°C)	Type of Equilibrium	Phase Reaction at Invariant Temperature
30	430 ± 5	Eutectic	$L \rightleftharpoons NaCl + 2NaCl \cdot UCl_4$
33.3	440 ± 5	Congruent melting point	$L \rightleftharpoons 2NaCl \cdot UCl_4$
47	370 ± 5	Eutectic	$L \rightleftharpoons 2NaCl \cdot UCl_4$ + unidentified compound
57	415 ± 5	Peritectic	$L + UCl_4 \rightleftharpoons$ unidentified compound

A phase diagram of this system has been reported by C. A. Kraus in *Phase Diagrams of Some Complex Salts of Uranium with Halides of the Alkali and Alkaline Earth Metals*, M-251 (July 1, 1943).

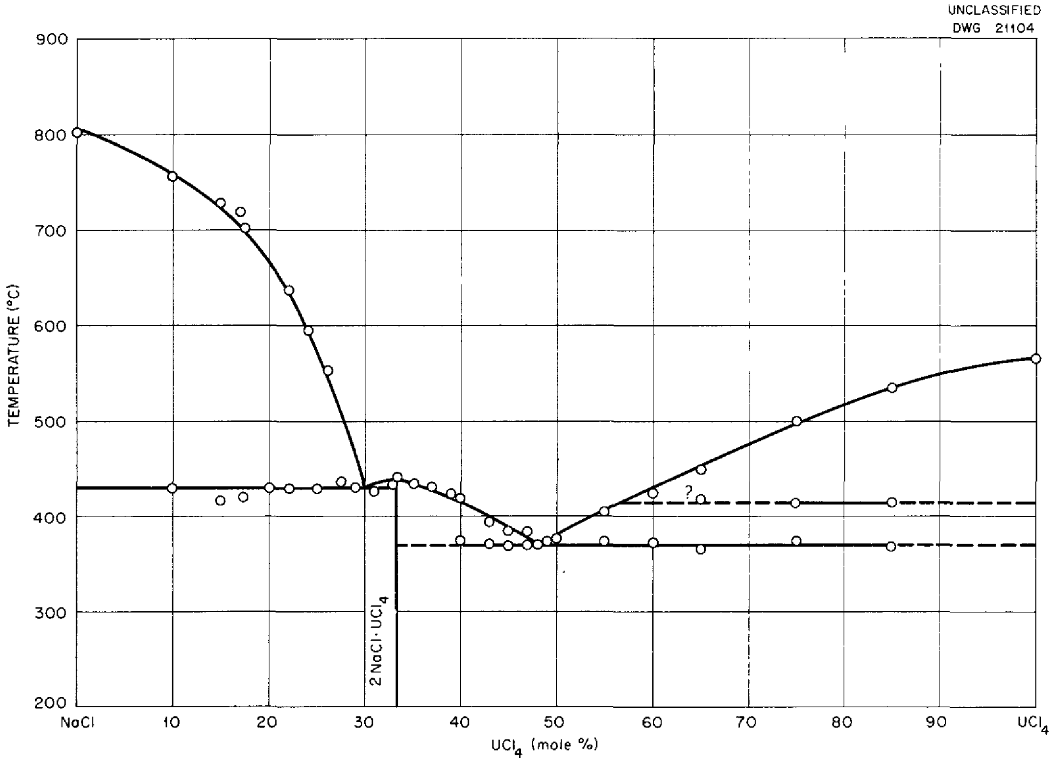

Fig. 3.84. The System $NaCl-UCl_4$.

3.85. The System $KCl–UCl_4$

C. J. Barton, A. B. Wilkerson, T. N. McVay, R. J. Sheil, and W. R. Grimes, unpublished work performed at the Oak Ridge National Laboratory, 1954.

Preliminary diagram.

Invariant Equilibria

Mole % UCl_4 in Liquid	Invariant Temperature (°C)	Type of Equilibrium	Phase Reaction at Invariant Temperature
25	550	Eutectic	$L \rightleftharpoons KCl + 2KCl{\cdot}UCl_4$
33.3	630	Congruent melting point	$L \rightleftharpoons 2KCl{\cdot}UCl_4$
44	330	Eutectic	$L \rightleftharpoons 2KCl{\cdot}UCl_4 + KCl{\cdot}UCl_4$
49	345	Peritectic	$L + KCl{\cdot}3UCl_4 \rightleftharpoons KCl{\cdot}UCl_4$
61	395	Peritectic	$L + UCl_4 \rightleftharpoons KCl{\cdot}3UCl_4$

A phase diagram of this system has been reported by C. A. Kraus in *Phase Diagrams of Some Complex Salts of Uranium with Halides of the Alkali and Alkaline Earth Metals*, M-251 (July 1, 1943).

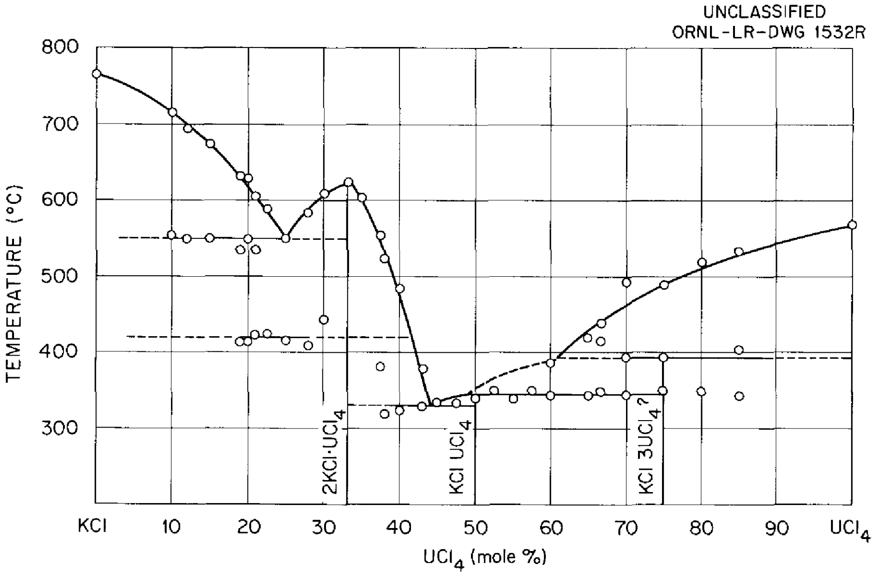

Fig. 3.85. The System $KCl–UCl_4$.

3.86. The System $RbCl-UCl_3$

C. J. Barton, R. J. Sheil, A. B. Wilkerson, and W. R. Grimes, unpublished work performed at the Oak Ridge National Laboratory, 1954.

Preliminary diagram.

Invariant Equilibria

Mole % UCl_3 in Liquid	Invariant Temperature (°C)	Type of Equilibrium	Phase Reaction at Invariant Temperature
15	610	Eutectic	$L \rightleftharpoons RbCl + 3RbCl{\cdot}UCl_3$
25	745 ± 10	Congruent melting point	$L \rightleftharpoons 3RbCl{\cdot}UCl_3$
40	560 ± 10	Peritectic	$L + 3RbCl{\cdot}UCl_3 \rightleftharpoons 2RbCl{\cdot}UCl_3$
45.5	513 ± 5	Eutectic	$L \rightleftharpoons 2RbCl{\cdot}UCl_3 + RbCl{\cdot}UCl_3$
49	550 ± 10	Peritectic	$L + UCl_3 \rightleftharpoons RbCl{\cdot}UCl_3$

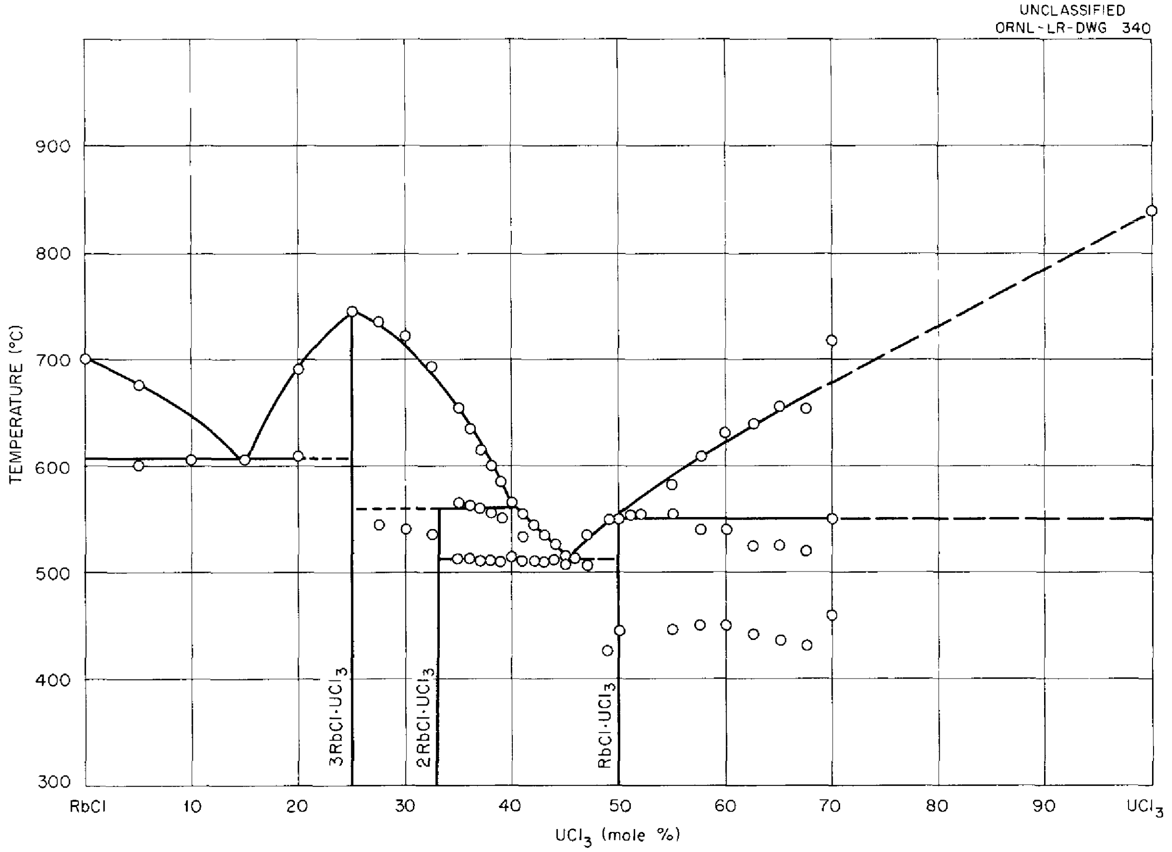

Fig. 3.86. The System $RbCl-UCl_3$.

3.87. The System $CsCl–UCl_4$

C. J. Barton, A. B. Wilkerson, and W. R. Grimes, unpublished work performed at the Oak Ridge National Laboratory, 1953.

Preliminary diagram.

Invariant Equilibria

Mole % UCl_4 in Liquid	Invariant Temperature (°C)	Type of Equilibrium	Phase Reaction at Invariant Temperature
20	505 ± 5	Eutectic	$L \rightleftharpoons CsCl + 2CsCl{\cdot}UCl_4$
33.3	657 ± 5	Congruent melting point	$L \rightleftharpoons 2CsCl{\cdot}UCl_4$
58	370 ± 5	Eutectic	$L \rightleftharpoons 2CsCl{\cdot}UCl_4 + CsCl{\cdot}2UCl_4$
63	382 ± 5	Peritectic	$L + UCl_4 \rightleftharpoons CsCl{\cdot}2UCl_4$

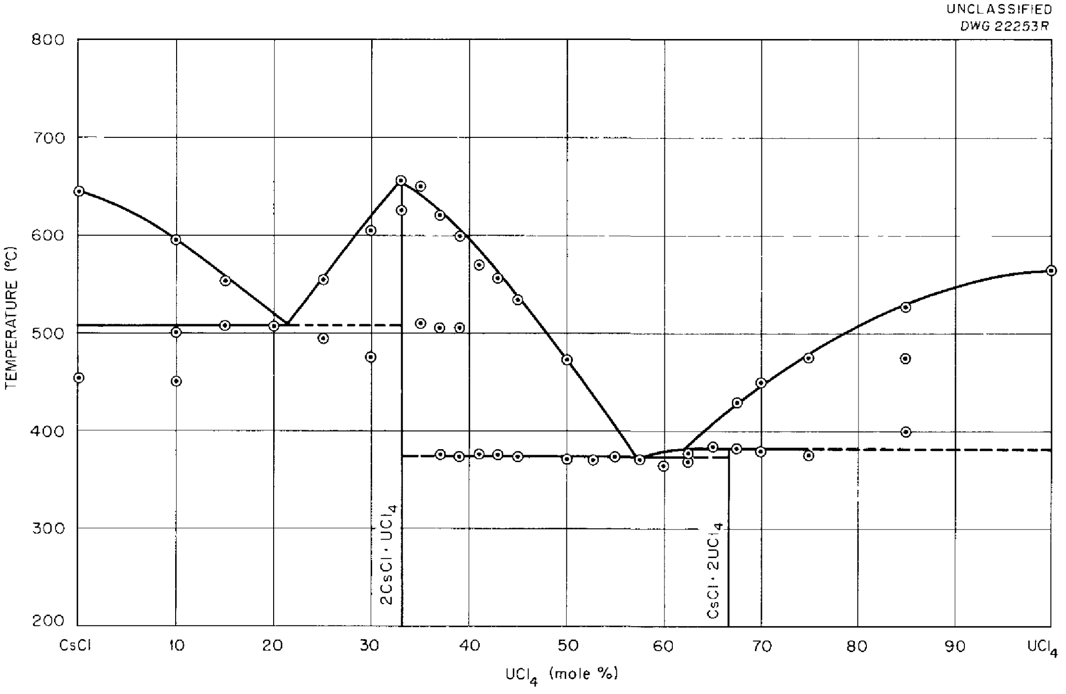

Fig. 3.87. The System $CsCl–UCl_4$.

3.88. The System K_3CrF_6–Na_3CrF_6–Li_3CrF_6

B. J. Sturm, L. G. Overholser, and W. R. Grimes, unpublished work performed at the Oak Ridge National Laboratory, 1951–52.

Preliminary diagram.

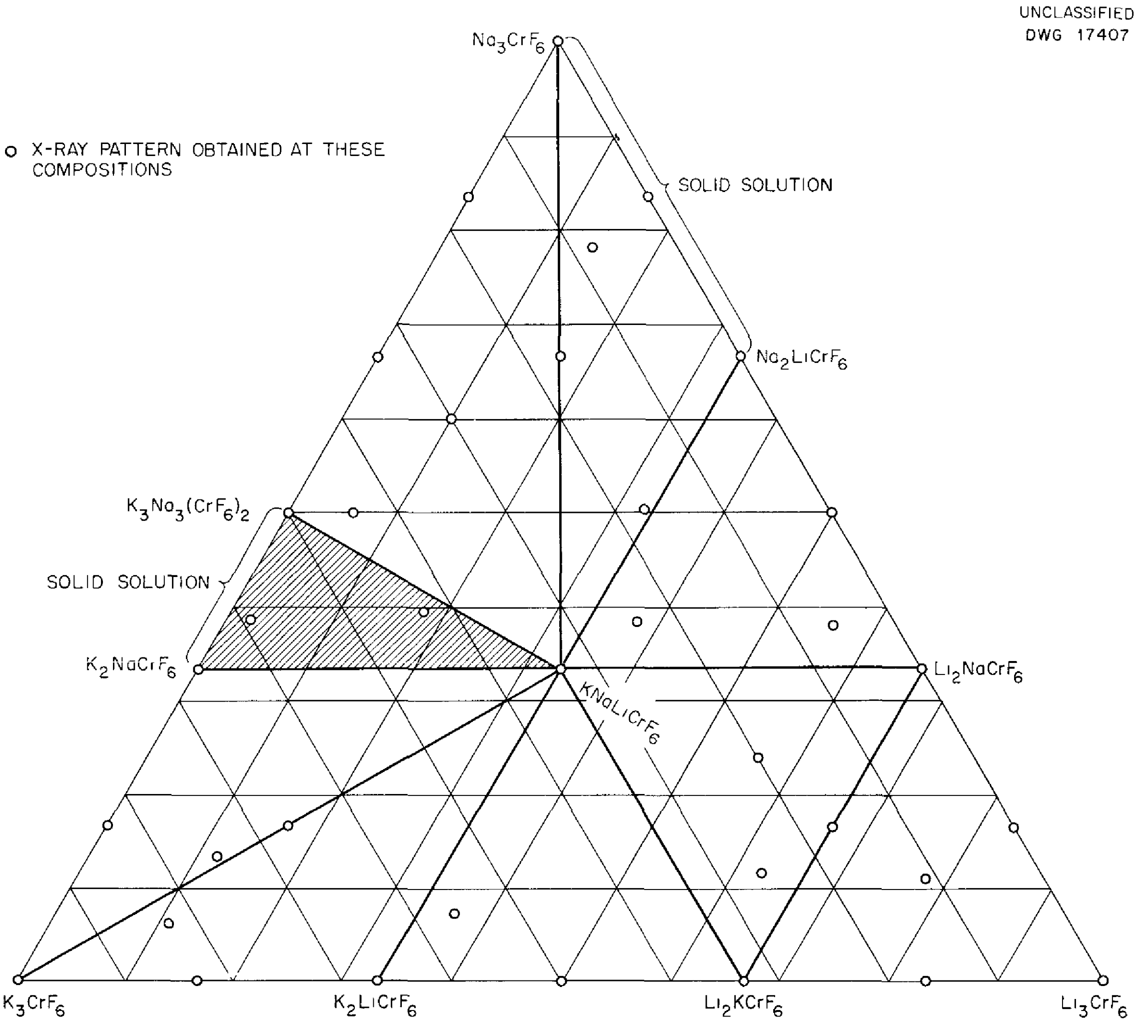

Fig. 3.88. The System K_3CrF_6–Na_3CrF_6–Li_3CrF_6.

4. OXIDE AND HYDROXIDE SYSTEMS

4.1. The System SiO_2–ThO_2

L. A. Harris, "A Preliminary Study of the Phase Equilibria Diagram of ThO_2–SiO_2," *J. Am. Ceram. Soc.* **42**, 74–77 (1959).

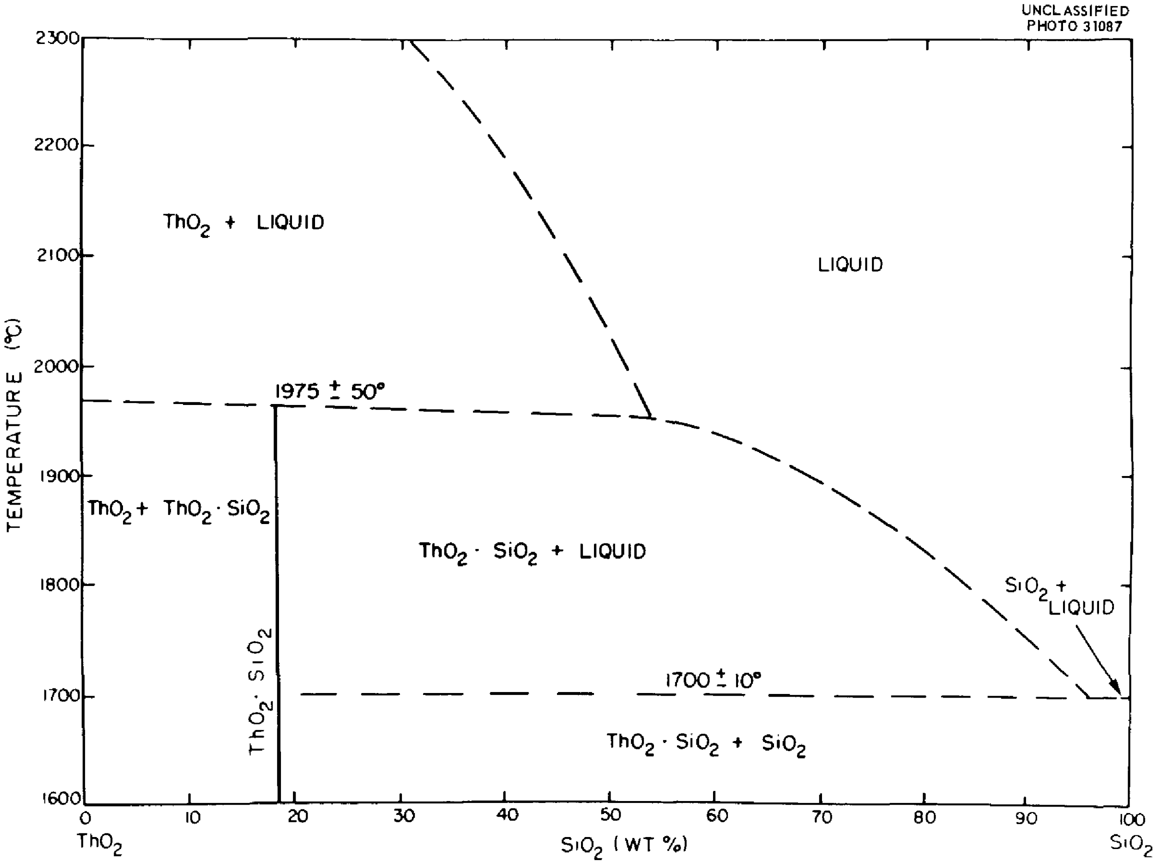

Fig. 4.1. The System SiO_2–ThO_2.

4.2. The System LiOH–NaOH

C. J. Barton, J. P. Blakely, K. A. Allen, W. C. Davis, and B. S. Weaver, unpublished work performed at the Oak Ridge National Laboratory, 1951.

Preliminary diagram. A phase diagram of the system LiOH–NaOH has been reported more recently by N. A. Reshetnikov and G. M. Oonzhakov, *Zhur. Neorg. Khim.* **3**, 1433 (1958).

Invariant Equilibria

Mole % LiOH in Liquid	Invariant Temperature (°C)	Type of Equilibrium	Phase Reaction at Invariant Temperature
27	219	Eutectic	$L \rightleftharpoons$ NaOH + α-NaOH·LiOH
40	250	Peritectic	L + LiOH $\rightleftharpoons$ α-LiOH·NaOH
–	180	Inversion	α-LiOH·NaOH $\rightleftharpoons$ β-LiOH·NaOH

UNCLASSIFIED
ORNL-LR-DWG 20463R

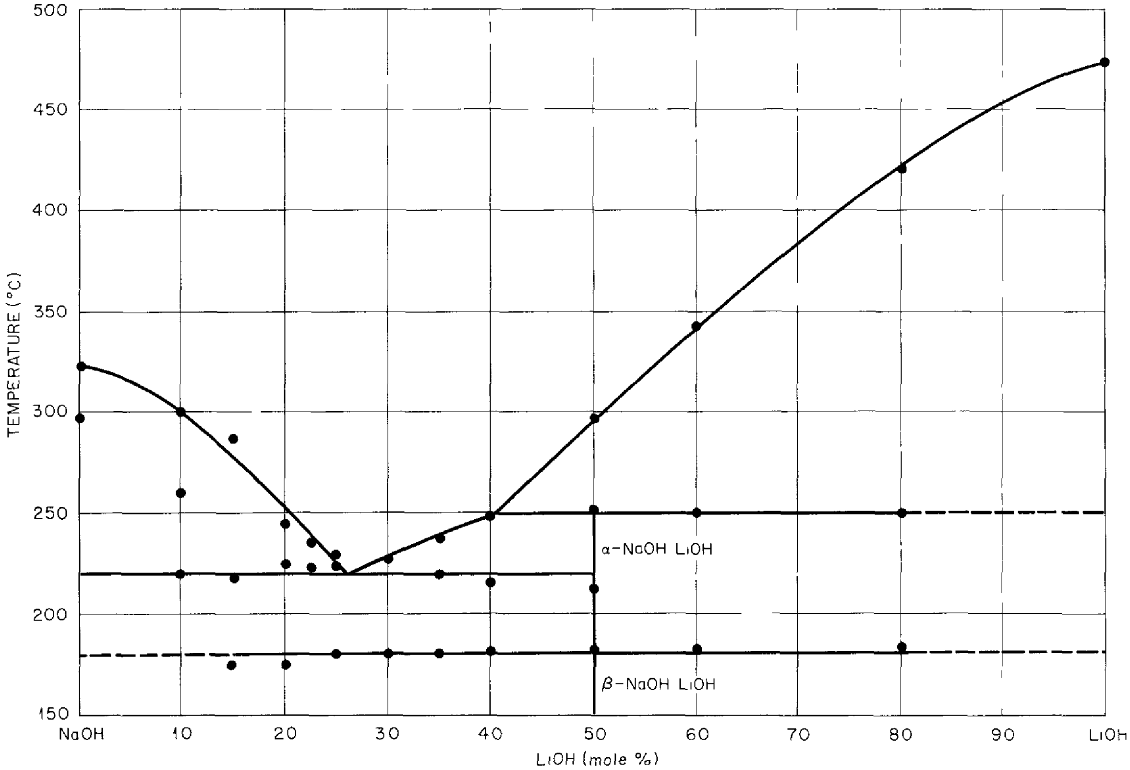

Fig. 4.2. The System LiOH–NaOH.

4.3. The System LiOH–KOH

C. J. Barton, J. P. Blakely, L. M. Bratcher, and W. R. Grimes, unpublished work performed at the Oak Ridge National Laboratory, 1951.

Preliminary diagram.

Invariant Equilibria

Mole % KOH in Liquid	Invariant Temperature (°C)	Type of Equilibrium	Phase Reaction at Invariant Temperature
40	315	Incongruent melting point of $3\text{LiOH}\cdot 2\text{KOH}$	$L + \text{LiOH} \rightleftharpoons 3\text{LiOH}\cdot 2\text{KOH}$
70	245	Eutectic	$L \rightleftharpoons 3\text{LiOH}\cdot 2\text{KOH} + \beta\text{-KOH}$

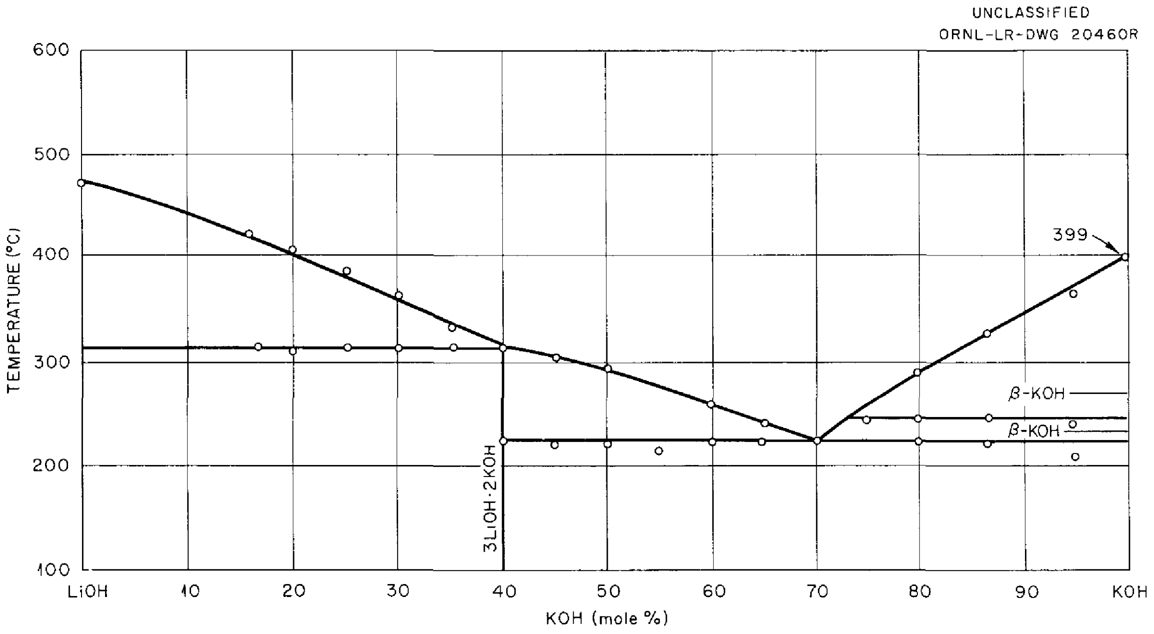

Fig. 4.3. The System LiOH–KOH.

4.4. The System NaOH–KOH

G. von Hevesy, "The Binary Systems NaOH–KOH, KOH–RbOH, and RbOH–NaOH," *Z. physik. Chem.* **73**, 667–84 (1910).

UNCLASSIFIED
ORNL-LR-DWG 20458

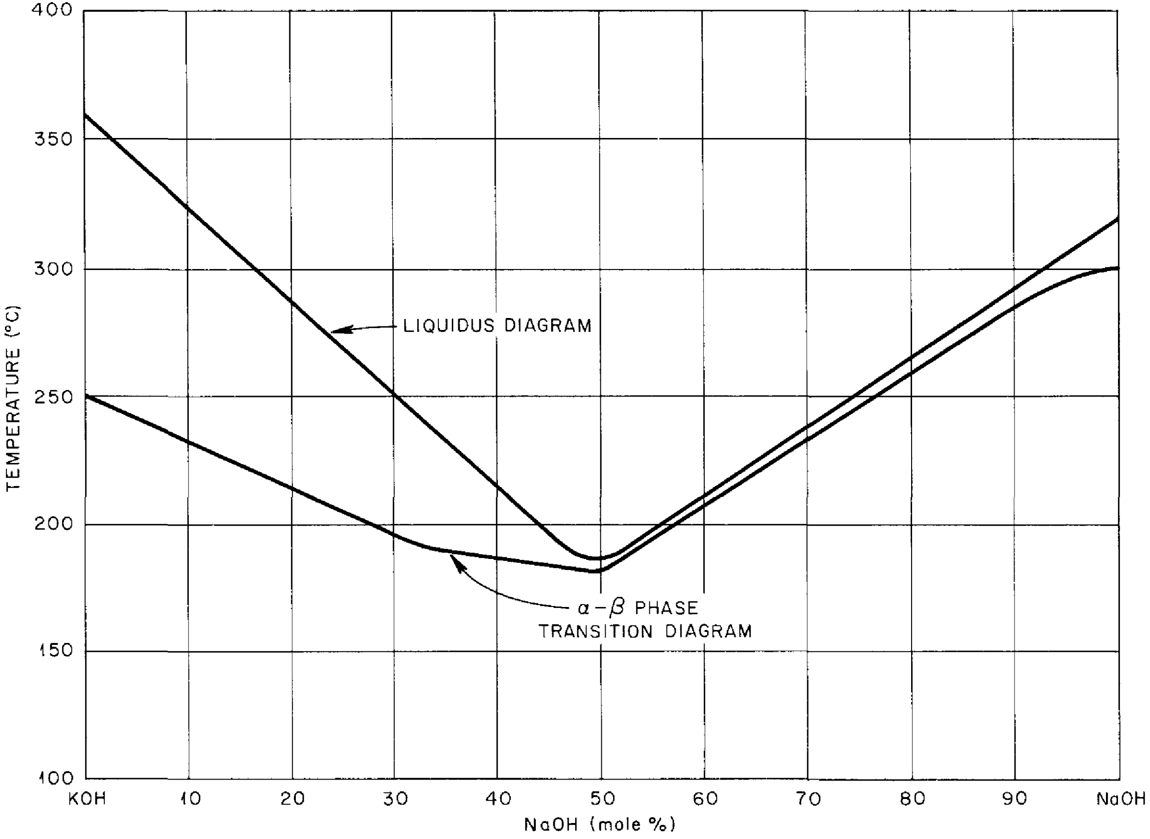

Fig. 4.4. The System NaOH–KOH.

4.5. The System NaOH–RbOH

G. von Hevesy, "The Binary Systems NaOH–KOH, KOH–RbOH, and RbOH–NaOH," *Z. physik. Chem.* **73**, 667–84 (1910).

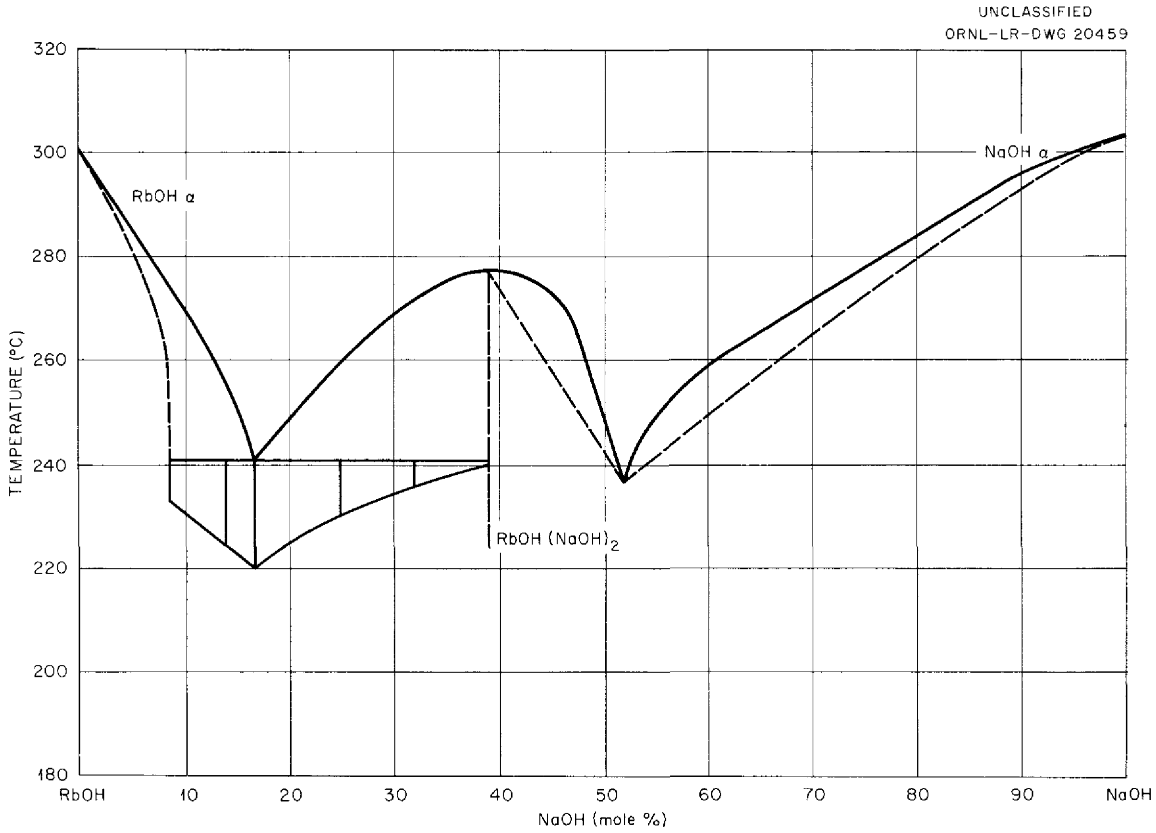

Fig. 4.5. The System NaOH–RbOH.

4.6. The System $Ba(OH)_2$–$Sr(OH)_2$

K. A. Allen, W. C. Davis, and B. S. Weaver, unpublished work performed at the Oak Ridge National Laboratory, 1951.

Preliminary diagram. The system $Ba(OH)_2$–$Sr(OH)_2$ contains a single eutectic at 37 $Sr(OH)_2$–63 $Ba(OH)_2$ (mole %), m.p. 360°C.

UNCLASSIFIED
ORNL-LR-DWG 20462R

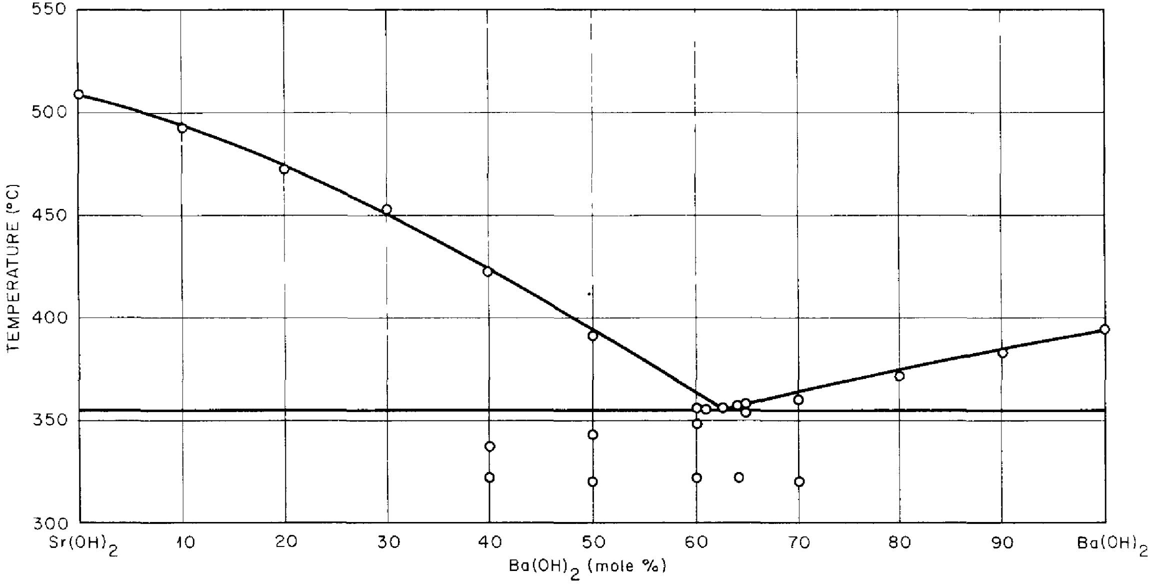

Fig. 4.6. The System $Ba(OH)_2$–$Sr(OH)_2$.

5.1. The System UO_2–P_2O_5–H_2O, 25°C Isotherm

J. M. Schreyer, "The Solubility of Uranium(IV) Orthophosphates in Phosphoric Acid Solutions," *J. Am. Chem. Soc.* **77**, 2972 (1955).

The transition point between $U(HPO_4)_2 \cdot 6H_2O$ and $U(HPO_4)_2 \cdot H_3PO_4 \cdot H_2O$ as stable solids was at 0.62 ± 0.02 *M* U (10.3 wt % UO_2) and 9.8 ± 0.1 *M* PO_4 (42.6 wt % P_2O_5), density 1.63 ± 0.03 g/ml. The compound $U(HPO_4)_2 \cdot H_3PO_4 \cdot H_2O$ is incongruently soluble in water.

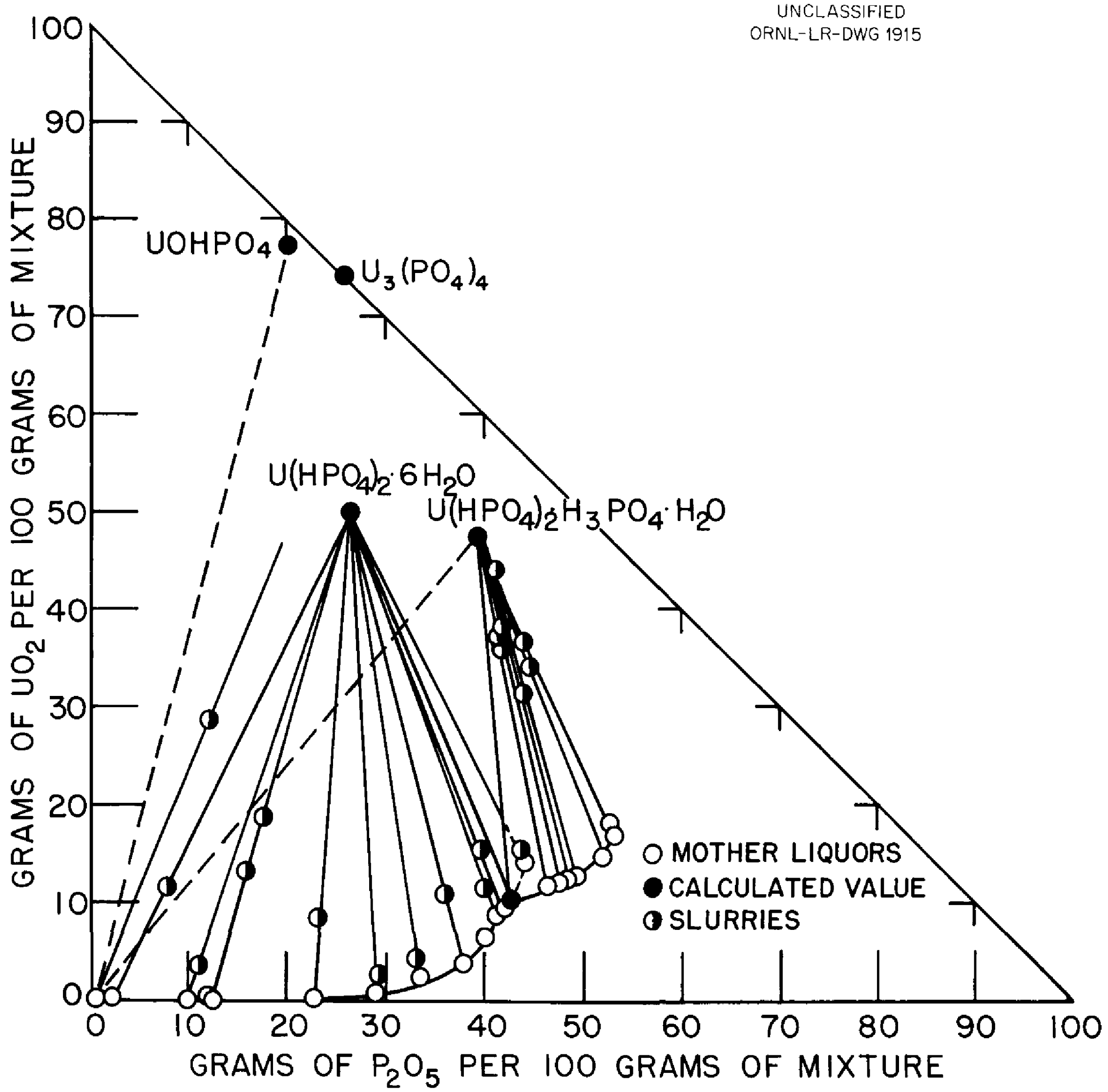

Fig. 5.1. The System UO_2–P_2O_5–H_2O, 25°C Isotherm.

5.2. The System UO_3–H_3PO_4–H_2O, 25°C Isotherm

J. M. Schreyer and C. F. Baes, Jr., "The Solubility of Uranium(VI) Orthophosphates in Phosphoric Acid Solution," *J. Am. Chem. Soc.* **76**, 354 (1954).

The normal phosphate $(UO_2)_3(PO_4)_2{\cdot}6H_2O$ is stable below 0.025 mole % H_3PO_4. The stability ranges are as follows:

Compound	Total Phosphate Molarity
$(UO_2)_3(PO_4)_2{\cdot}6H_2O$	<0.014
$UO_2HPO_4{\cdot}4H_2O$	0.014–6.1
$UO_2(H_2PO_4)_2{\cdot}3H_2O$	>6.1

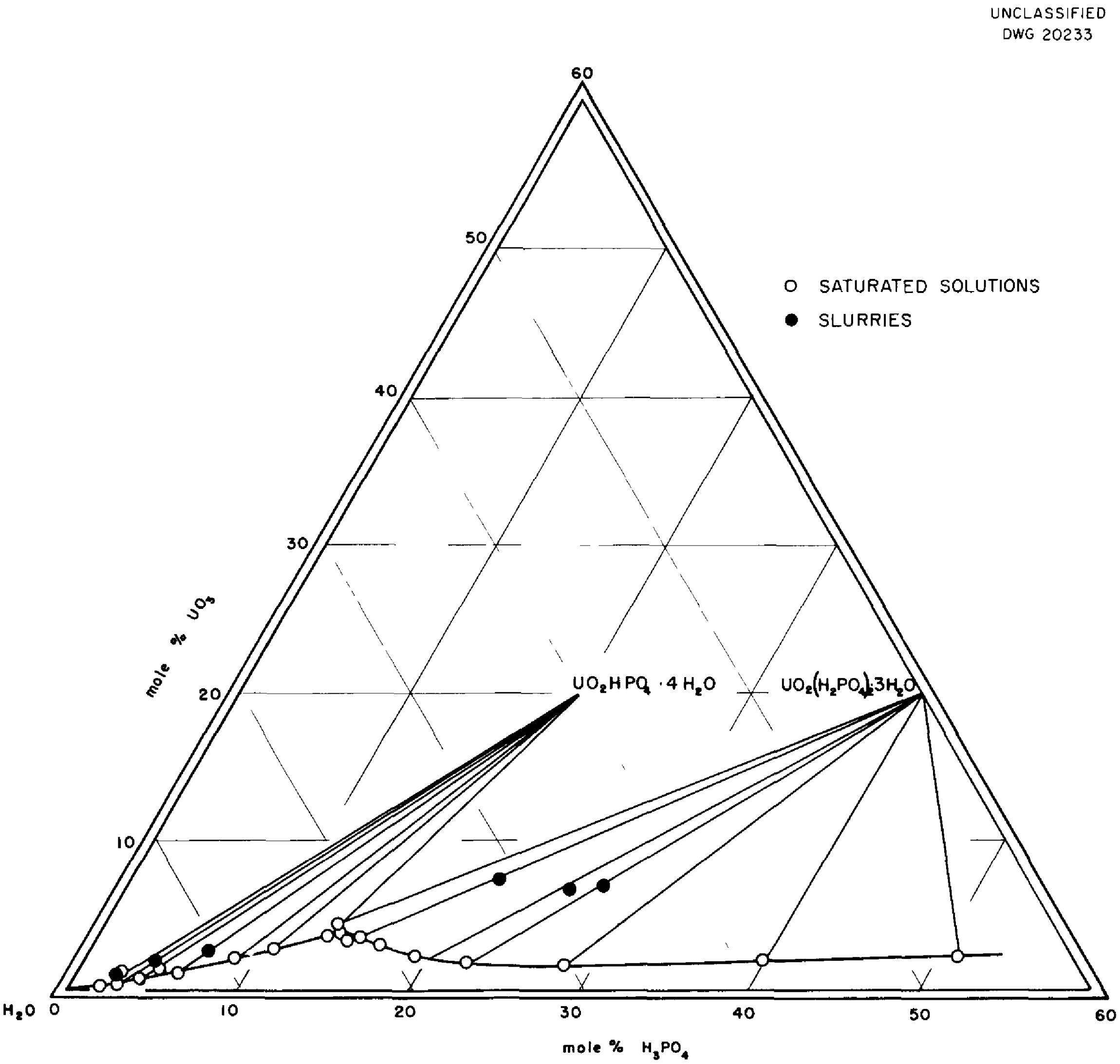

Fig. 5.2. The System UO_3–H_3PO_4–H_2O, 25°C Isotherm. 0–60 mole % UO_3, 0–60 mole % H_3PO_4.

5.3. The System $U(HPO_4)_2$–Cl_2O_7–H_2O, 25°C Isotherm

J. M. Schreyer and L. R. Phillips, "The Solubility of Uranium(VI) Orthophosphates in Perchloric Acid Solutions," *J. Phys. Chem.* **60**, 588 (1956).

The stable solids in this system are $U(HPO_4)_2 \cdot 2H_2O$, $U(H_2PO_4)_2(ClO_4)_2 \cdot 4H_2O$, and $U(H_2PO_4)_2(ClO_4)_2 \cdot 6H_2O$. Metastable anhydrous $U(HPO_4)_2$ formed readily in all solution compositions tested. X-ray diffraction patterns indicated the existence of three polymorphic forms of $U(H_2PO_4)_2(ClO_4)_2 \cdot 6H_2O$.

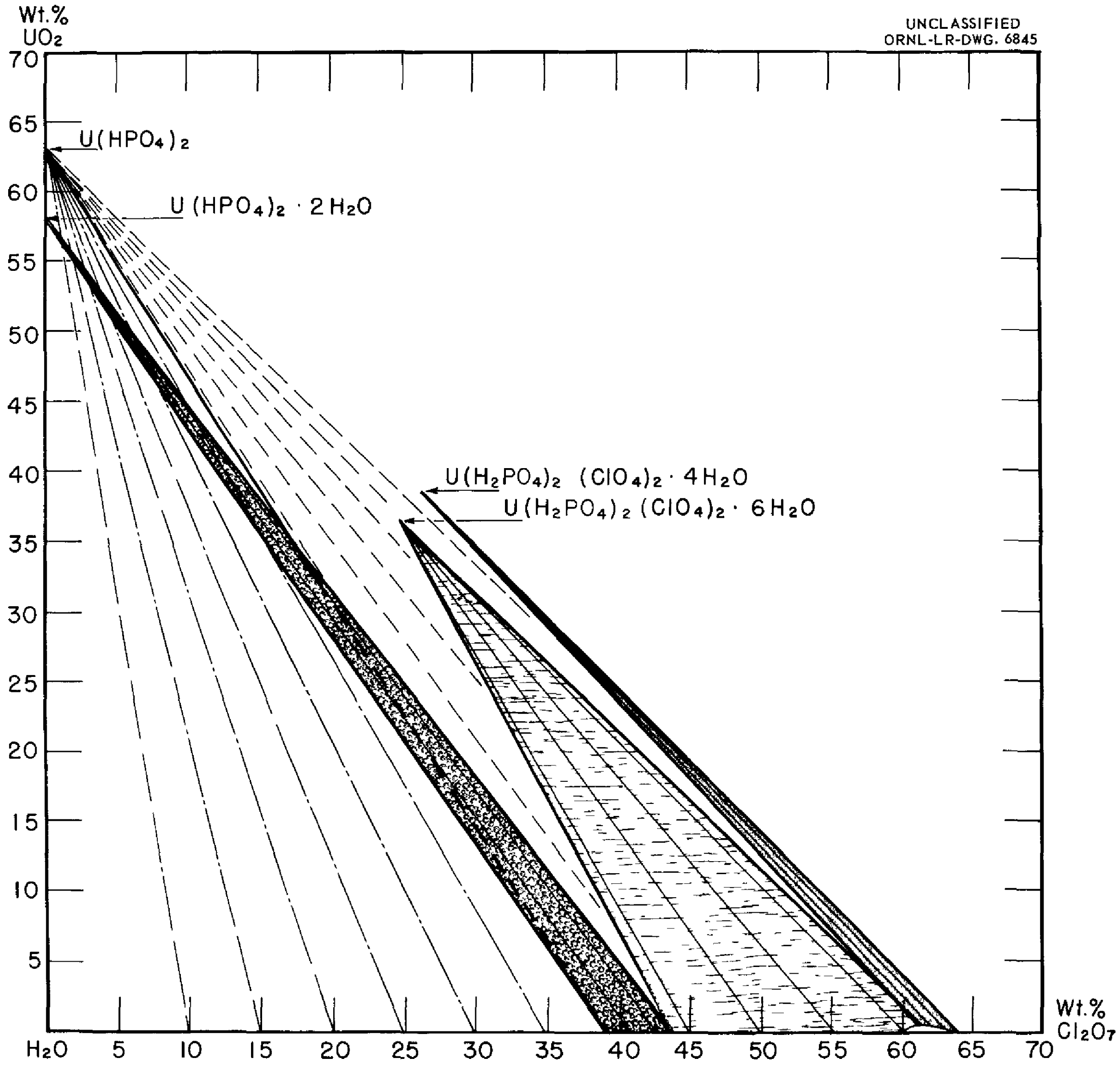

Fig. 5.3. Schreinemakers' Projection of the System UO_2–P_2O_5–Cl_2O_7–H_2O at 25°C. A projection on the UO_2–Cl_2O_7–H_2O face, plotted in rectangular coordinates.

5.4. The System UO_3–Na_2O–CO_2–H_2O, 26°C Isotherm

C. A. Blake, C. F. Coleman, K. B. Brown, D. G. Hill, R. S. Lowrie, and J. M. Schmitt, "Studies in the Carbonate–Uranium System," *J. Am. Chem. Soc.* **78**, 5978 (1956).

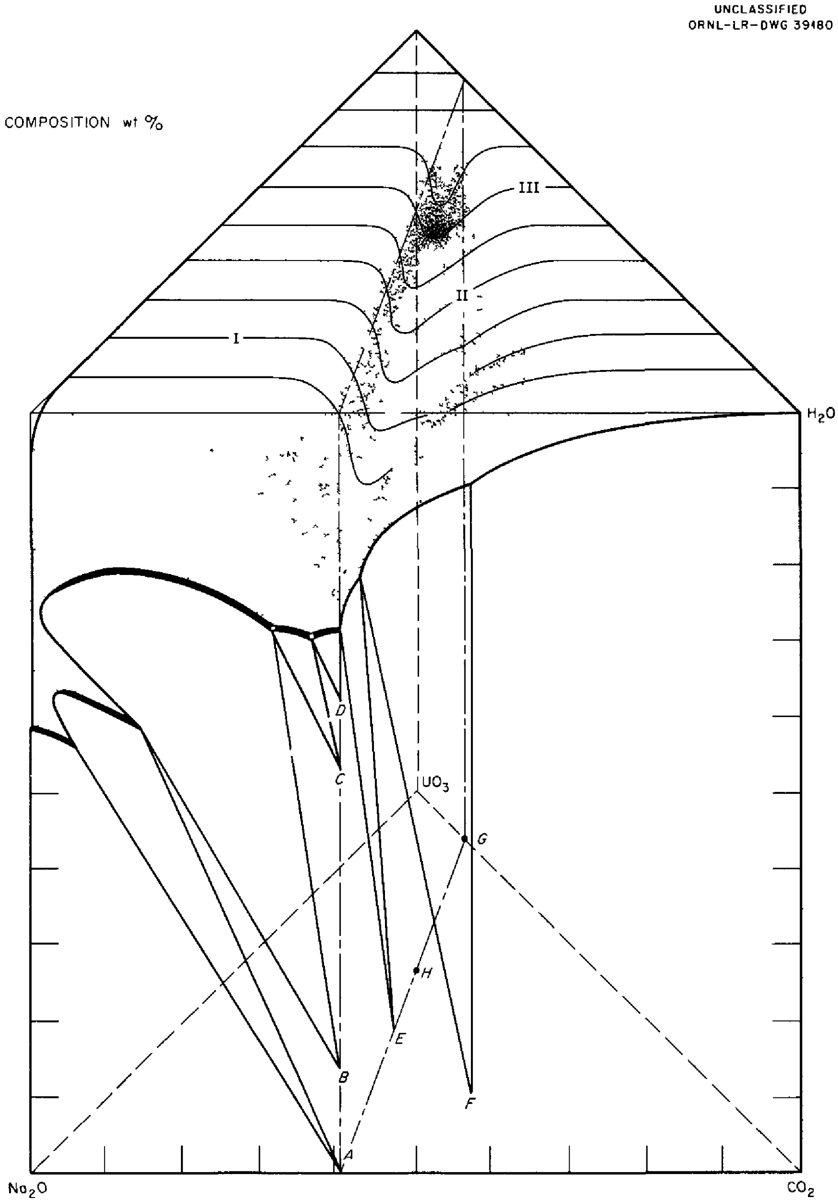

Fig. 5.4*a*. The System UO_3–Na_2O–CO_2–H_2O at 26°C. Compositions are plotted in weight per cent. I, solutions in equilibrium with sodium uranates; II, solutions in equilibrium with sodium uranyl tricarbonate; III, solutions in equilibrium with uranyl carbonate. *A*, Na_2CO_3; *B*, $Na_2CO_3 \cdot H_2O$; *C*, $Na_2CO_3 \cdot 7H_2O$; *D*, $Na_2CO_3 \cdot 10H_2O$; *E*, $Na_2CO_3 \cdot NaHCO_3 \cdot 2H_2O$ (trona); *F*, $NaHCO_3$, *G*, UO_2CO_3; *H*, $Na_4UO_2(CO_3)_3$. The entire upper face of the triangular prism represents pure water.

The stable uranium–carbonate solids found were UO_2CO_3 and $Na_4UO_2(CO_3)_3$. The solution composition at the transition point (not determined exactly) was at least 26 wt % UO_3, 5.6 wt % Na_2O, and 7.2 wt % CO_2 (mole ratio $UO_3:Na_2O:CO_2 = 1:1.0:1.8$).

Further data on this system are available from the American Documentation Institute (document No. 5079). These include compositions, pH's, and densities at points in and near the planes $Na_2O–CO_2–H_2O$, $UO_3–Na_2O–H_2O$, $UO_2CO_3–Na_2CO_3–H_2O$, $Na_4UO_2(CO_3)_3–NaHCO_3–H_2O$, $UO_3–Na_2CO_3–H_2O$, $UO_3–NaHCO_3–H_2O$, and $UO_2CO_3–Na_2O–H_2O$.

Related phase equilibria in the system $Na_2O–UO_3–H_2O$ at 50 and 75°C are reported by J. E. Ricci and F. J. Loprest, *J. Am. Chem. Soc.* **77**, 2119 (1955).

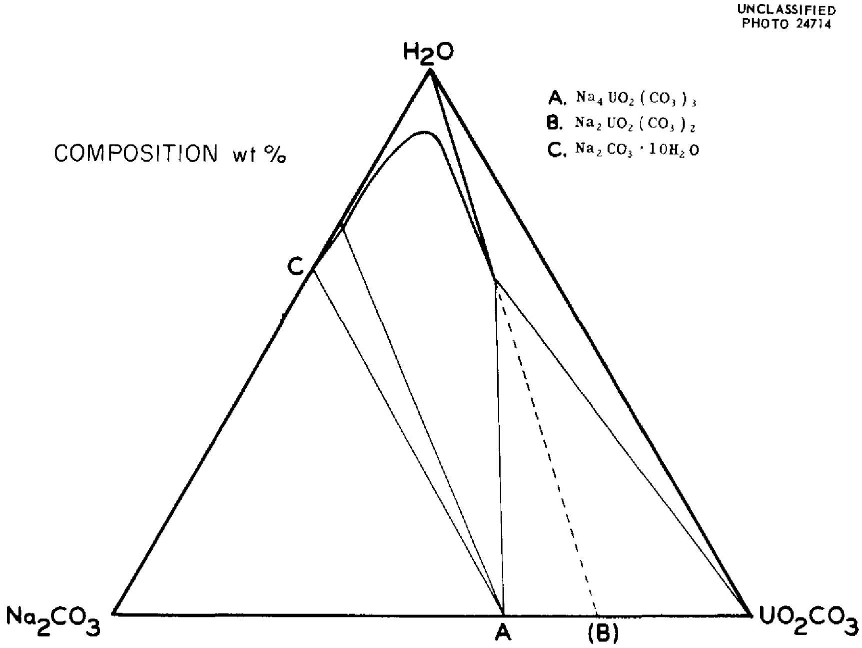

Fig. 5.4*b*. The Section $UO_2CO_3–Na_2CO_3–H_2O$ at 26°C.

5.5. Portions of the System $ThO_2-Na_2O-CO_2-H_2O$, 25°C Isotherm

F. A. Schimmel, unpublished work performed at the Oak Ridge National Laboratory, 1955. The stable thorium-carbonate solids found were $ThOCO_3 \cdot 8H_2O$ and $Na_6Th(CO_3)_5 \cdot 12H_2O$.

Ternary Points

Solid Phases Present	Composition of Solution (wt %)		
	ThO_2	Na_2O	CO_2
$Na_6Th(CO_3)_5 \cdot 12H_2O$, $NaHCO_3$, and $Na_2CO_3 \cdot NaHCO_3 \cdot 2H_2O$ (trona)	0.62	12.0	9.96
$Na_6Th(CO_3)_5 \cdot 12H_2O$, $Na_2CO_3 \cdot 10H_2O$, and trona	0.48	14.1	10.86

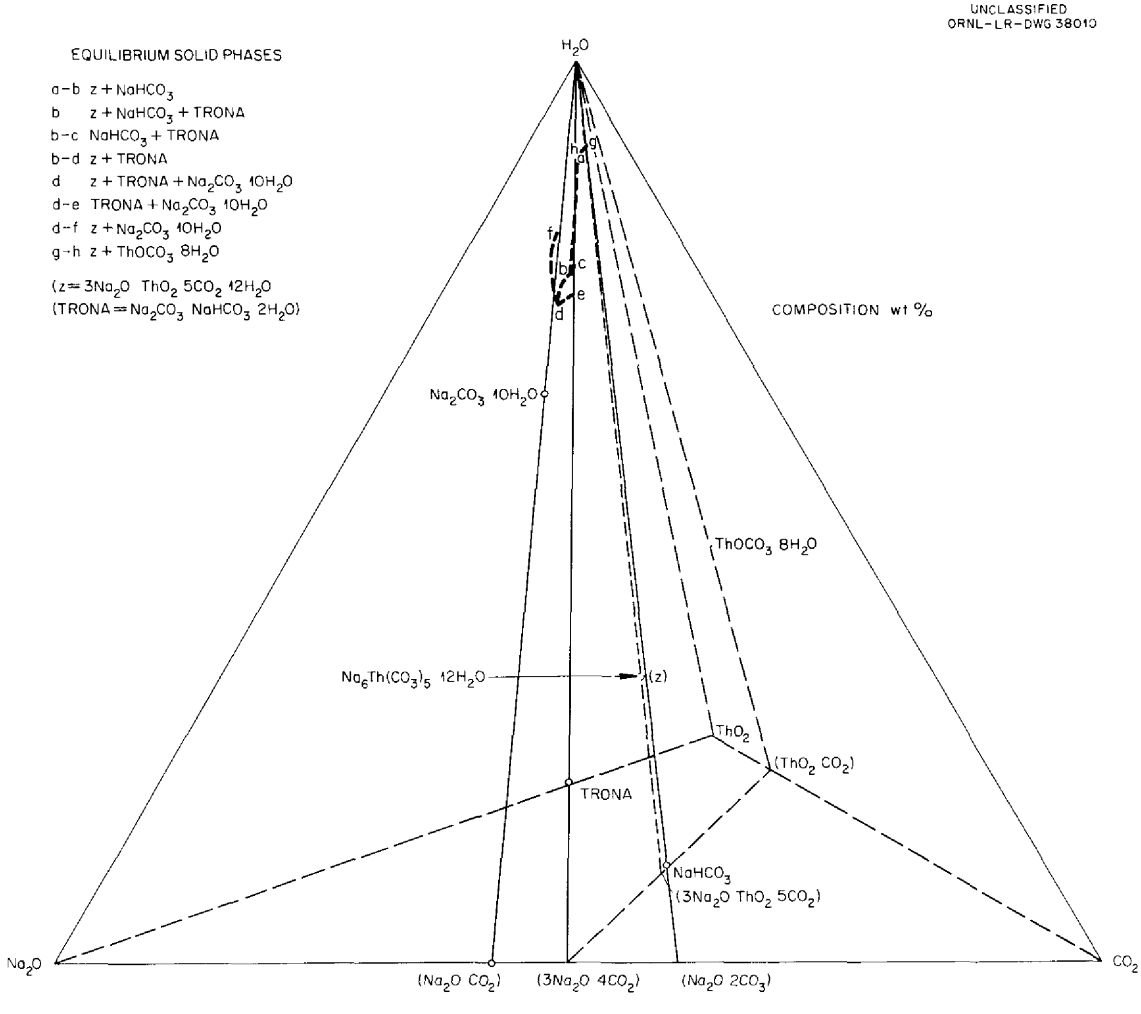

Fig. 5.5a. Perspective Representation of the System $ThO_2-Na_2O-CO_2-H_2O$ as a Tetrahedron.

The highest thorium solubility found was 3.35 wt % ThO_2 (3.06 wt % Na_2O, 3.60 wt % CO_2) in equilibrium with solid $Na_6Th(CO_3)_5 \cdot 12H_2O$ and $ThOCO_3 \cdot 8H_2O$. (The terminal points of this binary line were not established.) The maximum thorium solubility in equilibrium with $Na_6Th(CO_3)_5 \cdot 12H_2O$ and $Na_2CO_3 \cdot 10H_2O$ was 1.25 wt % ThO_2 (12.5 wt % Na_2O, 9.4 wt % CO_2); with $Na_6Th(CO_3)_5 \cdot 12H_2O$ and trona, the highest solubility was 0.7 wt % ThO_2 (12.6 wt % Na_2O, 10.4 wt % CO_2). The highest found with $Na_6Th(CO_3)_5 \cdot 12H_2O$ and $NaHCO_3$ was 1.2 wt % ThO_2 (5.0 wt % Na_2O, 6.0 wt % CO_2), which was the most dilute $NaHCO_3$ solution tested.

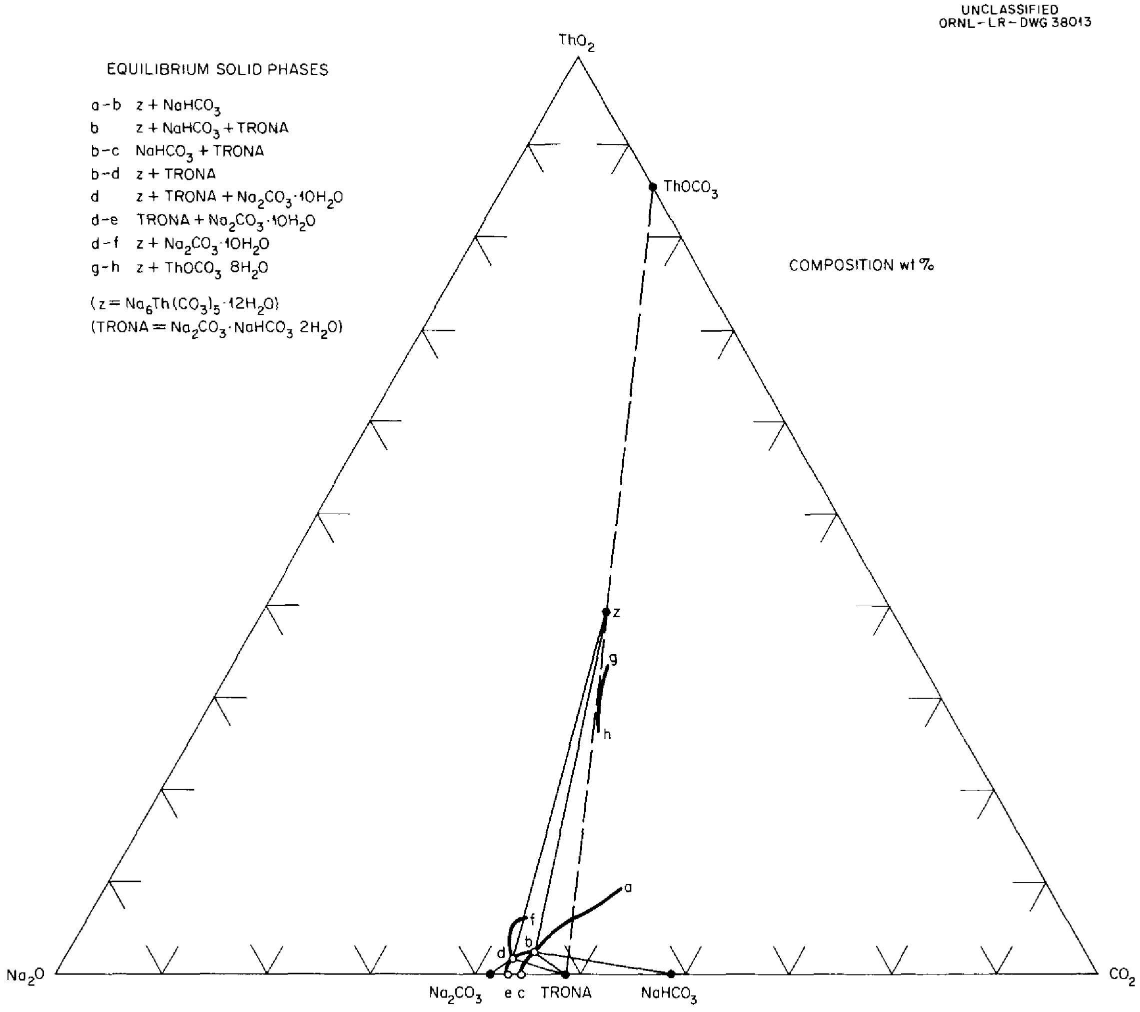

Fig. 5.5b. The System ThO_2–Na_2O–CO_2–H_2O at 25°C. Projection to the ThO_2–Na_2O–CO_2 face along radii from the H_2O vertex.

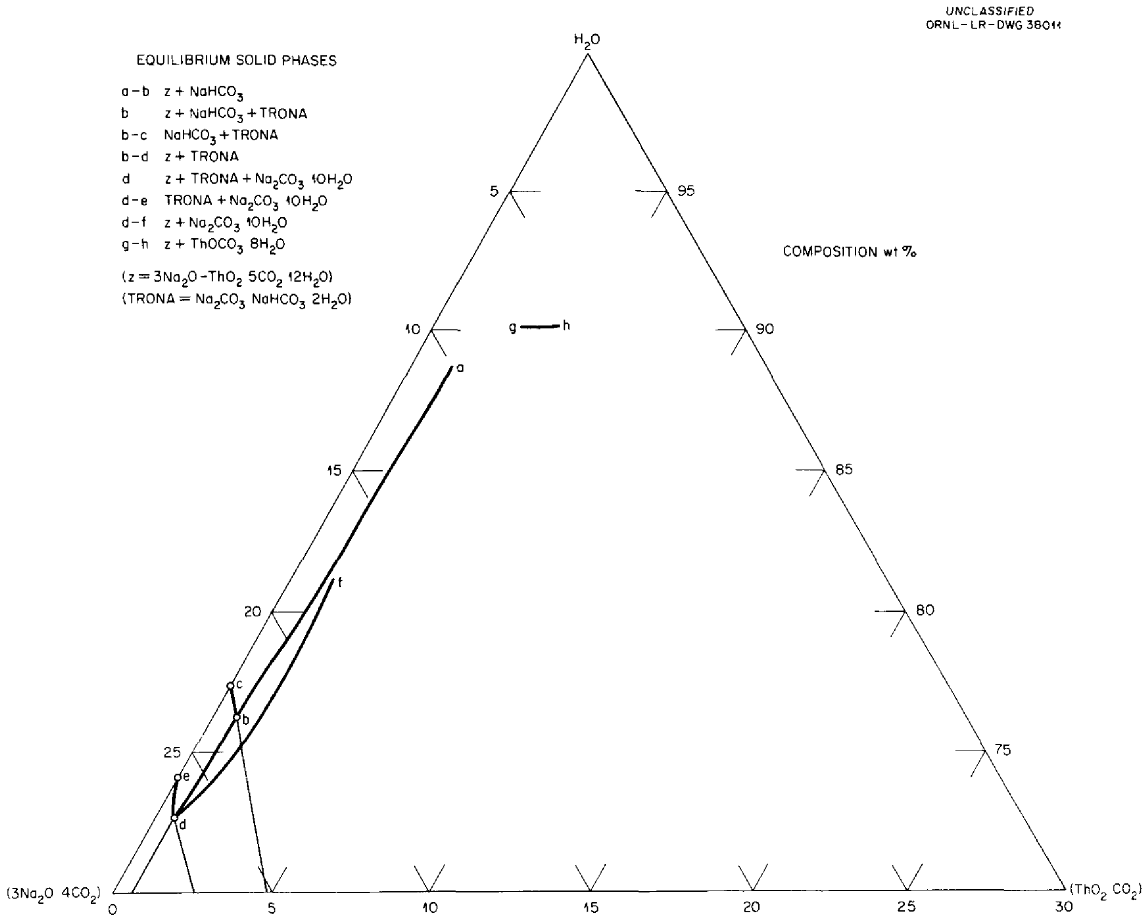

Fig. 5.5c. The System ThO_2–Na_2O–CO_2–H_2O at 25°C. Projection to the $ThO_2 \cdot CO_2$–$3Na_2O \cdot 4CO_2$–H_2O internal plane, represented as an equivalent triangle, along radii from the CO_2 vertex. Portion from 70 to 100 wt % H_2O.

5.6. The System Na_2O–CO_2–H_2O, 25°C Isotherm

F. A. Schimmel, unpublished work performed at the Oak Ridge National Laboratory, 1955.

Significant changes from the data of Freeth [*Phil. Trans. Roy. Soc. London* **233**, 35 (1922)] were found throughout the range; there was closer agreement in the bicarbonate range with the data of Hill and Bacon [*J. Am. Chem. Soc.* **49**, 2487 (1927)].

Transition Points

Solid Phases Present	Composition of Solution (wt %)	
	Na_2O	CO_2
$NaOH \cdot H_2O$ and Na_2CO_3	40.5	0.85
Na_2CO_3 and $Na_2CO_3 \cdot H_2O$	31.4	0.72
$Na_2CO_3 \cdot H_2O$ and $Na_2CO_3 \cdot 7H_2O$	18.7	6.9
$Na_2CO_3 \cdot 7H_2O$ and $Na_2CO_3 \cdot 10H_2O$	17.85	7.8
$Na_2CO_3 \cdot 10H_2O$ and $Na_2CO_3 \cdot NaHCO_3 \cdot 2H_2O$ (trona)	13.7	10.35
Trona and $NaHCO_3$	11.9	9.5

The System Na_2O–CO_2–H_2O, 25°C Isotherm

Composition of Saturated Solution (wt %)		Equilibrium Solid Phase
Na_2O	CO_2	
41.3	0	$NaOH \cdot H_2O$
40.5	0.85	Na_2CO_3
40.45	0.8	Na_2CO_3
31.6	0.67	Na_2CO_3
31.4	0.72	Na_2CO_3 and $Na_2CO_3 \cdot H_2O$
31.1	0.78	$Na_2CO_3 \cdot H_2O$
29.9	0.5	$Na_2CO_3 \cdot H_2O$
26.6	0.4	$Na_2CO_3 \cdot H_2O$
25.2	0.55	$Na_2CO_3 \cdot H_2O$
23.2	0.9	$Na_2CO_3 \cdot H_2O$
23.15	1.0	$Na_2CO_3 \cdot H_2O$
21.15	2.3	$Na_2CO_3 \cdot H_2O$
19.3	4.3	$Na_2CO_3 \cdot H_2O$
18.95	6.0	$Na_2CO_3 \cdot H_2O$
18.57	7.5	$Na_2CO_3 \cdot H_2O$ (metastable)
18.6	7.8	$Na_2CO_3 \cdot H_2O$ (metastable)
18.7	6.9	$Na_2CO_3 \cdot H_2O$ and $Na_2CO_3 \cdot 7H_2O$
18.5	6.75	$Na_2CO_3 \cdot 7H_2O$ (metastable)
17.7	7.95	$Na_2CO_3 \cdot 7H_2O$ (metastable)
18.3	7.3	$Na_2CO_3 \cdot 7H_2O$
17.85	7.8	$Na_2CO_3 \cdot 7H_2O$ and $Na_2CO_3 \cdot 10H_2O$
17.3	7.88	$Na_2CO_3 \cdot 10H_2O$
16.1	7.9	$Na_2CO_3 \cdot 10H_2O$
15.6	7.92	$Na_2CO_3 \cdot 10H_2O$
15.1	8.1	$Na_2CO_3 \cdot 10H_2O$
13.7	8.85	$Na_2CO_3 \cdot 10H_2O$
13.28	9.4	$Na_2CO_3 \cdot 10H_2O$
13.55	10.15	$Na_2CO_3 \cdot 10H_2O$
14.1	11.0	$Na_2CO_3 \cdot 10H_2O$ (metastable)
13.7	10.35	$Na_2CO_3 \cdot 10H_2O$ and trona*
17.0	13.0	Trona (metastable)
16.7	12.7	Trona (metastable)
13.8	10.35	Trona
11.9	9.5	Trona and $NaHCO_3$
11.55	9.3	$NaHCO_3$
10.5	8.8	$NaHCO_3$
9.4	8.0	$NaHCO_3$
8.1	7.5	$NaHCO_3$
6.4	6.5	$NaHCO_3$
5.4	5.75	$NaHCO_3$
3.9	5.0	$NaHCO_3$
3.56	4.95	$NaHCO_3$
3.47	4.93	$NaHCO_3$

*The formula of trona is $Na_2CO_3 \cdot NaHCO_3 \cdot 2H_2O$.

UNCLASSIFIED
ORNL-LR-DWG 38014

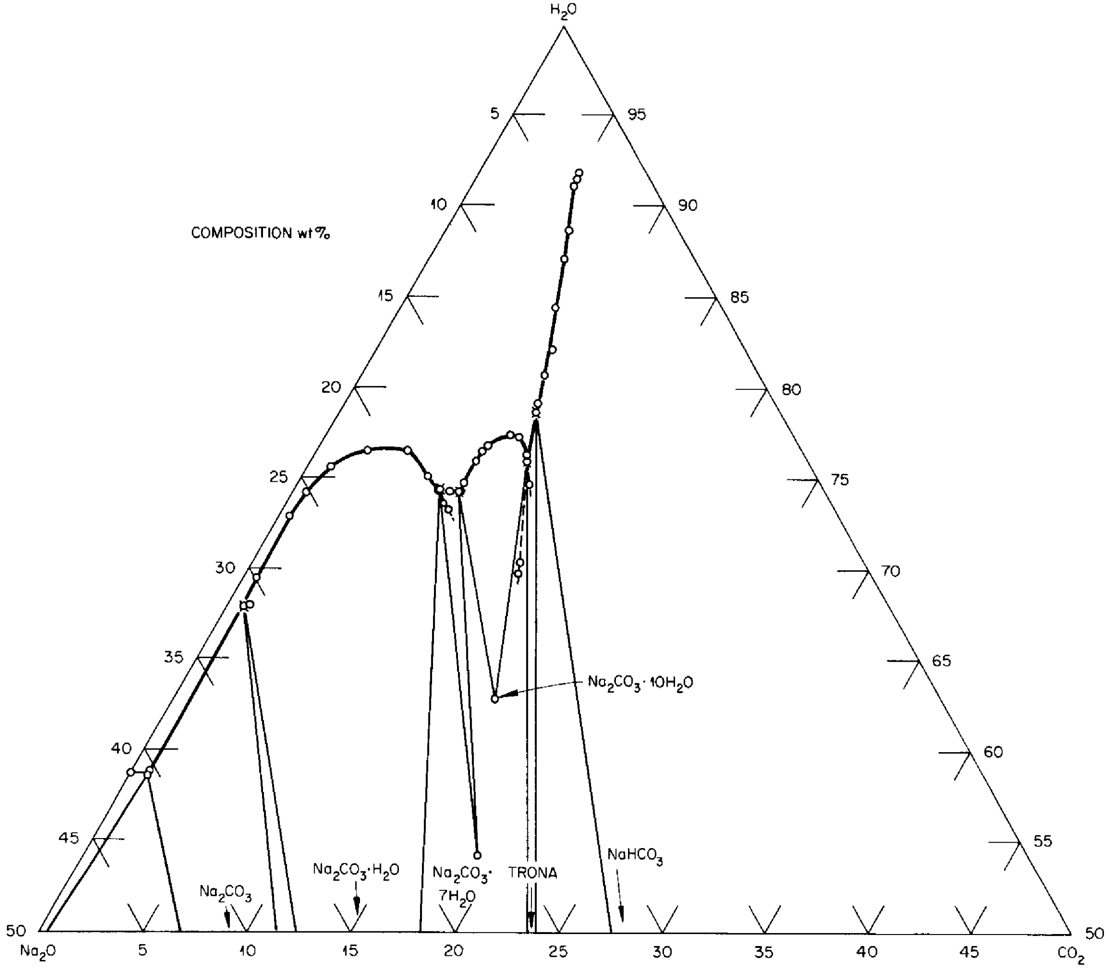

Fig. 5.6. The System Na_2O–CO_2–H_2O, 25°C Isotherm. 0–50 wt % Na_2O, 0–50 wt % CO_2.

5.7. Solubility of Uranyl Sulfate in Water

1. C. H. Secoy, *J. Am. Chem. Soc.* **72**, 3343 (1950) (data above 300°C).

2. C. H. Secoy, *J. Am. Chem. Soc.* **70**, 3450 (1948) (data up to 300°C).

3. L. Helmholtz and G. Friedlander, *Physical Properties of Uranyl Sulfate Solutions*, MDDC-808 (1943) (room temperature data).

4. C. Dittrich, *Z. physik. Chem.* **29**, 449 (1899).

5. E. V. Jones and W. L. Marshall, *HRP Quar. Prog. Rep. March 15, 1952*, ORNL-1280, p 180–83.

6. E. V. Jones and W. L. Marshall, *HRP Quar. Prog. Rep. Jan. 31, 1959*, ORNL-2696, p 210–11.

The two-liquid-phase region of this system in actuality must be represented by the three components UO_3, SO_3, and H_2O. The curve representing the boundary of liquid-liquid immiscibility is correct for stoichiometric solutions. However, the tie lines within the region of immiscibility do not connect two solutions containing stoichiometric UO_2SO_4 but rather connect solutions containing varying concentrations and ratios of UO_3 and SO_3 (Fig. 5.10). At low concentrations and high temperatures, that is, below 0.02 m UO_2SO_4 and above 250°C, hydrolysis occurs to produce a nonstoichiometric solution phase. The point of hydrolysis is dependent on concentration and temperature (see Sec 5.13).

Note: Revised data (ref 5) are used to construct the immiscibility boundary in the figure. Earlier data (ref 1) showed higher temperatures in this region and a possible likelihood of acid impurity in the solutions.

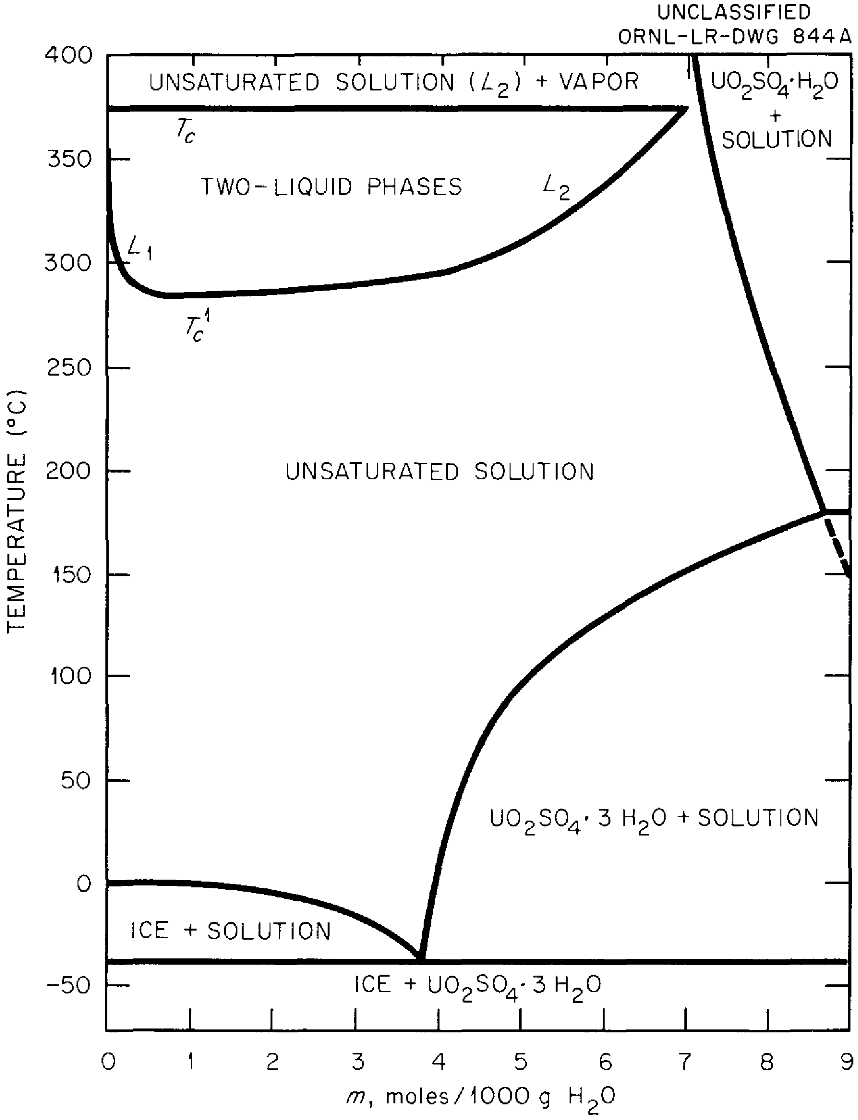

Fig. 5.7. The System UO_2SO_4–H_2O.

5.8. Two-Liquid-Phase Region of UO_2SO_4 in Ordinary and Heavy Water

E. V. Jones and W. L. Marshall, *HRP Quar. Prog. Rep. March 15, 1952,* ORNL-1280, p 180–83.

The two curves shown are boundary curves for liquid-liquid immiscibility obtained by observing the phase-transitional behavior of known UO_2SO_4–H_2O (D_2O) solutions in sealed tubes as a function of temperature. For later reference, this procedure is designated the visual-synthetic method. As was described in Sec 5.7, the concentrations and compositions of the two phases within the boundary region at equilibrium cannot be obtained from this figure. Mixtures which are solutions at lower temperatures separate into two liquid phases as the temperature is raised, according to the boundary curves.

UNCLASSIFIED
ORNL-LR-DWG 29314

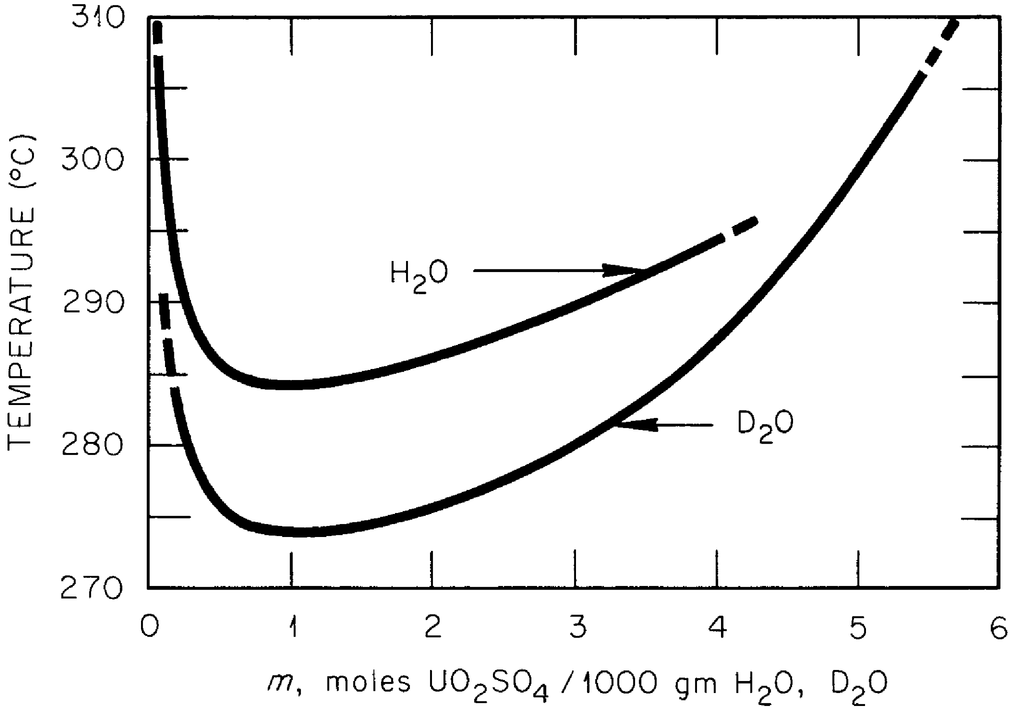

Fig. 5.8. Two-Liquid-Phase Region of UO_2SO_4 in Ordinary and Heavy Water.

5.9. The System UO_3–SO_3–H_2O

1. A. Colani, *Bull. soc. chim. France* [4] **43**, 754–62 (1928).

2. J. S. Gill, E. V. Jones, and C. H. Secoy, *HRP Quar. Prog. Rep. Oct. 31, 1953*, ORNL-1658, p 87.

The 25° data on the SO_3–rich side are those of Colani. The higher temperature data are those of Gill, Jones, and Secoy, obtained by filtration techniques at temperature. The number and identity of the solid phases in the UO_3–rich regions at 25, 100, and 175°C are somewhat uncertain. Subsequent unpublished work of F. E. Clark and C. H. Secoy has disclosed that the *K* solid is identical (x-ray diffraction) with the mineral uranopilite, $6UO_3 \cdot SO_3 \cdot xH_2O$, that the *G* solid is not identifiable as any known mineral, and that at least one additional unidentified solid phase occurs at 25 and 100°. The liquidus curves for the 25 and 100° isotherms are essentially correct as shown except that the transition points (two solid phases) occur at somewhat lower concentrations than those indicated.

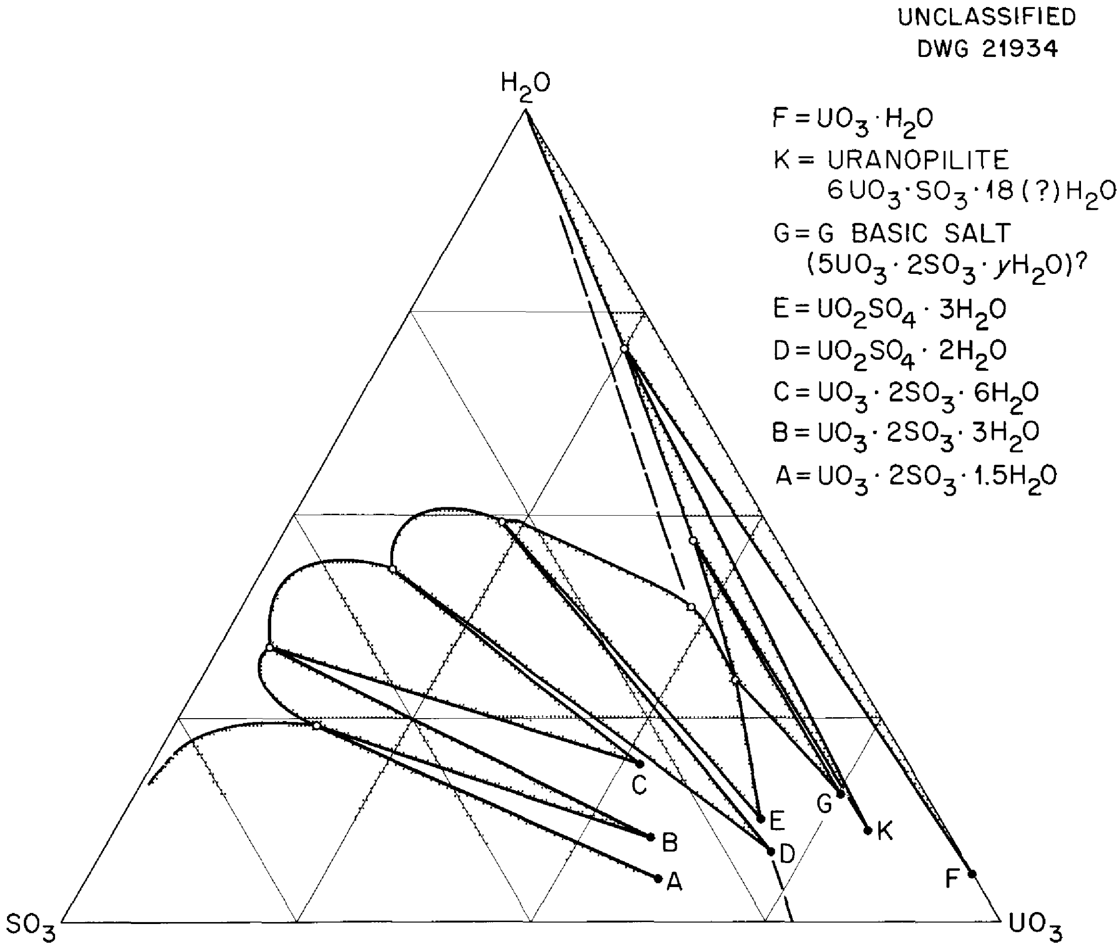

Fig. 5.9*a*. The System UO_3–SO_3–H_2O at 25°C.

UNCLASSIFIED
DWG 21935

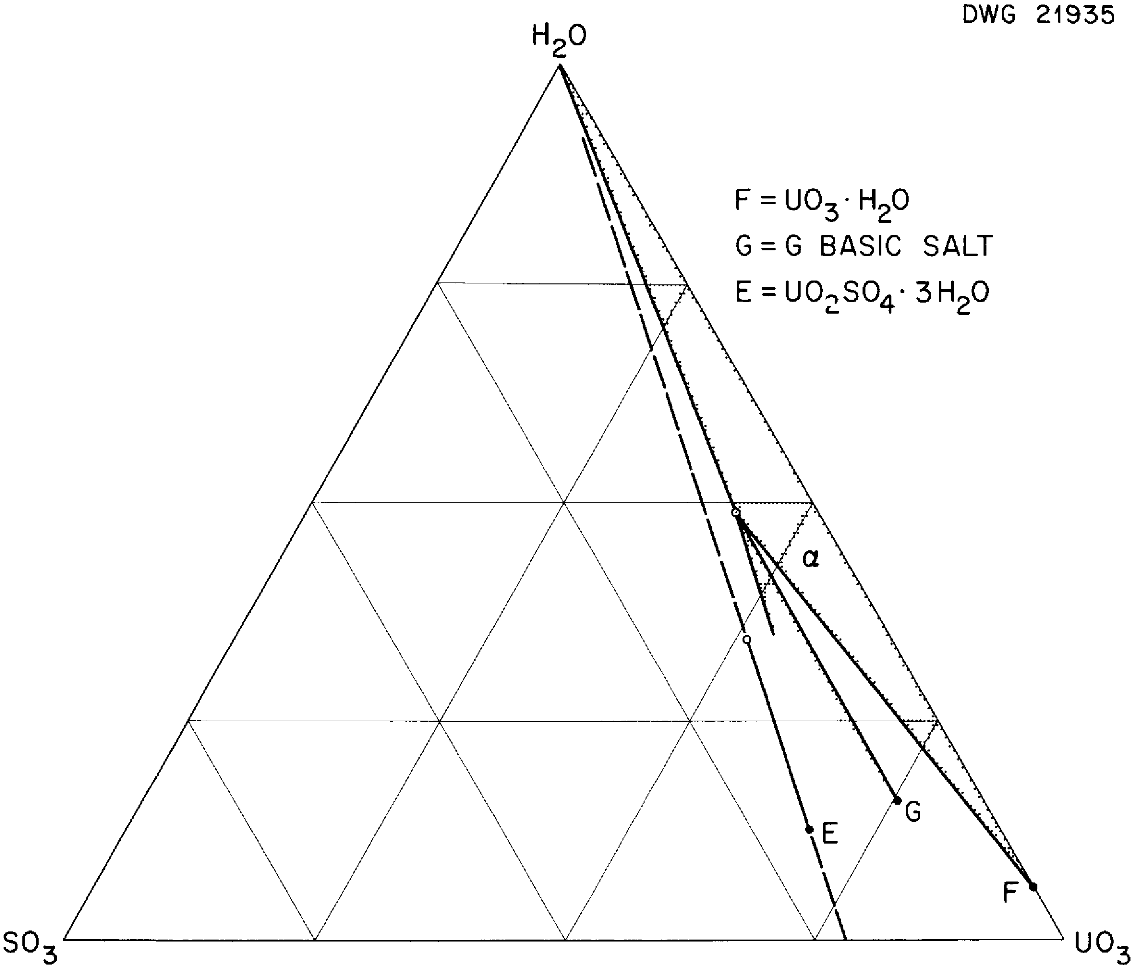

Fig. 5.9*b*. The System UO_3–SO_3–H_2O at 100°C.

UNCLASSIFIED
DWG 21936

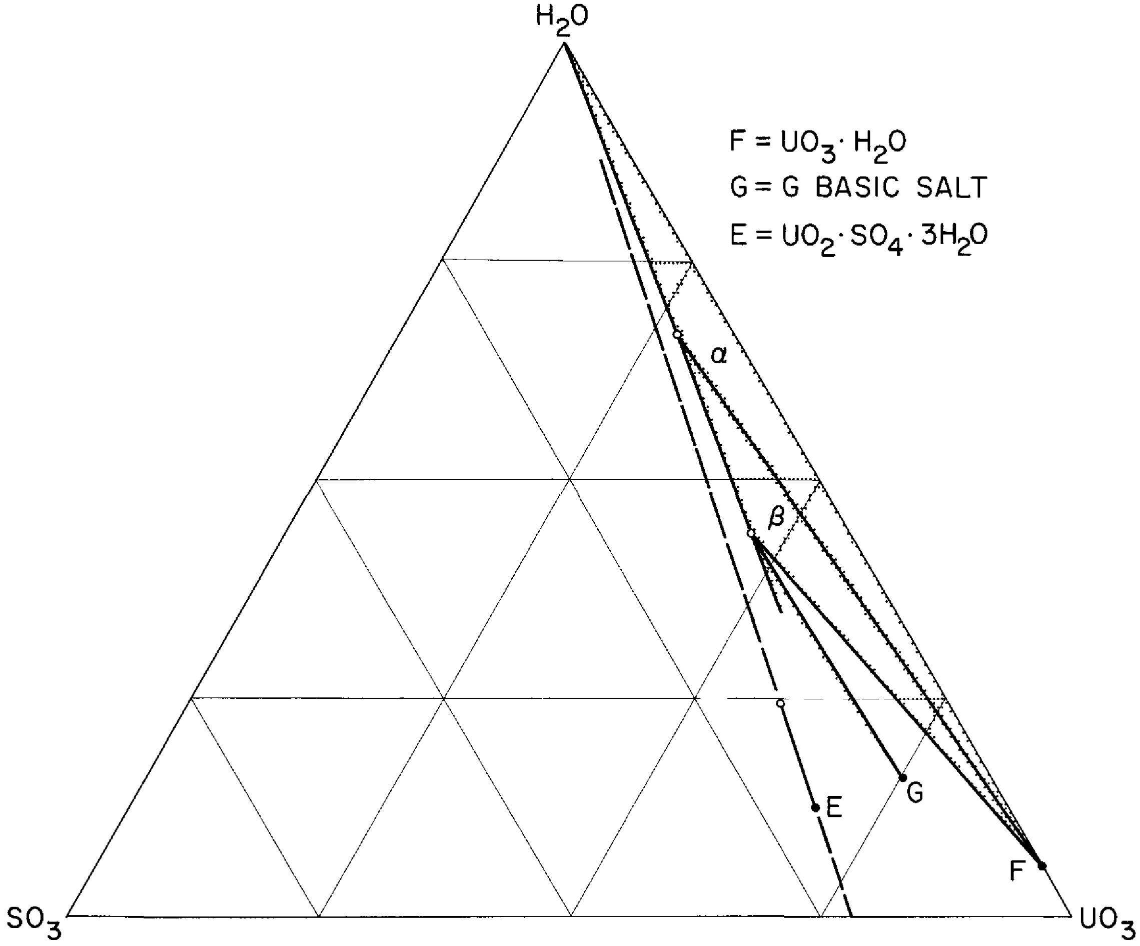

Fig. 5.9*c*. The System UO_3–SO_3–H_2O at 175°C.

UNCLASSIFIED
DWG 21937

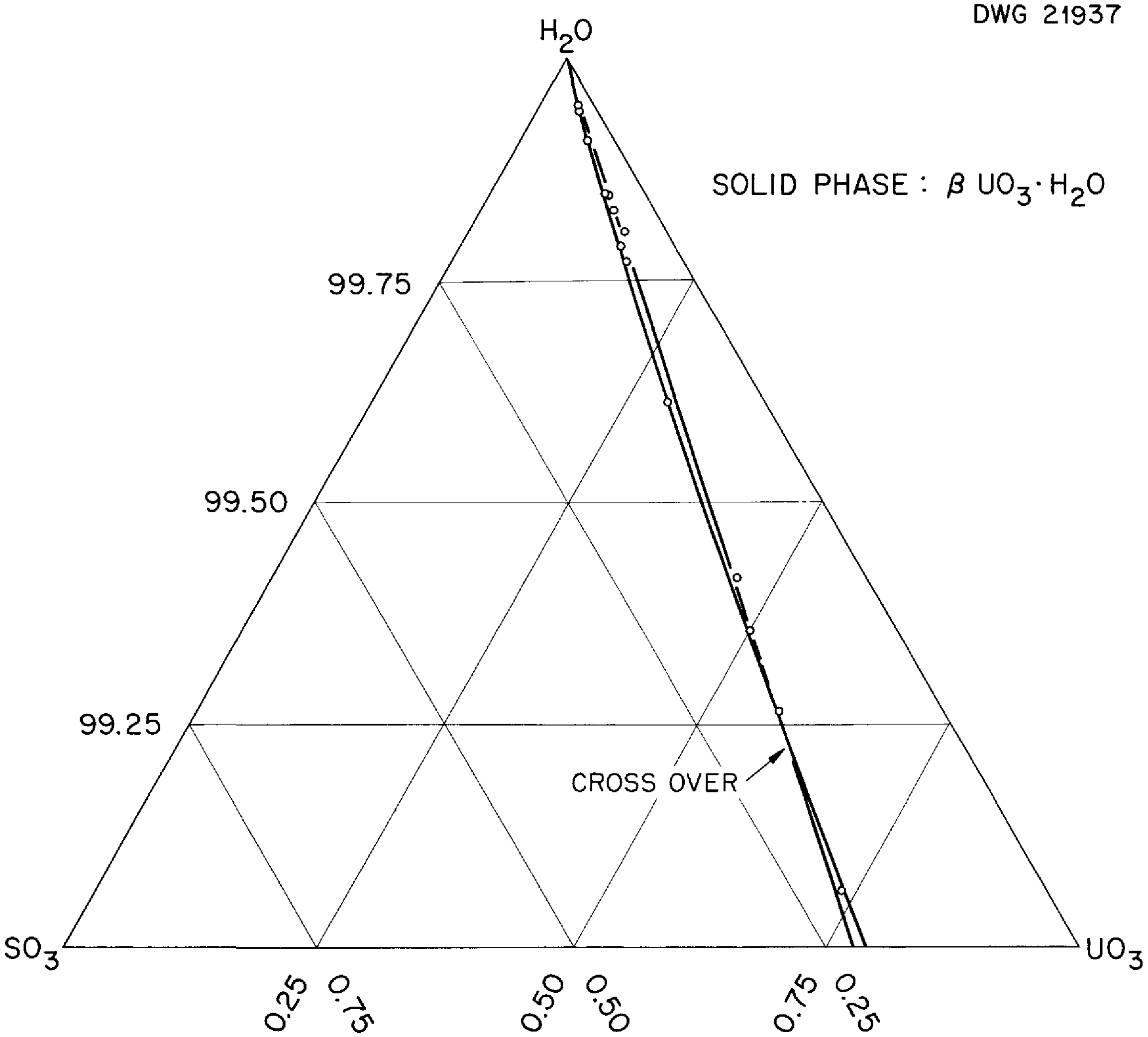

Fig. 5.9*d*. The System UO_3–SO_3–H_2O at 250°C.

5.10. Coexistence Curves for Two Liquid Phases in the System UO_2SO_4–H_2SO_4–H_2O

H. W. Wright, W. L. Marshall, and C. H. Secoy, *HRP Quar. Prog. Rep. Oct. 1, 1952,* ORNL-1424, p 108.

All curves in this figure must extrapolate to the critical temperature of water (374.2°C) at zero concentration of uranium. These are boundary curves which were determined by observing sealed tubes in which immiscibility occurred in UO_3–SO_3–H_2O solutions upon varying the temperature. As was explained in Sec 5.7, they do not represent concentrations and compositions of the two liquid phases within the temperature-concentration region of immiscibility but are lower solution boundary curves.

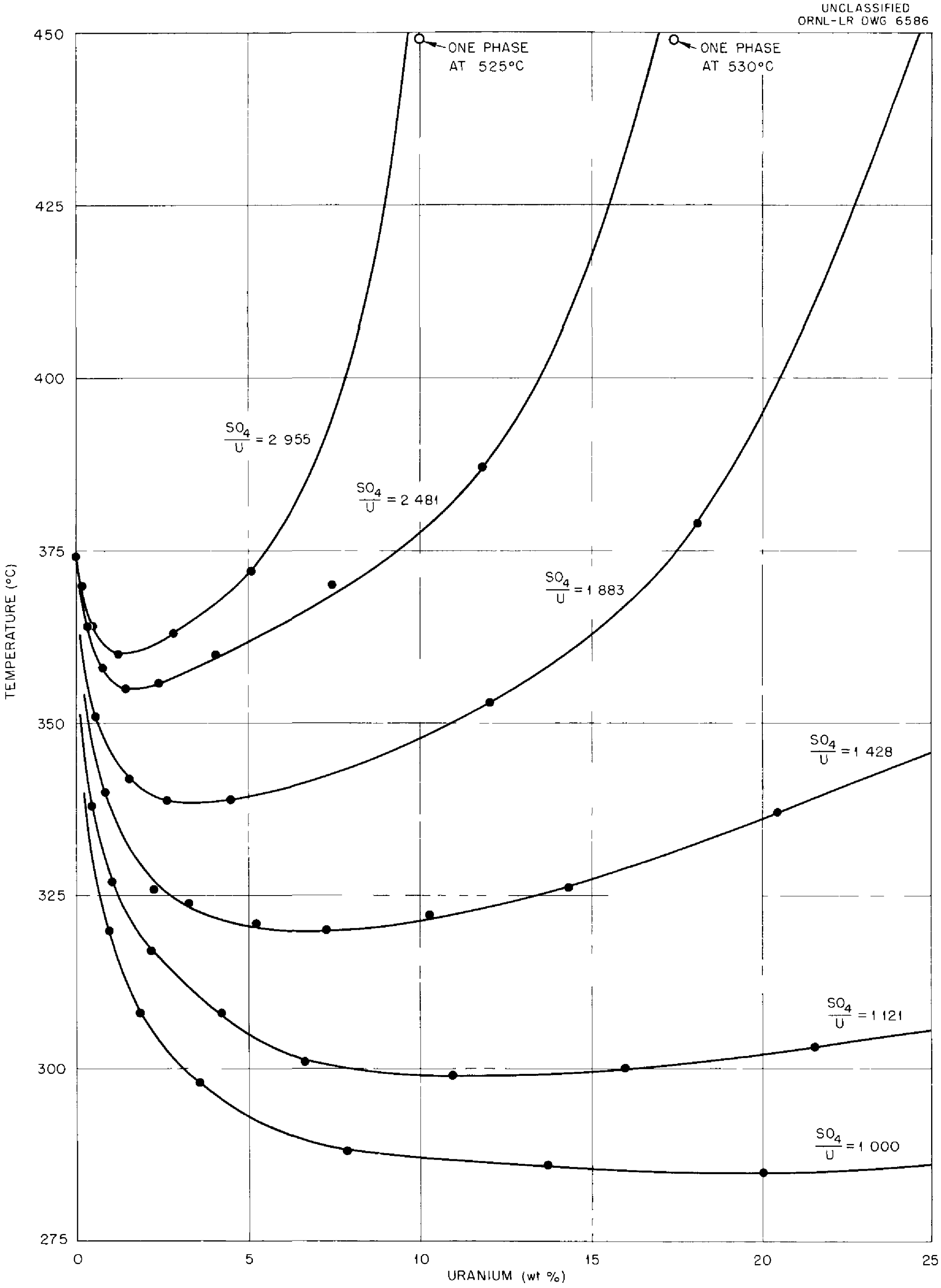

Fig. 5.10. Coexistence Curves for Two Liquid Phases in the System UO_2SO_4–H_2SO_4–H_2O.

5.11. Two-Liquid-Phase Region of the System $UO_2SO_4-H_2SO_4-H_2O$

R. E. Leed and C. H. Secoy, *Chem. Quar. Prog. Rep. Sept. 30, 1950*, ORNL-870, p 29–30; C. H. Secoy, *Chem. Quar. Prog. Rep. Dec. 31, 1949*, ORNL-607, p 33–38.

In contrast with the immiscibility curves shown in Fig. 5.10, each of these curves must extrapolate to a critical temperature curve for SO_3-H_2O in which a small or negligible amount of UO_3 is dissolved. Since SO_3 dissolved in H_2O (neglecting any dissolved UO_3) will elevate the critical temperature, the curves obtained from solutions containing a constant amount of free H_2SO_4 will all extrapolate to critical temperatures higher than that (374.2°C) for H_2O alone.

UNCLASSIFIED
DWG. 10085

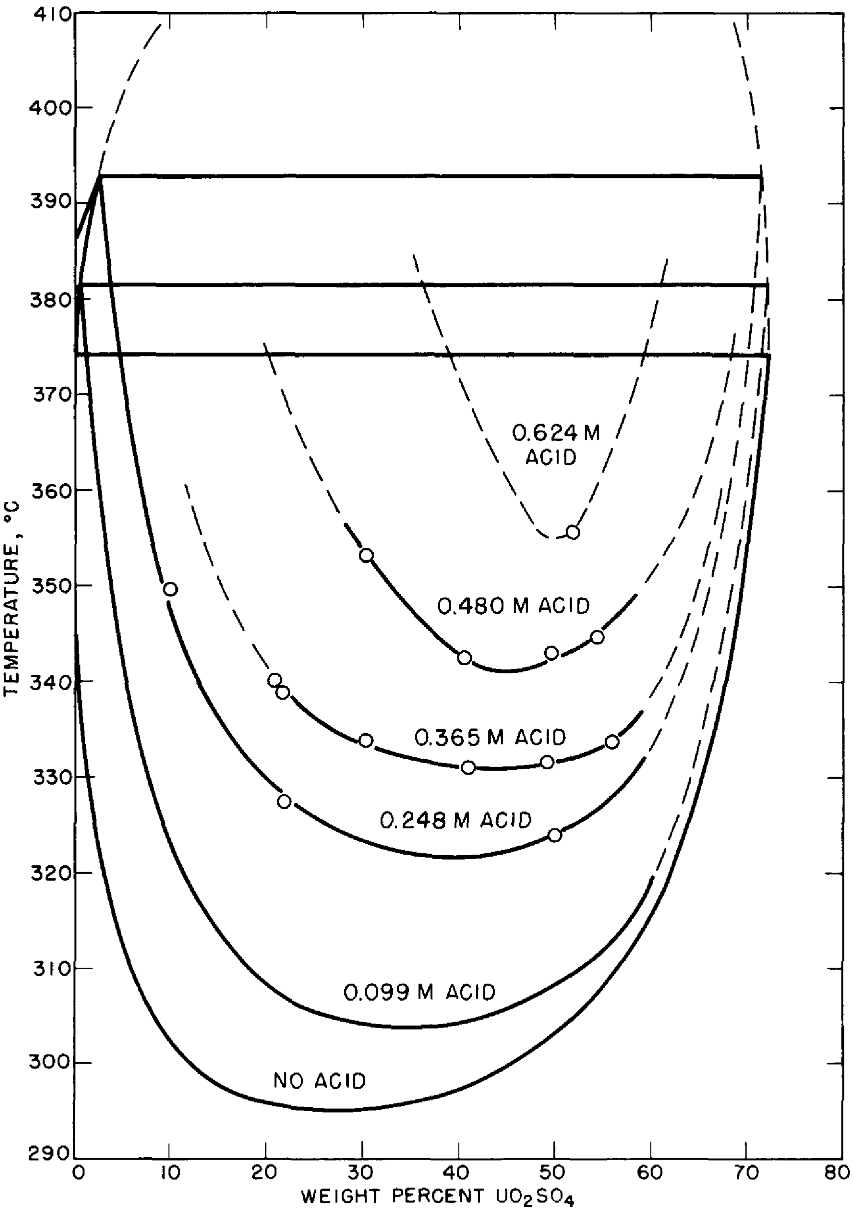

Fig. 5.11. Two-Liquid-Phase Region of the System $UO_2SO_4-H_2SO_4-H_2O$.

5.12. Two-Liquid-Phase Coexistence Curves for UO_3–Rich Solutions in the System UO_3–SO_3–H_2O With and Without HNO_3

E. V. Jones and W. L. Marshall, *HRP Quar. Prog. Rep. July 1, 1952,* ORNL-1318, p 147–48.

These curves have been obtained by the visual-synthetic method mentioned in Sec 5.8. They are therefore boundary curves and do not describe compositions and concentrations within the liquid-liquid immiscibility region.

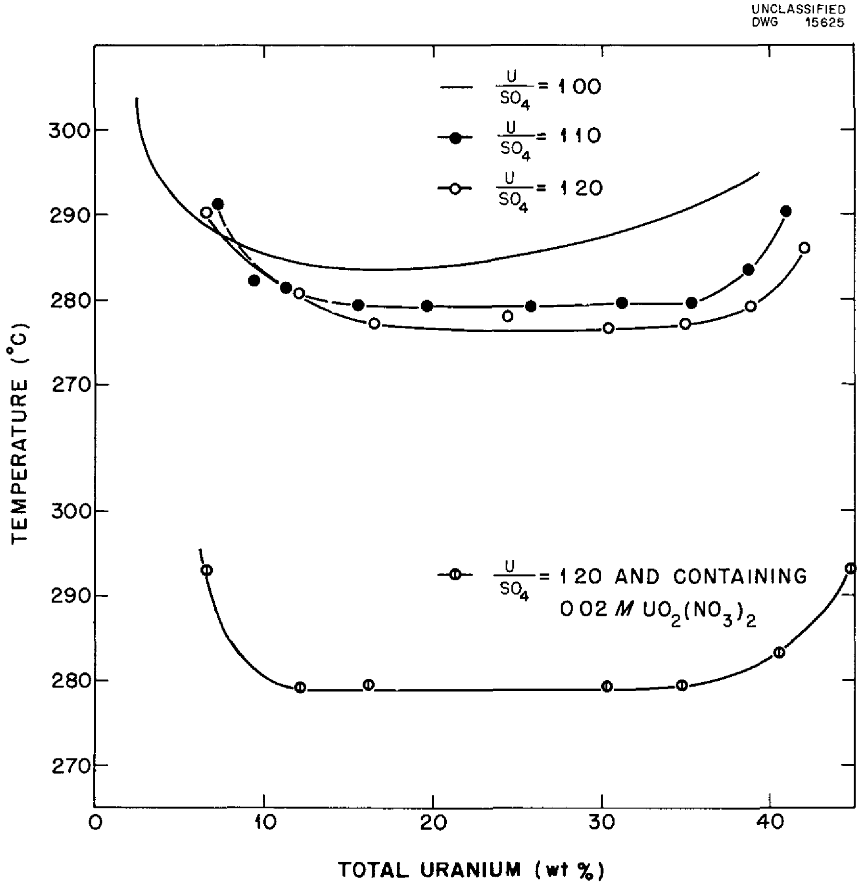

Fig. 5.12. Two-Liquid-Phase Coexistence Curves for UO_3–Rich Solutions in the System UO_3–SO_3–H_2O With and Without HNO_3.

5.13. Solubility of UO_3 in H_2SO_4–H_2O Mixtures

W. L. Marshall, *Anal. Chem.* **27**, 1923 (1955).

The data are represented in this manner in order to show the full concentration range on one figure and to best indicate the degree of precision. The solid phase is α-$UO_3 \cdot H_2O$ below 205°C and β-$UO_3 \cdot H_2O$ above 205°C. These curves represent hydrolysis equilibria.

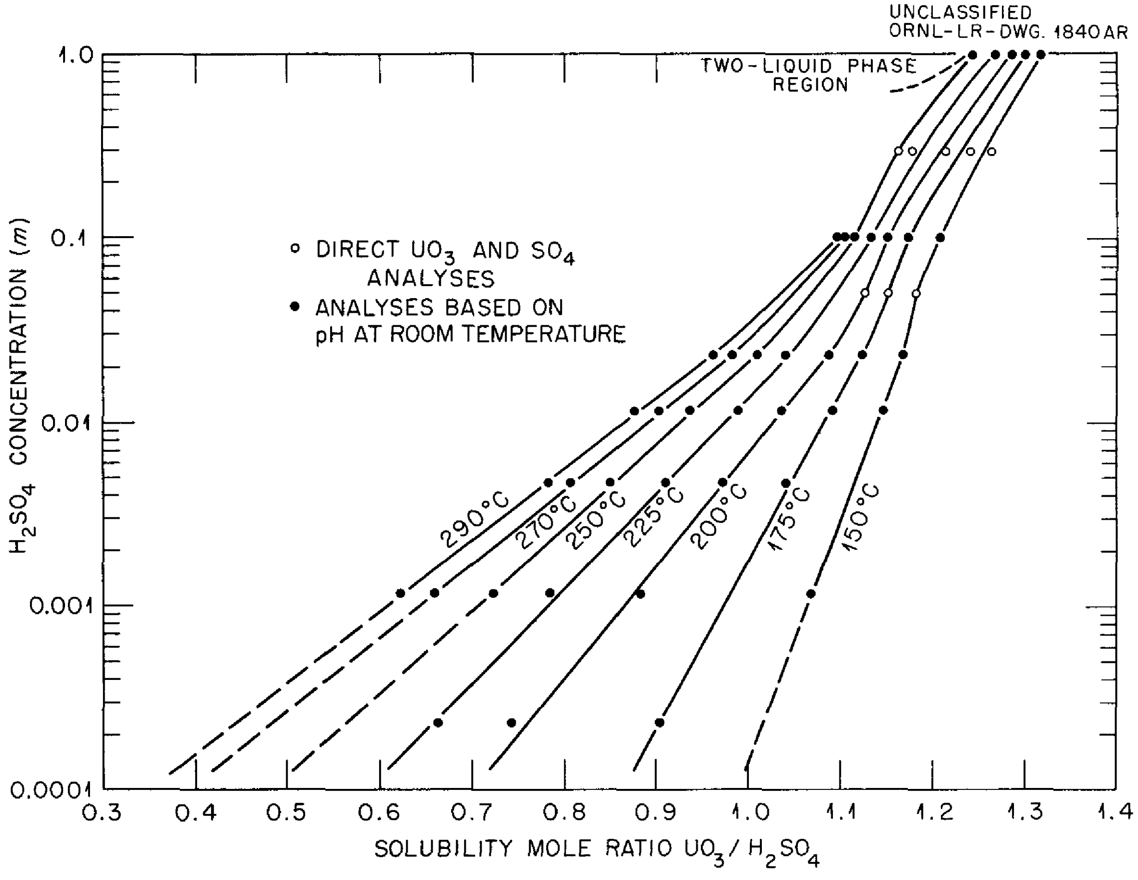

Fig. 5.13. Solubility of UO_3 in H_2SO_4–H_2O Mixtures.

5.14. Effect of Excess H_2SO_4 on the Phase Equilibria in Very Dilute UO_2SO_4 Solutions

1. W. L. Marshall, *Anal. Chem.* **27**, 1923 (1955).

2. H. W. Wright, W. L. Marshall, and C. H. Secoy, *HRP Quar. Prog. Rep. Oct. 1, 1952,* ORNL-1424, p 108.

The curves were drawn by C. H. Secoy from data used for Figs. 5.10 and 5.13.

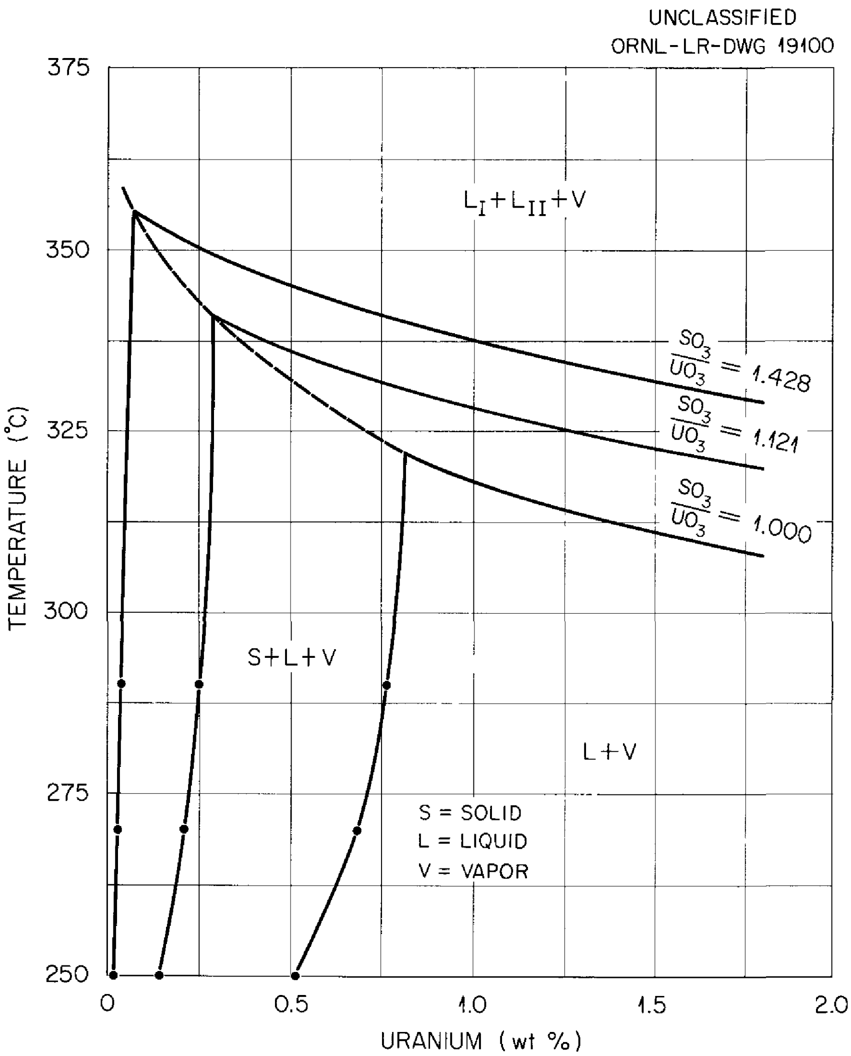

Fig. 5.14. Effect of Excess H_2SO_4 on the Phase Equilibria in Very Dilute UO_2SO_4 Solutions.

5.15. Second-Liquid-Phase Temperatures of UO_2SO_4–Li_2SO_4 Solutions

R. S. Greeley, S. R. Buxton, and J. C. Griess, "High Temperature Behavior of Aqueous UO_2SO_4–Li_2SO_4 and UO_2SO_4–$BeSO_4$," paper presented at American Nuclear Society 2nd Winter Meeting, New York City (Oct. 1957). Also R. S. Greeley and J. C. Griess, *HRP Dynamic Solution Corrosion Studies for Quarter Ending July 31, 1956*, ORNL CF-56-7-52, p 30–31.

These data were obtained by the visual-synthetic method mentioned in Sec 5.8.

UNCLASSIFIED
ORNL-LR-DWG 19101

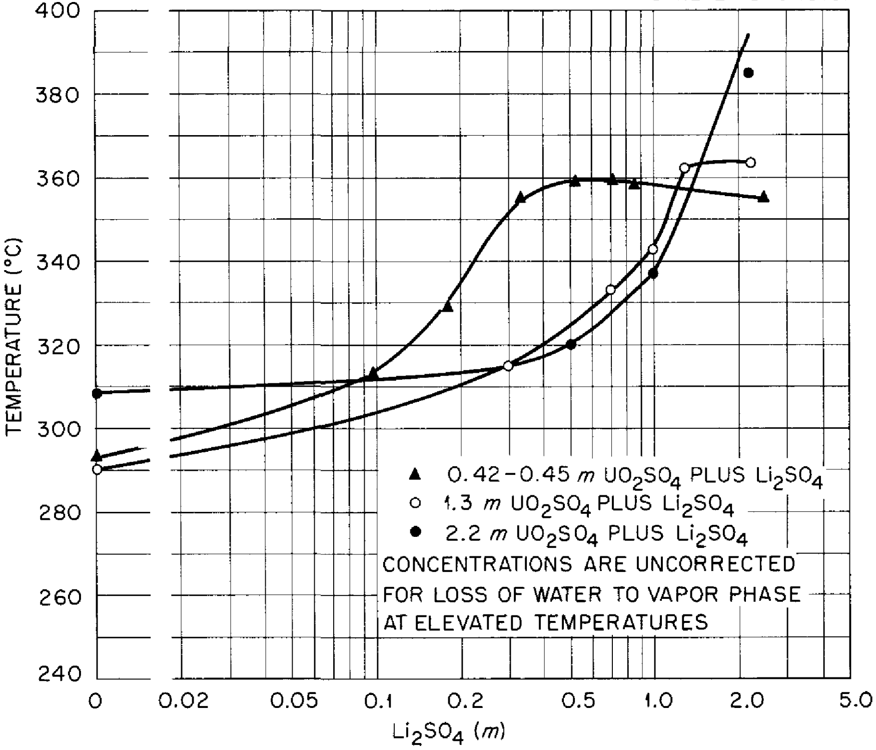

Fig. 5.15. Second-Liquid-Phase Temperatures of UO_2SO_4–Li_2SO_4 Solutions.

5.16. Second-Liquid-Phase Temperatures for UO_2SO_4 Solutions Containing Li_2SO_4 or $BeSO_4$

R. S. Greeley and J. C. Griess, *HRP Dynamic Solution Corrosion Studies for Quarter Ending July 31, 1956*, ORNL CF-56-7-52, p 30.

Liquid-liquid immiscibility occurs at the boundary curves as the temperature is raised.

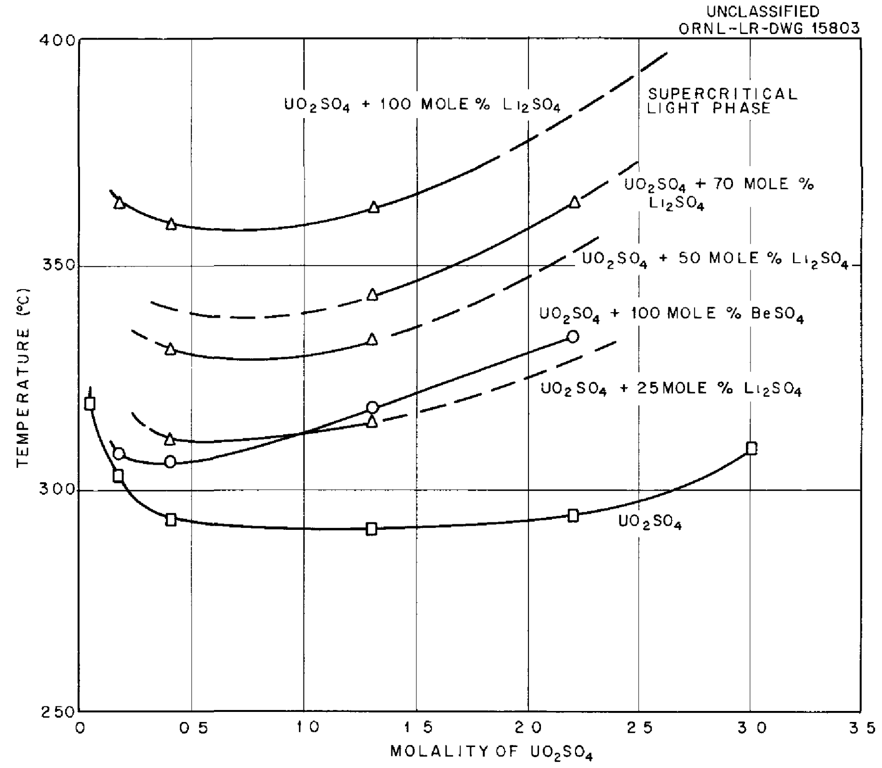

Fig. 5.16. Second-Liquid-Phase Temperatures for UO_2SO_4 Solutions Containing Li_2SO_4 or $BeSO_4$.

5.17. Second-Liquid-Phase Temperatures for $BeSO_4$ Solutions Containing UO_3

R. S. Greeley and J. C. Griess, *HRP Dynamic Solution Corrosion Studies for Quarter Ending July 31, 1956*, ORNL CF-56-7-52, p 31.

Liquid-liquid immiscibility occurs at the boundary curves as the temperature is raised.

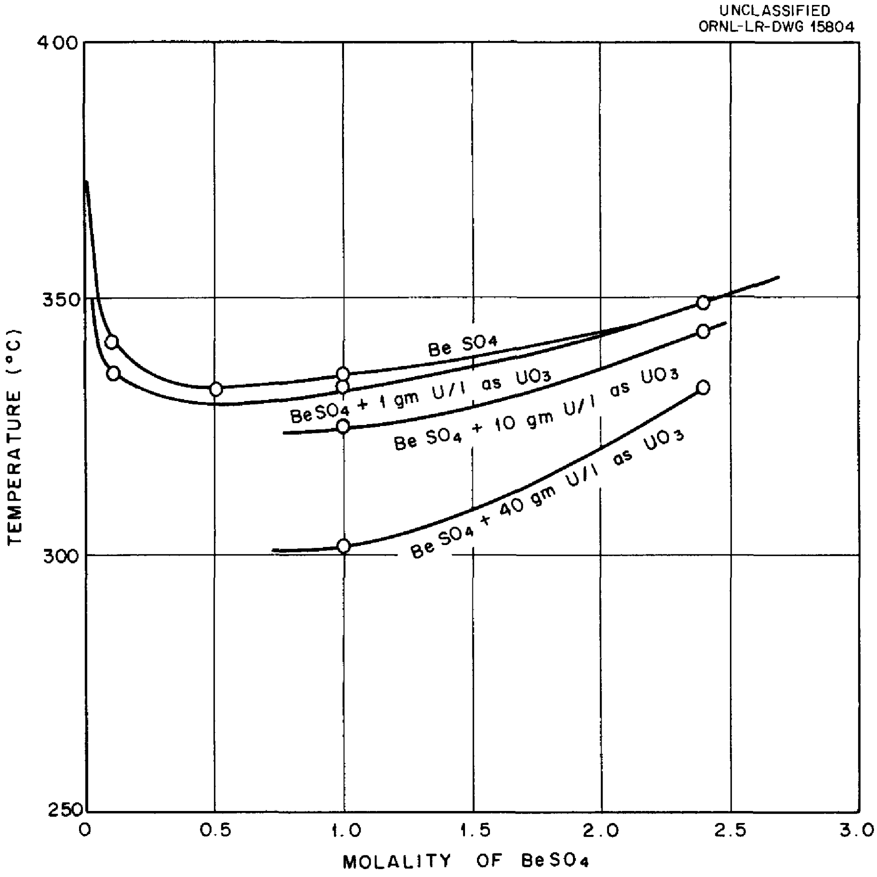

Fig. 5.17. Second-Liquid-Phase Temperatures for $BeSO_4$ Solutions Containing UO_3.

5.18. The System $NiSO_4$–UO_2SO_4–H_2O at 25°C

E. V. Jones, J. S. Gill, and C. H. Secoy, *HRP Quar. Prog. Rep. Oct. 31, 1954*, ORNL-1813, p 166–67.

Also included in the reference are solubility data for this system at 175 and 250°C. The data at high temperature are not in sufficient quantity for a diagram to be presented.

UNCLASSIFIED
ORNL–LR–DWG 3713A

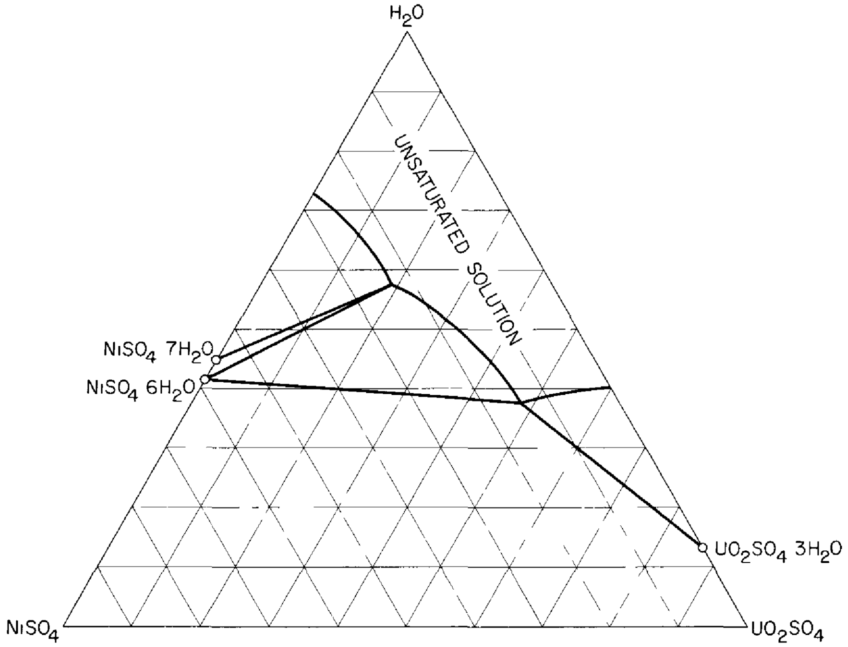

Fig. 5.18. The System $NiSO_4$–UO_2SO_4–H_2O at 25°C. Compositions are plotted in weight per cent.

5.19. Phase-Transition Temperatures in Solutions Containing $CuSO_4$, UO_2SO_4, and H_2SO_4

F. E. Clark, J. S. Gill, R. Slusher, and C. H. Secoy, *J. Chem. Eng. Data* 4, 12 (1959).

All data were obtained by the visual-synthetic method mentioned in Sec 5.8 and represent temperatures at which immiscibility occurred upon raising the temperature. No deductions can be made regarding compositions within the two-liquid-phase region.

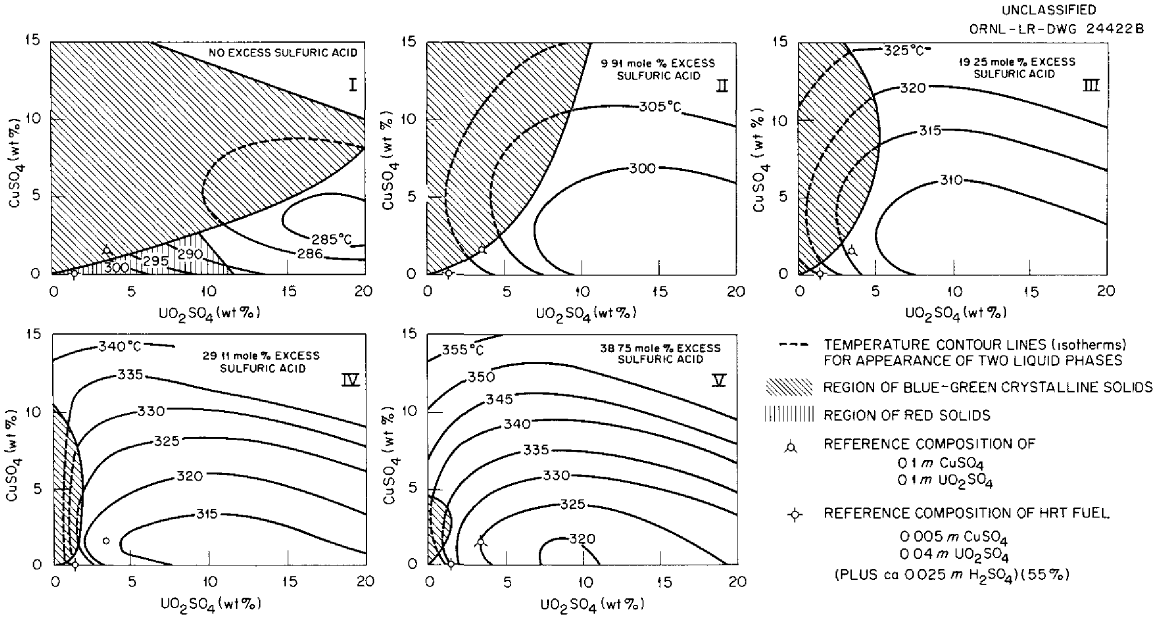

Fig. 5.19. Phase-Transition Temperatures in Solutions Containing $CuSO_4$, UO_2SO_4, and H_2SO_4.

5.20. The Effect of $CuSO_4$ and $NiSO_4$ on Phase-Transition Temperatures: 0.04 *m* UO_2SO_4; 0.01 *m* H_2SO_4

C. H. Secoy *et al.*, *HRP Quar. Prog. Rep. July 31, 1957*, ORNL-2379, p 163. Also additional data: F. Moseley, *Core Solution Stability in the Homogeneous Aqueous Reactor; the Effect of Corrosion Product and Copper Concentrations*, HARD(C)/P-41 (May 1957).

The curves for liquid-liquid immiscibility were drawn from data obtained by the visual-synthetic method mentioned in Sec 5.8. Saturation temperatures for solid-liquid equilibria were obtained by measuring solution concentrations as a function of temperature and determining a break in the curve. The numbers in parentheses are temperatures at which the indicated solid phase appeared upon raising the temperature. Solid phases indicated in parentheses were found in small quantity.

UNCLASSIFIED
ORNL-LR-DWG 23014A

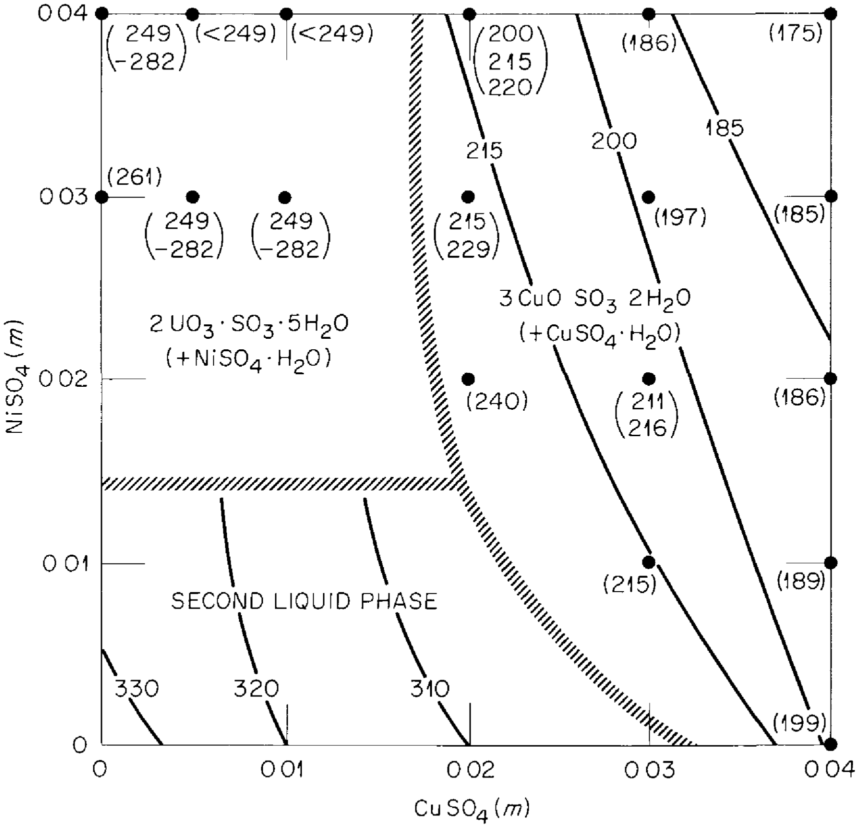

Fig. 5.20. The Effect of $CuSO_4$ and $NiSO_4$ on Phase-Transition Temperatures: 0.04 *m* UO_2SO_4; 0.01 *m* H_2SO_4.

5.21. The System UO_3–CuO–NiO–SO_3–D_2O at 300°C; 0.06 *m* SO_3

J. S. Gill, R. Slusher, and W. L. Marshall, *HRP Quar. Prog. Rep. Jan. 31, 1959*, ORNL-2696, p 205–13.

The variation in solution composition in the presence of one, two, and three solid phases was determined at 300°C from 0.04 to 0.2 *m* SO_3. Solubility relationships at 0.06 *m* SO_3 were obtained from these separate solubility curves, and the skeletal volume figure for the five-component system was drawn. Other skeletal figures can be drawn at various SO_3 concentrations. This investigation is still in progress, and the data are subject to revision.

UNCLASSIFIED
ORNL-LR-DWG. 35714A

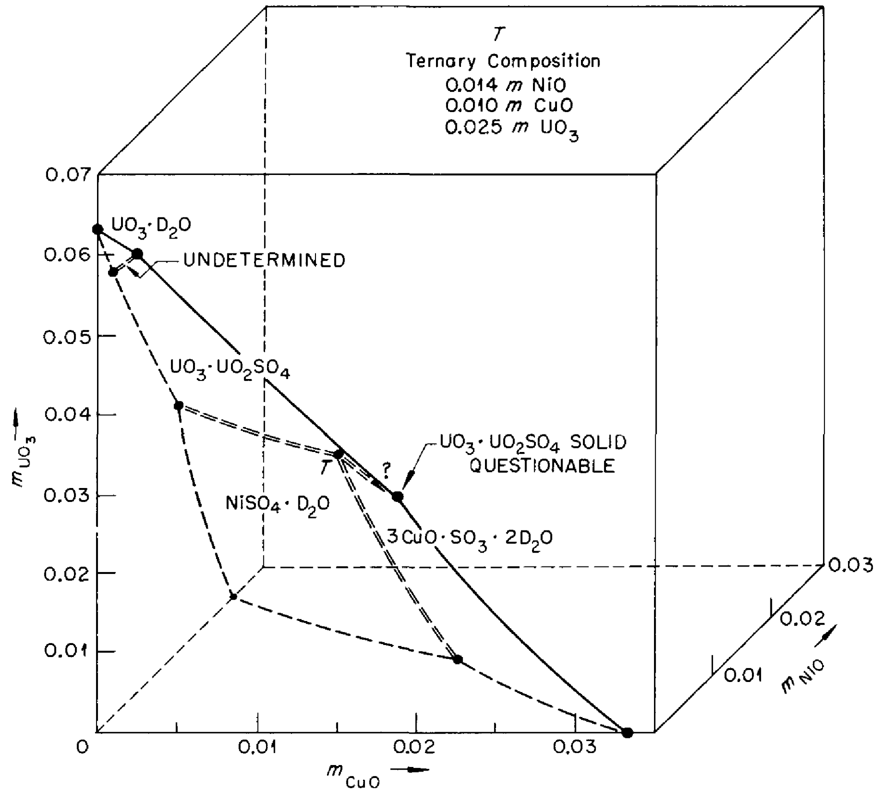

Fig. 5.21. The System UO_3–CuO–NiO–SO_3–D_2O at 300°C; 0.06 *m* SO_3.

5.22. Solubility of $Nd_2(SO_4)_3$ in 0.02 *m* UO_2SO_4 Solution Containing 0.005 *m* H_2SO_4 (180–300°C)

R. E. Leuze *et al.*, *HRP Quar. Prog. Rep. April 30, 1954*, ORNL-1753, p 176–79.

Also included in the reference are preliminary solubility data for rare earth sulfate mixtures as well as $Ce_2(SO_4)_3$ and $La_2(SO_4)_3$ in 0.02 *m* UO_2SO_4, 0.005 *m* H_2SO_4.

UNCLASSIFIED
ORNL-LR-DWG 925A

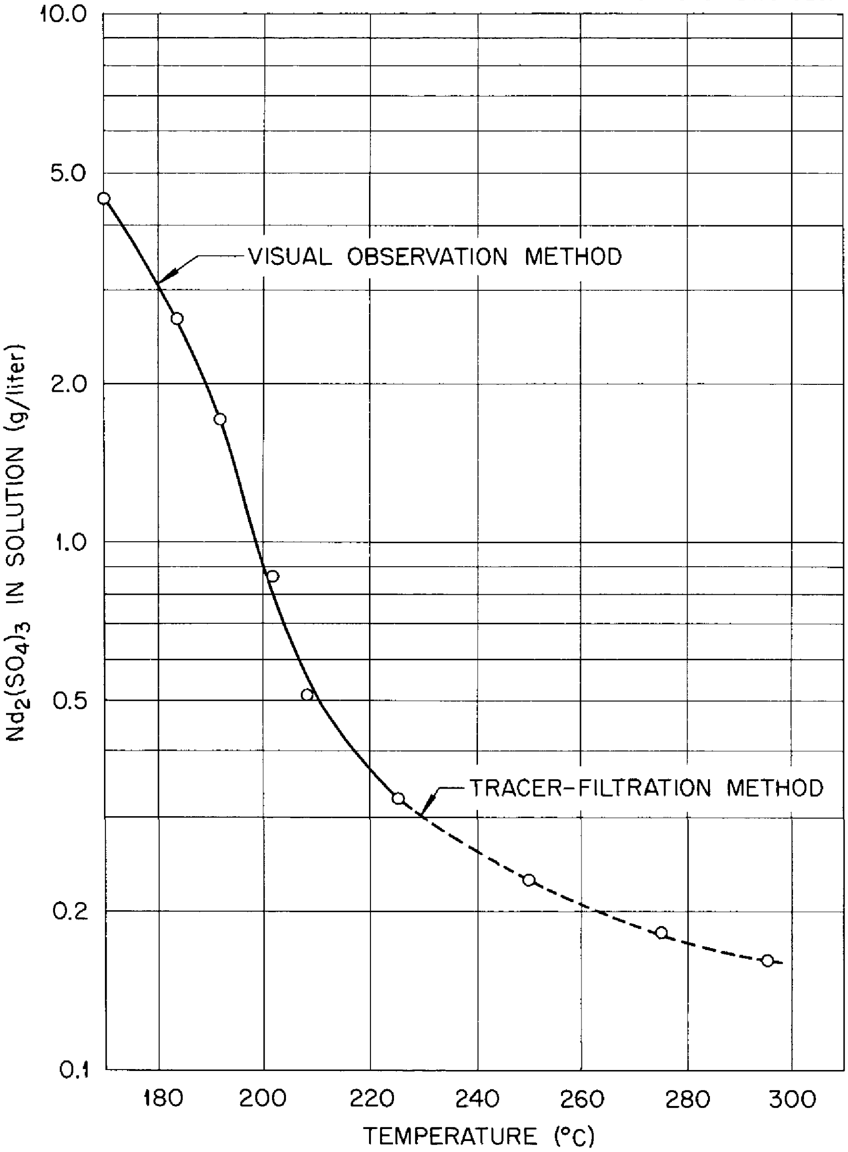

Fig. 5.22. Solubility of $Nd_2(SO_4)_3$ in 0.02 *m* UO_2SO_4 Solution Containing 0.005 *m* H_2SO_4 (180–300°C).

5.23. Solubility of $La_2(SO_4)_3$ in UO_2SO_4 Solutions

E. V. Jones, M. H. Lietzke, and W. L. Marshall, *J. Am. Chem. Soc.* **79**, 267 (1957); also *The Solubility of Several Metal Sulfates at High Temperatures and Pressures in Water and in Aqueous Uranyl Sulfate Solution*, ORNL CF-55-7-69 (declassified Aug. 23, 1955).

Experimental data for Figs. 5.23–5.27 were obtained by the visual-synthetic method described in Sec 5.8. The very large effect of UO_2SO_4 must be noted and indicates considerable solvation of other species by aqueous UO_2SO_4.

UNCLASSIFIED
DWG. 14640A

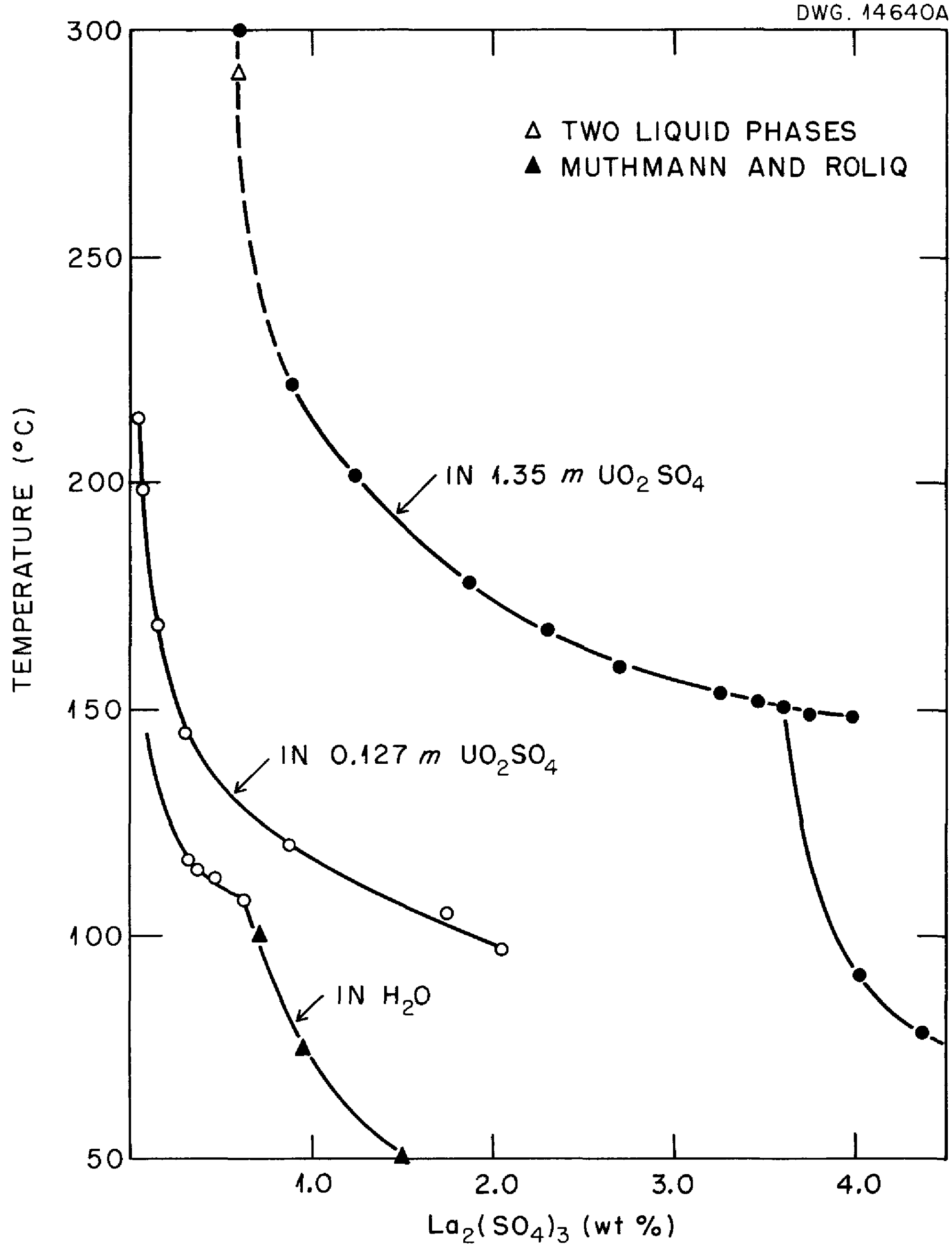

Fig. 5.23. Solubility of $La_2(SO_4)_3$ in UO_2SO_4 Solutions.

5.24. Solubility of $CdSO_4$ in UO_2SO_4 Solutions

E. V. Jones, M. H. Lietzke, and W. L. Marshall, *J. Am. Chem. Soc.* **79**, 267 (1957); also *The Solubility of Several Metal Sulfates at High Temperatures and Pressures in Water and in Aqueous Uranyl Sulfate Solution*, ORNL CF-55-7-69 (declassified Aug. 23, 1955).

See comments in Sec 5.23.

UNCLASSIFIED
DWG. 14613A

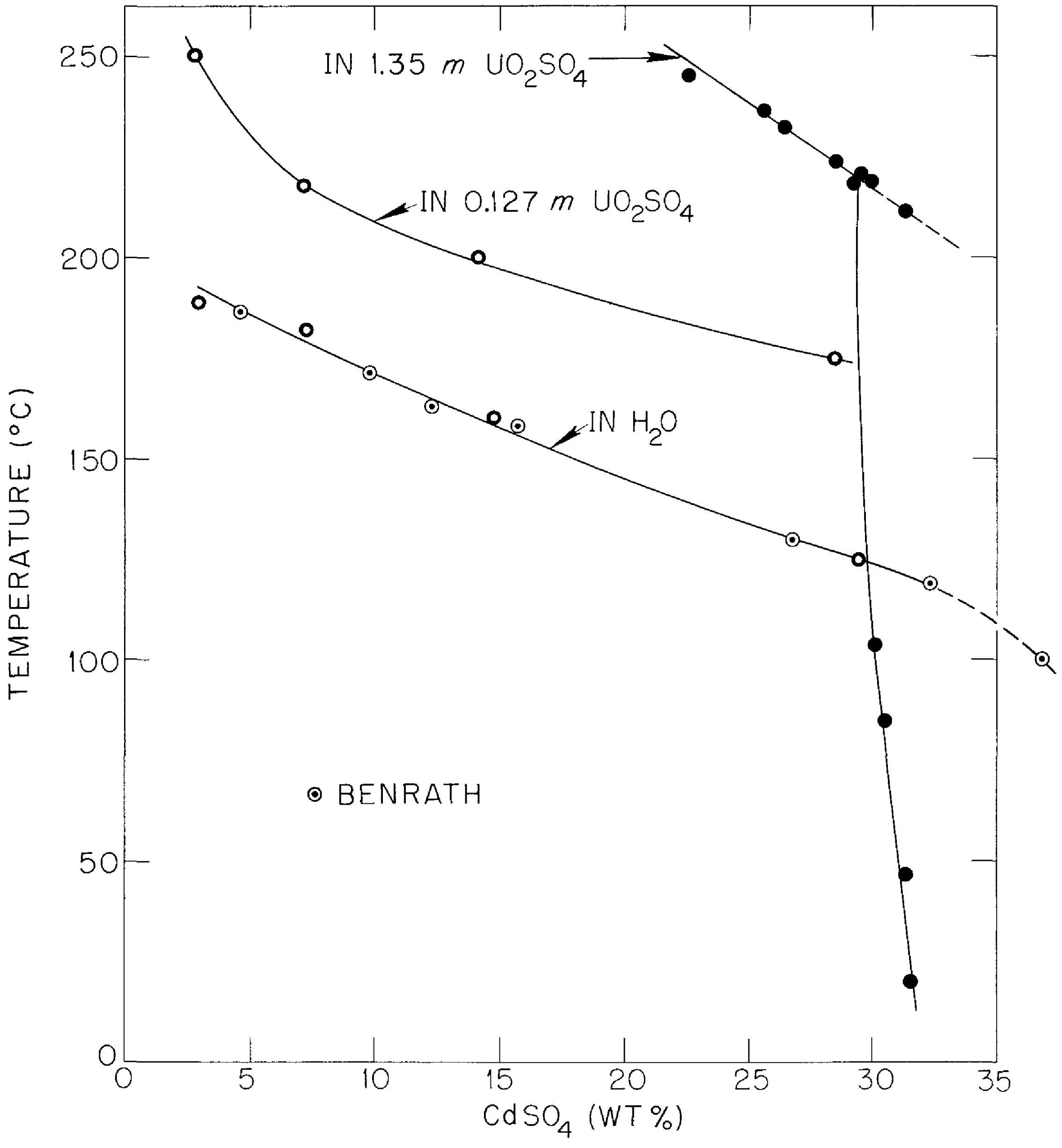

Fig. 5.24. Solubility of $CdSO_4$ in UO_2SO_4 Solutions.

5.25. Solubility of Cs_2SO_4 in UO_2SO_4 Solutions

E. V. Jones, M. H. Lietzke, and W. L. Marshall, *J. Am. Chem. Soc.* **79**, 267 (1957); also *The Solubility of Several Metal Sulfates at High Temperatures and Pressures in Water and in Aqueous Uranyl Sulfate Solution*, ORNL CF-55-7-69 (declassified Aug. 23, 1955).

See comments in Sec 5.23.

UNCLASSIFIED
DWG. 14617A

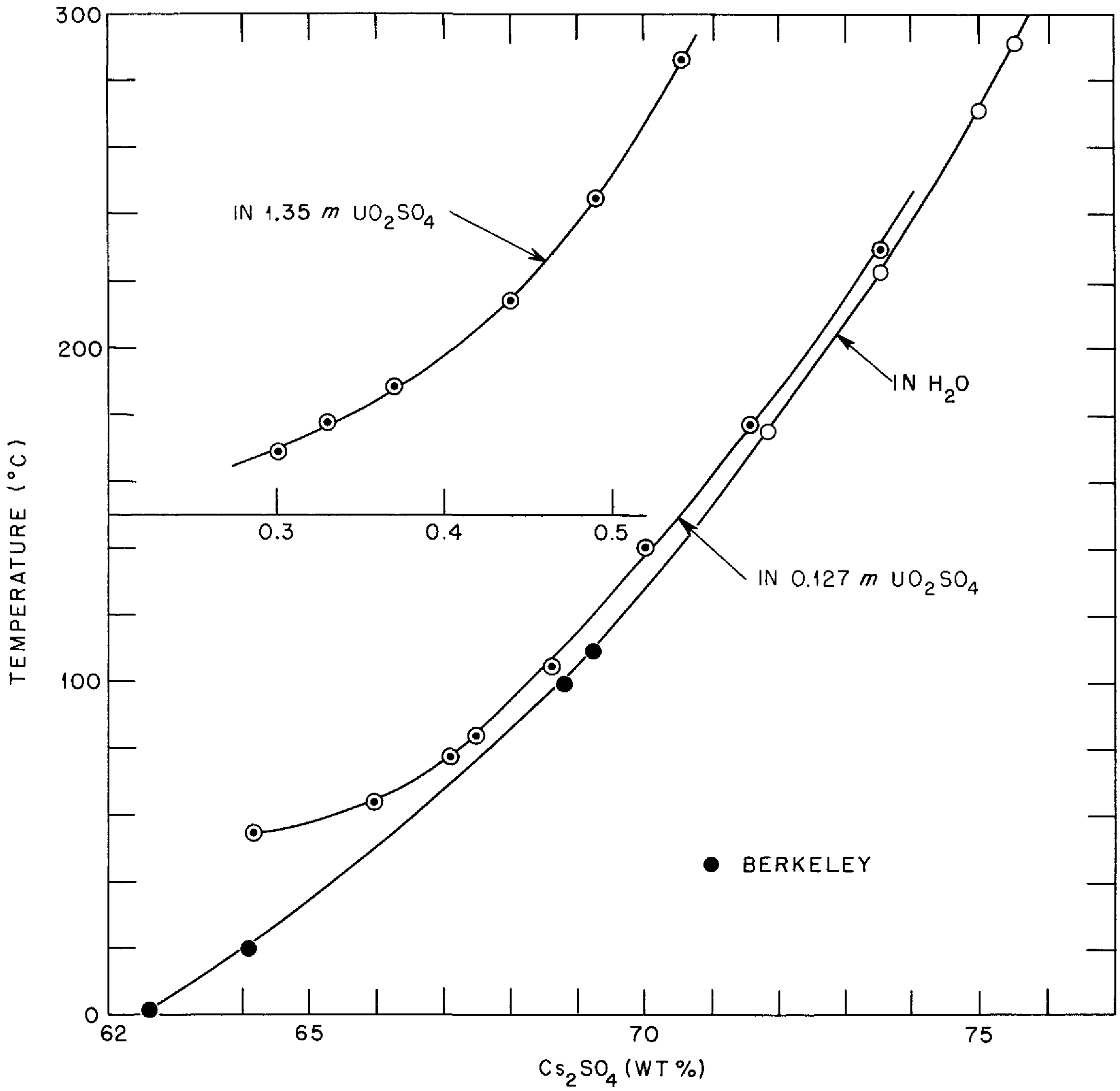

Fig. 5.25. Solubility of Cs_2SO_4 in UO_2SO_4 Solutions.

5.26. Solubility of $Y_2(SO_4)_3$ in UO_2SO_4 Solutions

E. V. Jones, M. H. Lietzke, and W. L. Marshall, *J. Am. Chem. Soc.* **79**, 267 (1957); also *The Solubility of Several Metal Sulfates at High Temperatures and Pressures in Water and in Aqueous Uranyl Sulfate Solution*, ORNL CF-55-7-69 (declassified Aug. 23, 1955).

See comments in Sec 5.23.

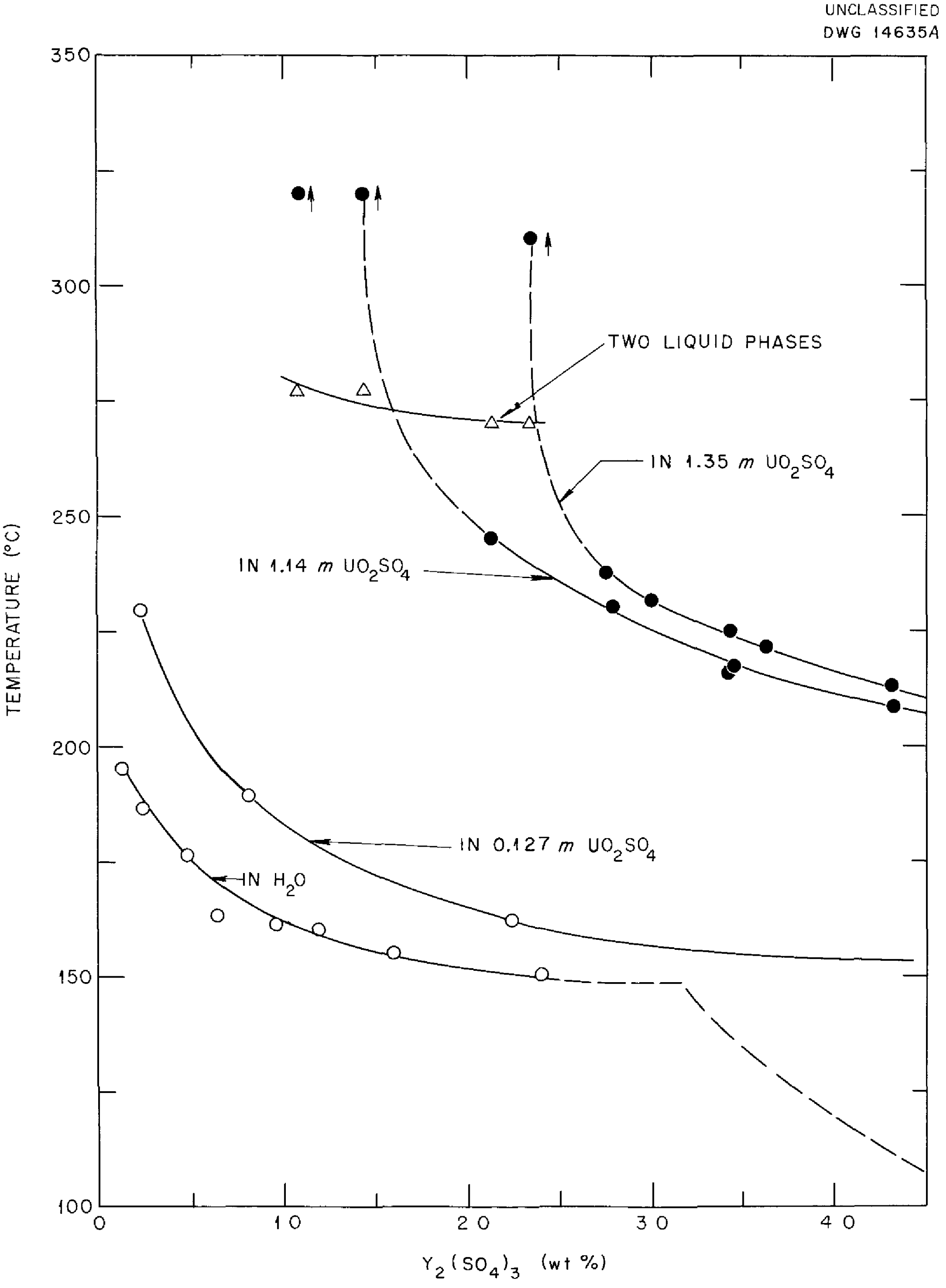

Fig. 5.26. Solubility of $Y_2(SO_4)_3$ in UO_2SO_4 Solutions.

5.27. Solubility of Ag_2SO_4 in UO_2SO_4 Solutions

E. V. Jones, M. H. Lietzke, and W. L. Marshall, *J. Am. Chem. Soc.* **79**, 267 (1957); also *The Solubility of Several Metal Sulfates at High Temperatures and Pressures in Water and in Aqueous Uranyl Sulfate Solution*, ORNL CF-55-7-69 (declassified Aug. 23, 1955).

See comments in Sec 5.23.

UNCLASSIFIED
DWG. 14615A

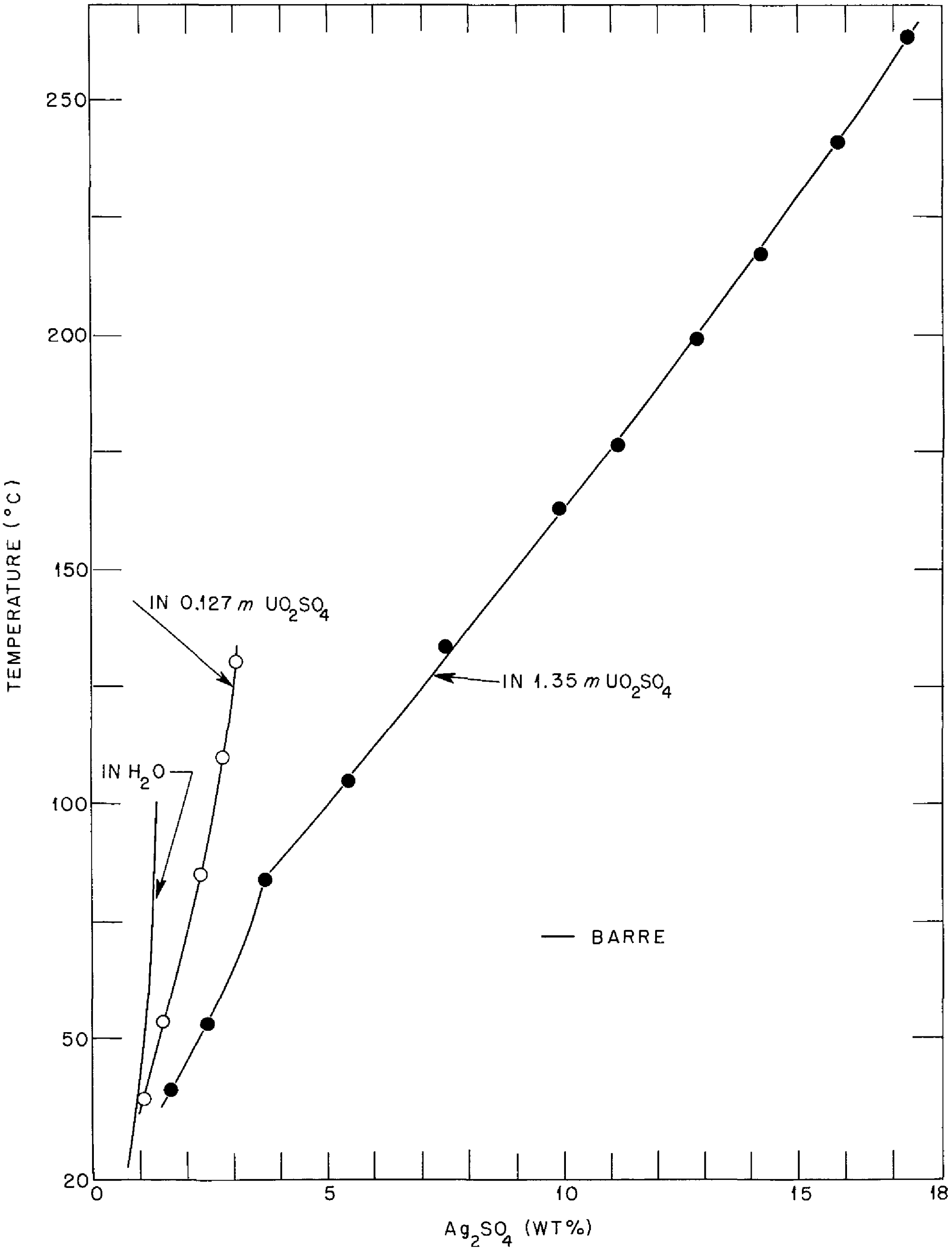

Fig. 5.27. Solubility of Ag_2SO_4 in UO_2SO_4 Solutions.

5.28. Solubility at 250°C of $BaSO_4$ in UO_2SO_4–H_2O Solutions

E. V. Jones, M. H. Lietzke, and W. L. Marshall, *J. Am. Chem. Soc.* **79**, 267 (1957); also *The Solubility of Several Metal Sulfates at High Temperatures and Pressures in Water and in Aqueous Uranyl Sulfate Solutions*, ORNL CF-55-7-69 (declassified Aug. 23, 1955).

Solutions were filtered from solids at 250°C to obtain the solubility of $BaSO_4$ in H_2O. Counting of radioactive barium was used to determine the solubility concentration. The very large effect of UO_2SO_4 must be noted and indicates considerable solvation of other species by aqueous UO_2SO_4.

UNCLASSIFIED
DWG. 15530 A

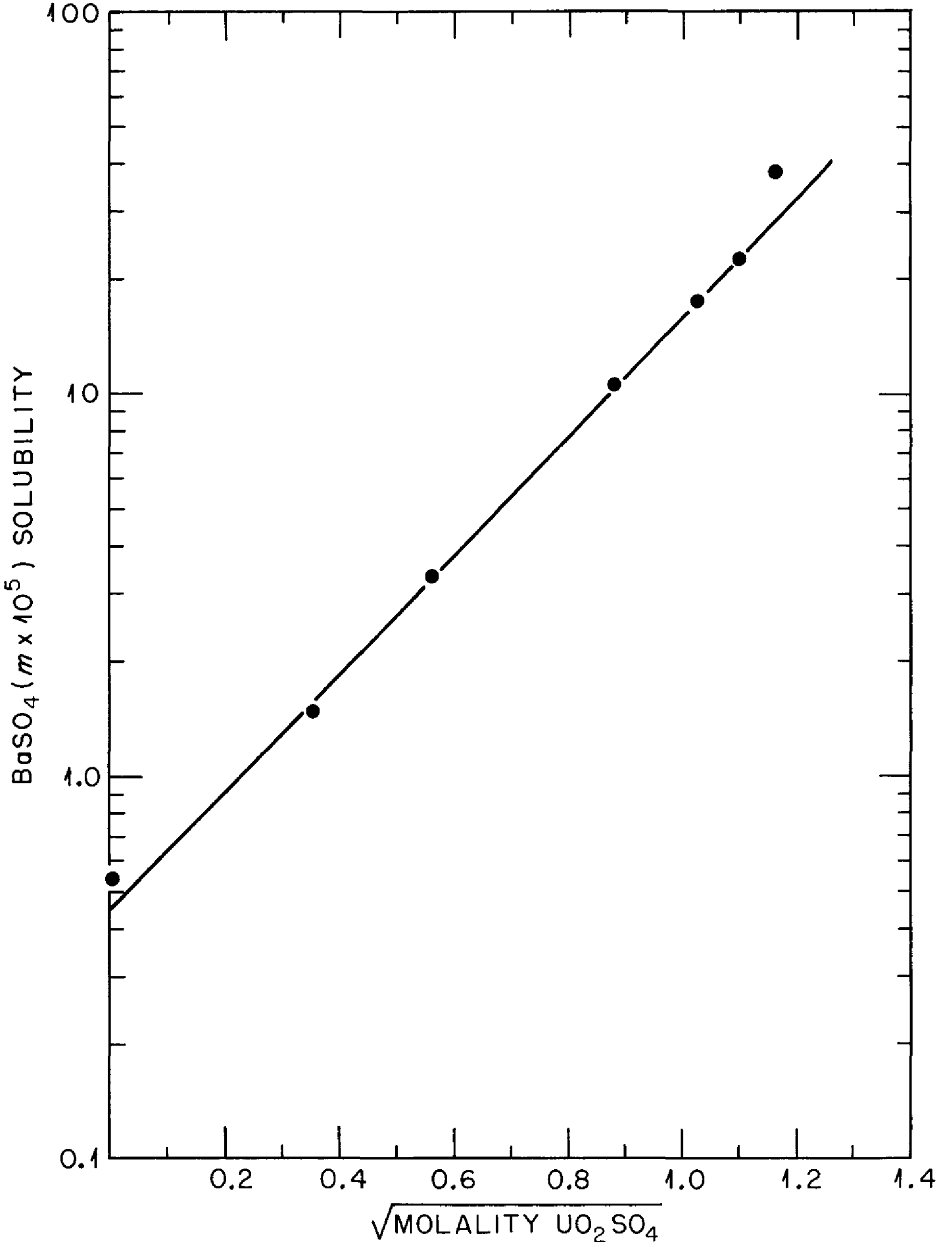

Fig. 5.28. Solubility at 250°C of $BaSO_4$ in UO_2SO_4–H_2O Solutions.

5.29. Solubility of H_2WO_4 in 0.126 and 1.26 *M* UO_2SO_4

C. E. Coffey, W. L. Marshall, and G. H. Cartledge, *HRP Quar. Prog. Rep. Oct. 31, 1953,* ORNL-1658, p 96–99.

The data shown in the figures were obtained by direct sampling of equilibrated solutions, by the filter bomb method, and by the synthetic method described previously in Sec 5.8. In 0.126 *M* UO_2SO_4 the solubility of H_2WO_4 first shows a positive temperature coefficient of solubility and then, above 100°C, a negative coefficient of solubility. In 1.26 *M* UO_2SO_4 the temperature coefficient of solubility is positive up to 285°, the temperature at which two liquid phases form – a characteristic of UO_2SO_4–H_2O solutions.

UNCLASSIFIED
DWG. 21760B

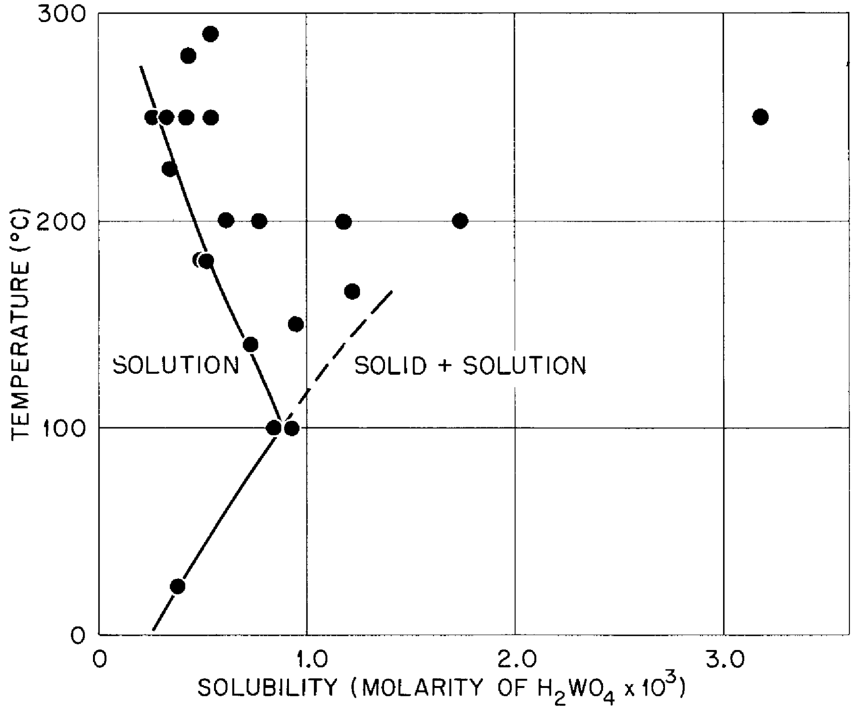

Fig. 5.29*a*. Solubility of H_2WO_4 in 0.126 *M* UO_2SO_4.

UNCLASSIFIED
DWG. 21757 B

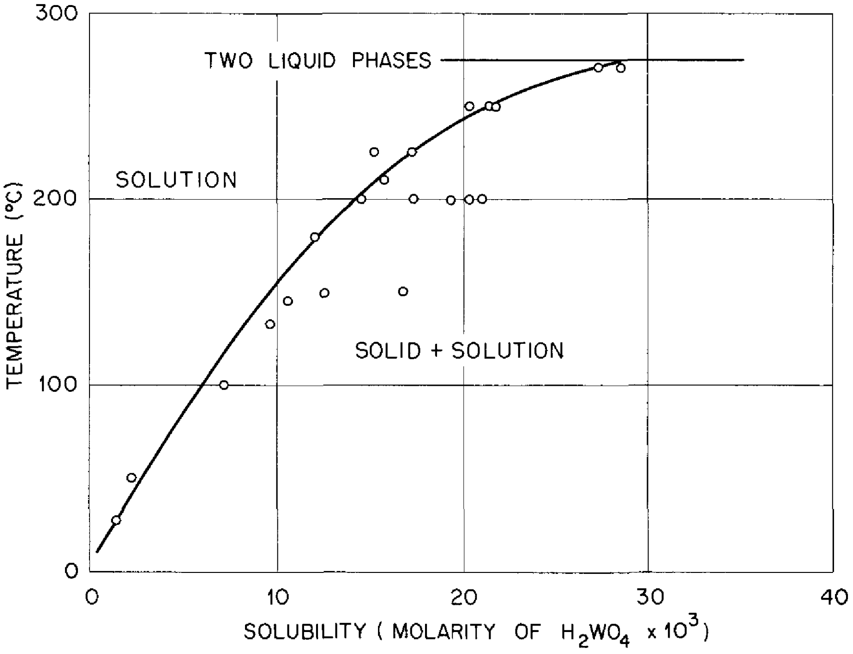

Fig. 5.29*b*. Solubility of H_2WO_4 in 1.26 *M* UO_2SO_4.

5.30. Phase Stability of H_2WO_4 in 1.26 *M* UO_2F_2

C. E. Coffey, W. L. Marshall, and G. H. Cartledge, *HRP Quar. Prog. Rep. Oct. 31, 1953,* ORNL-1658, p 96–99.

The methods of solubility and stability determination were the same as for analogous studies of H_2WO_4 in UO_2SO_4 (Sec 5.29). The data on the figure as drawn show temperatures at which hydrolytic precipitation of an unidentified solid phase occurs from solutions stable at lower temperatures.

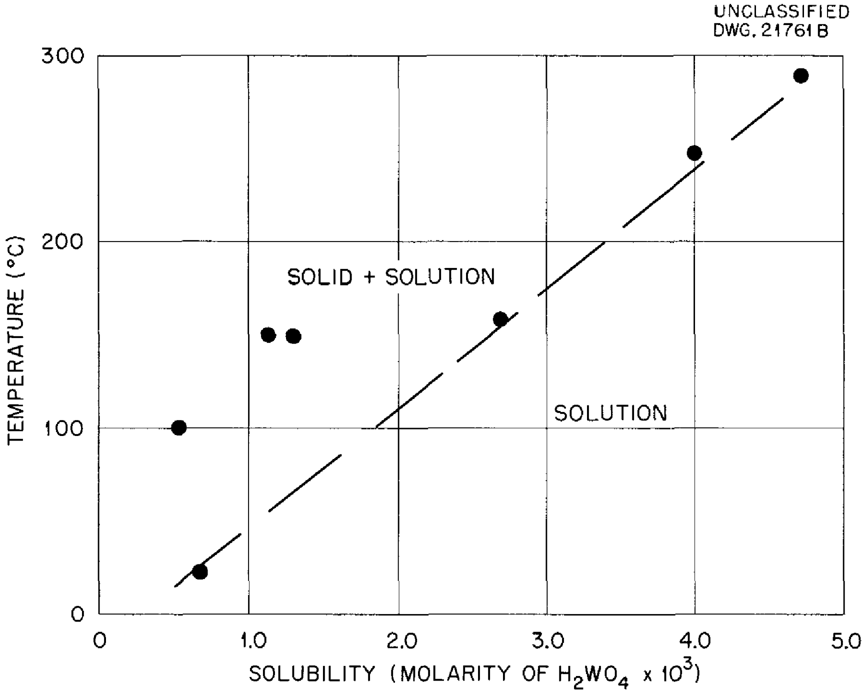

Fig. 5.30. Phase Stability of H_2WO_4 in 1.26 *M* UO_2F_2.

5.31. The System $UO_2(NO_3)_2$–H_2O

1. Reported in full by W. L. Marshall, J. S. Gill, and C. H. Secoy, *Chem. Quar. Prog. Rep. March 31, 1951*, ORNL-1053, p 22–25.

2. Reported in part by W. L. Marshall, J. S. Gill, and C. H. Secoy, *J. Am. Chem. Soc.* **73**, 1867 (1951).

As in the case of the system UO_2SO_4–H_2O, hydrolysis occurs at high temperatures and low concentrations, resulting in precipitation of $UO_3 \cdot H_2O$ from stoichiometric $UO_2(NO_3)_2$ solutions. In addition, decomposition of NO_3^- occurs at elevated temperature to produce an equilibrium vapor phase of nitrogen oxides. Letter *A* represents a region of complete solution. Data at low temperature up to point *F* were obtained by direct analysis of equilibrated solutions, whereas the high-temperature data were obtained by the visual-synthetic method described in Sec 5.8.

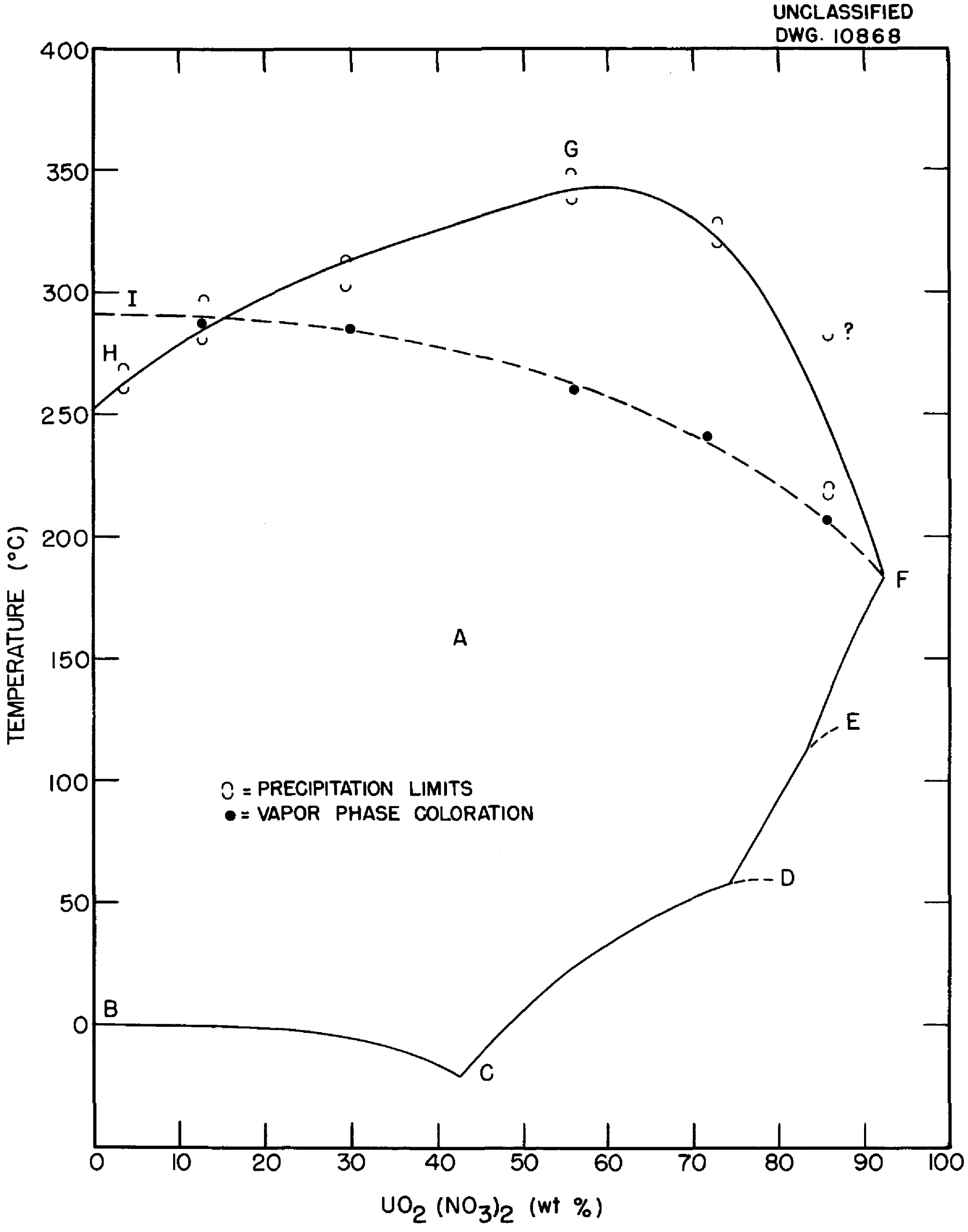

Fig. 5.31. The System $UO_2(NO_3)_2$–H_2O.

5.32. Phase Equilibria of UO_3 and HF in Stoichiometric Concentrations (Aqueous System)

W. L. Marshall, J. S. Gill, and C. H. Secoy, *J. Am. Chem. Soc.* **76**, 4279 (1954).

The two-liquid-phase region and the region of "basic" solid solution + saturated solution are in actuality segments of the three-component system UO_3–HF–H_2O, in which the equilibrium phases are nonstoichiometric with regard to UO_2F_2. This system is somewhat analogous to the system UO_3–H_2SO_4–H_2O (see Sec 5.7).

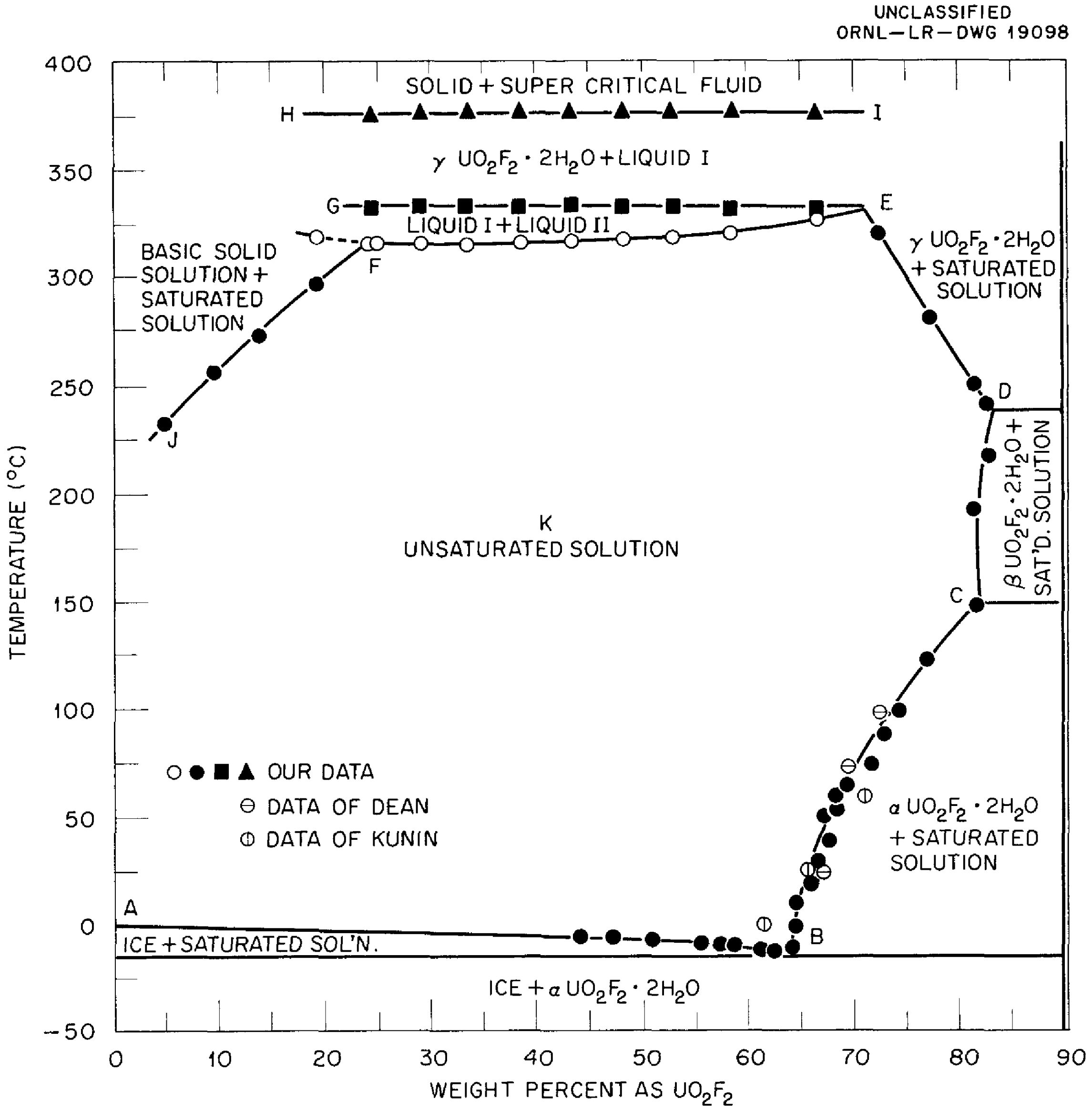

Fig. 5.32. Phase Equilibria of UO_3 and HF in Stoichiometric Concentrations (Aqueous System).

5.33. Solubility of Uranium Trioxide in Orthophosphoric Acid Solutions

W. L. Marshall, J. S. Gill, and H. W. Wright, *HRP Quar. Prog. Rep. May 15, 1951*, ORNL-1057, p 112–15.

The data were obtained for the most part by equilibrating solutions of known concentration in sealed tubes for various times at different temperatures. Phase changes were observed visually.

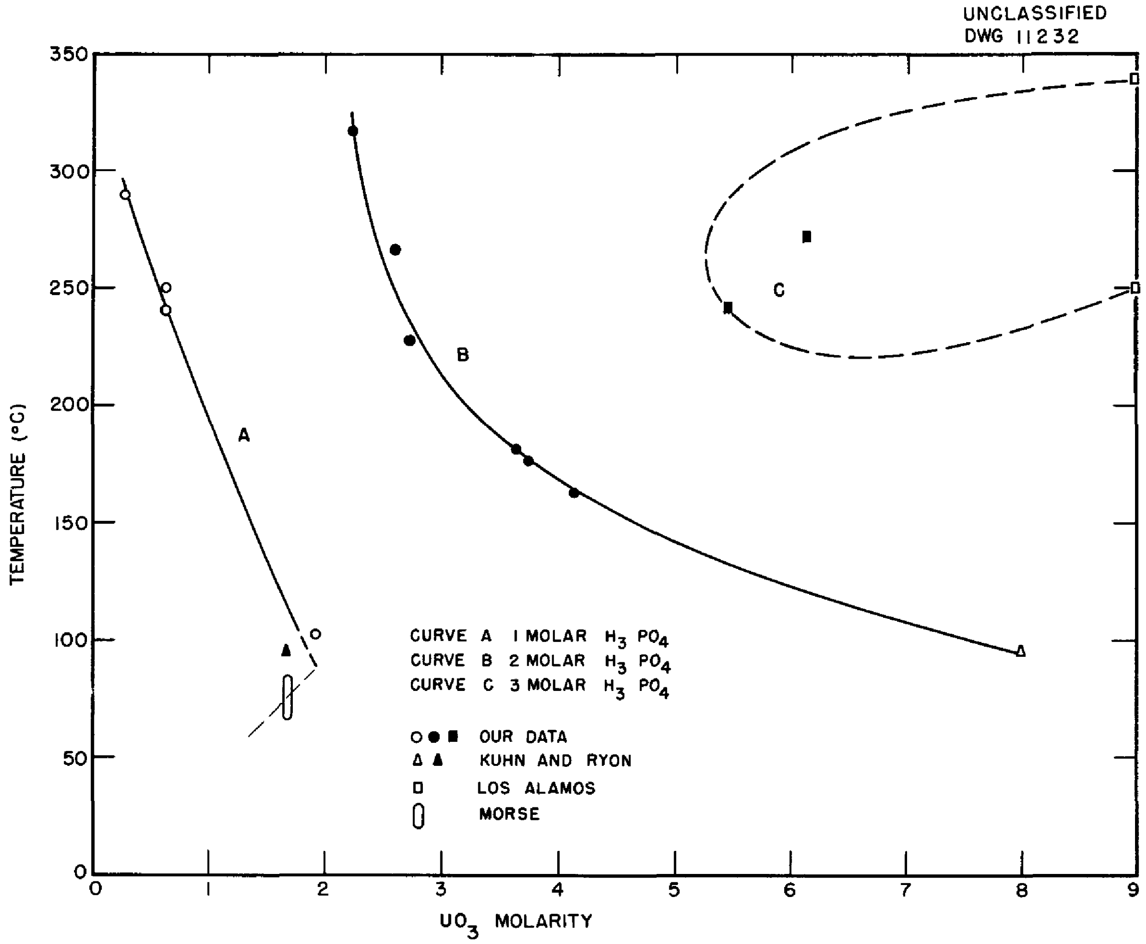

Fig. 5.33. Solubility of Uranium Trioxide in Orthophosphoric Acid Solutions.

5.34. Solubility of Uranium Trioxide in Phosphoric Acid at 250°C

J. S. Gill, W. L. Marshall, and H. W. Wright, *HRP Quar. Prog. Rep. Aug. 15, 1951,* ORNL-1121, p 119–21.

Solution and solid mixtures were equated at 250°C in sealed glass tubes. The tubes were cooled rapidly to room temperature, and the solution and solid phases were analyzed. The slow reversibility of equilibrium conditions made this procedure possible.

UNCLASSIFIED
DWG. 13000

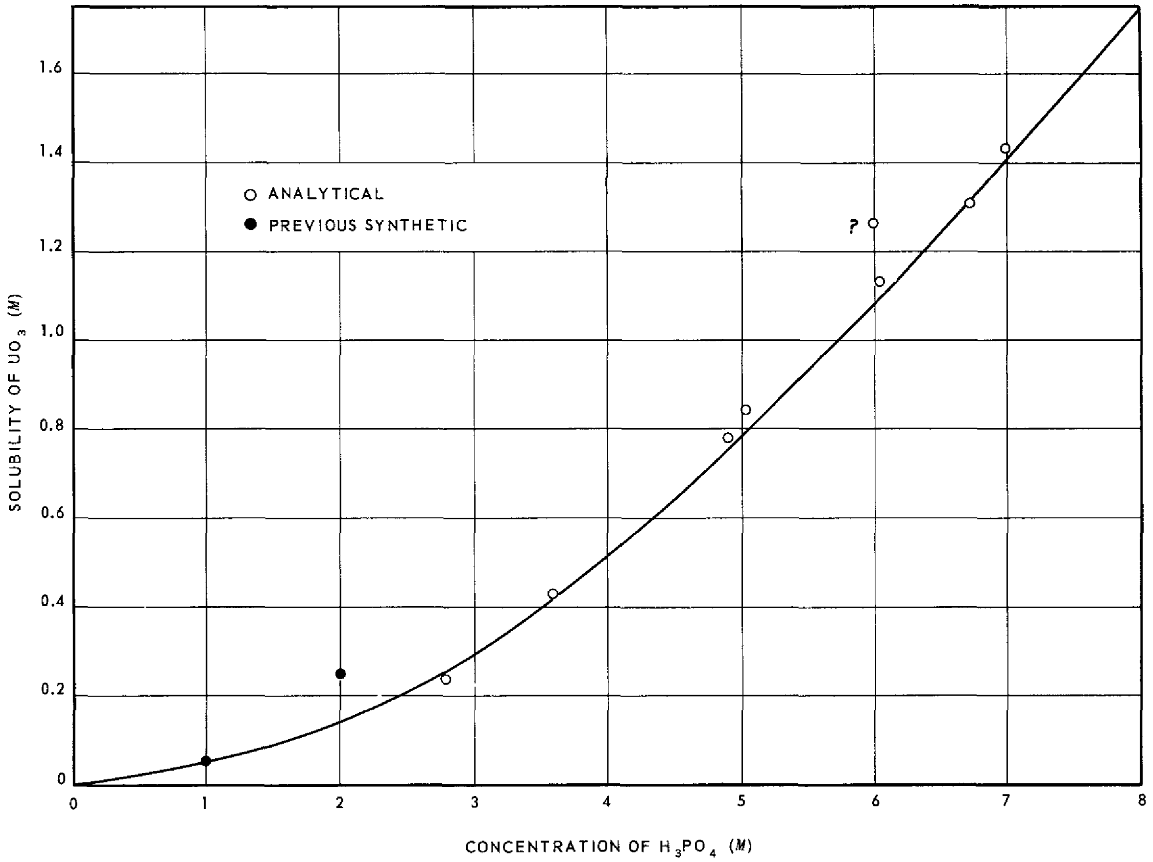

Fig. 5.34. Solubility of Uranium Trioxide in Phosphoric Acid at 250°C.

5.35. Solubility of UO_3 in H_3PO_4 Solution

B. J. Thamer *et al.*, *The Properties of Phosphoric Acid Solutions of Uranium as Fuels for Homogeneous Reactors*, LA-2043 (March 6, 1956); W. L. Marshall, J. S. Gill, and H. W. Wright, *HRP Quar. Prog. Rep. May 15, 1951*, ORNL-1057, p 112–15; and J. S. Gill, W. L. Marshall, and H. W. Wright, *HRP Quar. Prog. Rep. Aug. 15, 1951*, ORNL-1121, p 119–21.

This figure represents a compilation from the data of B. J. Thamer *et al.* of Los Alamos and W. L. Marshall *et al.* of Oak Ridge National Laboratory.

UNCLASSIFIED
ORNL-LR-DWG 29316

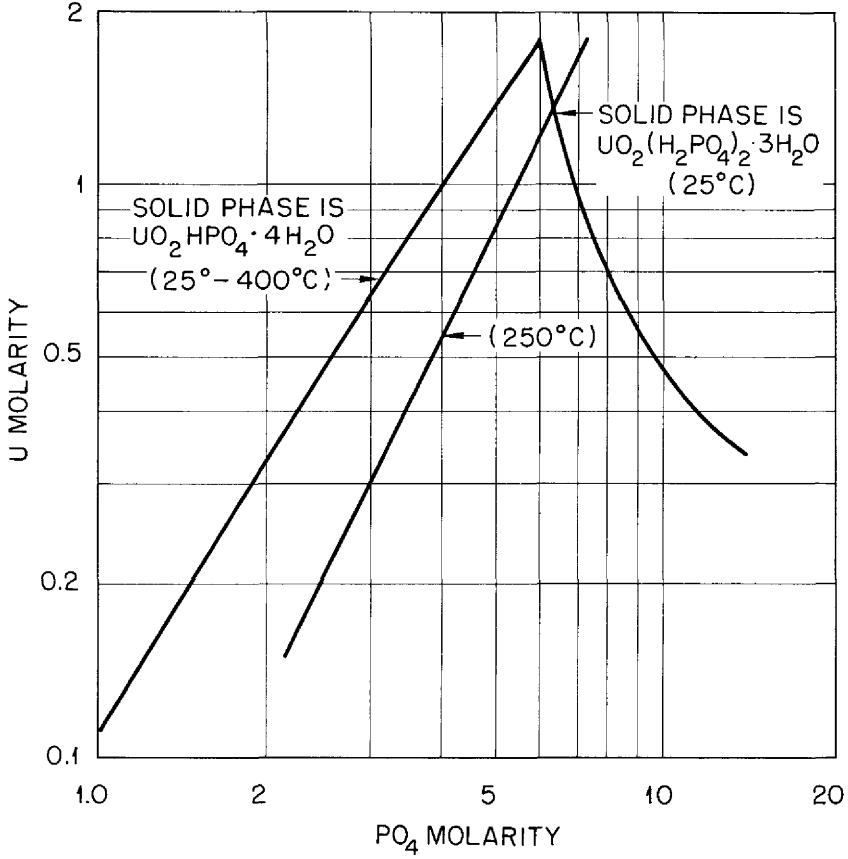

Fig. 5.35. Solubility of UO_3 in H_3PO_4 Solution.

5.36. The System UO_2CrO_4–H_2O

1. F. J. Loprest, W. L. Marshall, and C. H. Secoy, *J. Am. Chem. Soc.* **77**, 4705 (1955).
2. W. L. Marshall, *HRP Quar. Prog. Rep. March 31, 1953*, ORNL-1554, p 105–6.

The solid phases are $UO_2CrO_4 \cdot 5\frac{1}{2}H_2O$ (*A*) and $UO_2CrO_4 \cdot xH_2O$ (*B*). Curve *rs* represents the boundary of a region in which hydrolytic precipitation of a basic uranyl chromate occurs. In the same concentration range the dichromate, $UO_2Cr_2O_7$, is stable to the critical temperature and apparently dissolves in the supercritical fluid (ref 2).

UNCLASSIFIED
ORNL-LR-DWG 5144A

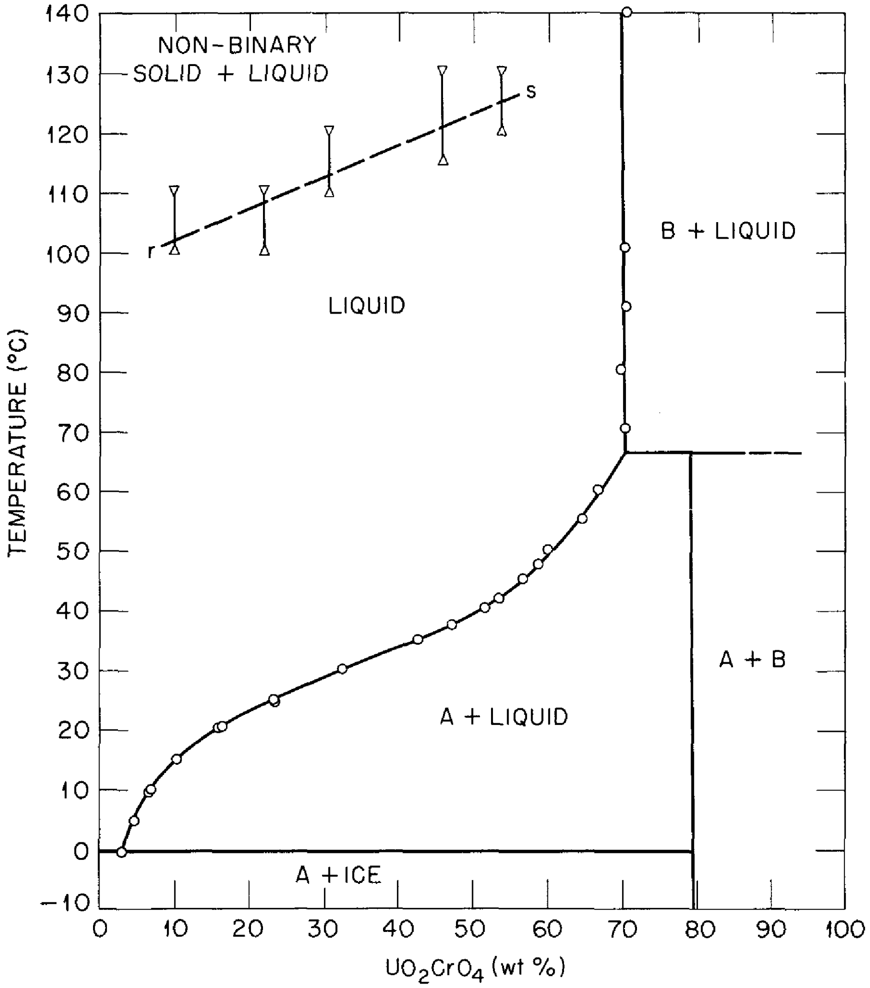

Fig. 5.36. The System UO_2CrO_4–H_2O.

5.37. Variation of Li_2CO_3 Solubility with UO_2CO_3 Concentration at Constant CO_2 Pressure (250°C)

1. F. J. Loprest, W. L. Marshall, and C. H. Secoy, *HRP Quar. Prog. Rep. July 31, 1955*, ORNL-1943, p 227–35.

2. W. L. Marshall, F. J. Loprest, and C. H. Secoy, *HRP Quar. Prog. Rep. Jan. 31, 1956*, ORNL-2057, p 131–32.

The solubility relationships in the figure indicate strong complexing of UO_2CO_3 with Li_2CO_3 under CO_2 pressure. The formation of HCO_3^- species in solution is indicated.

UNCLASSIFIED
ORNL-LR-DWG 11182A

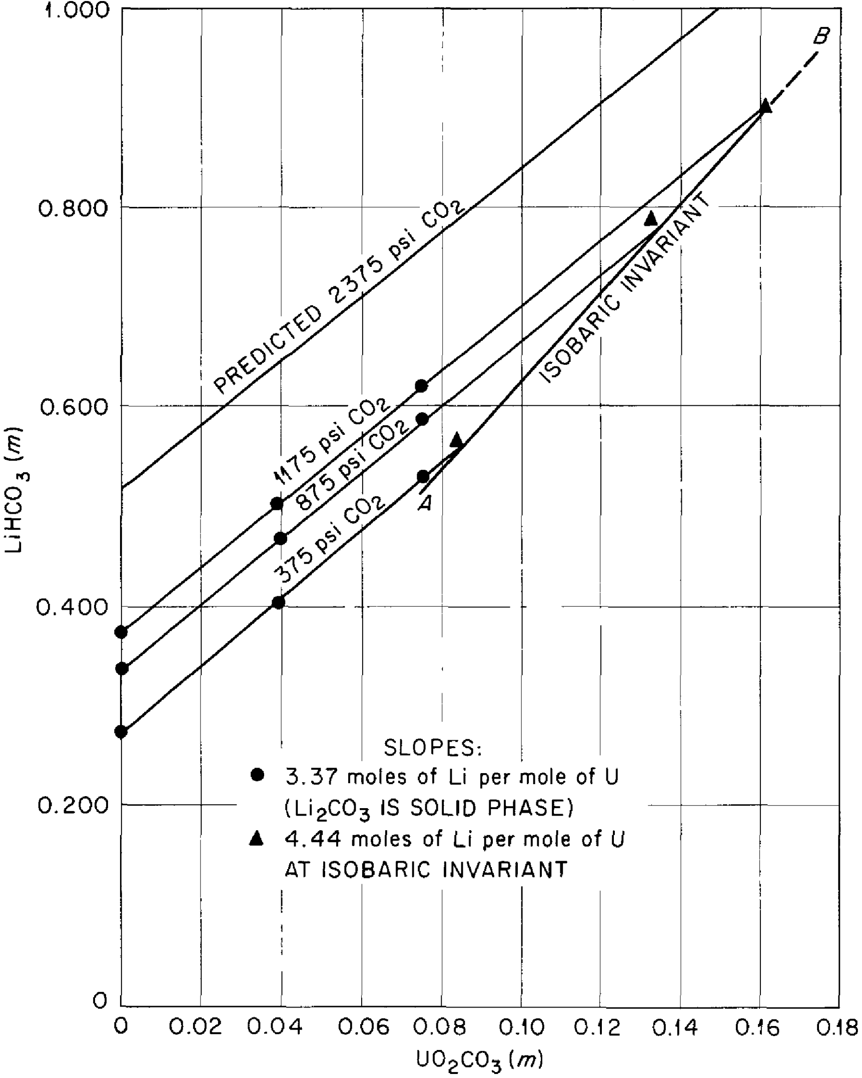

Fig. 5.37. Variation of Li_2CO_3 Solubility with UO_2CO_3 Concentration at Constant CO_2 Pressure (250°C).

5.38. The System $Li_2O-UO_3-CO_2-H_2O$ at 250°C and 1500 psi

1. F. J. Loprest, W. L. Marshall, and C. H. Secoy, *HRP Quar. Prog. Rep. July 31, 1955*, ORNL-1943, p 227–35.

2. W. L. Marshall, F. J. Loprest, and C. H. Secoy, *HRP Quar. Prog. Rep. Jan. 31, 1956*, ORNL-2057, p 131–32.

As CO_2 pressure is increased, the area of complete solution (indicated by the shading) increases. As temperature is increased, the solution area decreases.

UNCLASSIFIED
ORNL-LR-DWG 11342B

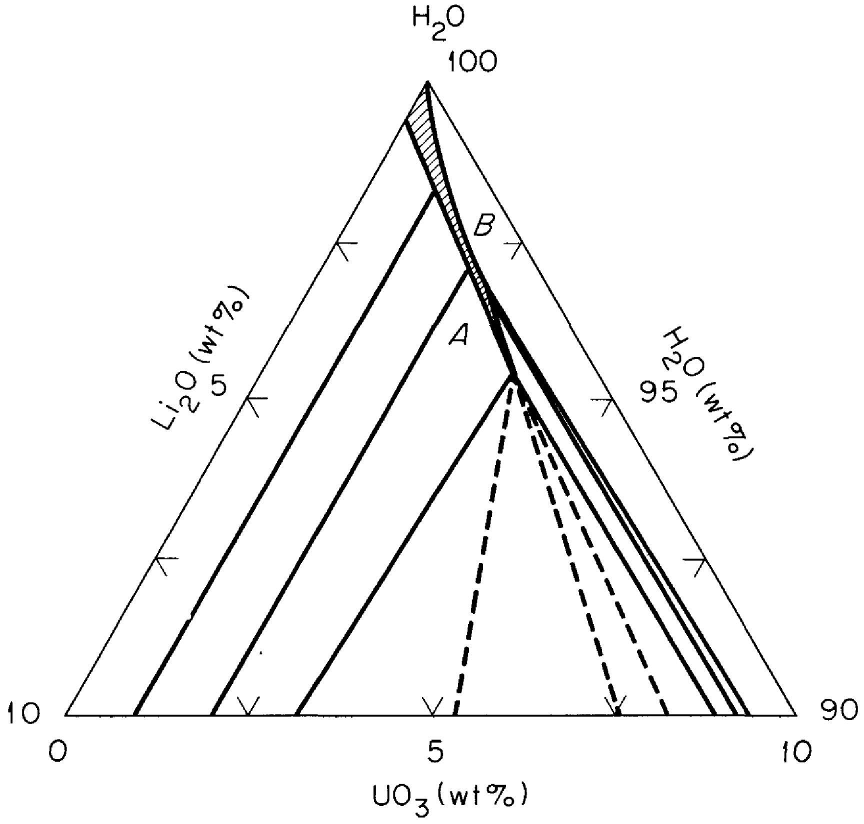

Fig. 5.38. The System $Li_2O-UO_3-CO_2-H_2O$ at 250°C and 1500 psi.

5.39. The System $Th(NO_3)_4$–H_2O

1. Reported in full by W. L. Marshall, J. S. Gill, and C. H. Secoy, *HRP Quar. Prog. Rep. Nov. 30, 1950*, ORNL-925, p 279–90.

2. W. L. Marshall, J. S. Gill, and C. H. Secoy, *J. Am. Chem. Soc.* **73**, 4991 (1951).

Hydrolytic precipitation of ThO_2 and thermal decomposition of NO_3^- in this system occur in an analogous manner to the reactions occurring in the system $UO_2(NO_3)_2$–H_2O (see Sec 5.31). At higher temperatures the two-component system in actuality must be considered in terms of the three components ThO_2, HNO_3, and H_2O.

UNCLASSIFIED
DWG. 9967

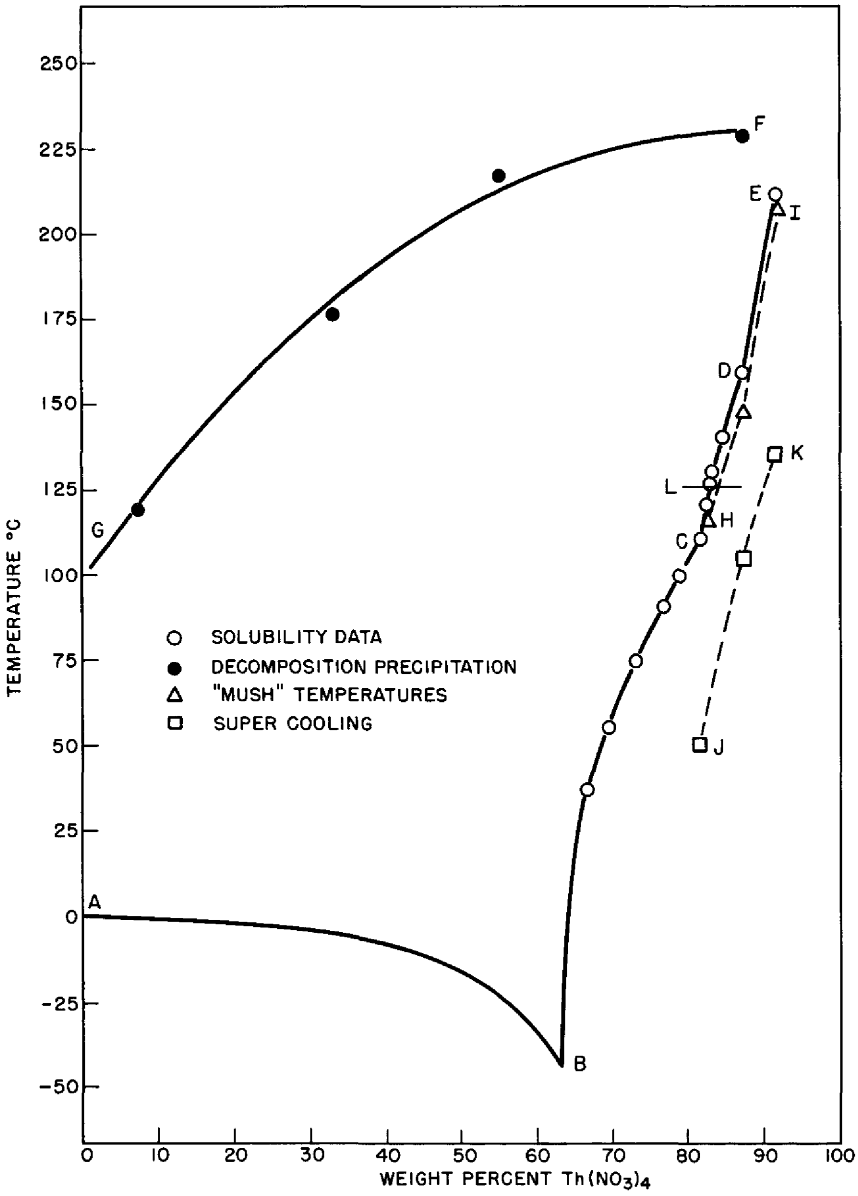

Fig. 5.39. The System $Th(NO_3)_4$–H_2O.

5.40. Hydrolytic Stability of Thorium Nitrate–Nitric Acid and Uranyl Nitrate Solutions

1. W. L. Marshall and C. H. Secoy, *HRP Quar. Prog. Rep. Oct. 31, 1953*, ORNL-1658, p 93–96.

2. W. L. Marshall, J. S. Gill, and C. H. Secoy, *Chem. Quar. Prog. Rep. March 31, 1951*, ORNL-1053, p 22–25.

The data used to draw the individual curves were obtained by observations at various temperatures of tubes that contained different solutions of known concentration. The procedure was analogous to that used for obtaining data for Fig. 5.33. The curve for hydrolytic precipitation of $UO_2(NO_3)_2$ is taken from ref 2.

UNCLASSIFIED
ORNL-LR-DWG. 21759B

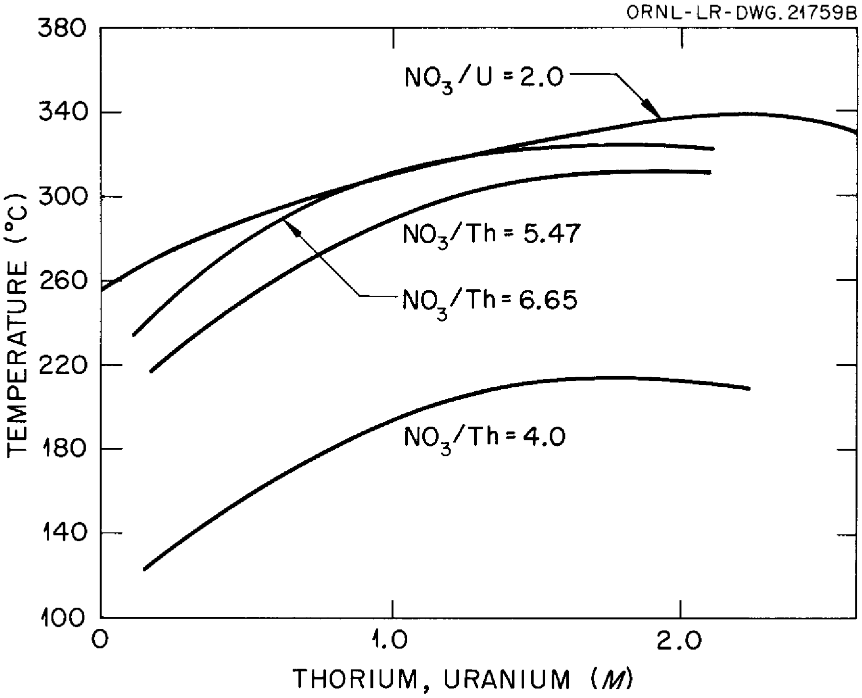

Fig. 5.40. Hydrolytic Stability of Thorium Nitrate–Nitric Acid and Uranyl Nitrate Solutions.

5.41. The System ThO_2–CrO_3–H_2O at 25°C

1. H. T. S. Britton, *J. Chem. Soc.* **123**, 1429 (1923).

2. W. L. Marshall, F. J. Loprest, and C. H. Secoy, *HRP Quar. Prog. Rep. Jan. 31, 1955*, ORNL-1853, p 205–6.

The phase diagram at 25° was determined by Britton. Points 1–7 indicate compositions investigated at high temperature by Marshall, Loprest, and Secoy. These solution compositions were phase stable up to 160°C for point 7 and 320°C for point 1.

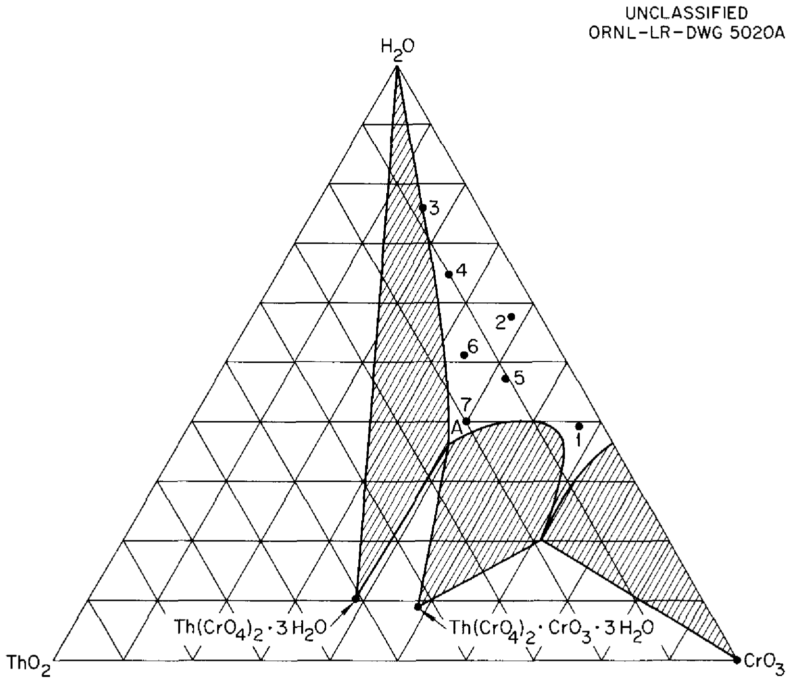

Fig. 5.41. The System ThO_2–CrO_3–H_2O at 25°C. Compositions are in weight per cent.

5.42. Phase Stability of ThO_2–H_3PO_4–H_2O Solutions at High Concentrations of ThO_2

W. L. Marshall, experimental data in ORNL research notebook 2881, p 35 (May 1953).

Solutions of appropriate concentrations were prepared and analyzed. These solutions were sealed in glass tubes and shaken at various temperatures for times varying from 1 hr to several days. In this manner the phase stability boundaries with respect to concentration and temperature were established. At first inspection of the figure it is surprising that more ThO_2 can be dissolved per liter at the lower H_3PO_4/ThO_2 ratio than at the higher ratio. Actually, there is a physical volume limitation due to the high fractional volumes occupied by ThO_2 and H_3PO_4 at these concentrations. As any solution is diluted with H_2O, hydrolysis of thorium in solution occurs. At room temperature, solutions in which the H_3PO_4/ThO_2 ratio is 5:1 are gels, whereas 10:1 ratio solutions are still fluid.

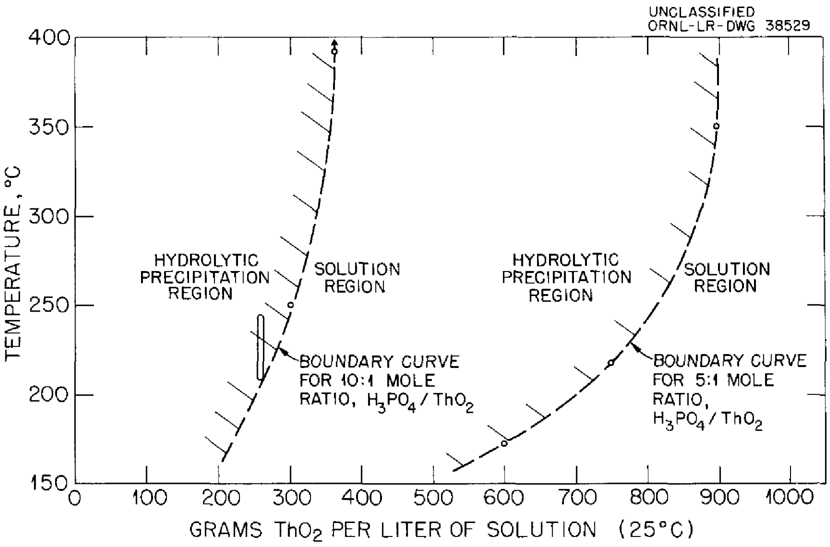

Fig. 5.42. Phase Stability of ThO_2–H_3PO_4–H_2O Solutions at High Concentrations of ThO_2.

ACKNOWLEDGMENT

Acknowledgment is made to the following for permission to reproduce copyrighted material:

American Ceramic Society
American Institute of Mining, Metallurgical, and Petroleum Engineers
Analytical Chemistry
Journal of Chemical and Engineering Data
Journal of Physical Chemistry
Journal of the American Chemical Society
U.S. Atomic Energy Commission

INTERNAL DISTRIBUTION

1\. R. D. Ackley
2\. R. E. Adams
3\. G. M. Adamson
4\. L. G. Alexander
5\. K. A. Allen
6\. C. F. Baes
7-11. C. J. Barton
12\. S. E. Beall
13\. P. R. Bell
14\. J. O. Betterton
15\. A. M. Billings
16\. D. S. Billington
17\. C. A. Blake
18\. J. P. Blakely
19\. R. E. Blanco
20\. F. F. Blankenship
21\. M. Blander
22\. E. P. Blizard
23\. C. M. Blood
24\. A. L. Boch
25\. E. G. Bohlman
26\. S. E. Bolt
27\. G. E. Boyd
28\. M. A. Bredig
29\. J. C. Bresee
30\. R. B. Briggs
31\. H. R. Bronstein
32\. J. R. Brown
33\. K. B. Brown
34\. W. E. Browning
35\. F. R. Bruce
36\. W. D. Burch
37\. S. R. Buxton
38\. S. Cantor
39\. W. H. Carr
40\. W. L. Carter
41\. G. H. Cartledge
42\. G. I. Cathers
43\. C. E. Center
44\. R. H. Chapman
45\. R. A. Charpie
46\. R. D. Cheverton
47\. H. C. Claiborne
48\. G. W. Clark
49\. C. F. Coleman
50\. E. L. Compere
51\. J. A. Cox
52\. J. H. Crawford
53\. C. R. Croft
54\. F. L. Culler
55\. J. S. Culver
56\. D. R. Cuneo
57\. J. E. Cunningham
58\. D. G. Davis
59\. R. J. Davis
60\. W. C. Davis
61\. J. H. DeVan
62\. R. R. Dickison
63\. L. M. Doney
64\. F. A. Doss
65\. J. S. Drury
66\. A. S. Dworkin
67\. L. B. Emlet (K-25)
68\. J. L. English
69\. J. E. Eorgan
70\. R. B. Evans
71\. D. E. Ferguson
72\. J. L. Fowler
73\. A. P. Fraas
74\. H. A. Friedman
75\. J. H. Frye, Jr.
76\. C. H. Gabbard
77\. W. R. Gall
78\. J. S. Gill
79\. J. H. Gillette
80\. L. O. Gilpatrick
81\. J. M. Googin (Y-12)
82\. R. S. Greeley
83\. A. T. Gresky
84\. J. C. Griess
85-89. W. R. Grimes
90\. E. Guth
91\. P. A. Haas
92\. P. H. Harley
93\. C. S. Harrill
94\. L. A. Harris
95\. P. N. Haubenreich
96\. G. M. Hebert
97\. H. L. Hemphill
98\. J. W. Hill
99\. E. C. Hise
100\. E. E. Hoffman
101\. H. W. Hoffman
102\. A. Hollaender
103\. R. W. Horton
104\. A. S. Householder
105\. H. Insley
106\. G. H. Jenks
107\. D. T. Jones
108\. E. V. Jones

109. W. H. Jordan
110. P. R. Kasten
111. G. W. Keilholtz
112. C. P. Keim
113. M. T. Kelley
114. M. J. Kelley
115. B. W. Kinyon
116. N. A. Krohn
117. J. A. Lane
118. S. Langer
119. C. G. Lawson
120. J. E. Lee, Jr.
121. R. E. Leed
122. R. E. Leuze
123. W. H. Lewis
124. M. H. Lietzke
125. T. A. Lincoln
126. S. C. Lind
127. R. B. Lindauer
128. R. S. Livingston
129. J. T. Long
130. R. A. Lorenz
131. R. E. Lowrie
132. M. I. Lundin
133. R. N. Lyon
134. J. P. McBride
135. W. B. McDonald
136. H. F. McDuffie
137. H. A. McLain
138. R. A. McNees
139. H. G. MacPherson
140. T. N. McVay
141. J. R. McWherter
142. W. D. Manly
143-147. W. L. Marshall
148. R. E. Meadows
149. R. P. Metcalf
150. R. P. Milford
151. A. J. Miller
152. J. W. Miller
153. C. S. Morgan
154. K. Z. Morgan
155. R. E. Moore
156. R. L. Moore
157. J. P. Murray (Y-12)
158. M. L. Nelson
159. G. J. Nessle
160. R. F. Newton
161. L. G. Overholser
162. L. F. Parsly, Jr.
163. R. L. Pearson
164. F. N. Peebles
165. D. Phillips
166. L. R. Phillips (Y-12)
167. M. L. Picklesimer
168. W. T. Rainey
169. A. D. Redman
170. S. A. Reed
171. P. M. Reyling
172. D. M. Richardson
173. R. C. Robertson
174. A. D. Ryon
175. H. C. Savage
176. H. W. Savage
177. F. A. Schimmel (Y-12)
178. J. M. Schmitt
179. J. M. Schreyer (Y-12)
180. H. E. Seagren
181. C. H. Secoy
182. C. L. Segaser
183. J. H. Shaffer
184. E. M. Shank
185. R. J. Sheil
186. R. P. Shields
187. E. D. Shipley
188. M. D. Silverman
189. M. J. Skinner
190. R. Slusher
191. N. V. Smith
192. W. T. Smith, Jr.
193. A. H. Snell
194. B. A. Soldano
195. I. Spiewak
196. H. H. Stone
197. R. A. Strehlow
198. B. J. Sturm
199. C. D. Susano
200. J. E. Sutherland
201. J. A. Swartout
202. A. Taboada
203. E. H. Taylor
204-213. R. E. Thoma
214. D. G. Thomas
215. M. Tobias
216. D. S. Toomb
217. D. B. Trauger
218. J. Truitt
219. W. E. Unger
220. R. Van Winkle
221. F. C. VonderLage
222. W. T. Ward
223. G. M. Watson
224. B. S. Weaver
225. C. F. Weaver

226. A. M. Weinberg
227. K. W. West
228. M. E. Whatley
229. G. C. Williams
230. C. E. Winters
231. H. W. Wright
232. J. P. Young
233. F. C. Zapp
234. P. H. Emmett (consultant)
235. H. Eyring (consultant)
236. D. G. Hill (consultant)
237. C. E. Larson (consultant)
238. W. O. Milligan (consultant)
239. J. E. Ricci (consultant)
240. G. T. Seaborg (consultant)
241. E. P. Wigner (consultant)
242. Biology Library
243-244. Central Research Library
245. Health Physics Library
246-265. Laboratory Records Department
266. Laboratory Records, ORNL R.C.
267. Reactor Experimental Engineering Library
268. ORNL – Y-12 Technical Library, Document Reference Section

EXTERNAL DISTRIBUTION

269-270. Stanford Research Institute, Menlo Park, Calif. (1 copy ea. to D. Cubicciotti and J. W. Johnson)
271-272. National Lead Co., P. O. Box 158, Cincinnati 39, Ohio (1 copy ea. to R. E. DeMarco and K. Notz)
273. Geophysical Laboratory, Carnegie Institution of Washington, 2801 Upton St., Washington 8, D.C. (J. W. Grieg)
274. Mound Laboratory, Miamisburg, Ohio (E. F. Eichelberger)
275-276. Minnesota Mining and Manufacturing Co., Central Research Dept., 2301 Hudson Rd., St. Paul 9, Minn. (1 copy ea. to J. R. Johnson and G. D. White)
277. Chemical Separations and Development Branch, Nuclear Technology, Division of Reactor Development, AEC, Washington 25, D.C. (F. Kerze, Jr.)
278. Dept. of Chemistry, Brown University, Providence 12, R.I. (C. A. Kraus)
279. Mallinckrodt Chemical Works, Uranium Division, P.O. Box 472, St. Charles, Mo. (C. W. Kuhlman)
280. Portland Cement Association Fellowship, National Bureau of Standards, Washington 25, D. C. (E. M. Levin)
281-282. National Carbon Research Laboratories, P.O. Box 6116, Cleveland, Ohio (1 copy ea. to G. W. Mellors and S. Senderoff)
283. College of Mineral Industries, Pennsylvania State University, University Park, Pa. (E. F. Osborn)
284. Los Alamos Scientific Laboratory, P.O. Box 1663, Los Alamos, N. M. (B. J. Thamer)
285. Dept. of Physics, University of Chicago, Chicago, Ill. (W. H. Zachariasen)
286. Reaction Motors Division, Thiokol Chemical Corp., Denville, N.J. (F. L. Loprest)
287. National Bureau of Standards, Washington 25, D. C. (H. F. McMurdie)
288. U.S. Geological Survey, Washington 25, D. C. (G. W. Morey)
289. National Carbon Co., Union Carbide Corporation, Parma, Ohio (F. E. Clark)
290. Division of Research and Development, AEC, Washington
291. Division of Research and Development, AEC, ORO
292. Division of Reactor Development, AEC, Washington
293. Division of Reactor Development, AEC, ORO
294. Oak Ridge Institute of Nuclear Studies, Oak Ridge
295-851. Given distribution as shown in TID-4500 (15th ed.) under Chemistry-General category (75 copies - OTS)